



**UNIVERSITÀ DEGLI STUDI DI TRIESTE**  
**e**  
**UNIVERSITÀ CA' FOSCARI DI VENEZIA**

**XXXI CICLO DEL DOTTORATO DI RICERCA IN**  
**CHIMICA**

**STUDY OF 1,3,5-TRIAZINE-BASED AMIDATION**  
**AGENTS AND THEIR APPLICATION IN**  
**CONDENSATION REACTIONS, COLLAGEN**  
**CROSS-LINKING AND POLYMER GRAFTING**

Settore scientifico-disciplinare: **CHIM/04**

**DOTTORANDO**  
**LODOVICO AGOSTINIS**

**COORDINATORE**  
**PROF. BARBARA MILANI**

**SUPERVISORE DI TESI**  
**PROF. VALENTINA BEGHETTO**

**ANNO ACCADEMICO 2018/2019**



**UNIVERSITY OF TRIESTE**  
and  
**CA' FOSCARI UNIVERSITY OF VENICE**

**XXXI CYCLE OF RESEARCH DOCTORATE IN  
CHEMISTRY**

**STUDY OF 1,3,5-TRIAZINE-BASED AMIDATION  
AGENTS AND THEIR APPLICATION IN  
CONDENSATION REACTIONS, COLLAGEN  
CROSS-LINKING AND POLYMER GRAFTING**

Scientific-disciplinary sector: **CHIM/04**

**ACADEMIC YEAR 2018/2019**

PhD STUDENT  
**LODOVICO AGOSTINIS**

PhD COORDINATOR  
**PROF. BARBARA MILANI**

THESIS SUPERVISOR  
**PROF. VALENTINA BEGHETTO**

*in collaboration with:*



## *Abstract*

# **Study of 1, 3, 5-triazine-based amidation agents and their application in condensation reactions, collagen cross-linking and polymer grafting**

---

*Lodovico Agostinis*

Amide bonds are important for the synthesis or functionalization of many biological macromolecules and a wide range of pharmaceutical products, polymers and fibers. 4-(4,6-dimethoxy-1,3,5-triazin-2-yl)-4-methyl-morpholinium chloride (DMTMM) is an unexploited amidation agent capable to work in wide pH range, water solvent and room temperature. Starting from DMTMM, this thesis focuses on the synthesis of new amidation agents, more active and stable, leading to the drafting of two patents, one of which international. Moreover, this work examines the application of these new compounds for the cross-linking of atoxic and metal-free collagen. Finally, the functionalization of polymers by DMTMM is investigated for the modification of polymer surfaces.



*To my families*

## INDEX

<b>SYNTHESIS OF AMIDATION AGENTS AND THEIR REACTIVITY IN COUPLING REACTIONS</b>	<b>6</b>
<b>1 – INTRODUCTION</b>	<b>7</b>
1.1 Importance of amides synthesis reactions	8
1.2 Condensation reaction activators	8
1.3 Acyl chlorides	9
1.4 Acyl Azides	9
1.5 1-hydroxybenzotriazole derivates, uronium and phosphonium salts	10
1.6 Carbodiimides	12
1.7 Triazine derivatives as amidation agents	15
<b>2 – SCOPE OF THE WORK</b>	<b>18</b>
<b>3 – RESULTS AND DISCUSSION</b>	<b>21</b>
3.1 Synthesis of 2-chloro-4,6-disubstituted-1,3,5-triazines	23
3.1.1 Synthesis of 2-chloro-4,6-bis-diisopropylamino-1,3,5-triazine (DIAT)	24
3.1.2 Synthesis of 2-chloro-4,6-bis-diethylamino-1,3,5-triazine (DEAT)	26
3.1.3 Synthesis of 2-chloro-4-methoxy-6-diisopropylamino-1,3,5-triazine (MAT)	28
3.1.4 Synthesis of <i>N,N'</i> -(oxybis(4,1-phenylene))bis(2-chloro-4-methoxy-1,3,5-triazin-6-amine) (MODAM)	32
3.1.5 Synthesis of <i>N,N'</i> -(methylenebis(4,1-phenylene))bis(2-chloro-4-methoxy-1,3,5-triazin-6-amine) (MMDAM)	38
3.2 Synthesis of 2,4-dichloro-6-substituted-1,3,5-triazines	41
3.2.1 Synthesis of 2,4-dichloro-6-methoxy-1,3,5-triazine (MMT)	42
3.2.2 Synthesis of 2,4-dichloro-6-diisopropylamino-1,3,5-triazine (MIAT)	44
3.2.3 Synthesis of 2,4-dichloro-6-diethylamino-1,3,5-triazine (MEAT)	45
3.2.4 Synthesis of <i>N<sub>1</sub>N<sub>2</sub></i> -bis(2,4-dichloro-1,3,5-triazin-6-yl)- <i>N<sub>1</sub>N<sub>2</sub></i> -diethylethane-1,2-diamine (CDEDC)	47
3.2.5 Syntheses of <i>N,N'</i> -(oxybis(4,1-phenylene))bis(2,4-dichloro-1,3,5-triazin-6-amine) (CODAC) and <i>N,N'</i> -(methylenebis(4,1-phenylene))bis(2,4-dichloro-1,3,5-triazin-6-amine) (CMDAC)	52
3.3 Synthesis of quaternary multi-ammonium salts derived from 2,4-dichloro-6-substituted-1,3,5-triazine	56
3.3.1 Synthesis of quaternary bis-ammonium salts derived from 2,4-dichloro-6-methoxy-1,3,5-triazine (MMT)	56
3.3.1.1 Synthesis of quaternary bis-ammonium salt of 2,4-dichloro-6-methoxy-1,3,5-triazine in the presence of <i>N</i> -methylmorpholine (MMTMM)	57
3.3.1.2 Synthesis of quaternary bis-ammonium salt of 2,4-dichloro-6-methoxy-1,3,5-triazine in the presence di <i>N</i> -ethylmorpholine	59
3.3.1.3 Synthesis of quaternary bis-ammonium salts of 2,4-dichloro-6-methoxy-1,3,5-triazine in the presence of <i>N</i> -methylpiperidine (MMTMP) and of <i>N</i> -ethylpiperidine (MMTEP)	62
3.3.1.4 Synthesis of quaternary bis-ammonium salt of 2,4-dichloro-6-methoxy-1,3,5-triazine in the presence of <i>N</i> -methylpyrrolidine (MMTMPD)	64
3.3.1.5 Synthesis of quaternary bis-ammonium salts of 2,4-dichloro-6-methoxy-1,3,5-triazine in the presence of trimethylamine (MMTTMA) and triethylamine (MMTTEA)	66
3.3.2 Synthesis of quaternary bis-ammonium salts derived from 2,4-dichloro-6-diisopropylamino-1,3,5-triazine (MIAT)	67
3.3.2.1 Synthesis of quaternary bis-ammonium salts of 2,4-dichloro-6-diisopropylamino-1,3,5-triazine in the presence of <i>N</i> -methylmorpholine (MIATMM) and <i>N</i> -ethylmorpholine (MIATEM)	68
3.3.2.2 Synthesis of quaternary bis-ammonium salts of 2,4-dichloro-6-diisopropylamino-1,3,5-triazine in the presence of <i>N</i> -methylpiperidine (MIATMP) and <i>N</i> -ethylpiperidine (MIATEP)	70
3.3.2.3 Synthesis of quaternary bis-ammonium salt of 2,4-dichloro-6-diisopropylamino-1,3,5-triazine in the presence of <i>N</i> -methylpyrrolidine (MIATMPD)	72
3.3.2.4 Synthesis of quaternary bis-ammonium salt of 2,4-dichloro-6-diisopropylamino-1,3,5-triazine in the presence of <i>N</i> -methylimidazole (MIATMI)	74
3.3.2.5 Synthesis of quaternary bis-ammonium salts of 2,4-dichloro-6-diisopropylamino-1,3,5-triazine in the presence of trimethylamine (MIATTMA) and triethylamine (MIATTEA)	79
3.3.3 Synthesis of quaternary bis-ammonium salts derived from 2,4-dichloro-6-diethylamino-1,3,5-triazine (MEAT)	80
3.3.3.1 Synthesis of quaternary bis-ammonium salts of 2,4-dichloro-6-diethylamino-1,3,5-triazine in the presence of <i>N</i> -methylmorpholine (MEATMM) and <i>N</i> -ethylmorpholine (MEATEM)	81
3.3.3.2 Synthesis of quaternary bis-ammonium salts of 2,4-dichloro-6-diethylamino-1,3,5-triazine in the presence of <i>N</i> -methylpiperidine (MEATMP) and <i>N</i> -ethylpiperidine (MEATEP)	83

3.3.3.3 Study of quaternary bis-ammonium salt of 2,4-dichloro-6-diethylamino-1,3,5-triazine in the presence of <i>N</i> -methylpyrrolidine (MEATMPD)	85
3.3.3.4 Synthesis of quaternary bis-ammonium salts of 2,4-dichloro-6-diethylamino-1,3,5-triazine in the presence of trimethylamine (MEATMA) and triethylamine (MEATTEA)	85
3.3.4 Study of quaternary tetrakis-ammonium salt derived from <i>N</i> <sub>1</sub> , <i>N</i> <sub>2</sub> -bis(2,4-dichloro-1,3,5-triazin-6-yl)- <i>N</i> <sub>1</sub> , <i>N</i> <sub>2</sub> -diethylethane-1,2-diamine in the presence of <i>N</i> -methylmorpholine (MMDEDMM)	87
3.4 Summary table of synthesized agents and their stability in aqueous solution and inert atmosphere	91
3.5 Amidation reactions by use of quaternary bis-ammonium salts	92
3.5.1 Amidation reactions with benzoic acid and phenylethylamine	92
3.5.2 Amidation reactions with dodecanoic acid and phenylethylamine	95
<b>4 – CONCLUSIONS</b>	<b>99</b>
<b>5 – EXPERIMENTAL SECTION</b>	<b>102</b>
5.1 General methods	103
5.2 Synthesis of mono-1,3,5-triazine compounds and their derived ammonium salts	104
5.2.1 Preparation of 2-chloro-4,6-disubstituted-1,3,5-triazine	105
5.2.1.1 Synthesis of 2-chloro-4,6-bis-diisopropylamino-1,3,5-triazine (DIAT)	105
5.2.1.2 Synthesis of 2-chloro-4,6-bis-diethylamino-1,3,5-triazine (DEAT)	106
5.2.1.3 Synthesis of 2-chloro-4-methoxy-6-diisopropylamino-1,3,5-triazine (MAT)	106
5.2.2 Preparation of 2,4-dichloro-6-substituted-1,3,5-triazine	108
5.2.2.1 Synthesis of 2,4-dichloro-6-methoxy-1,3,5-triazine (MMT)	108
5.2.2.2 Synthesis of 2,4-dichloro-6-diisopropylamino-1,3,5-triazine (MIAT) and 2,4-dichloro-6-diethylamino-1,3,5-triazine (MEAT)	108
5.2.3 Preparation of quaternary bis-ammonium salts derived from 2,4-dichloro-6-substituted-1,3,5-triazine	110
5.2.3.1 Synthesis of quaternary bis-ammonium salts derived from 2,4-dichloro-6-methoxy-1,3,5-triazine (MMT)	110
5.2.3.2 Synthesis of quaternary bis-ammonium salts derived from 2,4-dichloro-6-diisopropylamino-1,3,5-triazine (MIAT)	112
5.2.3.3 Synthesis of quaternary bis-ammonium salts derived from 2,4-dichloro-6-diethylamino-1,3,5-triazine (MEAT)	114
5.3 Synthesis of bis-1,3,5-triazine compounds and their derived ammonium salts	116
5.3.1 Preparation of 2,4-disubstituted-6-anilino-bis-1,3,5-triazines with chloro or methoxy groups	117
5.3.1.1 Synthesis of <i>N,N'</i> -(oxybis(4,1-phenylene))bis(2-chloro-4-methoxy-1,3,5-triazin-6-amine) (MODAM) and Synthesis of <i>N,N'</i> -(methylenebis(4,1-phenylene))bis(2-chloro-4-methoxy-1,3,5-triazin-6-amine) (MMDAM)	117
5.3.1.2 Synthesis of <i>N,N'</i> -(oxybis(4,1-phenylene))bis(2,4-dichloro-1,3,5-triazin-6-amine) (CODAC) and <i>N,N'</i> -(methylenebis(4,1-phenylene))bis(2,4-dichloro-1,3,5-triazin-6-amine) (CMDAC)	118
5.3.2 Preparation of 2,4-disubstituted-6-amino-bis-1,3,5-triazine derived from <i>N,N'</i> -diethylethylene diamine	119
5.3.2.1 Synthesis of <i>N</i> <sub>1</sub> , <i>N</i> <sub>2</sub> -bis(2,4-dichloro-1,3,5-triazin-6-yl)- <i>N</i> <sub>1</sub> , <i>N</i> <sub>2</sub> -diethylethane-1,2-diamine (CDEDC)	119
5.3.2.2 Synthesis of <i>N</i> <sub>1</sub> , <i>N</i> <sub>2</sub> -bis(2,4-dimethoxy-1,3,5-triazin-6-yl)- <i>N</i> <sub>1</sub> , <i>N</i> <sub>2</sub> -diethylethane-1,2-diamine (DDEDD)	120
5.3.3 Study of quaternary tetrakis-ammonium salt derived from <i>N</i> <sub>1</sub> , <i>N</i> <sub>2</sub> -bis(2,4-dichloro-1,3,5-triazin-6-yl)- <i>N</i> <sub>1</sub> , <i>N</i> <sub>2</sub> -diethylethane-1,2-diamine in the presence of <i>N</i> -methylmorpholine (MMDEDMM)	121
5.4 Application of amidation agents in condensation reactions	122
5.4.1 Isolation of <i>N</i> -phenylethyl-benzamide	122
5.4.2 Isolation of <i>N</i> -phenylethyl-dodecanamide	122
5.4.3 Synthesis of an amide in the presence of quaternary ammonium salts with <i>IPP</i> protocol	123
5.4.4 Synthesis of an amide in the presence of quaternary ammonium salts with <i>in situ</i> protocol	123
<b>6 – ATTACHMENT</b>	<b>124</b>
6.1 Calibration line for synthesis of <i>N</i> -phenylethyl-benzamide	125
6.2 Calibration line for synthesis of <i>N</i> -phenylethyl-dodecanamide	126
<b>COLLAGEN CROSS-LINKING</b>	<b>128</b>
<b>7 – INTRODUCTION</b>	<b>129</b>
7.1 Collagen	130
7.1.1 Structure of collagen	130
7.1.2 Role of water in collagen	131

7.1.3 Denaturation process of collagen	132
7.2 Chemical cross-linking of collagen	133
7.2.1 Mineral cross-linking agents	135
7.2.2 Vegetable and aldehydic cross-linking agents	135
7.2.3 Zero-length cross-linking agents	135
<b>8 - SCOPE OF THE WORK</b>	<b>137</b>
<b>9 – RESULTS AND DISCUSSION</b>	<b>139</b>
9.1 Optimization of cross-linking process with 1,3,5-triazine salts	141
9.2 Collagen cross-linking with 1,3,5-triazine quaternary bis-ammonium salts	143
<b>10 – CONCLUSIONS</b>	<b>146</b>
<b>11 – EXPERIMENTAL SECTION</b>	<b>148</b>
11.1 General methods	149
11.2 Synthesis and characterization	150
11.2.1 Preparation of 1,3,5-triazine precursors and quaternary ammonium salts	150
11.2.1.1 Synthesis of 2-chloro-4,6-dimethoxy-1,3,5-triazine (CDMT)	150
11.2.1.2 Synthesis of 4-(4,6-dimethoxy-1,3,5-triazin-2-yl)-4-methylmorpholinium chloride (DMTMM)	151
11.2.2 Collagen cross-linking with 1,3,5-triazine quaternary ammonium salts	151
11.2.2.1 Collagen cross-linking in the presence of quaternary ammonium salts with <i>IPP</i> protocol	151
11.2.2.2 Collagen cross-linking in the presence of quaternary ammonium salts with <i>in situ</i> protocol	152
11.2.2.3 Collagen cross-linking in tanning process with DMTMM	152
11.2.3 Shrinkage temperature characterization	152
<b>POLYMER GRAFTING</b>	<b>153</b>
<b>12 – INTRODUCTION</b>	<b>154</b>
12.1 Polymers Modification	155
12.1.1 Polymers blends	155
12.1.2 Curing process	155
12.2 Polymer grafting	156
12.2.1 Free radical grafting and reactive extrusion (REX)	157
12.2.1.1 Polypropylene reactive extrusion	157
12.2.1.2 Polylactic acid reactive extrusion	159
12.2.2 Grafting by use of amidation agents	161
<b>13 – SCOPE OF THE WORK</b>	<b>163</b>
<b>14 – RESULTS AND DISCUSSION</b>	<b>165</b>
14.1 Grafting by reactive extrusion (REX)	166
14.1.1 REX grafting of polypropylene	169
14.1.1.1 Polypropylene- <i>grafted</i> -fumaric acid (PP- <i>g</i> -FMA)	169
14.1.1.2 Polypropylene- <i>grafted</i> -linoleic acid (PP- <i>g</i> -LNA)	174
14.1.2 REX grafting of polylactic acid	178
14.1.2.1 Polylactic acid- <i>grafted</i> -fumaric acid (PLA- <i>g</i> -FMA)	179
14.1.2.2 Polylactic acid- <i>grafted</i> -linoleic acid (PLA- <i>g</i> -LNA)	184
14.2 Surface grafting by use of 4-(4,6-dimethoxy-1,3,5-triazin-2-yl)-4-methylmorpholinium chloride (DMTMM)	187
<b>15 – CONCLUSIONS</b>	<b>193</b>
<b>16 – EXPERIMENTAL SECTION</b>	<b>195</b>
16.1 General methods	196
16.2 Reactive extrusion processes and characterizations	197
16.2.1 Reactive extrusion of polypropylene (PP)	198
16.2.1.1 Synthesis of polypropylene- <i>grafted</i> -fumaric acid (PP- <i>g</i> -FMA)	198
16.2.1.2 Synthesis of polypropylene- <i>grafted</i> -linoleic acid (PP- <i>g</i> -LNA)	199
16.2.1.3 Synthesis of polypropylene- <i>grafted</i> -maleic anhydride (PP- <i>g</i> -MA)	200
16.2.2 Reactive extrusion of polylactic acid (PLA)	201
16.2.2.1 Synthesis of polylactic acid- <i>grafted</i> -fumaric acid (PLA- <i>g</i> -FMA)	201
16.2.2.2 Synthesis of polylactic acid- <i>grafted</i> -linoleic acid (PLA- <i>g</i> -LNA)	202
16.3 Synthesis of 2-chloro-4,6-dimethoxy-1,3,5-triazine (CDMT) and 4-(4,6-dimethoxy-1,3,5-triazin-2-yl)-4-methylmorpholinium chloride (DMTMM)	203
16.4 Surface grafting treatment with DMTMM	204
16.5 Contact angle characterization	205
<b>17 – REFERENCES</b>	<b>206</b>

**STUDY OF AMIDATION AGENTS**

**SYNTHESIS OF AMIDATION AGENTS AND  
THEIR REACTIVITY IN COUPLING REACTIONS**



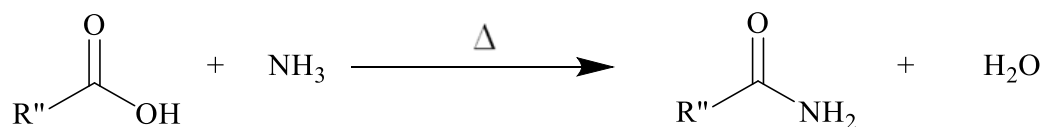
## **CHAPTER 1**

### **INTRODUCTION**

### **SYNTHESIS OF AMIDATION AGENTS AND THEIR REACTIVITY IN COUPLING REACTIONS**

## 1.1 Importance of amides synthesis reactions

The synthesis of amides is nowadays of great importance since these compounds are widely used in many industrial sectors for the production of drugs, biomaterials, polypeptides, etc.<sup>[1,2]</sup>. One of the historically known methods for the synthesis of amides, reported by Mitchell *et al.*,<sup>[3]</sup> consists in the direct reaction between an aliphatic carboxylic acid and ammonia at high temperature (at least 160-180 °C). Water distillation in steam streaming, carried out during the process, allows to push reaction balance to the products, favouring amide formation with high yields. (**Scheme 1.1**).



**Scheme 1.1:** Carboxylic acids activation promoted by heat.

This method involves some advantages:<sup>[4]</sup>

- Easy and economic protocol application;
- Short reaction times;
- Possibility to carry out the reaction in absence of catalyst or solvent;

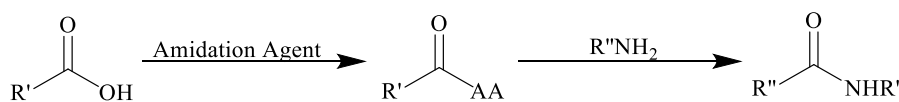
Nevertheless, some disadvantages are present:

- The reaction is limited only to thermostable reagents or products;
- Reagents should be melt at the operative temperatures in order to grant homogenous phases in the reaction conditions;
- Low-boiling or sublimable substances may be lost at high temperature from the reaction environment.

This method is applicable only for compounds resistant to high temperatures. Condensation agents have been developed to activate carboxylic acids towards amidation reaction under mild conditions.<sup>[4]</sup>

## 1.2 Condensation reaction activators

Condensation activators are agents that promote formation of amides under mild conditions. As example, the general process of a condensation reaction activated by an amidation agent (AA) is reported below. (**Scheme 1.2**)



**Scheme 1.2:** General process of an amidation reaction activated by a condensation agent.

Moreover, these compounds are reported to be able to activate carboxylic acid also towards ester, thioester and anhydrides and their use allows to protect other functionalizations eventually present in the molecule from thermal decomposition.<sup>[5,6]</sup>

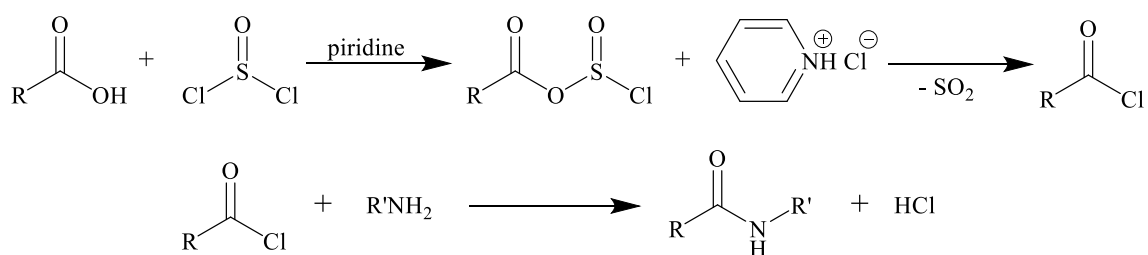
In literature many of these compounds are known and divided in many different families:<sup>[5]</sup>

- Acyl chlorides;
- Acyl azides;
- 1-hydroxybenzotriazole derivatives, uronium and phosphonium salts;
- Carbodimides;
- Triazine derivatives.

### 1.3 Acyl chlorides

One of the first methods to activate a carboxylic groups is the conversion into an acyl chloride.<sup>[5]</sup>

(Scheme 1.3)



**Scheme 1.3:** Carboxylic acid activation by acyl chloride.

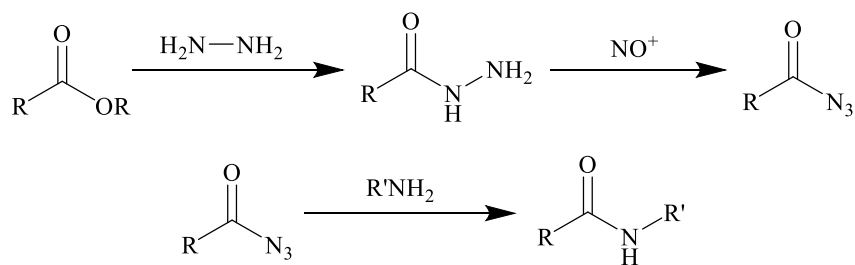
The acyl chloride can be obtained by reaction between the carboxylic acid and a chlorinating agent, typically thionyl chloride, in the presence of a weak non nucleophilic base. Therefore, the desired amide is obtained by reaction with an amine, usually in an anhydrous solvent.

This activation process presents many issues:

- Thionyl chloride is dangerous by contact or inhalation;
- The main byproduct of the reaction is sulfur dioxide, a toxic and pollutant compound;
- HCl formation may lead to subreaction with acid sensitive substrates.

### 1.4 Acyl azides

The activation of carboxylic groups using acyl azides, known since long time in literature,<sup>[7]</sup> provides four distinct steps.<sup>[5,8]</sup> (Scheme 1.4)



**Scheme 1.4:** Carboxylic acid activation by acyl azides.

The steps are carried out as reported below:

1. Conversion of carboxylic acid to the corresponding methyl, ethyl or benzyl ester;
2. Reaction between the ester and an excess of hydrazine carried out in alcohol solution at *r.t.* for the synthesis of hydrazide, later isolated by solvent evaporation and purified;
3. Conversion of the hydrazide to acylazide by nitrosation with sodium nitrite in acetic acid and HCl. This step must be carried out at a low temperature to avoid the decomposition of the product with consequent release of N<sub>2</sub>;
4. The acylazide is finally extracted with organic solvent and reacted with an amine to obtain the desired amide.

The esters of many carboxylic acid are commercially available. Nevertheless, their use for amide synthesis is not common, due to the slow reaction between the azide and the amine. Moreover, the acylazides may decompose at higher temperature or undergo rearrangement processes into alkylisocyanate.<sup>[2]</sup>

### 1.5 1-hydroxybenzotriazole derivatives, uronium and phosphonium salts

In literature, 1-hydroxybenzotriazole (HOBt) and 1-hydroxy-7-azabenzotriazole (HOAt), are widely known and used as activators agents, generally for peptide synthesis.<sup>[9]</sup> (**Figure 1.1**)



**Figure 1.1:** Chemical formula of 1-hydroxybenzotriazole (HOBt) and 1-hydroxy-7-azabenzotriazole (HOAt).

Also phosphonium and uronium salts are derivatives of HOBt and HOAt known as amidation agents.<sup>[9]</sup> Among the most used uronium salts, hexafluorophosphate azabenzotriazole tetramethyl uronium (HATU) and hexafluorophosphate benzotriazole tetramethyl uronium (HBTU) are of particular relevance.<sup>[2]</sup> Nevertheless, this compounds may lead to the formation of potentially toxic

guanidine byproducts.<sup>[10]</sup> The use of phosphonium salts do not present this disadvantage and among these are worthy of mention (benzotriazol-1-yloxy)tris(dimethylamino)-phosphonium hexafluorophosphate (BOP) and (benzotriazol-1-yloxy)-tripyrrolidino-phosphonium hexafluorophosphate (PyBOP).<sup>[5]</sup> HOBt and its derivatives are explosive,<sup>[11]</sup> therefore, the development of safer activating agents has led to the synthesis of (1-cyano-2-ethoxy-2-oxoethylideneaminoxy)dimethylamino-morpholino-carbenium hexafluorophosphate (COMU).<sup>[12]</sup> Finally, the structures of the most important 1-hydroxybenzotriazole derivatives and of COMU are reported below. (**Figure 1.2**)

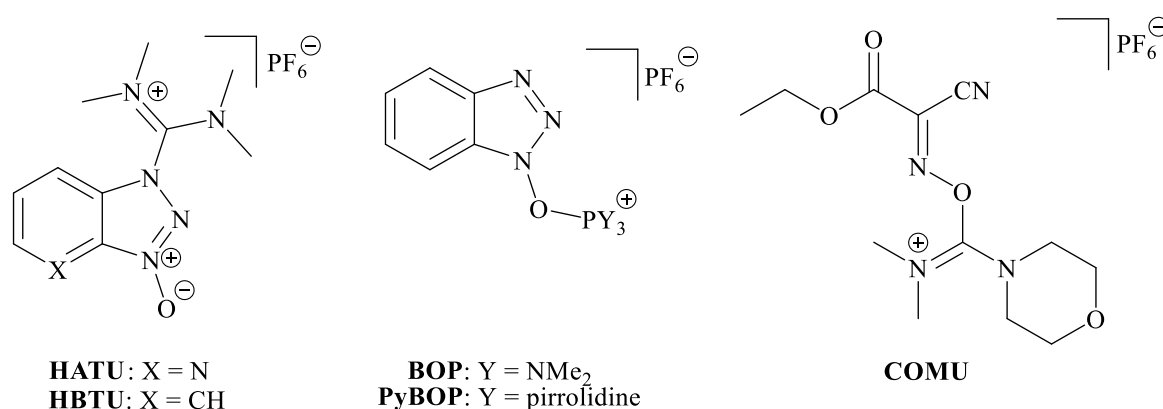
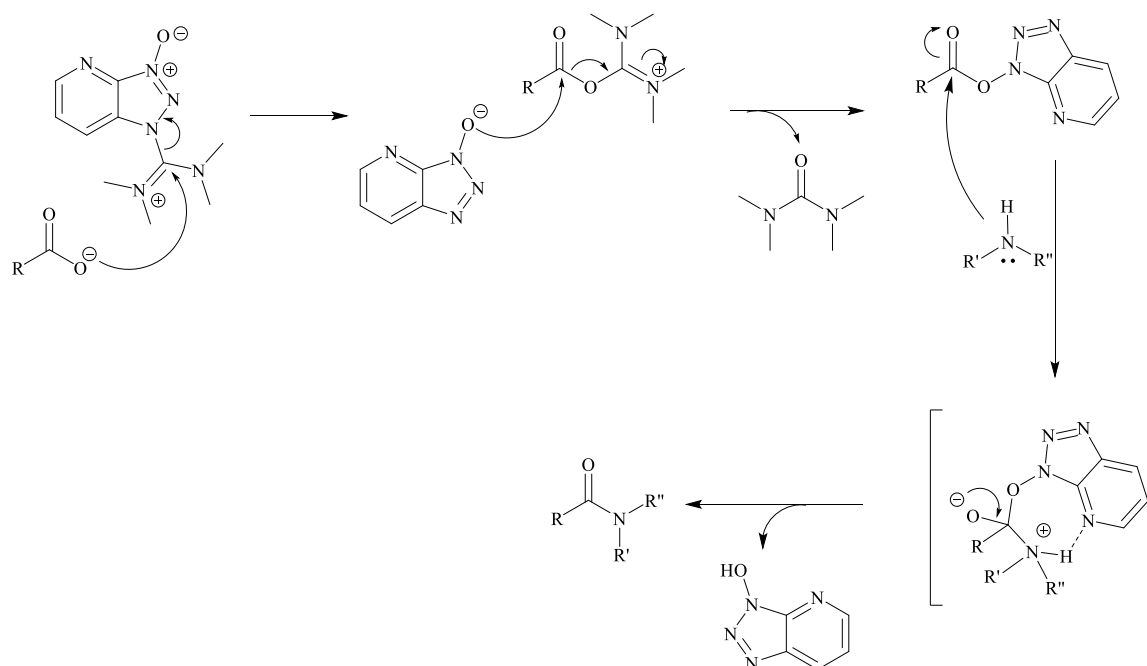


**Figure 1.2:** Chemical formulas of 1-hydroxybenzotriazole derivatives and COMU.

Uronium and phosphonium salts activate carboxylic acids with the same reaction mechanism. As example, the amidation reaction in presence of HATU is reported below. (**Scheme 1.5**)



**Scheme 1.5:** Amidation mechanism of a carboxylic acids in presence of hexafluorophosphate azabenzotriazole tetramethyl uronium (HATU).

## 1.6 Carbodiimides

Another class of activators traditionally used in the synthesis of amide bonds are carbodiimides.<sup>[5]</sup> Among these activators dicyclohexylcarbodiimide (DCC), known since 1955,<sup>[13]</sup> is of particular relevance and used for amidation reaction in organic solvent. (**Figure 1.3**)

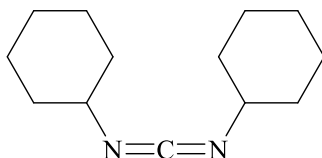
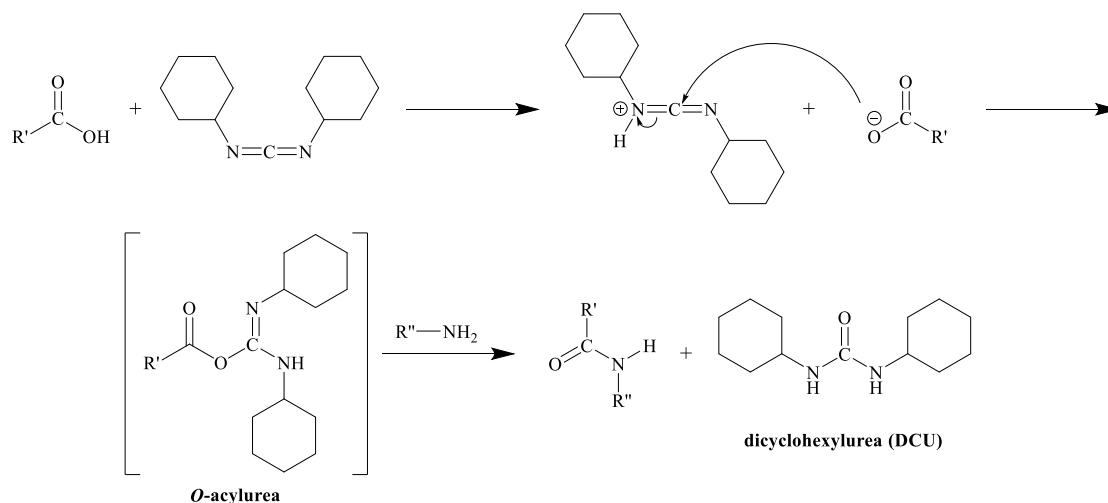


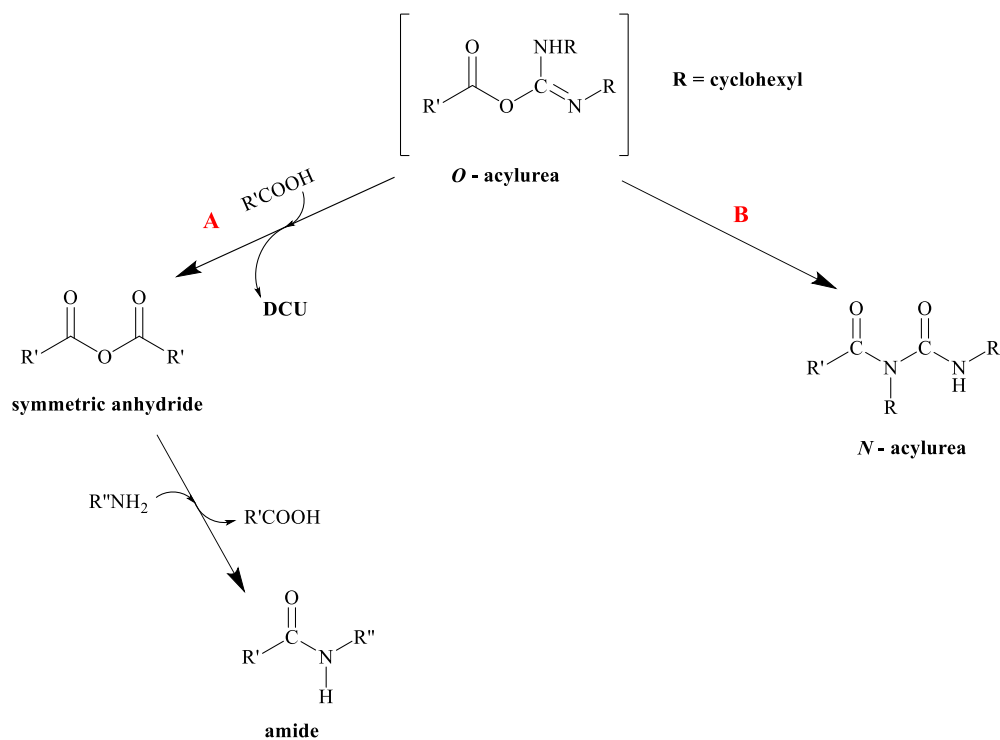
**Figure 1.3:** Chemical formula of dicyclohexylcarbodiimide (DCC).

The reaction of carboxylic acids activated by carbodiimides for synthesis of amides is reported below, using DCC as example. (**Scheme 1.6**)



**Scheme 1.6:** Amidation reaction of carboxylic acids activated by dicyclohexylcarbodiimide (DCC).

In the reaction mechanism reported above (**Scheme 1.6**), DCC is protonated and undergoes nucleophilic attack by carboxylate group, with the formation of *O*-acylurea. This intermediate reacts with the amine, leading to the formation of the desired amide and dicyclohexylurea (DCU) as a byproduct. *O*-acylurea is a very reactive species and may undergo two other possible reactions, reported below. (**Scheme 1.7**)



**Scheme 1.7:** Possible secondary reactions of *O*-acylurea.

In the presence of an excess of carboxylic acid (**Scheme 1.7, route A**), *O*-acylurea can undergo protonation on the second nitrogen atom with the formation of a symmetrical anhydride and DCU. However, symmetrical anhydrides present a very low reactivity with amines.<sup>[14]</sup>

A second possible reaction (**Scheme 1.7, route B**) is an intramolecular rearrangement of *O*-acylurea to *N*-acylurea, a stable and inert compound. This undesired reaction, that occurs in solvent such as *N,N*-dimethylformamide or dichloromethane, leads to a decrease in yield as it involves use of carboxylic acid and activation agent without the formation of the desired amide.<sup>[5]</sup>

Moreover, the application of DCC as amidation agent presents some drawbacks:

- 1) use limited to organic solvents.
- 2) Dicyclohexylurea (DCU) is a toxic byproduct
- 3) DCU removal is complicated, byproduct traces are still present even after chromatographic separation.<sup>[5]</sup>

*N*-(3-dimethylaminopropyl)-*N'*-ethylcarbodiimide (EDC) is an atoxic watersoluble carbodiimide developed in 1961.<sup>[15]</sup> (**Figure 1.4**)

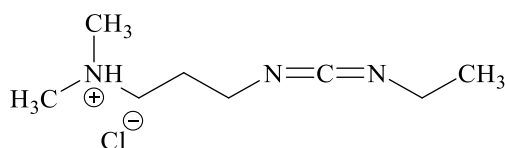


**Figure 1.4:** Chemical structure of *N*-(3-dimethylaminopropyl)-*N'*-ethylcarbodiimide (EDC).

Nowadays, this carbodiimide is widely used in condensation reactions between an amine and a carboxylic acid thanks to the watersolubility of both EDC and its urea byproduct, that is consequently easily separable.<sup>[5]</sup> EDC follows the same activation mechanism for carboxylic acids of DCC (**Scheme 1.6**), but its application presents some issues:<sup>[16]</sup>

- *O*-acylurea is easily hydrolyzable and it is formed at acid pH (4-5). In this pH range, the amine are in their protonated forms with a consequent lose in reactivity and a decrease in final yield,<sup>[14]</sup>
- EDC is ten times more expensive than DCCit requires to be preserved;
- EDC is thermally unstable and need to be stored at -20 °C.

Even if *N*-(3-dimethylaminopropyl)-*N'*-ethylcarbodiimide (EDC) may be used as condensation agent, usually it is used with stoichiometric (or higher) quantity of *N*-hydroxysuccinimide (NHS). (**Figure 1.5**)

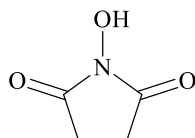
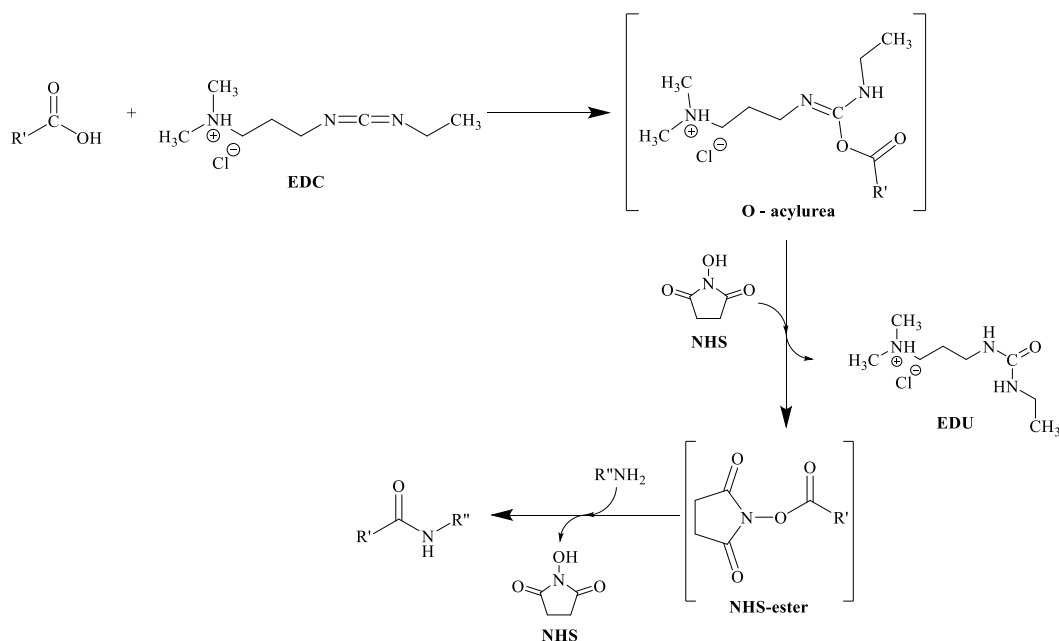


**Figure 1.5:** Chemical formula of *N*-hydroxysuccinimide (NHS).

Application of NHS additive prevents the rearrangement to *N*-acylurea and leads to an increase in amidation yield.<sup>[17]</sup> The mechanism of EDC/NHS for carboxylic acids activation is reported below.

(**Scheme 1.8**)



**Scheme 1.8:** Carboxylic acids activation by EDC/NHS .

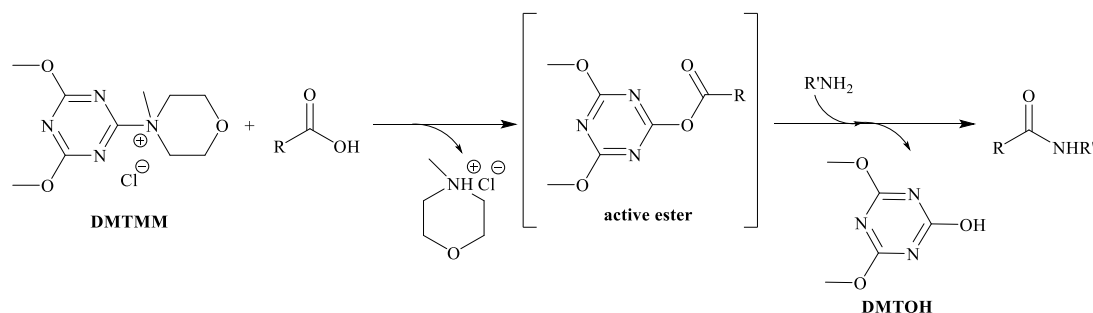


The reaction between carboxylic acid and EDC leads to the intermediate *O*-acylurea. This later undergoes nucleophilic attack by NHS leading to the formation of 1-ethyl-3-(3-dimethylammonium propyl)urea chloride (EDU) and NHS-ester, an intermediate stable to hydrolysis in aqueous solution. Finally, NHS-ester reacts with the amine and the desired amide is formed.

## 1.7 Triazine derivatives as amidation agents

Quaternary ammonium salts of 2-chloro-4,6-dimethoxy-1,3,5-triazine (CDMT) are known as efficient activators for amide synthesis and are a valid alternative to carbodiimides.<sup>[18-20]</sup>

In particular, Kunishima *et al.* report a mechanism for condensation reaction between an amine and a carboxylic acid in presence of 4-(4,6-dimethoxy-1,3,5-triazin-2-yl)-4-methylmorpholinium chloride (DMTMM).<sup>[21]</sup> (**Scheme 1.9**)



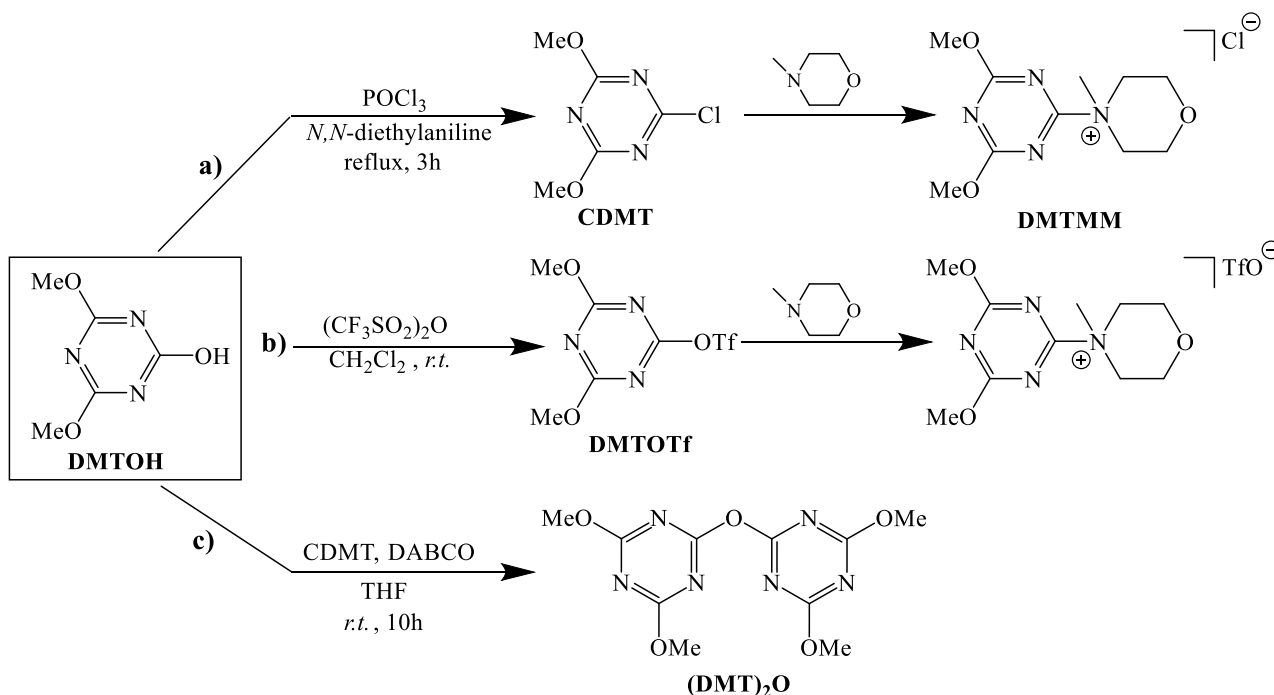
**Scheme 1.9:** Amidation mechanism of carboxylic acids in presence of 4-(4,6-dimethoxy-1,3,5-triazin-2-yl)-4-methylmorpholinium chloride (DMTMM).

The activation mechanism provides the nucleophilic substitution of the carboxylate group to the triazine ring. This leads to the formation of a first byproduct, *N*-methylmorpholinium chloride, and an intermediate called "active ester".<sup>[20]</sup> Triazine electronic withdraw effect activates the carbonyl group to the nucleophilic substitution by the amine leading to the formation of the desired amide and a second byproduct, 2-hydroxy-4,6-dimethoxy-1,3,5-triazine (DMTOH).<sup>[22]</sup>

Both Kunishima and Jastrzabek report that DMTOH is easily separable and recyclable in new activation agents.<sup>[23,24]</sup> Kunishima proposes a treatment for DMTOH with  $\text{POCl}_3$ , to restore CDMT, or with triflic anhydride, to synthesize 2-trifluoromethylsulfonyl-4,6-dimethoxy-1,3,5-triazine (DMTOTf). These are later reacted with *N*-methylmorpholine to synthesize active triazine *N*-methylmorpholinium salts respectively with a chloride (DMTMM) or a triflate as counterions.<sup>[23]</sup> (**Scheme 1.10, route a and b**)

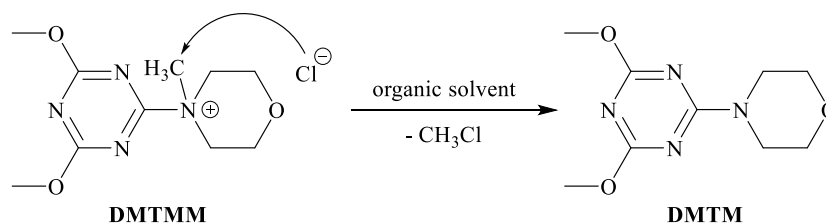
Jastrzabek suggests to react fresh CDMT with DMTOH in presence of 1,4-diazabicyclo[2.2.2]-

octane (DABCO) in order to synthesize bis(4,6-dimethoxy-1,3,5-triazin-2-yl)ether [(DMT)<sub>2</sub>O]. Even if fresh CDMT is required for the synthesis, (DMT)<sub>2</sub>O is reported to display good potential for coupling of lipophilic substrates, due to his non ionic nature.<sup>[24]</sup> (**Scheme 1.10, route c**)



**Scheme 1.10:** Recyclability of DMTOH in new activation agents.

DMTMM is active in a 5-8 pH range and allows to conduct amidation reactions in water and alcohols but also in some organic solvents. Kunishima and Kaminski report that, under anhydrous conditions or under heating, quaternary ammonium chloride salts are prone to dealkylation in a process analogous to the Von Braun reaction.<sup>[19,20,25-27]</sup> (**Scheme 1.11**)



**Scheme 1.11:** decomposition mechanism of DMTMM by demethylation in organic solvent.

When DMTMM is solubilized in solvents like dichloromethane, chloroform and acetonitrile, the chloride nucleophilic attack to morpholinium methyl group is particularly favoured. This reaction leads the formation of chloromethane and of 4-(4,6-dimethoxy-1,3,5-triazin-2-yl)-morpholine (DMTM), which presents no reactivity as activator in amidation reactions.

Kunishima *et al.* report DMTMM complete decomposition after 3 hours in CH<sub>2</sub>Cl<sub>2</sub> or DMSO and after 18 hours in THF.<sup>[19]</sup> Instead, Rydergren reports an higher resistance to decomposition in polar

solvents like water or alcohols (ca. 50% decomposition in 50 h at 35 °C, ca. 89% after 48 hours at 50 °C).<sup>[28]</sup>

In order to reduce demethylation processes, Kaminski reported the possibility to synthesize the ammonium salt directly in reaction environment, with a process called “*in situ*”: CDMT and *N*-methylmorpholine are reacted in presence of a carboxylic acid and DMTMM acts as an intermediate. [29]

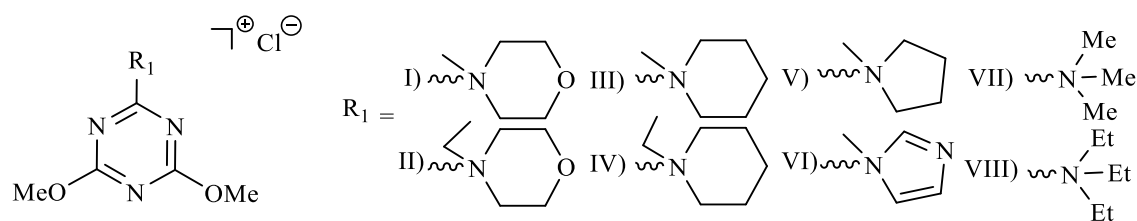
The nucleophilic nature of DMTMM counterion has been recognized as a cause of demethylation processes and  $\text{BF}_4^-$  or  $\text{ClO}_4^-$  are alternatives to chloride anion commonly used.<sup>[21,30]</sup>

Recently, Kolesinska *et al.* investigated the substitution of DMTMM counterion with less nucleophilic anions, such as camphorsulfonate ( $\text{CsO}^-$ ), methanesulfonate ( $\text{MsO}^-$ ), trifluoromethane sulfonate ( $\text{TfO}^-$ ) and toluenesulfonate ( $\text{TsO}^-$ ). The latter has been identified as the species that grants the best stability to the salt.<sup>[22,31]</sup>

Many studies reports that it is possible to increase the reactivity of DMTMM by modification of the triazine substituents. First studies by Kaminski *et al.* focused on the substitution of methoxy group with phenoxy, cycloalkoxy or long chain alkoxy substituents.<sup>[29,32]</sup> Recently, Kunishima and Kitamura reported substitution of one methoxy moiety with an amido or imido substituent, achieving an increased reactivity for amide reactions.<sup>[33,34]</sup>

Finally, Kunishima *et al.* proposed the substitution of *N*-methylmorpholine with other tertiary amines, reporting a "library" of compounds similar to DMTMM with different ammonium moieties.

<sup>[21]</sup> (Scheme 1.12)



**Scheme 1.12:** examples of compounds similar to DMTMM with different ammonium moieties.

The amidation agent reported in literature, can activate only one carboxylic group for each molecule, before being turned into its byproducts. To the best of our knowledge, no study has been reported regarding the synthesis and use of amidation agents able to activate more than one carboxylic acid at time. One possible exception is proposed by Kaminski, who reports that *in situ* process may be used to trigger activation of two carboxylic groups by application of 2,4-dichloro-6-methoxy-1,3,5-triazine. Nevertheless, no triazine multi-ammonium salt isolation is reported.<sup>[29]</sup>

Hence, triazine multi-ammonium salts are unexploited amidation agents that may enhance reactivity, leading to the reduction of activators used for coupling reactions.

## **CHAPTER 2**

### **SCOPE OF THE WORK**

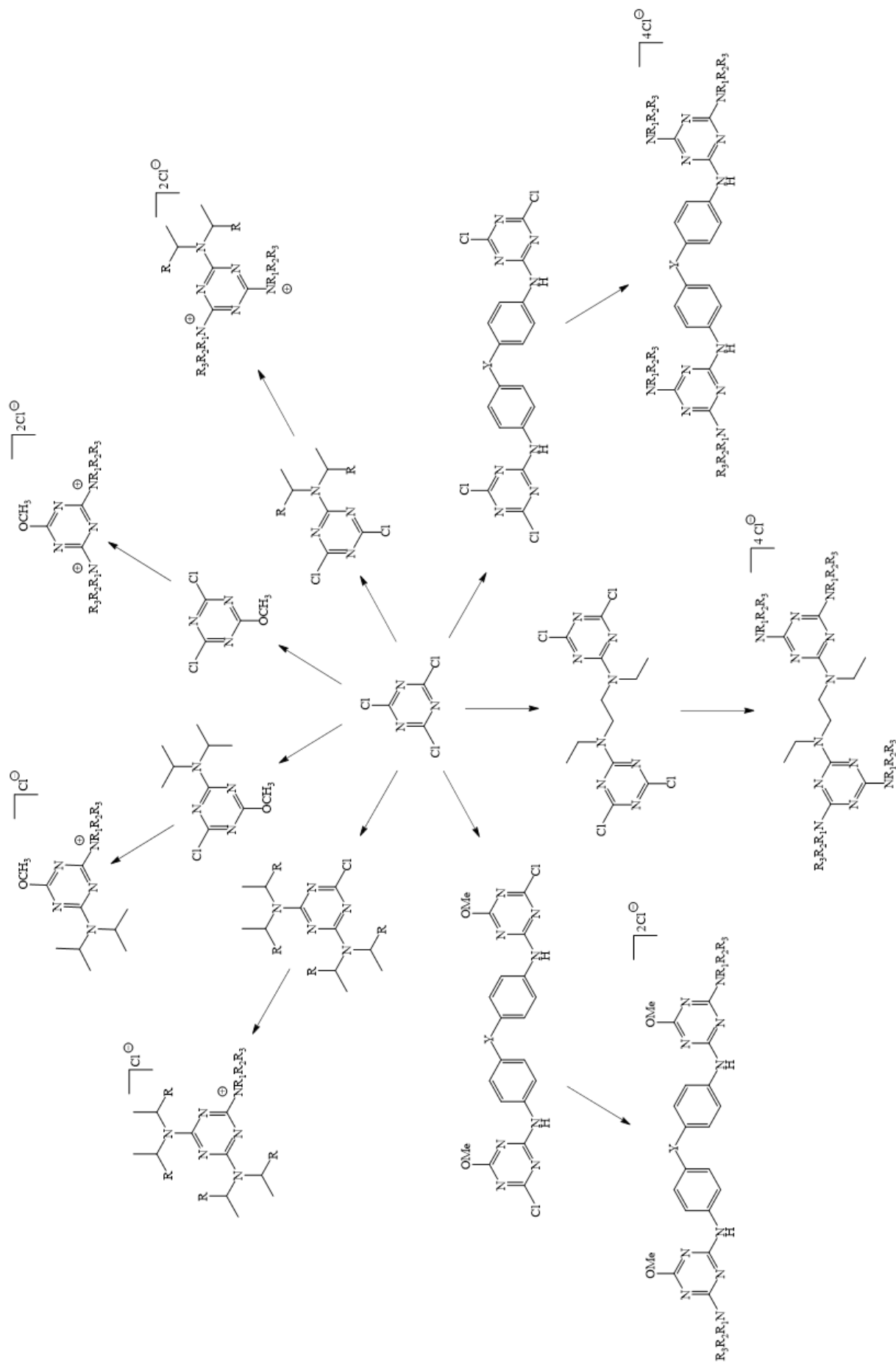
### **SYNTHESIS OF AMIDATION AGENTS AND THEIR REACTIVITY IN COUPLING REACTIONS**

The scope of this part of PhD thesis is the development of a new library of 1,3,5-triazine-based compounds. Specifically, the research will focus on the syntheses of quaternary ammonium salts derivated from 2-chloro-4,6-disubstituted-1,3,5-triazines and 2,4-dichloro-6-substituted-1,3,5-triazines as well as their activity as amidation agents. (**Scheme 2.1**)

Thanks to the knowledge acquired by the research group where this work has been carried out, the development of a new class of quaternary mono-, bis- and tetrakis-ammonium salts was investigated. The results obtained in this work will be compared in order to identify the most stable products and to evaluate, when possible, the steric and electronic characteristics that promote the formation of highly reactive ammonium salts.

The triazine quaternary ammonium salts will be tested in the reaction between aromatic or aliphatic carboxylic acids and phenylethylamine to evaluate their reactivity as amidation agents.

Moreover, two different protocols will be compared by application of preformed quaternary ammonium salts (“*isolated product procedure*”, *IPP*) or by formation of the active species “*in situ*” starting from chloro-triazines and a tertiary amine. Indeed, as reported in literature,<sup>[29]</sup> chloro-1,3,5-triazines in the presence of tertiary amine may activate carboxylic groups towards amidation reaction as well. This protocol is of particular interest because it allows a cost reduction for application in industrial sector thanks to a reduced number of synthesis steps.

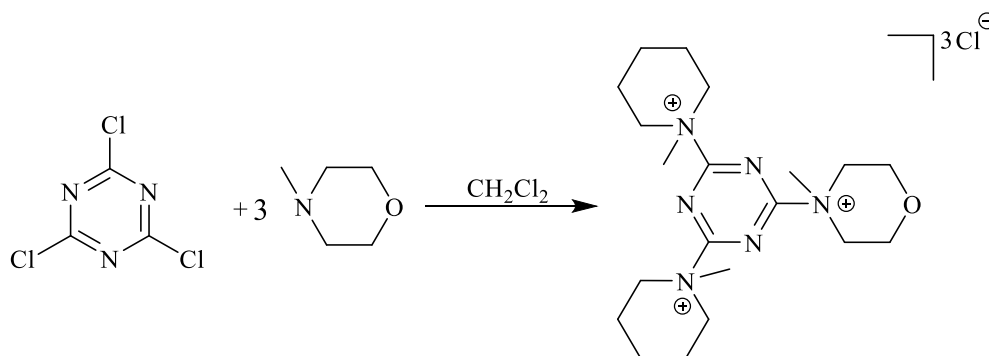


**Scheme 2.1:** Syntheses of quaternary ammonium salts derived from new 2-chloro-4,6-disubstituted-1,3,5-triazines and 2,4-dichloro-6-substituted-1,3,5-triazines.

## **CHAPTER 3**

### **RESULTS AND DISCUSSION SYNTHESIS OF AMIDATION AGENTS AND THEIR REACTIVITY IN COUPLING REACTIONS**

Condensation agents reported in literature, such as 4-(4,6-dimethoxy-1,3,5-triazin-2-yl)-4-methylmorpholinium chloride (DMTMM), are capable to activate no more than one carboxylic group for each molecule. The presence of two or more ammonium moieties on the triazine ring may improve their performances, leading to the reduction of activators needed for amidation reactions. A study by Azarifar *et al.* reports the synthesis of a triazine tris-ammonium salt [2,4,6-tris-(4-methylmorpholinium)-1,3,5-triazine trichloride (TMMT)] by the direct reaction between cyanuric chloride and *N*-methylmorpholine in CH<sub>2</sub>Cl<sub>2</sub>.<sup>[35]</sup> (**Scheme 3.1**)



**Scheme 3.1:** Synthesis of 2,4,6-tris-(4-methylmorpholinium)-1,3,5-triazine trichloride (TMMT).

The reactivity of TMMT in condensation reactions is not reported. Nevertheless, use of dichloromethane as solvent is in disagreement with what reported by Kunishima *et al.* about demethylation of ammonium salts (**Chapter 1.7**).<sup>[19,20]</sup> Experimental data, carried out on first attempts to synthesis multi-ammonium salts directly from cyanuric chloride, led to results in agreement with Kunishima's study. Indeed, a mixture of triazines substituted by a combination of *N*-methylmorpholinium and demethylated morpholine has been obtained. Similar results have been achieved using different solvents such as acetone and THF. This behaviour may be attributable to high reactivity of cyanuric chloride, that does not allow to control properly the reaction, even when carried out at low temperature.

Compared to cyanuric chloride, dichloro- or monochloro-substituted triazines have proven to be better reagents generally leading to the synthesis of non-dealkylated compounds. For this reason, no ammonium salts, directly derived from cyanuric chloride, have been further studied.

The research of this thesis investigated the synthesis and characterization of multi-ammonium salts and their precursors, in addition to their performances as activators of amidation reactions.

In the first part (**Chapter 3.1**), the synthesis of new 2-chloro-4,6-disubstituted-1,3,5-triazines has been studied. These compounds have a structure similar to 2-chloro-4,6-dimethoxy-1,3,5-triazine (CDMT), but present different substituent groups in positions 4 and 6. Moreover, another class of compounds bearing two triazine rings, bridged by a diamino or dianilino moieties, is also reported.



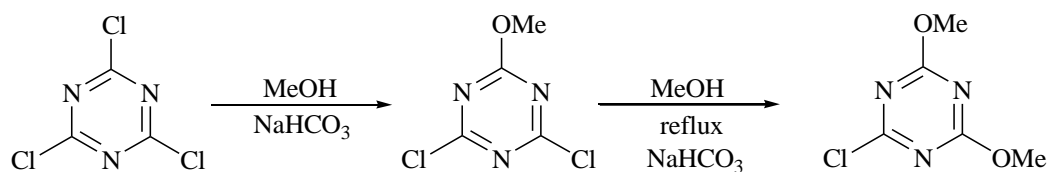
In the second part (**Chapter 3.2**), syntheses of 2,4-dichloro-6-substituted-1,3,5-triazines, as well as 2,4-dichloro-bis-1,3,5-triazines, have been investigated. These compounds are precursors for the synthesis of multi-ammonium quaternary salts.

In the third part (**Chapter 3.3**), syntheses and characterizations of triazine multi-ammonium salts have been studied.

Finally, the fourth part (**Chapter 3.4**) focuses on the reactivity of triazine multi-ammonium salts in amidation reactions of different substrates.

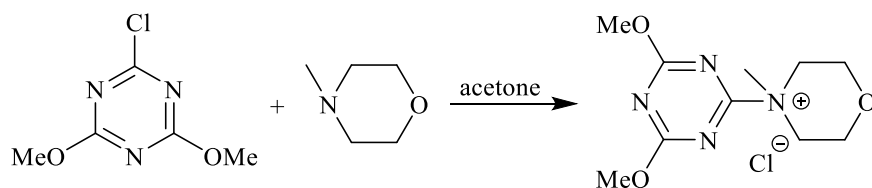
### 3.1 Synthesis of 2-chloro-4,6-disubstituted-1,3,5-triazines

In literature, the synthesis of quaternary ammonium salts obtained by the reaction between 2-chloro-4,6-dimethoxy-1,3,5-triazine (CDMT) and a tertiary amine is reported.<sup>[21]</sup> CDMT is synthesized from cyanuric chloride (CC) in methanol and in the presence of a base. The first substitution by a methoxy group is carried out at room temperature, while the second needs reflux in order to be achieved.<sup>[29]</sup> (**Scheme 3.2**)



**Scheme 3.2:** Synthesis of 2-chloro-4,6-dimethoxy-1,3,5-triazine (CDMT).

The reaction between CDMT and *N*-methylmorpholine, carried out at room temperature, leads to the synthesis of 4-(4,6-dimethoxy-1,3,5-triazin-2-yl)-4-methylmorpholinium chloride (DMTMM).<sup>[32]</sup> (**Scheme 3.3**)



**Scheme 3.3:** Synthesis of 4-(4,6-dimethoxy-1,3,5-triazin-2-yl)-4-methylmorpholinium chloride (DMTMM).

This quaternary ammonium salt is widely employed as condensing agent in the reactions between carboxylic acids and amines for the formation of the corresponding amides.<sup>[19]</sup> Moreover, as reported by Kunishima *et al.*, it is possible to create a "library" of compounds similar to DMTMM by the reaction of CDMT and different tertiary amines.<sup>[21]</sup>

Studies have revealed that, under anhydrous conditions or under heating, quaternary ammonium chloride salts are prone to dealkylation in a process analogous to the Von Braun reaction.<sup>[20,25-27]</sup>

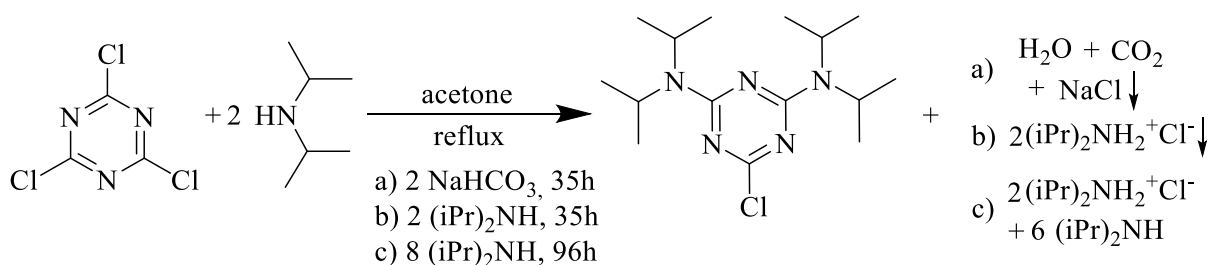
For example, demethylation of DMTMM leads to the formation of methyl chloride and 2-(morphol-4-yl)-4,6-dimethoxy-1,3,5-triazine, inactive as amidation agent. Thus, in this work, synthesis and application of quaternary ammonium salts have been carried out at *r.t.* and in solvents such as water, alcohols or acetone in order to avoid dealkylation processes.

Below, the results obtained for the synthesis of 2-chloro-4,6-diisopropylamino-1,3,5-triazine (DIAT) and 2-chloro-4,6-diethylamino-1,3,5-triazine (DEAT) are reported. Moreover, triazine compounds with an alkoxy and an amino group have been synthesized, such as 2-chloro-4-methoxy-6-diisopropylamino-1,3,5-triazine (MAT).

Another class of compounds bearing two triazine rings is also reported: *N,N'*-(oxybis(4,1-phenylene))bis(2-chloro-4-methoxy-1,3,5-triazin-6-amine) (MODAM) and *N,N'*-(methylenebis(4,1-phenylene))bis(2-chloro-4-methoxy-1,3,5-triazin-6-amine) (MMDAM).

### 3.1.1 Synthesis of 2-chloro-4,6-bis-diisopropylamino-1,3,5-triazine (DIAT)

In a study by Katritzky *et al.*,<sup>[36]</sup> a synthesis of DIAT is proposed by reacting cyanuric chloride with neat diisopropylamine under reflux for 8 hours in acetone. The reaction reported requests a very large excess of diisopropylamine. Thus, a similar protocol to the one used for synthesis of CDMT has been investigated, using an inorganic base in heterogeneous phase. (**Scheme 3.4**).



**Scheme 3.4:** Synthesis of 2-chloro-4,6-diisopropylamino-1,3,5-triazine (DIAT).

It has been observed that diisopropylamine partly acts as HCl scavenger formed during the reaction, leading to a conversion of 8% by gas-chromatographic analyses. (**Scheme 3.4, route a**) This can be attributed to diisopropylamine higher basicity ( $pK_a=11.05$ )<sup>[37]</sup> compared to  $NaHCO_3$  ( $pK_a=10.33$ ) and to the presence of the amine and inorganic base in two different phases. Later on, a new protocol has been tested using an excess of diisopropylamine acting both as reagent and as scavenger for chloridric acid which is formed as byproduct (**Scheme 3.4, route b**). Gas-chromatographic analyses showed that, after 35 hours under reflux, conversion was at 16%. Therefore, synthesis reported by Katritzky has been followed,<sup>[36]</sup> but by experimental experience, complete conversion has been reached after 96 hours of reflux (**Scheme 3.4, route c**).

As reported by Bird,<sup>[38]</sup> triazines possess an aromaticity value equivalent to benzene, but differences lie on the replacement of three CH groups with N atoms that localizes electronic charge on the nitrogen atoms. 1,3,5-triazines do not exhibit the typical electrophilic substitution reactions of benzene, but undergo nucleophilic addition with same rules known for other aromatic rings.<sup>[39]</sup>

Therefore, it is possible that the substitution of 1,3,5-triazine with an amine, a known electron donating group, disfavors the substitution in meta position. For this reason, a large excess of diisopropylamine and high temperatures are needed, as reported by Katritzky *et al.*,<sup>[36]</sup> in addition to long reaction times.

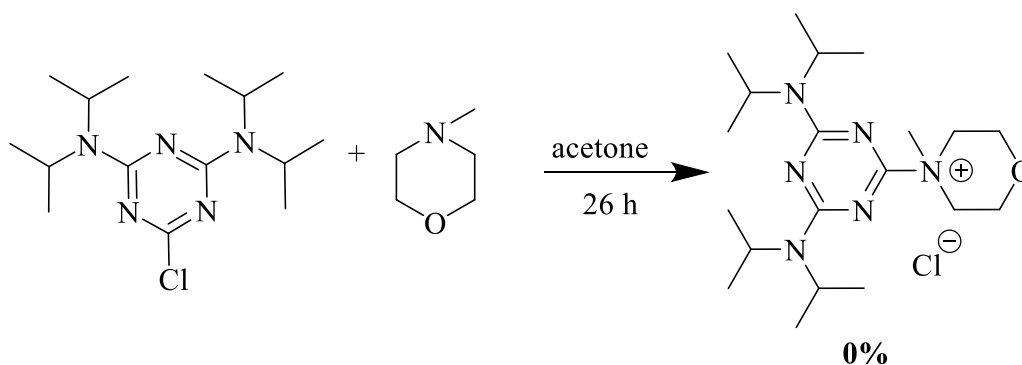
<sup>1</sup>H NMR, <sup>13</sup>C NMR and FT-IR spectra confirmed the synthesis of DIAT as a powder with yield of 80% (purity 94%). Data are in agreement with characterizations reported by Katritzky *et al.*:<sup>[36]</sup>

<sup>1</sup>H NMR (300 MHz, CDCl<sub>3</sub>, ppm): 4.38 (4H, m broad, CH(CH<sub>3</sub>)<sub>2</sub>), 1.33 (24H, d, CH(CH<sub>3</sub>)<sub>2</sub>).

<sup>13</sup>C NMR (300 MHz, CDCl<sub>3</sub>, ppm): 167.43, 163.69, 45.76, 20.57, 20.26.

In <sup>13</sup>C NMR of DIAT two signals are present at 20.57 ppm and 20.26 ppm, both assignable to primary carbons of isopropyl groups. This behaviour is attributable to decoalescence effect caused by the restricted bond rotation around Triazine-N bond, that will be examined in depth in **Chapter 3.2**.

DIAT has been reacted with *N*-methylmorpholine for the synthesis of 4-(4,6-bis-diisopropylamino-1,3,5-triazin-2-yl)-4-methylmorpholinium chloride (DIATMM), the corresponding quaternary ammonium salt (**Scheme 3.5**).

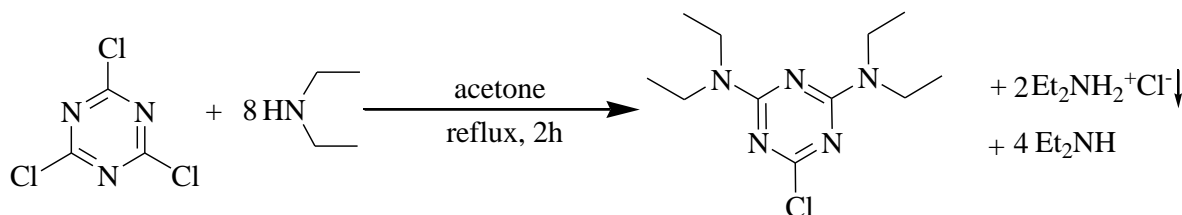


**Scheme 3.5:** Synthesis of 4-(4,6-bis-diisopropylamino-1,3,5-triazin-2-yl)-4-methylmorpholinium chloride (DIATMM).

Despite long reaction times, no product formation has been observed. The reaction is probably disfavored toward nucleophilic substitution by tertiary amine due to the presence of two electron donating groups as substituents of the triazine ring, in a mechanism similar to what may be considered for a benzene ring.<sup>[38,39]</sup>

### 3.1.2 Synthesis of 2-chloro-4,6-bis-diethylamino-1,3,5-triazine (DEAT)

Considering the results obtained with DIAT, the substitution of diisopropyl groups with ethyl moieties makes the amine a weaker electron donating substituent for the triazine ring. In a study by Katritzky *et al.* is reported a possible synthesis for 2,4,6-tris-diethylamino-1,3,5-triazine (TEAT) by reaction between cyanuric chloride with an excess of diethylamine, under reflux for 8 hours in DMF.<sup>[36]</sup> Thus, 2-chloro-4,6-bis-diethylamino-1,3,5-triazine (DEAT) has been synthesized, considering that it is a reaction step in the synthesis of TEAT. (Scheme 3.6)



Scheme 3.6: Synthesis of 2-chloro-4,6-bis-diethylamino-1,3,5-triazine (DEAT).

<sup>1</sup>H NMR, <sup>13</sup>C NMR and FT-IR spectra confirmed the synthesis of DEAT as an oil with a yield of 84% (purity 96%). Data are in agreement with characterizations reported by Katritzky *et al.*<sup>[36]</sup>

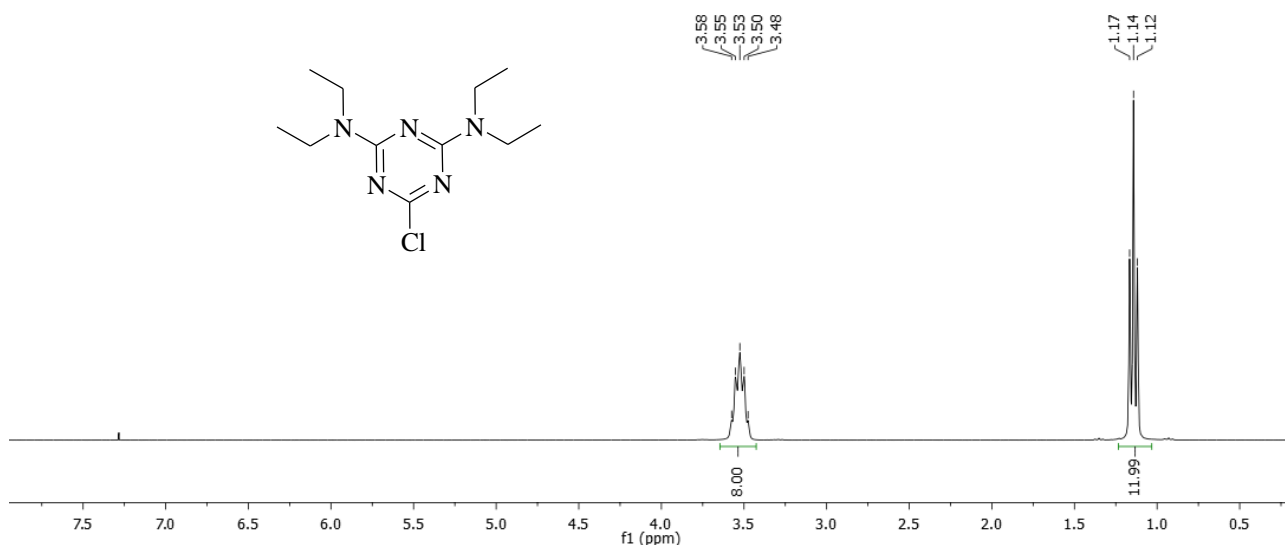
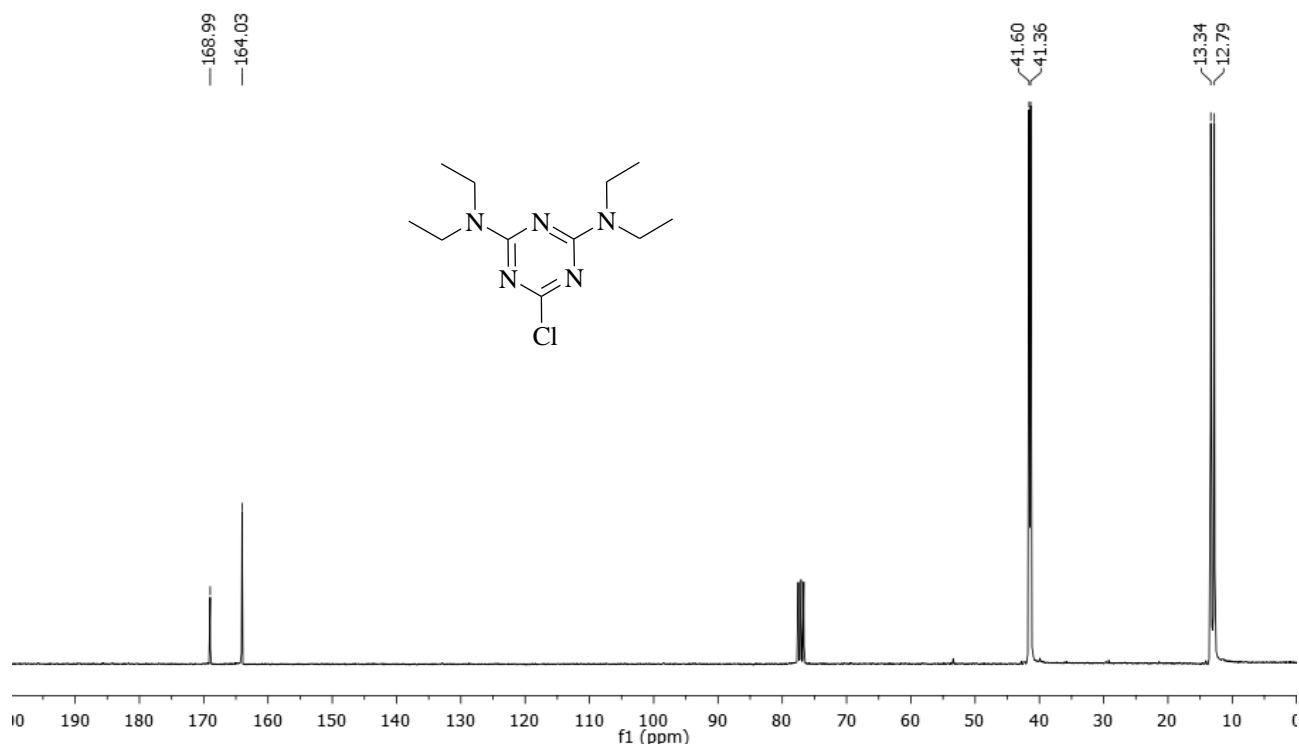


Figure 3.1: <sup>1</sup>H NMR spectrum (CDCl<sub>3</sub>) of 2-chloro-4,6-bis-diethylamino-1,3,5-triazine (DEAT).

<sup>1</sup>H NMR (300 MHz, CDCl<sub>3</sub>, ppm): 3.53 (8H, qi, CH(CH<sub>3</sub>)<sub>2</sub>), 1.14 (12H, t, CH(CH<sub>3</sub>)<sub>2</sub>).

In <sup>1</sup>H NMR spectrum (Figure 3.1), signals of ethyl moieties are observable as a quintet at 3.53 ppm and as a triplet at 1.14 ppm, respectively attributable to CH<sub>2</sub>CH<sub>3</sub> and CH<sub>2</sub>CH<sub>3</sub> protons.



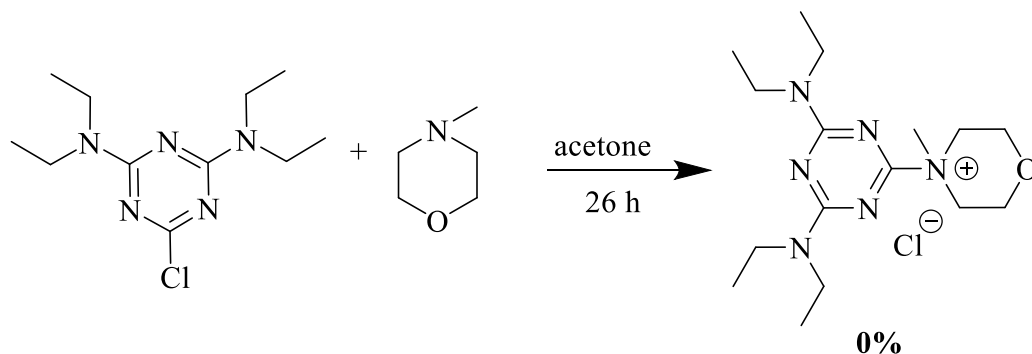
**Figure 3.2:** <sup>13</sup>C NMR spectrum (CDCl<sub>3</sub>) of 2-chloro-4,6-diethylamino-1,3,5-triazine (DEAT).

<sup>13</sup>C NMR (300 MHz, CDCl<sub>3</sub>, ppm): 168.99, 164.03, 41.60, 41.36, 13.34, 12.79.

In <sup>13</sup>C NMR spectrum (**Figure 3.2**), triazine carbons are attributable to signals at 168.99 ppm and at 164.03 ppm. Two couples of signals are present at 41.60-41.36 ppm and 13.34-12.79 ppm, respectively assignable to secondary and primary carbons of ethyl groups.

In both <sup>1</sup>H and <sup>13</sup>C NMR spectra, it is possible to observe decoalescences effects due to restricted bond rotation around Triazine-N bond, this behaviour will be examined in depth in **Chapter 3.2**.

DEAT has been reacted with *N*-methylmorpholine for the synthesis of 4-(4,6-bis-diethylamino-1,3,5-triazin-2-yl)-4-methylmorpholinium chloride (DEATMM), the corresponding quaternary ammonium salt (**Scheme 3.7**).



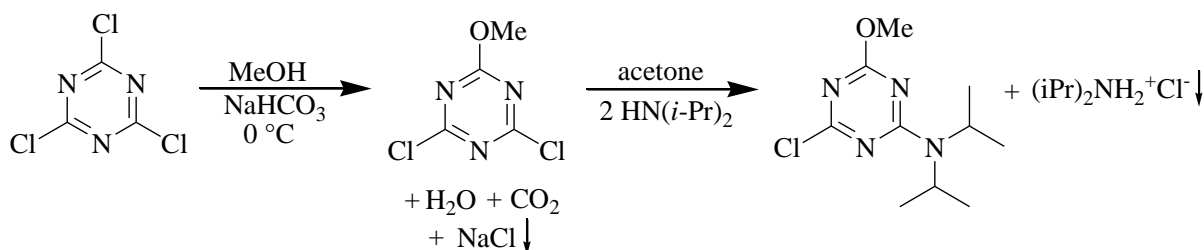
**Scheme 3.7:** Synthesis of 4-(4,6-bis-diethylamino-1,3,5-triazin-2-yl)-4-methylmorpholinium chloride (DEATMM).

Despite long reaction times, no product formation has been observed. Therefore, it is possible that diethylamino substituent is still an electron donating group strong enough to disfavor the nucleophilic substitution on the triazine with a mechanism similar to what may be considered for aromatic cycles.<sup>[38,39]</sup> Considering lack of reactivity observed in 2-chloro-4,6-bis-dialkylamino-1,3,5-triazine with *N*-methylmorpholine, it has been decided to change one amino substituent with an alkoxy group.

### 3.1.3 Synthesis of 2-chloro-4-methoxy-6-diisopropylamino-1,3,5-triazine (MAT)

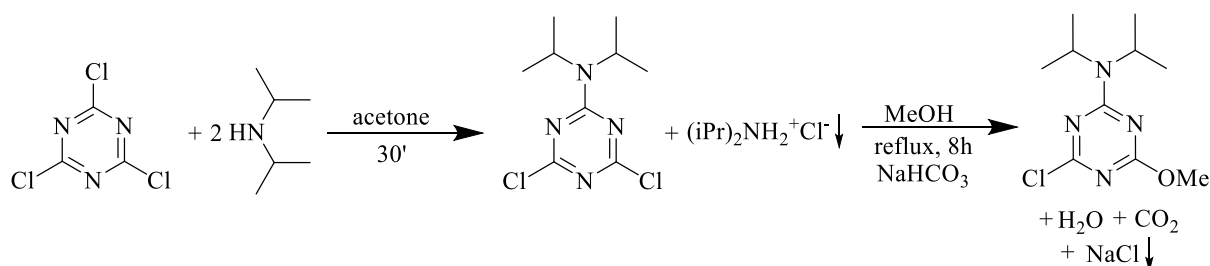
A triazine containing both alkoxy and amine substituents has been synthesized, specifically: 2-chloro-4-methoxy-6-diisopropylamino-1,3,5-triazine. Two different methods have been tested.

In the first method, cyanuric chloride has been dissolved in methanol, at 0 °C, in the presence of a base and later reacted with diisopropylamine. (**Scheme 3.8**)



**Scheme 3.8:** Synthesis of 2-chloro-4-methoxy-6-diisopropylamino-1,3,5-triazine (MAT) (Method 1).

In the second method the reaction has been carried out in acetone in the presence of cyanuric chloride and an excess of diisopropylamine, that is used both as reagent and as scavenger for hydrochloric acid formed during the reaction. Thus, the solvent has been removed and methanol has been added in the presence of a base. (**Scheme 3.9**)



**Scheme 3.9:** Synthesis of 2-chloro-4-methoxy-6-diisopropylamino-1,3,5-triazine (MAT) (Method 2).

Thanks to gas-chromatographic analyses, it is possible to monitor the reaction, that is led to complete conversion in 4.5 hours at *r.t.* for the first method and after 8 hours at reflux using the second method.

The yields of weighed product are:

- Method 1: 66%
- Method 2: 74%

As reported before (**Chapter 3.1.1**),<sup>[38,39]</sup> a possible explanation to what has been experimentally observed is that the presence of diisopropylamine as substituent of triazine ring (Method 2) disfavors the nucleophilic substitution in meta position and thus higher temperatures are required. Instead, the presence of a weaker electron donating group bonded to the triazine ring, such as methoxy group, allows the second substitution to be carried out at room temperature (Method 1). Finally, the differences in yield between the two methods can be explained by the slight solubility in water of 2,4-dichloro-6-methoxy-1,3,5-triazine experimentally observed in the work up.

$^1\text{H}$ ,  $^{13}\text{C}$  NMR and FT-IR spectra confirmed that both methods lead to 2-chloro-4-methoxy-6-diisopropylamino-1,3,5-triazine.

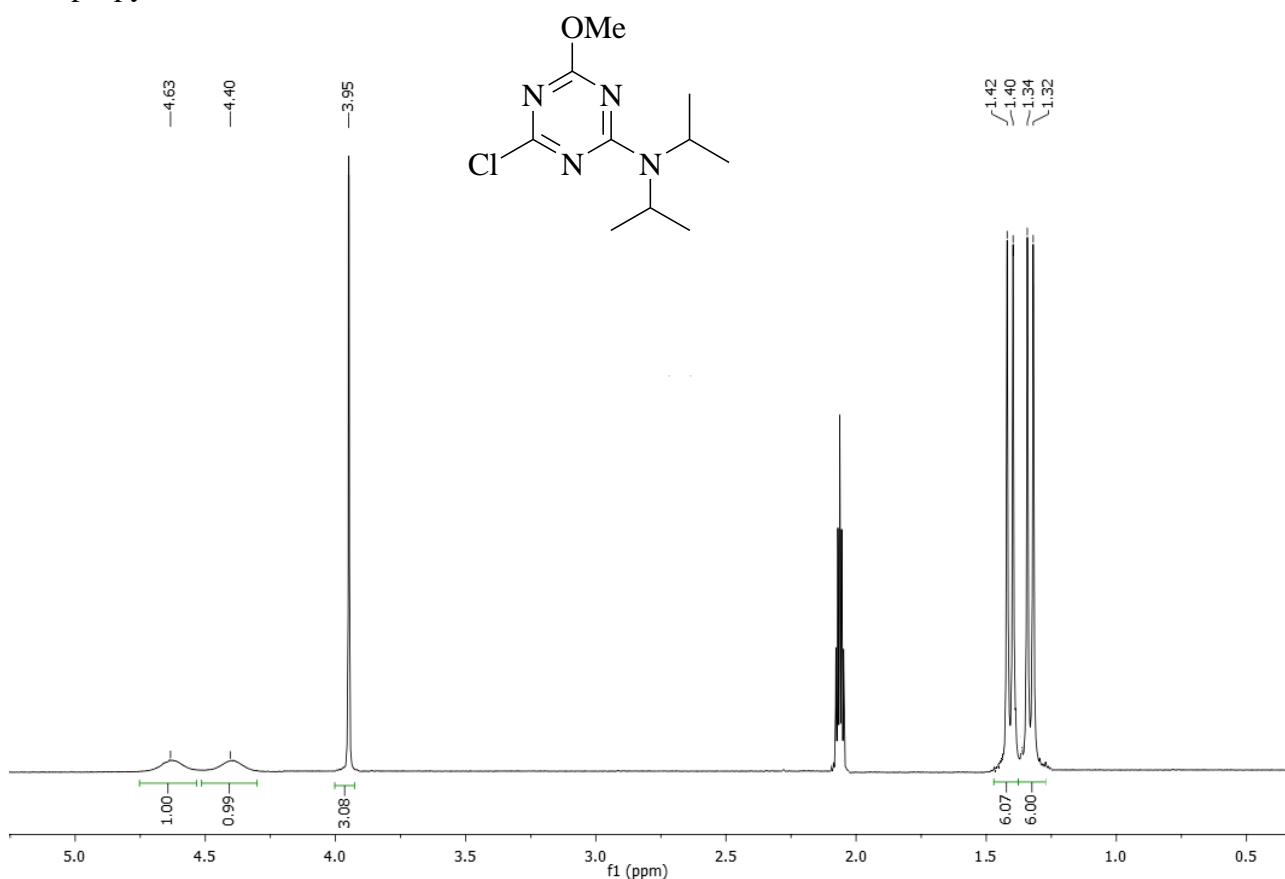


**Figure 3.3:**  $^1\text{H}$  NMR spectrum (acetone- $d_6$ ) of 2-chloro-4-methoxy-6-diisopropylamino-1,3,5-triazine (MAT).

$^1\text{H}$  NMR (300 MHz, acetone- $d_6$ , ppm): 4.61-4.39 (2H, m broad,  $\text{NCH}(\text{CH}_3)_2$ ), 3.93 (3H, s,  $\text{OCH}_3$ ), 1.38-1.31 (12H, d,  $\text{NCH}(\text{CH}_3)_2$ ).

In  $^1\text{H}$  NMR spectrum (**Figure 3.3**), it is possible to observe two distinct sets of signals assignable to the diisopropylamino group, multiplets at 4.63 ppm and at 4.40 ppm are attributable to protons bonded to carbons in  $\alpha$  position to nitrogen. These signals occur at higher ppm compared to protons in the same position  $[(\text{CH})_\alpha]$  in an aromatic amine (ca. 3.00 ppm) due to the electron withdrawing effect of the triazine.<sup>[40]</sup> Signals of  $\text{NCH}(\text{CH}_3)_2$  protons are observable as a couple of doublets at 1.42 ppm and at 1.34 ppm. Finally, the methoxy group is assignable to the singlet at 3.95 ppm.

Katritzky *et al.* report a study about NMR spectra of 2-chloro-4,6-bis-dialkylamino-1,3,5-triazine and their restricted rotation around N-Ar and N- $\text{C}_\alpha$  bonds.<sup>[36,41]</sup> In this study Katritzky analyses the  $^1\text{H}$  NMR spectrum of 2-chloro-4,6-bis-diisopropylamino-1,3,5-triazine from 120 °C until -65 °C and reports the differences observed for protons in  $\alpha$  and  $\beta$  position of diisopropyl moieties. Unfortunately, no spectrum gathered at 25 °C is reported. Nevertheless, in  $^1\text{H}$  NMR spectrum at 120 °C, only one signal for each  $\alpha$  and  $\beta$  proton is reported, a completely free rotation around N-Ar and N- $\text{C}_\alpha$  bonds can be supposed. At -60 °C, Katritzky reports two signals for  $\alpha$  protons and two for  $\beta$  protons, while at -65 °C,  $^1\text{H}$  NMR shows the presence of two signals for  $\alpha$  protons and four signals for  $\beta$  protons. It may be assumed that between 120 °C and -60 °C the rotation around N-Ar bond is disfavoured giving rise to two different signals for  $\alpha$  protons, while rotations of N- $\text{C}_\alpha$  bonds is blocked only below -65 °C leading to the presence of four different signals.<sup>[41]</sup>

$^1\text{H}$  NMR spectrum (**Figure 3.3**) has been gathered at 25 °C and it may be assumed that the presence of two distinct sets of signals is attributable to the restricted bond rotation around N-Ar bond, while N- $\text{C}_\alpha$  bonds are free to rotate. This situation leads to the presence of two sets of signals for protons bonded to primary and tertiary carbon of diisopropyl moieties due to non-equivalent steric positions. (**Figure 3.4**)

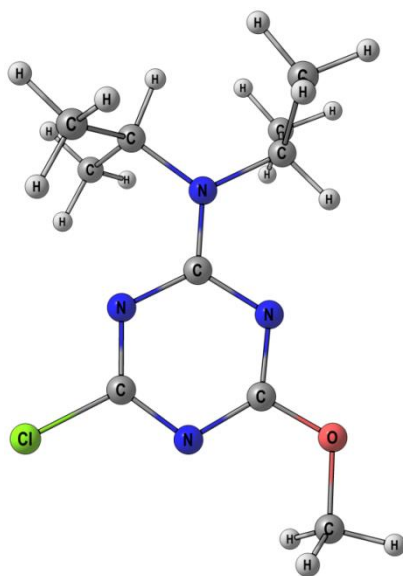


**Figure 3.4:** Spatial arrangement of 2-chloro-4-methoxy-6-diisopropylamino-1,3,5-triazine (MAT).



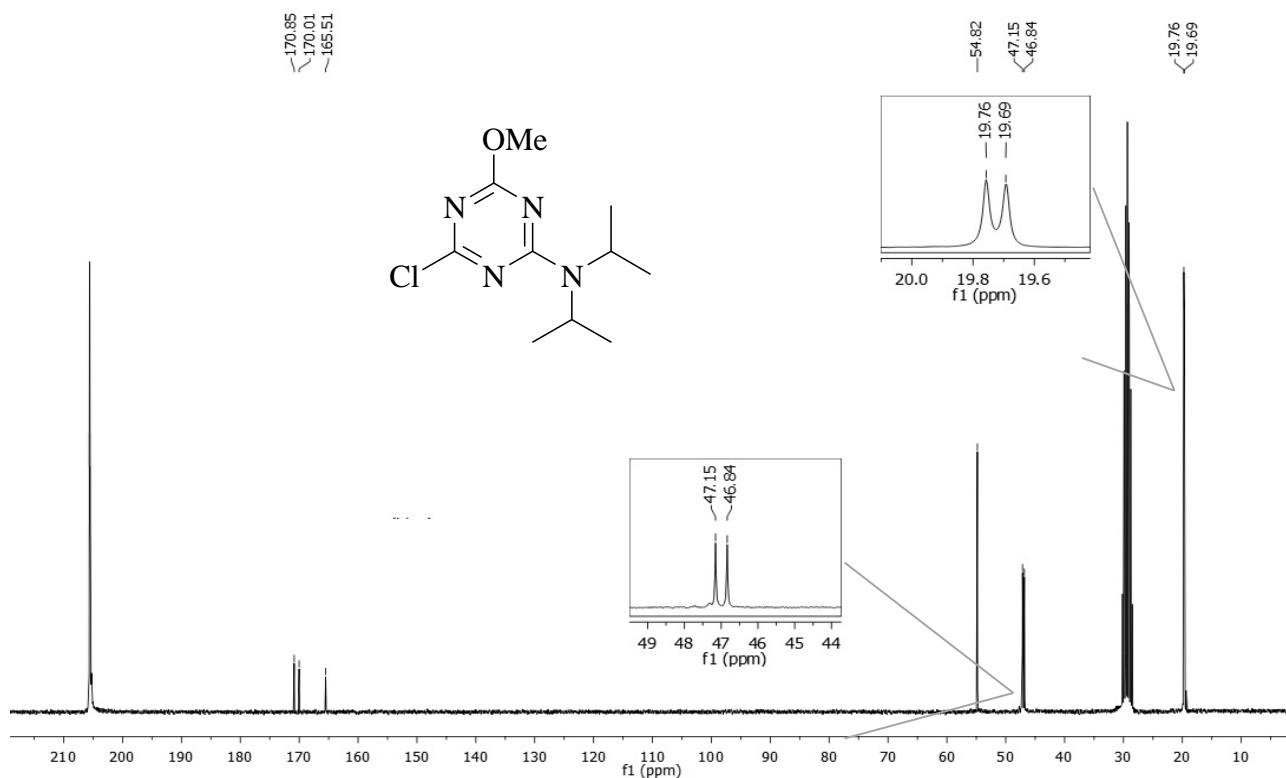
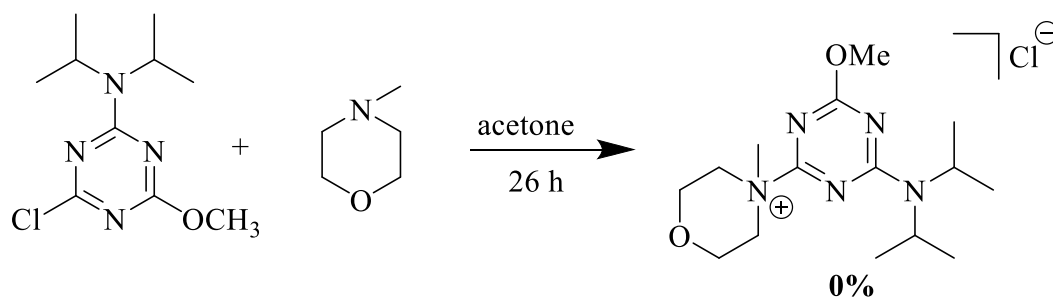


**Figure 3.5:** <sup>13</sup>C NMR spectrum (acetone-d<sub>6</sub>) of 2-chloro-4-methoxy-6-diisopropylamino-1,3,5-triazine (MAT).

<sup>13</sup>C NMR (300 MHz, acetone-d<sub>6</sub>, ppm): 170.85, 170.01, 165.51, 54.82, 47.15, 46.84, 19.76, 19.69.

<sup>13</sup>C NMR spectrum (**Figure 3.5**) confirms what has been supposed by <sup>1</sup>H NMR analysis. Indeed, it is possible to observe signals of tertiary and primary carbons of the diisopropylamino group respectively at 47.16-46.84 ppm and at 19.76-19.69 ppm, this can be attributable to the restricted rotation around N-Ar bond. Carbon of methoxy group is observable at 54.82 ppm, while signals between 170.87 ppm and 165.53 ppm are assignable to triazine ring carbons.

MAT has been reacted with *N*-methylmorpholine for the synthesis of 4(4-methoxy-6-diisopropylamino-1,3,5-triazin-2-yl)-4-methylmorpholinium chloride (MATMM), the derived quaternary ammonium salt (**Scheme 3.10**).



**Scheme 3.10:** Synthesis of 4(4-methoxy-6-diisopropylamino-1,3,5-triazin-2-yl)-4-methylmorpholinium chloride (MATMM).

Despite long reaction times, no product formation has been observed. It can be assumed that the presence of an electron donating groups strong as diisopropylamine, disfavors the nucleophilic substitution by tertiary amine in a mechanism similar to what may be considered for a benzene ring.<sup>[38,39]</sup>

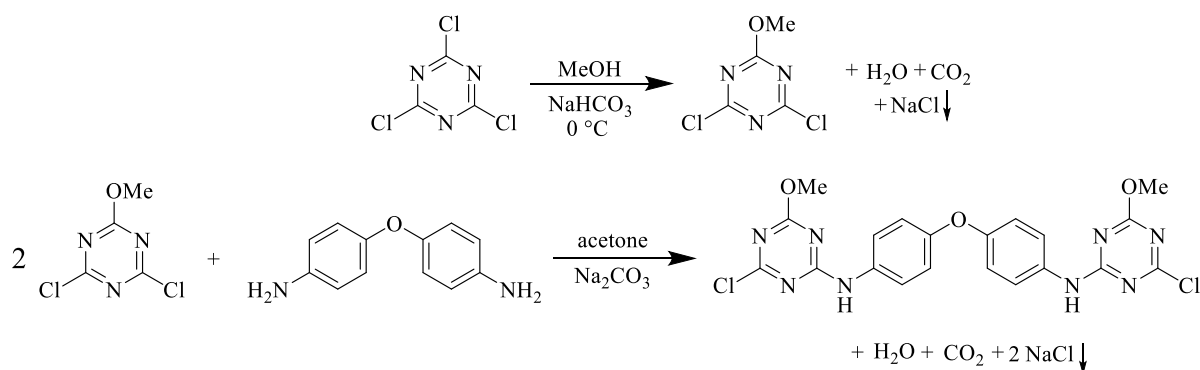
Experimental data have shown that amino substituents are electron donating groups too strong and disfavour nucleophilic substitution in meta position even in the presence of a methoxy moiety, well know substituent for the synthesis of triazine ammonium salts.<sup>[21,32]</sup> Hence, it has been decided to do not continue with the study of alkoxy-alkylamino-substituted-1,3,5-triazines.

### 3.1.4 Synthesis of *N,N'*-(oxybis(4,1-phenylene))bis(2-chloro-4-methoxy-1,3,5-triazin-6-amine) (MODAM)

Many studies are present in literature about triazine substituted by anilino-derivatives used as antimicrobials<sup>[42,43]</sup>, ultraviolet ray absorbers<sup>[44]</sup> or as insecticides.<sup>[45]</sup>

For example, Mewada *et al.* report the synthesis of anilino-methoxy substituted triazines with promising biological activities,<sup>[46]</sup> while Kusano *et al.* and Yuan *et al.* investigated the synthesis of bis-triazine compounds bridged by dianilines for supramolecular studies.<sup>[47,48]</sup> Hence, it has been decided to investigate the reaction of methoxy substituted triazine with 4,4'-oxydianiline (ODA) and 4,4'-methyldianiline (MDA) in order to synthesize ammonium salts precursors with two triazine rings.

Below, the synthesis of *N,N'*-(oxybis(4,1-phenylene))bis(2-chloro-4-methoxy-1,3,5-triazin-6-amine) (MODAM) is reported starting from cyanuric chloride dissolved in methanol at 0 °C and later reacted with 4,4'-oxydianiline, both steps were carried out in the presence of an inorganic base (**Scheme 3.11**). Differently to what reported for DIAT and DEAT (**Chapters 3.1.1 and 3.1.2**), para-aryl-substituted aniline derivatives possess a pKa ca. 4.2<sup>[49]</sup> and do not compete with an inorganic base for HCl scavenging. Hence, the yield is quantitative without the need to use an excess of dianiline.



**Scheme 3.11:** Synthesis of *N,N'*-(oxybis(4,1-phenylene))bis(2-chloro-4-methoxy-1,3,5-triazin-6-amine) (MODAM).

$^1\text{H}$  NMR,  $^{13}\text{C}$  NMR and FT-IR spectra confirmed the isolation of the desired product, MODAM, with 86% of yield (purity 91%).

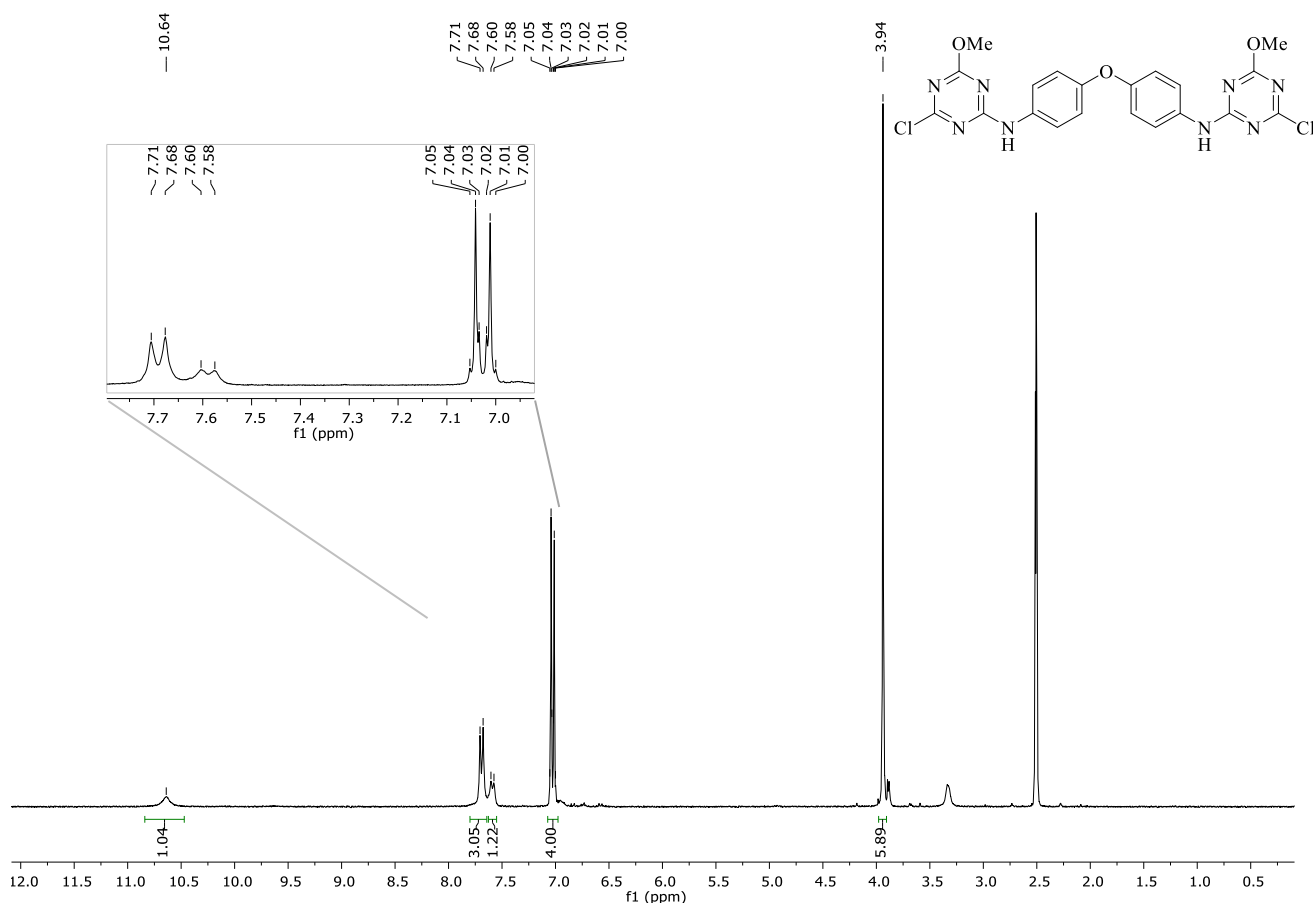


**Figure 3.6:**  $^1\text{H}$  NMR spectrum ( $\text{DMSO-d}_6$ ) of  $N,N'$ -(oxybis(4,1-phenylene))bis(2-chloro-4-methoxy-1,3,5-triazin-6-amine) (MODAM) at 298 K.

In  $^1\text{H}$  NMR spectrum (**Figure 3.6**), it is possible to observe the signal of triazine methoxy group at 3.94 ppm and the signals of amino and phenyl protons respectively at 10.64 ppm and between 7.71 ppm and 7.00 ppm. Small signals at 7.01 ppm and at 3.94 ppm are attributable to the presence of byproducts.

The aromatic signal at 7.05 ppm shows the typical behavior of a second order magnetic molecule, leading to a doublet of triplets. While the signal at 7.71 ppm and the doublet at 7.60 ppm are attributable to a phenomenon of decoalescence.

Indeed, both these phenomena occur when an amino group is attached to a molecule with  $\pi$  bonding, such as an amide or an aromatic system.<sup>[50,51]</sup> The lone pair of the nitrogen conjugates with the  $\pi$  aromatic system to create a partial double bond, shifting amino protons signal to low field of the spectrum. This effect creates significant barrier to rotation between the amino and the aromatic systems, leading to the formation of two possible rotamers. (**Figure 3.7**)

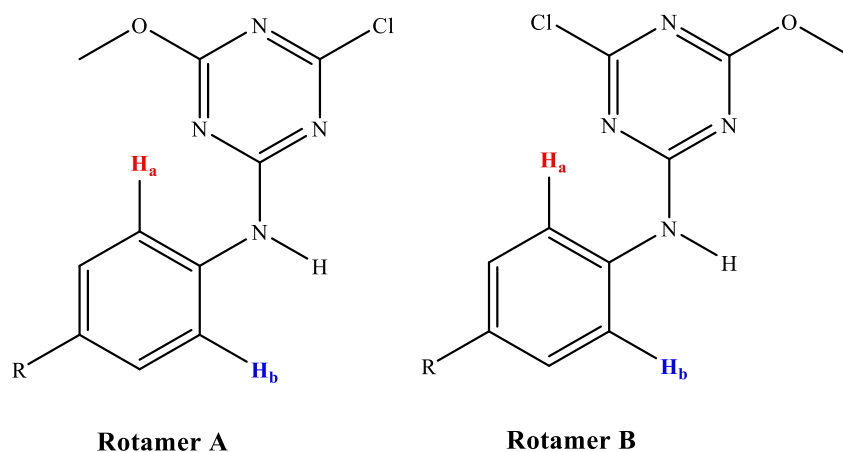


**Figure 3.7:** Example of rotamers formed due to partially  $sp^2$  hybridization of the amino group.

The rotational barrier is the activation energy required to trigger free rotation and convert one rotamer into another, preventing the possibility to discern them: at low temperatures, two separate proton signals are observed, but as temperature is raised, rate of rotation of the bond increases and the two signals coalesce. The phenomenon is reported below, where it is possible to see the coalescence of the signals at 338 K (**Figure 3.8**), where a doublet is formed, thanks to the free rotation of Triazine-N-Ar bonds. Moreover, also the signal at 7.01 ppm, a doublet of triplets at 298 K, is simplified into a doublet at 338 K.

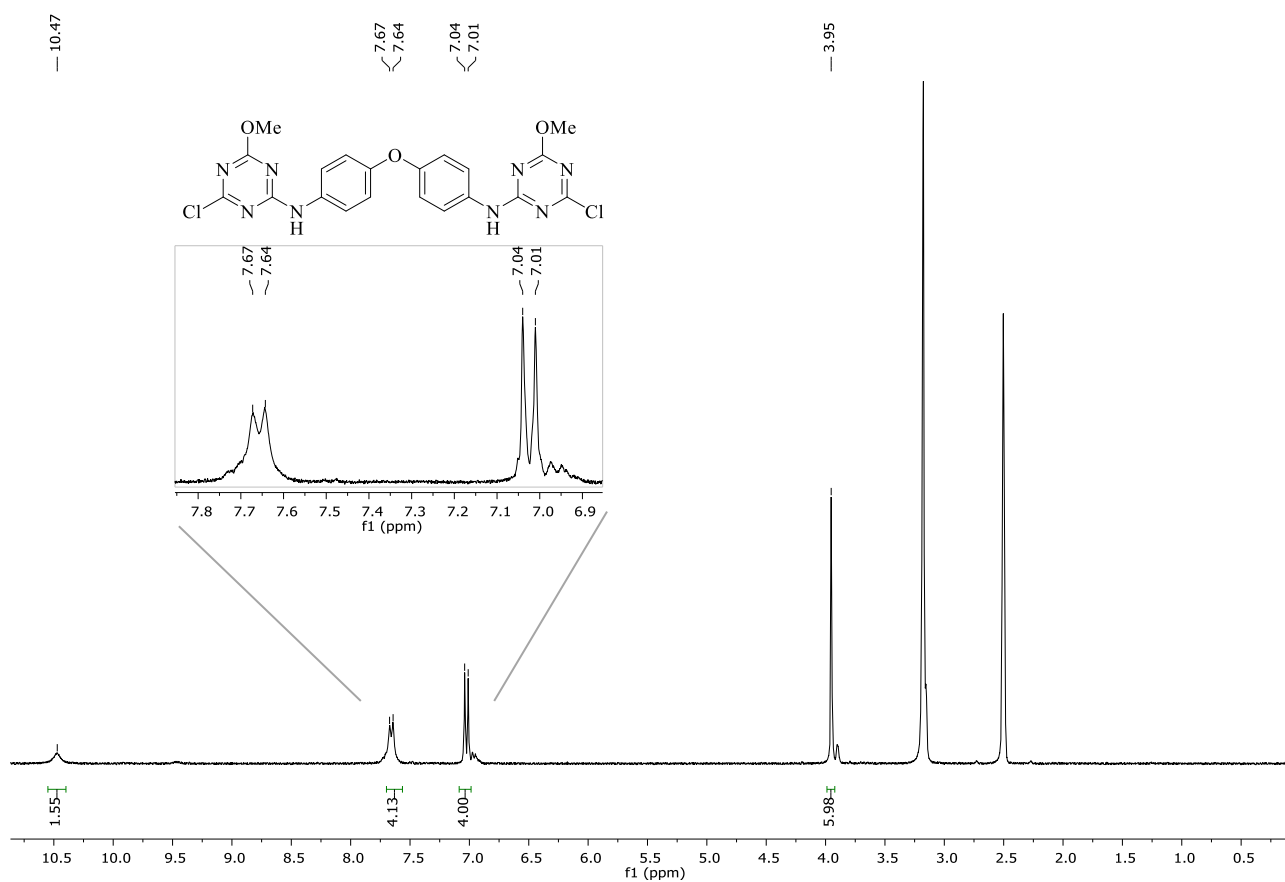


**Figure 3.8:**  $^1\text{H}$  NMR spectrum ( $\text{DMSO-d}_6$ ) of *N,N'*-(oxybis(4,1-phenylene))bis(2-chloro-4-methoxy-1,3,5-triazin-6-amine) (MODAM) at 338 K.

As a further demonstration of the decoalescence effect, COSY NMR spectrum at 298 K is reported (**Figure 3.9**), where it is possible to observe the coupling between the signal at 7.04 ppm and both the doublets at 7.70 and at 7.61 ppm.

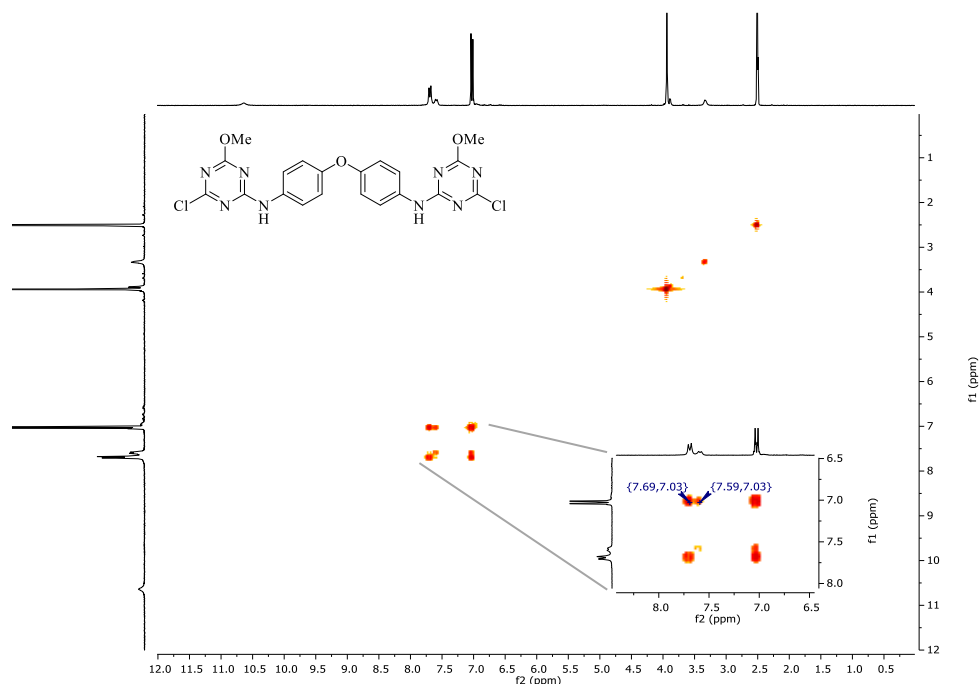


**Figure 3.9:** COSY NMR spectrum (DMSO- $d_6$ ) of *N,N'*-(oxybis(4,1-phenylene))bis(2-chloro-4-methoxy-1,3,5-triazin-6-amine) (MODAM) at 298 K.

In  $^{13}\text{C}$  NMR spectrum as well, it is possible to observe the effect of coalescence, below it is reported a comparison between spectra gather at 338 K and 298 K. (**Figure 3.10**)

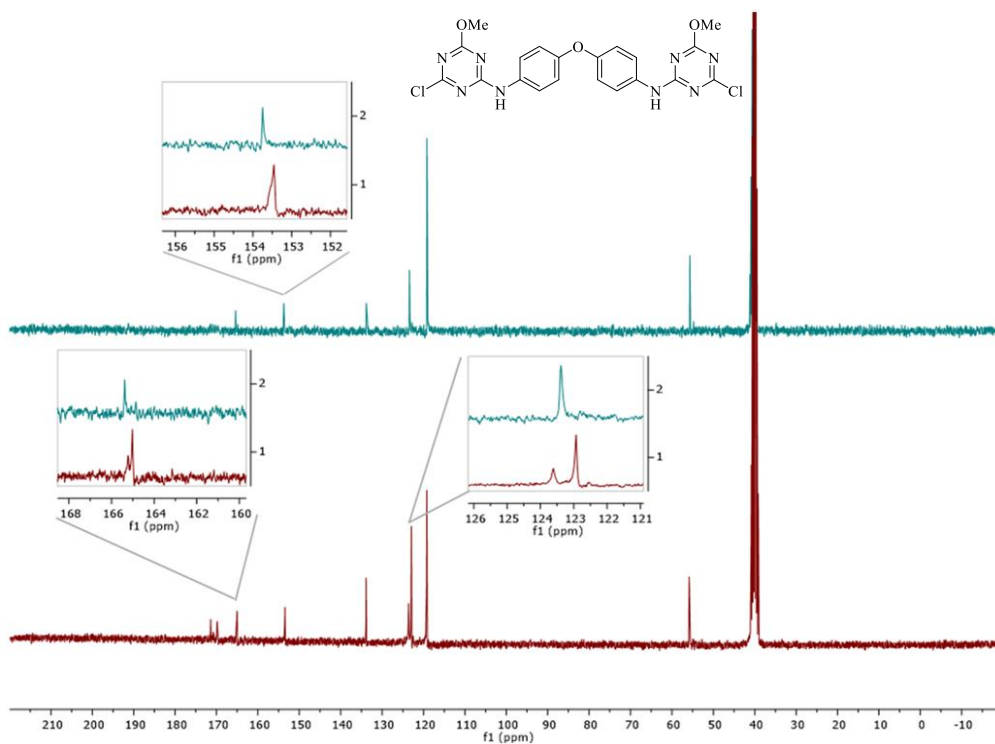


**Figure 3.10:** Comparison between  $^{13}\text{C}$  NMR spectra (DMSO- $d_6$ ) of *N,N'*-(oxybis(4,1-phenylene))bis(2-chloro-4-methoxy-1,3,5-triazin-6-amine) (MODAM) at 338 K (upper) and 298 K (bottom).

In  $^{13}\text{C}$  NMR spectrum at 298K (**Figure 3.10**), it is possible to observe two couples of signals at 165.23-162.22 ppm and at 123.61-122.93 ppm, that coalesce into singlets at 338 K. Signal at 153.46 ppm is affected as well: due to low resolution of NMR, a shoulder on its left side is observable and attributable to a second carbon signal, that is not present at higher temperature and can be explained by decoalescence effect.

Thanks to coalescence, it is possible to assign the signals to carbons affected by the rotation hindrance effect. Thus, signals at 165.23 ppm and at 153.46 ppm (**Figure 3.10**) can be attributed to carbons directly bonded to amino nitrogen atoms, respectively of triazine and phenyl rings. Signals at 123.61-122.93 ppm can be assigned to phenyl carbons in ortho position to amino substituent groups, which are more affected by steric difference between the two rotamers and present signals of the relative carbons farther from each other in the  $^{13}\text{C}$  NMR spectrum at 298 K.

Finally, APT NMR (**Figure 3.11**) and HMQC NMR (**Figure 3.12**), are reported for a complete assignment of  $^{13}\text{C}$  NMR spectrum.

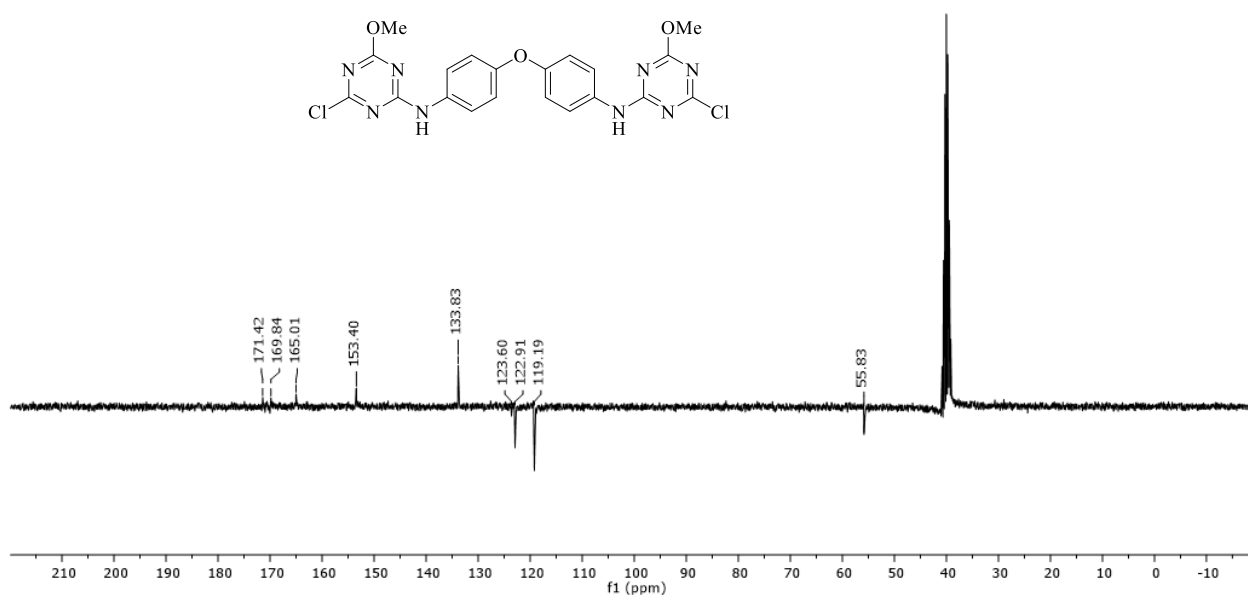


**Figure 3.11:** APT NMR spectrum ( $\text{DMSO-d}_6$ ) of *N,N'*-(oxybis(4,1-phenylene))bis(2-chloro-4-methoxy-1,3,5-triazin-6-amine) (MODAM) at 298 K.

Thanks to APT spectrum (**Figure 3.11**), it is possible to discern primary and tertiary carbons (negative phase) from secondary and quaternary carbons (positive phase). Thus, it is possible to attribute the signals between 172.42 ppm and 165.01 ppm to triazine quaternary carbons. Signals at 153.40 ppm and at 133.83 ppm are assignable to aromatic quaternary carbons. Finally, signals of methoxy and aromatic tertiary carbons can be observed between 123.60 ppm and 55.83 ppm.

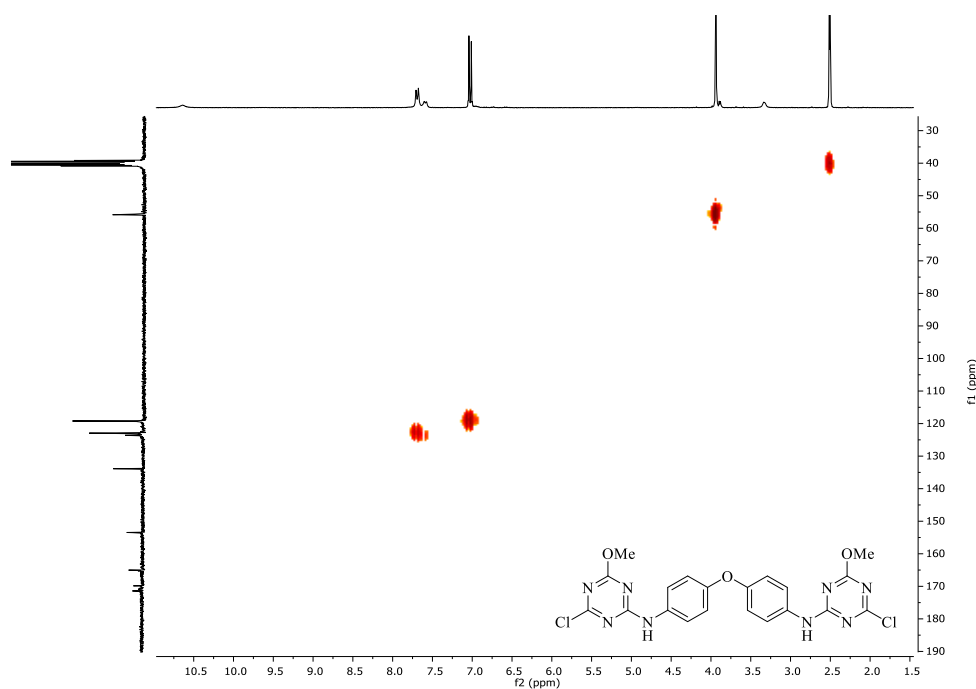


**Figure 3.12:** HMQC NMR spectrum (DMSO-d<sub>6</sub>) of *N,N'*-(oxybis(4,1-phenylene))bis(2-chloro-4-methoxy-1,3,5-triazin-6-amine) (MODAM) at 298 K.

In HMQC spectrum (**Figure 3.12**), it is possible to observe the coupling between protons and carbons of methoxy groups and between aromatic protons and corresponding carbons directly bonded.

Hence, <sup>1</sup>H NMR and <sup>13</sup>C NMR assignments of MODAM (**Figure 3.13**) are:

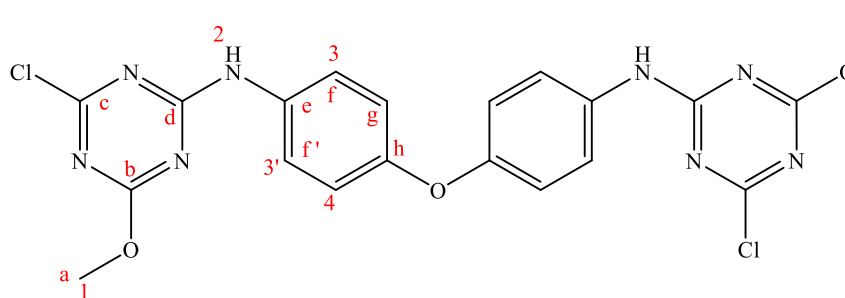
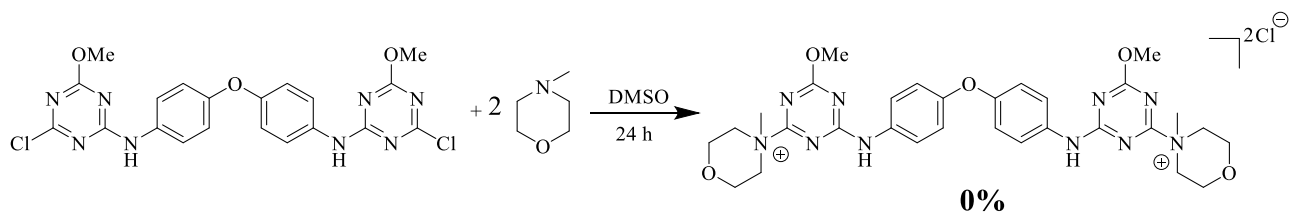


**Figure 3.13:** Formula of *N,N'*-(oxybis(4,1-phenylene))bis(2-chloro-4-methoxy-1,3,5-triazin-6-amine) (MODAM) where <sup>1</sup>H are assigned with numbers and <sup>13</sup>C with letters.

<sup>1</sup>H NMR (300 MHz, DMSO-d<sub>6</sub>, ppm): 10.64 (2H, m, H<sub>2</sub>), 7.71-7.58 (4H, dd, H<sub>3/3'</sub>), 7.05-7.00 (4H, dt, H<sub>4</sub>), 3.94 (6H, s, H<sub>1</sub>).

<sup>13</sup>C NMR (300 MHz, DMSO-d<sub>6</sub>, ppm): 171.42-169.85 (Cb,c), 165.23-165.02 (Cd/d'), 153.46 (Ce)133.86, (Ch), 123.61-122.93 (Cf/f'), 119.21 (Cg), 55.83 (Ca).

The isolated solid product has proved to be insoluble in all commonly used organic solvents except for dimethyl sulfoxide. Therefore, MODAM has been employed for synthesis of the quaternary bis-ammonium salt by reaction in the presence of *N*-methyl morpholine in DMSO. (**Scheme 3.12**).



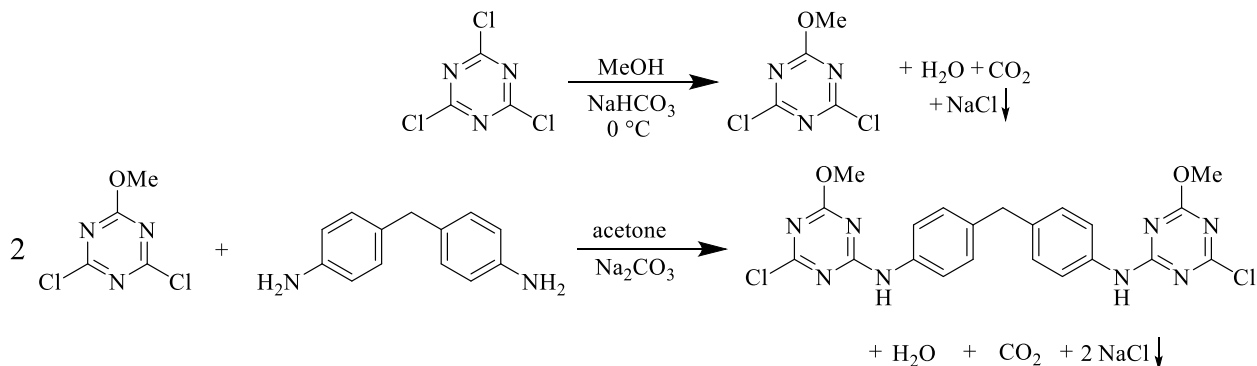
**Scheme 3.12:** Synthesis of quaternary ammonium salt derived from the reaction of MODAM and *N*-methyl morpholine.

Despite long reaction times, no product has been isolated. The reaction is probably hampered by the deactivation of halogenated carbon toward nucleophilic substitution by a tertiary amine.

### 3.1.5 Synthesis of *N,N'*-(methylenebis(4,1-phenylene))bis(2-chloro-4-methoxy-1,3,5-triazin-6-amine) (MMDAM)

Synthesis of *N,N'*-(methylenebis(4,1-phenylene))bis(2-chloro-4-methoxy-1,3,5-triazin-6-amine) (MMDAM) has been investigated. In the presence of an inorganic base, cyanuric chloride has been dissolved in methanol and later reacted with 4,4'-diaminodiphenylmethane. (**Scheme 3.13**)

As reported before (**Chapter 3.1.4**), para-aryl substituted aniline derivatives do not compete with an inorganic base for HCl scavenging due to low pKa (ca. 4.2),<sup>[49]</sup> thus yield is quantitative without the need to use an excess of dianiline.



**Scheme 3.13:** Synthesis of *N,N'*-(methylenebis(4,1-phenylene))bis(2-chloro-4-methoxy-1,3,5-triazin-6-amine) (MMDAM).

<sup>1</sup>H NMR, <sup>13</sup>C NMR and FT-IR spectra confirmed isolation of the desired product, MMDAM, with 94% of yield (purity 96%).

In <sup>1</sup>H NMR spectrum (**Figure 3.14**), it is possible to observe the signal of methoxy group at 3.93 ppm and the signal of methylene group at 3.88 ppm. Signal at 10.59 ppm is attributable to nitrogen-bonded protons. Finally, signals between 7.62 ppm and 7.19 ppm are assignable to protons of the aromatic rings.



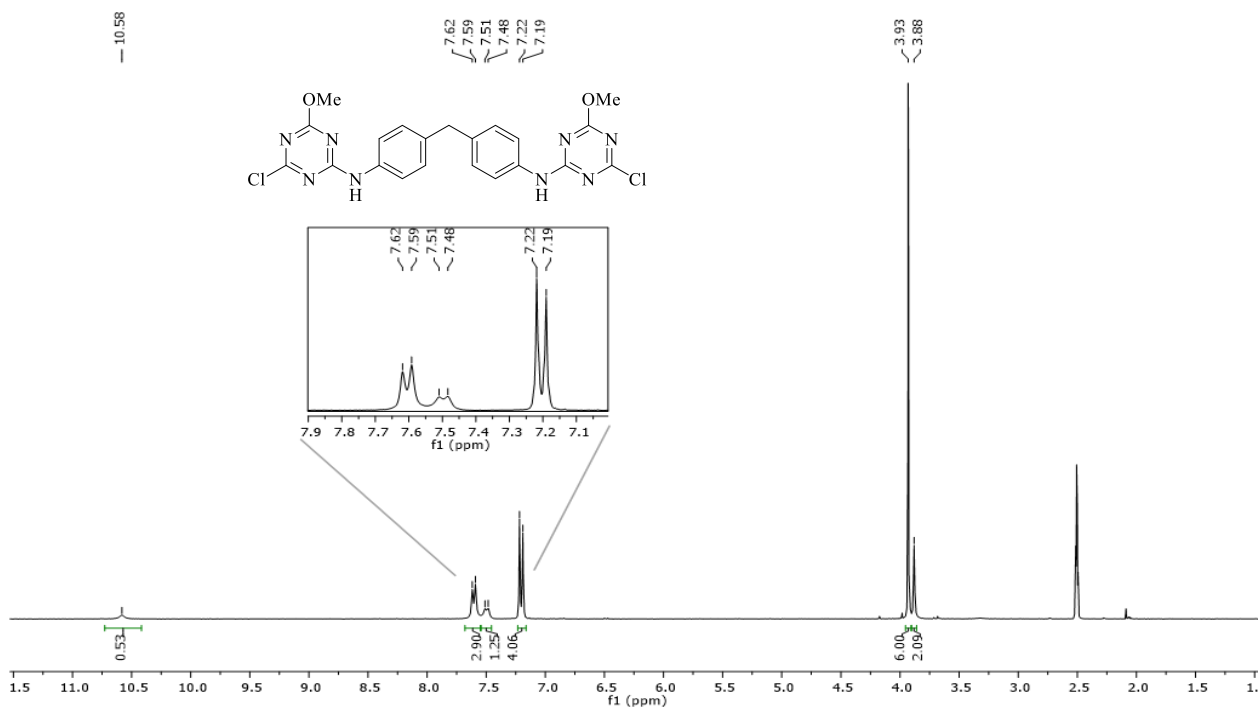


**Figure 3.14:**  $^1\text{H}$  NMR spectrum (DMSO- $d_6$ ) of *N,N'*-(methylenebis(4,1-phenylene))bis(2-chloro-4-methoxy-1,3,5-triazin-6-amine) (MMDAM) at 298 K.

As described before (**Chapter 3.1.4**), hindrance to rotation caused by partial  $sp^2$  hybridization of the nitrogen atom leads to the formation of two rotamers. This effect is observed thanks to coalescence of the signals at 7.62 ppm and 7.48 ppm that occurs in  $^1\text{H}$  NMR at 338 K (**Figure 3.15**).

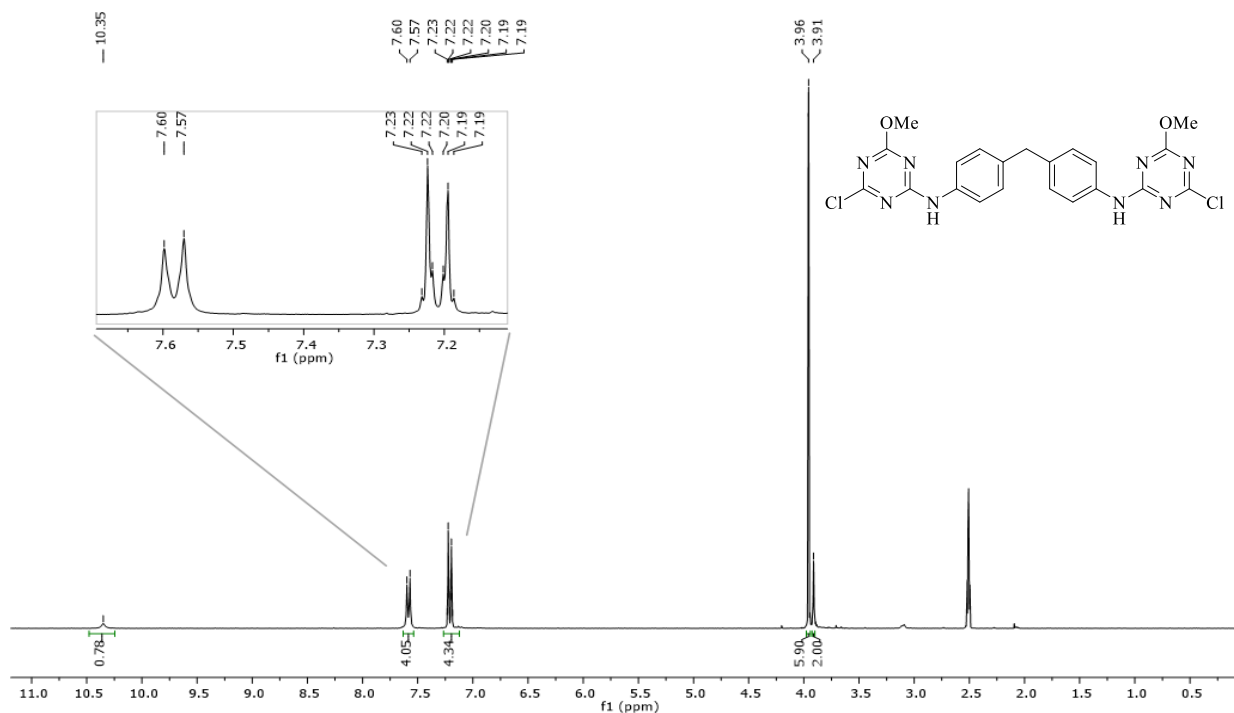


**Figure 3.15:**  $^1\text{H}$  NMR spectrum (DMSO- $d_6$ ) of *N,N'*-(methylenebis(4,1-phenylene))bis(2-chloro-4-methoxy-1,3,5-triazin-6-amine) (MMDAM) at 338 K.

In  $^{13}\text{C}$  NMR spectra of MMDAM, it is possible to observe as well the coalescence of carbon signals close to aniline nitrogen. Increasing temperature from 298 K to 338 K, the set of signals at 165.15-165.00 ppm, at 121.99-121.30 ppm and at 137.54-137.40 ppm coalesce into one, as shown in **Figure 3.16**, where magnifications for the affected signals are reported.

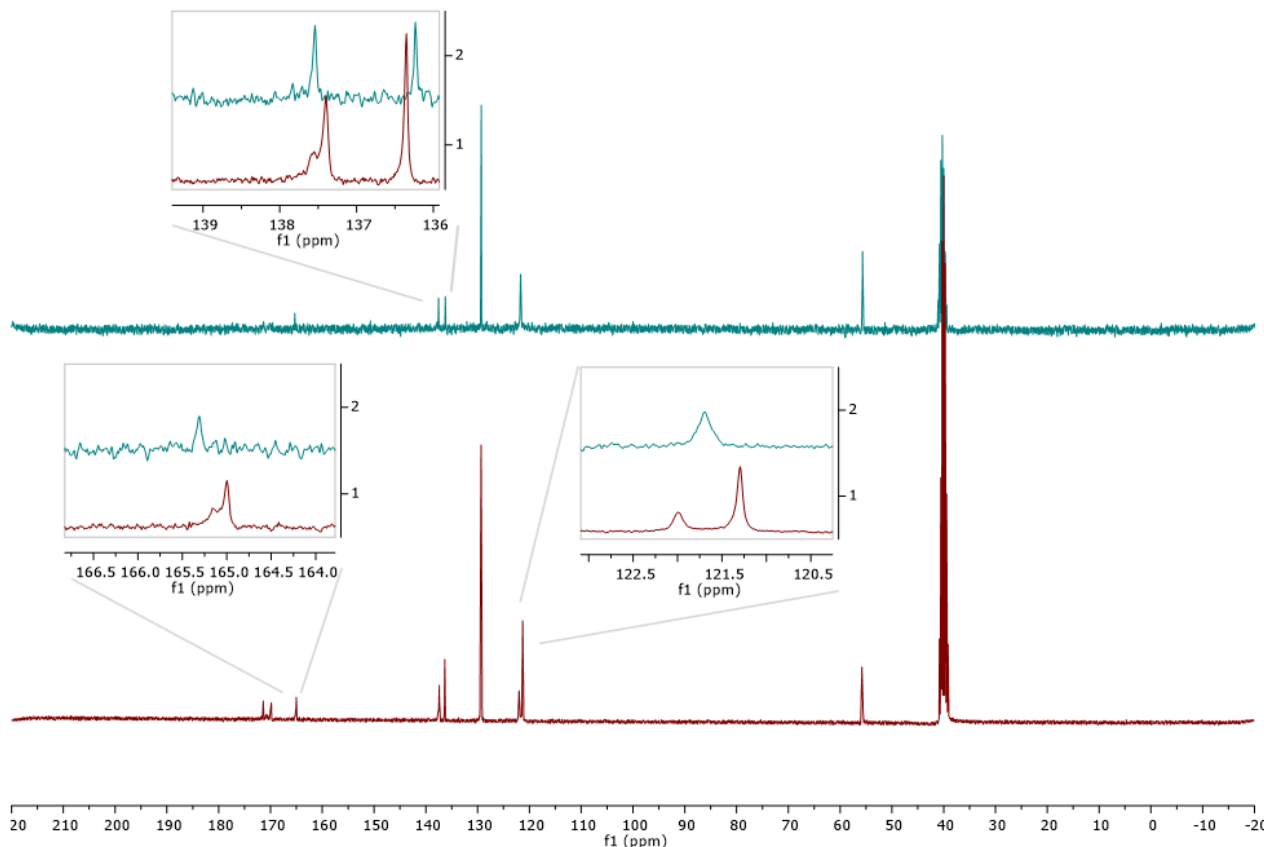


**Figure 3.16:** Comparison between  $^{13}\text{C}$  NMR spectra (DMSO- $d_6$ ) of *N,N'*-(methylenebis(4,1-phenylene))bis(2-chloro-4-methoxy-1,3,5-triazin-6-amine) (MMDAM) at 338 K (upper) and 298 K (bottom).

Coalescence effect in NMR spectra allows attribution of carbons to the signals affected. Thus, signals at 165.16 ppm and at 137.58 ppm are attributed respectively to triazine and phenyl carbons bonded to the amino nitrogen atoms. Signals at 121.99 ppm, instead, can be assigned to phenyl carbons in ortho position to the nitrogen groups.

Therefore,  $^1\text{H}$  and  $^{13}\text{C}$  NMR assignments for MMDAM (**Figure 3.17**) are:

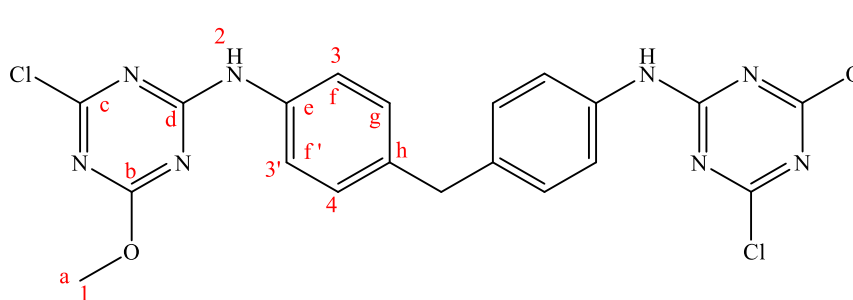
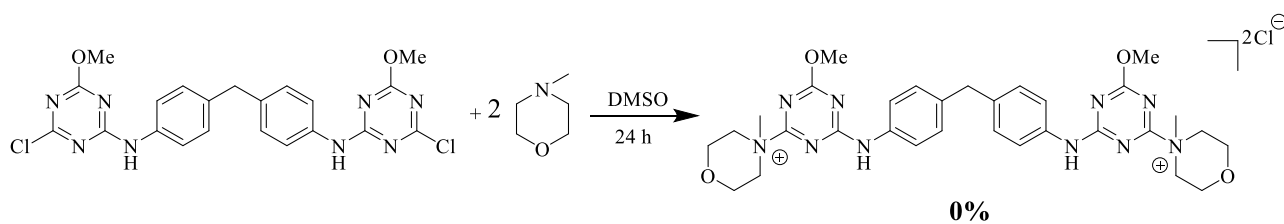


**Figure 3.17:** Formula of *N,N'*-(methylenebis(4,1-phenylene))bis(2-chloro-4-methoxy-1,3,5-triazin-6-amine) (MMDAM) where  $^1\text{H}$  are assigned with numbers and  $^{13}\text{C}$  with letters.

$^1\text{H}$  NMR (300 MHz, DMSO- $d_6$ , ppm): 10.58 (2H, m,  $\text{H}_2$ ), 7.62-7.48 (4H, dd,  $\text{H}_{3/3'}$ ), 7.22-7.19 (4H, d,  $\text{H}_4$ ), 3.93 (6H, s,  $\text{H}_1$ ), 3.38 (2H, s,  $\text{H}_5$ ).

$^{13}\text{C}$  NMR (300 MHz, DMSO- $d_6$ , ppm): 171.40-169.84 (Cb,c), 165.16-165.00 (Cd/d'), 137.58-137.40 (Ce), 136.35 (Ch), 129.33 (Cg), 121.98-121.30 (Cf/f'), 55.79 (Ca), 40.39 (Ci).

Finally, the isolated solid product has proved to be insoluble in all commonly used organic solvents except for dimethyl sulfoxide, thus, MMDAM has been employed for synthesis of the quaternary ammonium salt by reaction in the presence of *N*-methylmorpholine in DMSO (**Scheme 3.14**).



**Scheme 3.14:** Synthesis of quaternary ammonium salt derived from the reaction of MMDAM and *N*-methylmorpholine.

Similarly to what has been observed for MODAM (**Chapter 3.1.4**), despite long reaction times, no product has been isolated.

Thanks to experimental data, it can be assumed that anilino-methoxy substituted triazines are unreactive toward nucleophilic substitution of chlorine bonded carbon by a tertiary amine. It may be supposed that extra stability given by the partial  $sp^2$  hybridization of anilino nitrogen, combined to the presence of an electron donating group such as methoxy substituent, is responsible for the observed reagents inactivity. Hence, it has been decided to do not continue with the study of 2-chloro-4,6-disubstituted-1,3,5-triazines.

### 3.2 Synthesis of 2,4-dichloro-6-substituted-1,3,5-triazines

On the basis of the results gathered with the synthesis of 2-chloro-4,6-disubstituted-1,3,5-triazines, it has been decided to study the synthesis and the reactivity of 2,4-dichloro-6-substituted-1,3,5-triazines. In particular, compounds with one triazine ring, such as 2,4-dichloro-6-methoxy-1,3,5-triazine and 2,4-dichloro-6-dialkylamino-1,3,5-triazine have been taken into account, in order to synthesize their derived ammonium salts. Moreover, compounds with two triazine rings have been investigated as well, having moieties such as *N,N'*-diethylethylenediamine (DED), 4,4'-oxydianiline (ODA) and 4,4'-methylenedianiline (MDA) acting as bridges between the triazines.

Theoretically, the main advantage of these compounds is the presence of more potential reactive sites for synthesis of multi-ammonium salts that could lead to an increased efficiency in condensation reactions.

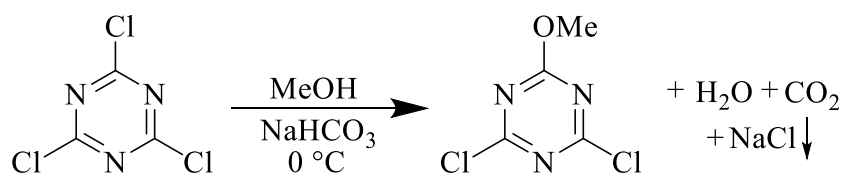
Below, the results obtained in the synthesis of 2,4-dichloro-6-methoxy-1,3,5-triazine (MMT), 2,4-dichloro-6-diisopropylamino-1,3,5-triazine (MIAT), 2,4-dichloro-6-diethylamino-1,3,5-triazine (MEAT) are reported for what concerns mono-triazine compounds. Later on, bis-triazine products are reported as well, such as,  $N_1,N_2$ -bis(2,4-dichloro-1,3,5-triazin-6-yl)- $N_1,N_2$ -diethylethane-1,2-diamine (CDEDC),  $N,N'$ -(oxybis(4,1-phenylene))bis(2,4-dichloro-1,3,5-triazin-6-amine) (CODAC) and  $N,N'$ -(methylenebis(4,1-phenylene))bis(2,4-dichloro-1,3,5-triazin-6-amine) (CMDAC).

### 3.2.1 Synthesis of 2,4-dichloro-6-methoxy-1,3,5-triazine (MMT)

2,4-dichloro-6-methoxy-1,3,5-triazine (MMT) is widely known in literature as building block for many applications and more than 150 publications exist concerning its use. As instance, MMT has been used for OLED technology,<sup>[52]</sup> synthesis of antimicrobials and peptides,<sup>[22,53]</sup> or in patents for production of antitumor drugs.<sup>[54,55]</sup>

To the best of our knowledge, only few examples exist about application of 2,4-dichloro-6-methoxy-1,3,5-triazine as precursor of ammonium salts. Kunishima *et al.* have recently published studies about ammonium salts synthesized from 2-chloro-4-methoxy-6-amido-1,3,5-triazine and 2-chloro-4-methoxy-6-imido-1,3,5-triazine,<sup>[33,34]</sup> where MMT is used as reagent for 2-chloro-4,6-disubstituted triazine synthesis. Only one case of bis-ammonium salts directly derived by 2,4-dichloro-6-methoxy-1,3,5-triazine is known: an untranslated french-belgian patent published by Sandoz Ltd. (now Novartis International AG) for antifouling and antitumoral applications.<sup>[55]</sup>

As reported by Kaminski,<sup>[29]</sup> MMT has been synthesized starting from cyanuric chloride in methanol, in the presence of an inorganic base. In order to avoid formation of CDMT by second substitution on the triazine ring, the reaction has been carried out at 0 °C. (**Scheme 3.15**).



**Scheme 3.15:** Synthesis of 2,4-dichloro-6-methoxy-1,3,5-triazine (MMT).

The reaction is monitored by gas-chromatographic analyses and it is led to complete conversion in 1 hour.  $^1\text{H}$  NMR,  $^{13}\text{C}$  NMR and FT-IR spectra confirmed the isolation of the desired product, MMT, with 97% of yield (purity 98%).

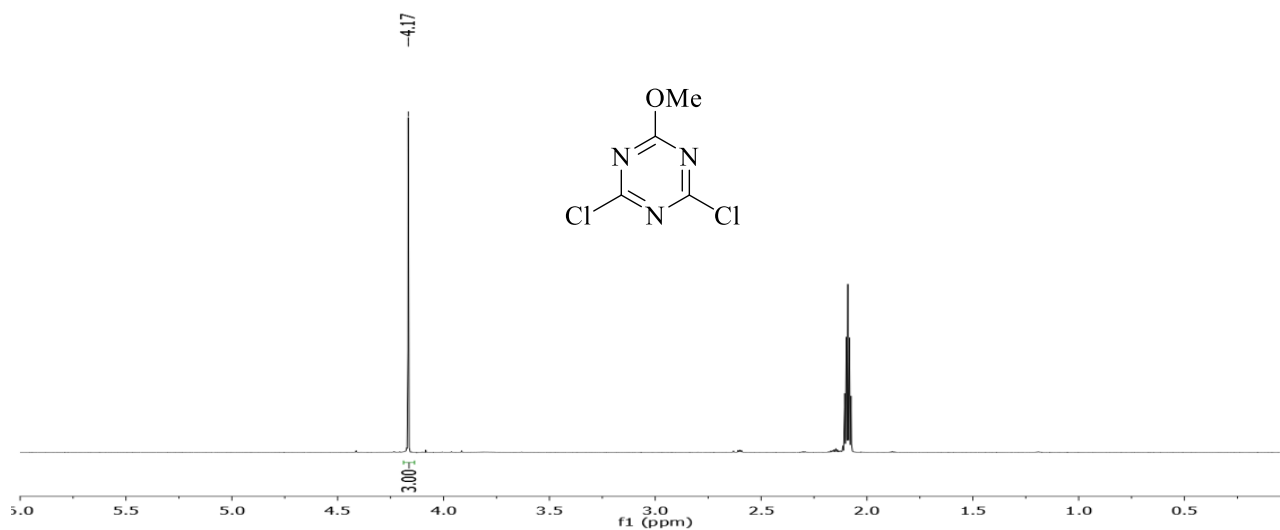


**Figure 3.18:**  $^1\text{H}$  NMR spectrum (acetone- $d_6$ ) of 2,4-dichloro-6-methoxy-1,3,5-triazine (MMT).

$^1\text{H}$  NMR (300 MHz, acetone- $d_6$ , ppm): 4.17 (3H, s,  $\text{OCH}_3$ ).

In  $^1\text{H}$  NMR spectrum (**Figure 3.18**), a singlet is present at 4.17 ppm, attributable to protons of the methoxy group.

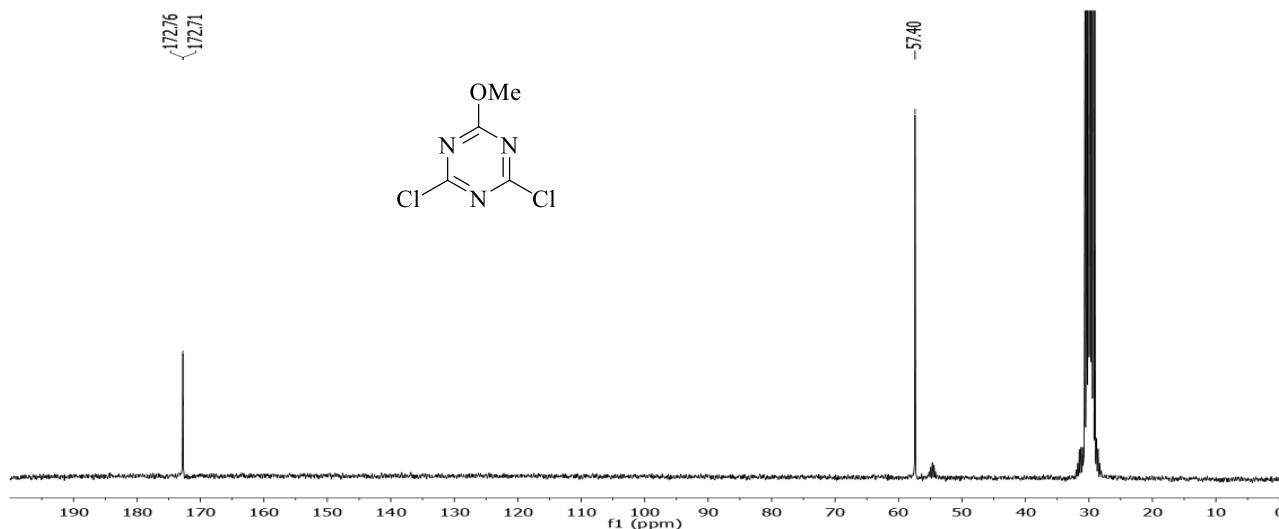


**Figure 3.19:**  $^{13}\text{C}$  NMR spectrum (acetone- $d_6$ ) of 2,4-dichloro-6-methoxy-1,3,5-triazine (MMT).

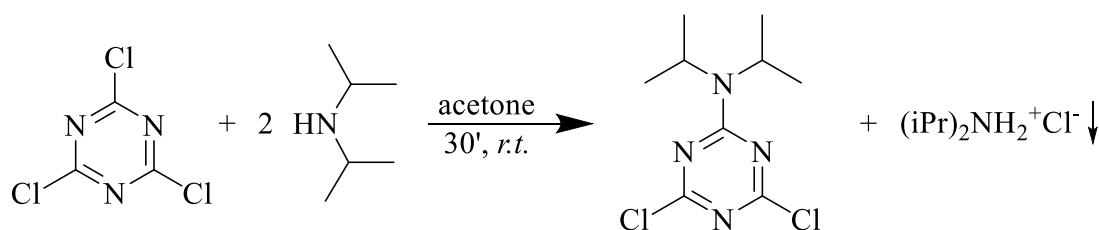
$^{13}\text{C}$  NMR (300 MHz, acetone- $d_6$ , ppm): 172.76, 172.71, 57.40.

In  $^{13}\text{C}$  NMR spectrum (**Figure 3.19**), signals at 172.76 ppm and at 172.71 ppm are attributable to triazine carbons, while the signal at 57.40 ppm is assignable to methoxy group carbon.

Finally, 2,4-dichloro-6-methoxy-1,3,5-triazine (MMT) has been successfully used for synthesis of bis-ammonium salts and reported later in this work. (**Chapter 3.3.1**)

### 3.2.2 Synthesis of 2,4-dichloro-6-diisopropylamino-1,3,5-triazine (MIAT)

Many studies are reported in literature about application of 2,4-dichloro-6-diisopropylamino-1,3,5-triazine (MIAT) as building block for compounds with biological activities.<sup>[56,57]</sup> MIAT is a reaction intermediate for the synthesis of 2-chloro-4,6-bis-diisopropylamine-1,3,5-triazine (DIAT) reported above (**Chapter 3.1.1**). The synthesis has been carried out by reaction of cyanuric chloride with an excess of diisopropylamine in acetone solution at *r.t.*. In this case the amine is employed both as reagent and as scavenger for chloridric acid formed during the reaction. (**Scheme 3.16**)



**Scheme 3.16:** Synthesis of 2,4-dichloro-6-diisopropylamine-1,3,5-triazine (MIAT).

Thanks to gas-chromatographic analyses, it is possible to monitor the reaction, led to complete conversion in 20 minutes. <sup>1</sup>H NMR, <sup>13</sup>C NMR and FT-IR spectra confirmed the isolation of the desired product, MIAT, with 95% of yield (purity 96%).

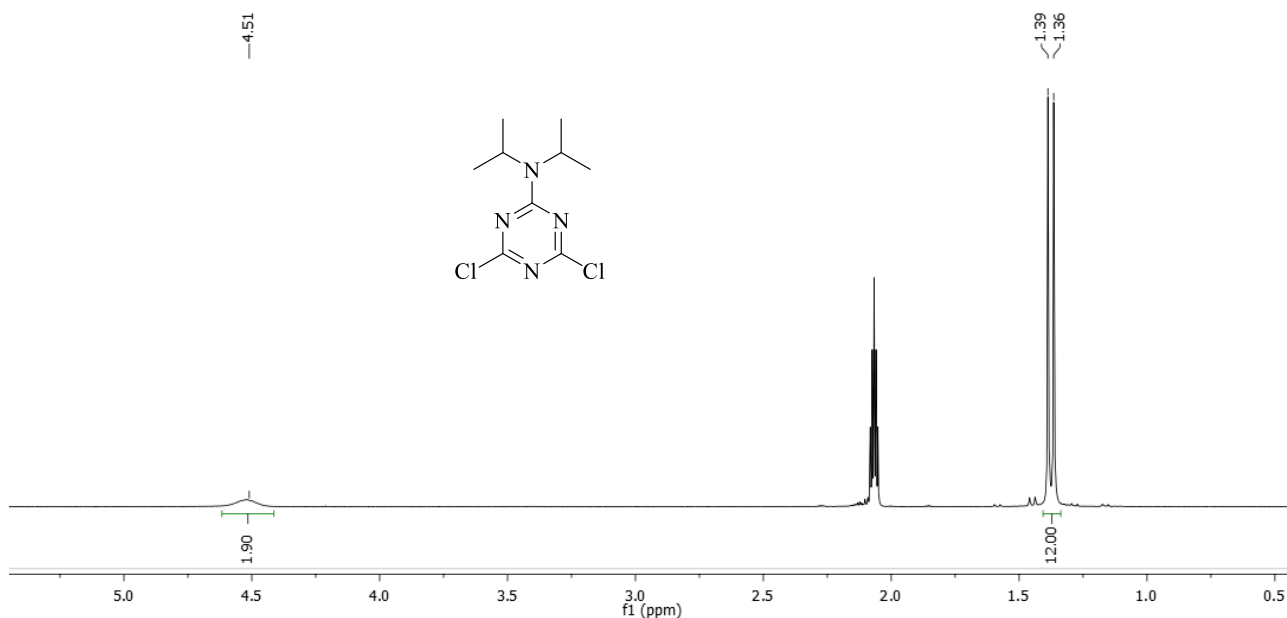


**Figure 3.20:** <sup>1</sup>H NMR spectrum (acetone-d<sub>6</sub>) of 2,4-dichloro-6-diisopropylamine-1,3,5-triazine (MIAT).

<sup>1</sup>H NMR (300 MHz, acetone-d<sub>6</sub>, ppm): 4.51 (2H, m broad, NCH(CH<sub>3</sub>)<sub>2</sub>), 1.39 (12H, d, NCH(CH<sub>3</sub>)<sub>2</sub>).

$^1\text{H}$  NMR spectrum (**Figure 3.20**) presents a broad signal at 4.54 ppm attributable to  $\text{NCH}(\text{CH}_3)_2$  proton of isopropyl group, while the doublet at 1.39 ppm is assignable to  $\text{NCH}(\text{CH}_3)_2$  protons.

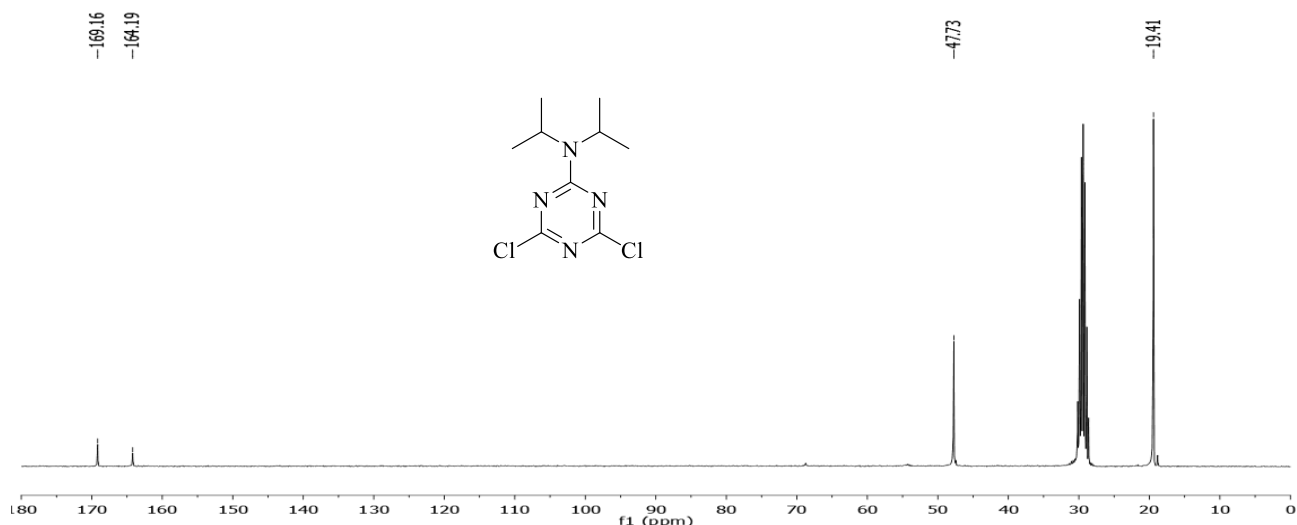


**Figure 3.21:**  $^{13}\text{C}$  NMR spectrum (acetone- $d_6$ ) of 2,4-dichloro-6-diisopropylamine-1,3,5-triazine (MIAT).

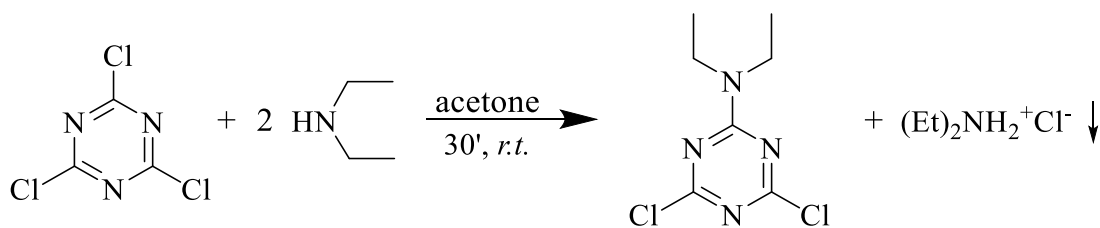
$^{13}\text{C}$  NMR (300 MHz, acetone- $d_6$ , ppm): 169.16, 164.19, 47.73, 19.41.

In  $^{13}\text{C}$  NMR (**Figure 3.21**), signals at 169.19 ppm and at 164.19 ppm are attributable to C-Cl and C-N carbons of triazine ring. Signal at 47.73 ppm is attributable to tertiary carbons of isopropyl groups, while signal at 19.41 ppm is attributable to primary carbons.

Finally, 2,4-dichloro-6-diisopropylamine-1,3,5-triazine (MIAT) has been successfully used for synthesis of bis-ammonium salts and reported later in this work. (**Chapter 3.3.2**)

### 3.2.3 Synthesis of 2,4-dichloro-6-diethylamino-1,3,5-triazine (MEAT)

2,4-dichloro-6-diethylamine-1,3,5-triazine (MEAT) is known in literature for its application as building block for the synthesis of antimalarian compounds<sup>[56]</sup> or as ligand in the synthesis for noble metals complexes.<sup>[58]</sup> MEAT is a reaction intermediate for the synthesis of 2-chloro-4,6-bis-diethylamine-1,3,5-triazine (DEAT) reported above. (**Chapter 3.1.2**) In particular, the synthesis has been carried out adding dropwise an excess of diethylamine to an acetone solution of cyanuric chloride. As reported before, the amine acts as reagent and scavenger to chloridric acid formed during the reaction. (**Scheme 3.17**)



**Scheme 3.17:** Synthesis of 2,4-dichloro-6-diethylamino-1,3,5-triazine (MEAT).

Thanks to gas-chromatographic analyses, it is possible to monitor the reaction, carried out to complete conversion in 30 minutes.  $^1\text{H}$  NMR,  $^{13}\text{C}$  NMR and FT-IR spectra confirmed isolation of the desired product, MEAT, with 92% of yield (purity 97%).

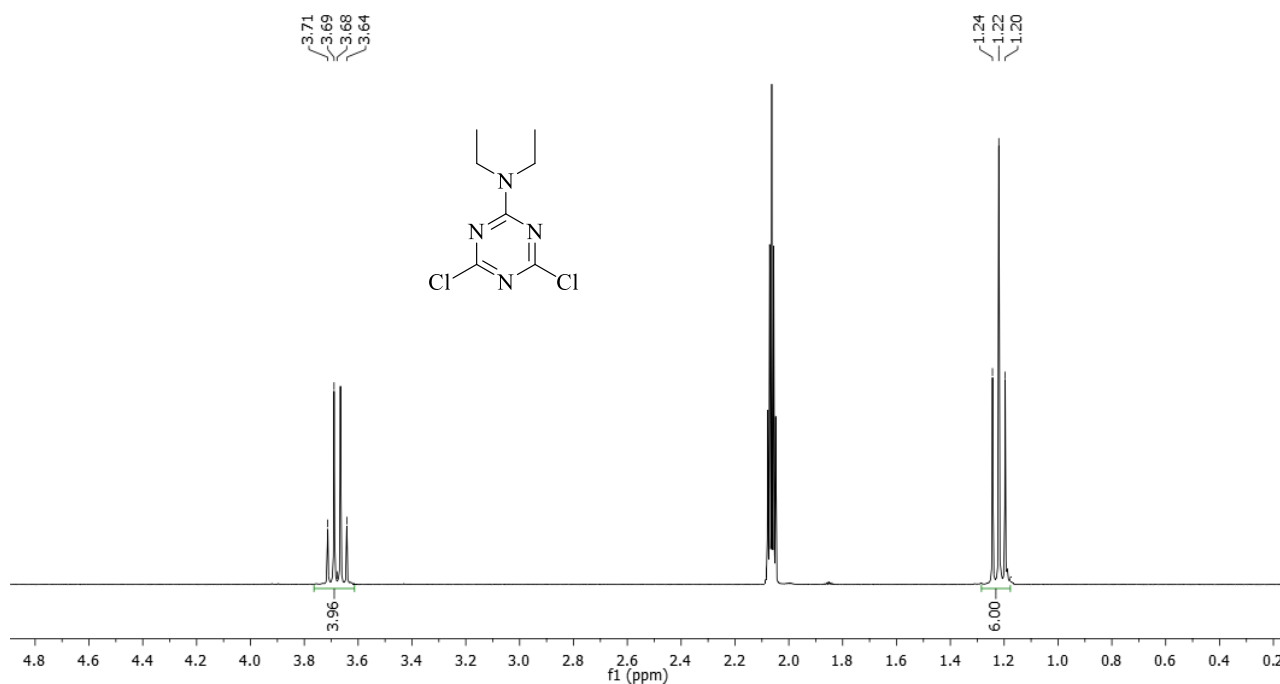


**Figure 3.22:**  $^1\text{H}$  NMR spectrum (acetone- $d_6$ ) of 2,4-dichloro-6-diethylamino-1,3,5-triazine (MEAT).

$^1\text{H}$  NMR (300 MHz, acetone- $d_6$ , ppm): 3.71 (4H, q,  $\text{NCH}_2\text{CH}_3$ ), 1.22 (6H, t,  $\text{NCH}_2\text{CH}_3$ ).

In the  $^1\text{H}$  NMR (**Figure 3.22**), it is possible to observe a quartet at 3.72 ppm and a triplet at 1.25 ppm attributable respectively to ( $\text{NCH}_2\text{CH}_3$ ) and ( $\text{NCH}_2\text{CH}_3$ ) protons of the ethyl groups.

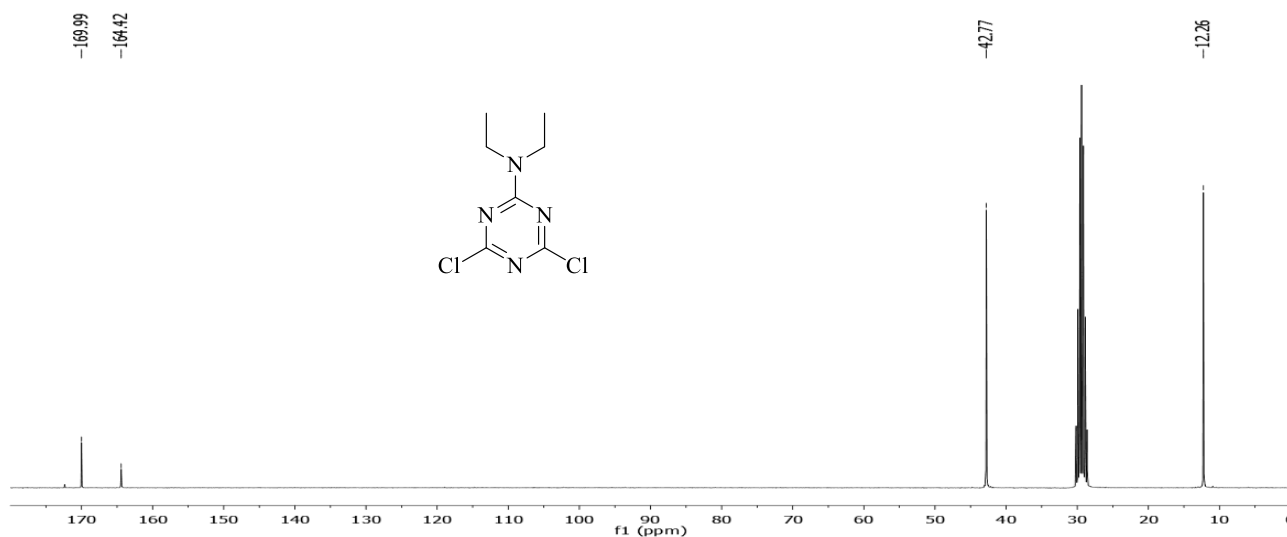


**Figure 3.23:**  $^{13}\text{C}$  NMR spectrum (acetone- $d_6$ ) of 2,4-dichloro-6-diethylamino-1,3,5-triazine (MEAT).

$^{13}\text{C}$  NMR (300 MHz, acetone- $d_6$  ppm): 169.99, 164.42, 42.77, 12.26.



In  $^{13}\text{C}$  NMR spectrum (**Figure 3.23**), signals of the triazine carbons are observable at 169.99 ppm and at 164.42 ppm, attributable respectively to chloro-substituted and nitrogen-substituted carbons. Signals at 42.77 ppm and at 12.26 ppm are assignable to the secondary and primary carbons of ethyl groups.

Finally, 2,4-dichloro-6-diethylamine-1,3,5-triazine (MEAT) has been successfully used for synthesis of bis-ammonium salts and reported later in this work. (**Chapter 3.3.3**)

### 3.2.4 Synthesis of $N_1,N_2$ -bis(2,4-dichloro-1,3,5-triazin-6-yl)- $N_1,N_2$ -diethylethane-1,2-diamine (CDEDC)

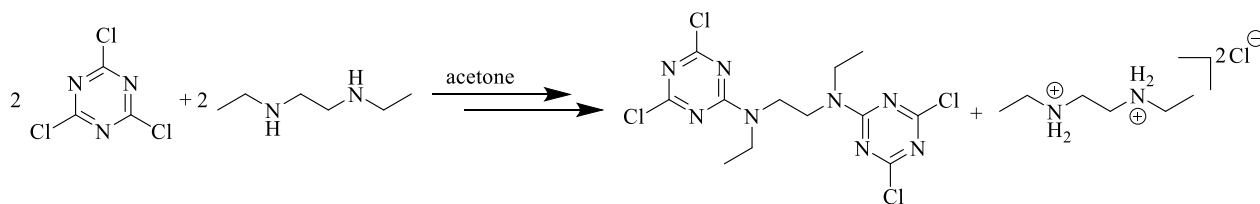
In literature alkyldiamines are used with 1,3,5-triazine for the synthesis of polyguanamines: many studies are reported by application of primary diamines in polycondensations with 2,4-dichloro-6-substituted-1,3,5-triazines at high temperatures, with a ratio diamine:triazine of 1:1.<sup>[59,60]</sup>

To the best of our knowledge, only one study is known reporting a ratio 1:2 for reactions between an alkyldiamine and 2-chloro-4,6-disubstituted-1,3,5-triazines: Austin *et al.* investigated the alkylation of tertiary bis-ammonium salts for chemoterapeutic purposes.<sup>[61]</sup>

Reactions between diamine and 1,3,5-triazine with at least two reactive sites, such as cyanuric chloride are susceptible to polymerization and oligomerization issues. Thus, synthesis of  $N_1,N_2$ -bis(2,4-dichloro-1,3,5-triazin-6-yl)- $N_1,N_2$ -diethylethane-1,2-diamine (CDEDC) requires low temperature and great attention to stoichiometry.

First trials for the synthesis of CDEDC have been carried out by reacting cyanuric chloride and  $N,N'$ -diethylethylenediamine (DED) with a ratio 2:1, using  $\text{NaHCO}_3$  as scavenger for HCl formed during the reaction. Unfortunately gas-chromatographic analyses showed that, after 5 hours, conversion was at 50%, NMR analyses of the precipitated solid suggested the formation of  $N,N'$ -diethylethane-1,2-bis-ammonium dichloride. Similarly to what has been reported for DIAT (**Chapter 3.1.1**),  $\text{NaHCO}_3$  is in heterogeneous phase and does not compete efficiently with the diamine for HCl scavenging (pKa 10.46 for DED and pKa 10.33 for  $\text{NaHCO}_3$ ).<sup>[62]</sup>

Therefore, CDEDC has been synthesized by the reaction of cyanuric chloride and DED with a stoichiometric ratio of 1:1. In order to avoid oligomerization issues by the second substitution of the triazine ring, the reaction has been carried out at 0 °C with two aliquotes of DED added at 30 minutes distance. (**Scheme 3.18**)



**Scheme 3.18:** Synthesis of  $N_1,N_2$ -bis(2,4-dichloro-1,3,5-triazin-6-yl)- $N_1,N_2$ -diethylethane-1,2-diamine (CDEDC).

The reaction was monitored by gas-chromatographic analyses and it is led to complete conversion in 90 minutes.  $^1\text{H}$  NMR,  $^{13}\text{C}$  NMR and FT-IR spectra confirmed the desired product isolation, CDEDC, with 97% of yield (purity 98%).

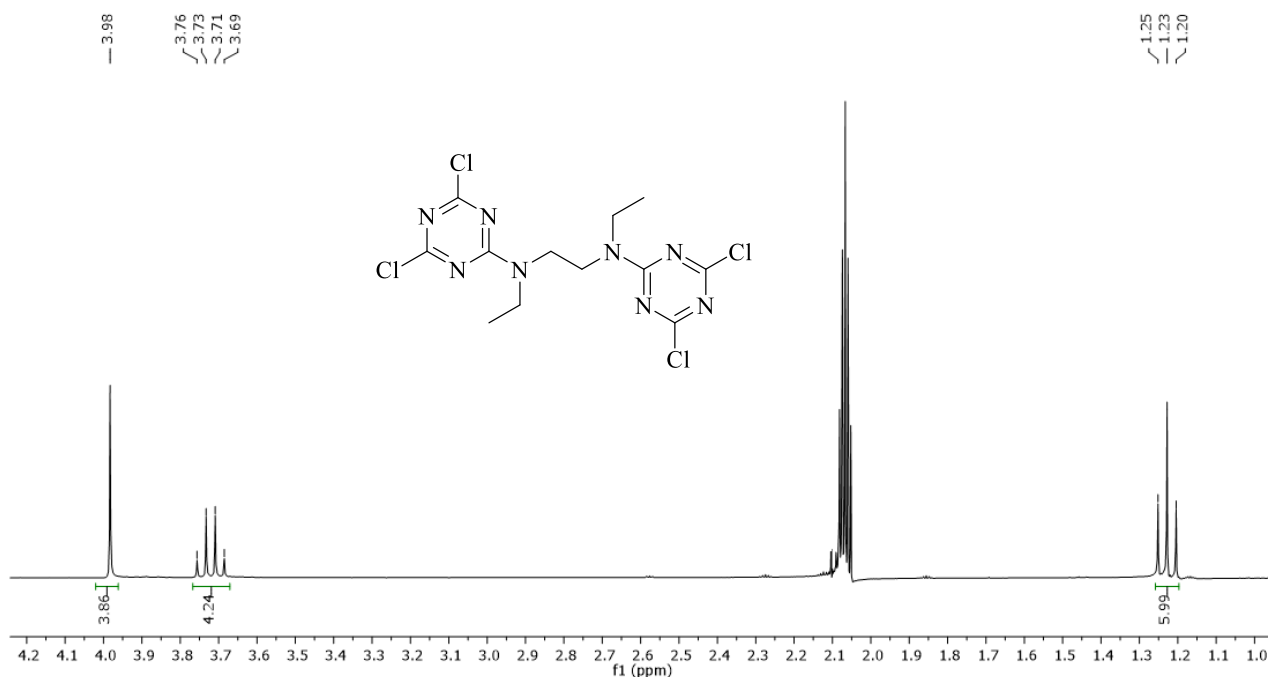


**Figure 3.24:**  $^1\text{H}$  NMR spectrum (acetone- $d_6$ ) of  $N_1,N_2$ -bis(2,4-dichloro-1,3,5-triazin-6-yl)- $N_1,N_2$ -diethylethane-1,2-diamine (CDEDC).

$^1\text{H}$  NMR (300 MHz, acetone- $d_6$ , ppm): 3.98 (4H, m s,  $\text{NCH}_2\text{CH}_2\text{N}$ ), 3.73 (4H, q,  $\text{NCH}_2\text{CH}_3$ ), 1.23 (6H, t,  $\text{NCH}_2\text{CH}_3$ ).

In  $^1\text{H}$  NMR spectrum (**Figure 3.24**), it is possible to observe the signals of ethyl groups: a quadruplet at 3.73 ppm and a triplet at 1.23 ppm respectively for  $\text{NCH}_2\text{CH}_3$  and  $\text{NCH}_2\text{CH}_3$  protons. Singlet at 3.98 ppm is assignable to ethylene bridging group. Considering the  $^1\text{H}$  NMR spectrum of the reagent  $N,N'$ -diethylethylenediamine (DED):

$^1\text{H}$  NMR (300 MHz, acetone- $d_6$ , ppm): 2.64 (4H, m s,  $\text{NCH}_2\text{CH}_2\text{N}$ ), 2.63 (4H, q,  $\text{NCH}_2\text{CH}_3$ ), 1.62 (2H, s broad,  $\text{NH}_2$ ), 1.07 (6H, t,  $\text{NCH}_2\text{CH}_3$ ).

It is possible to observe that in CDEDC  $\alpha$  protons signals shift to low field due to the electron withdrawing effect of the triazine.

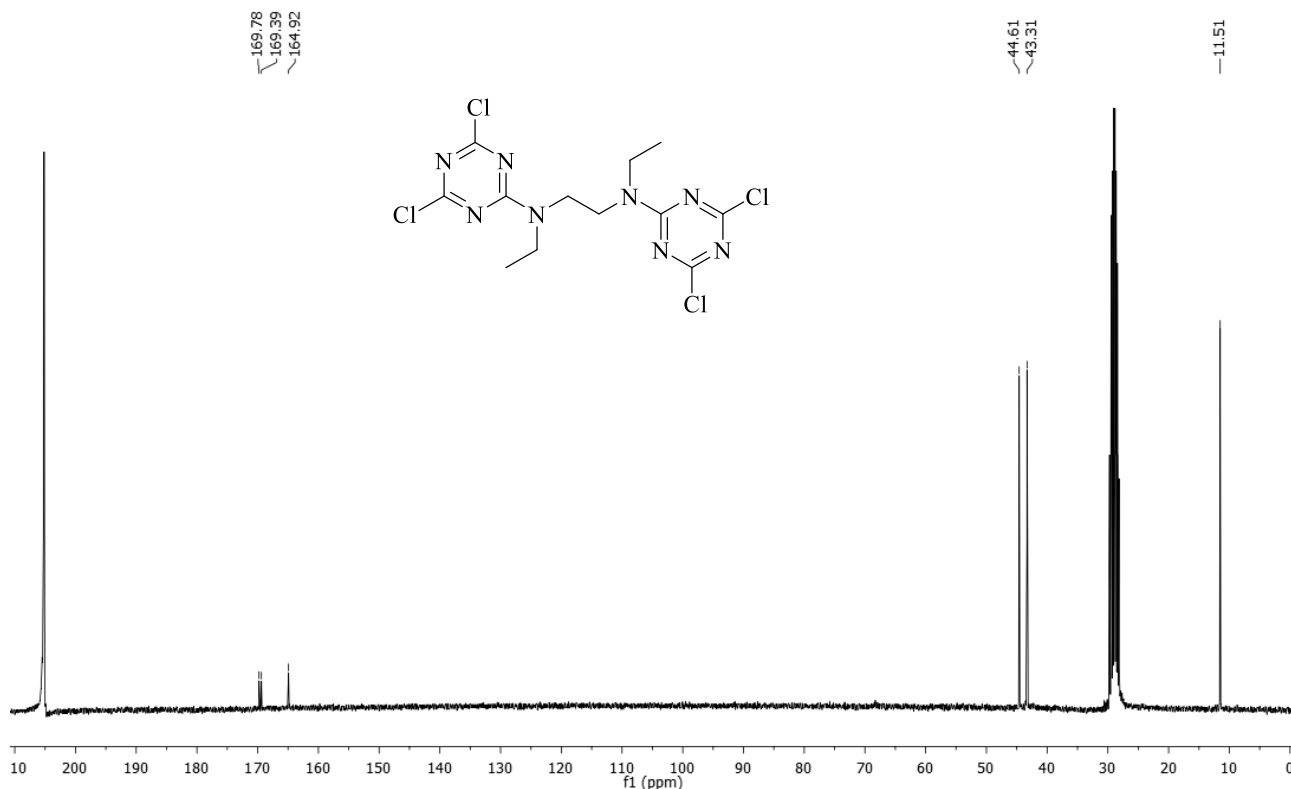


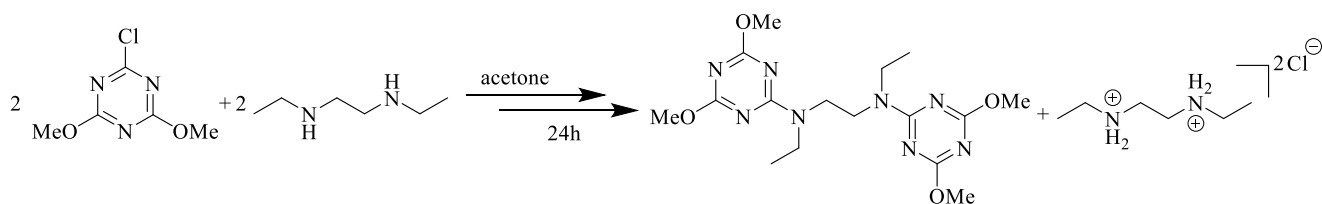
**Figure 3.25:**  $^{13}\text{C}$  NMR spectrum (acetone- $d_6$ ) of  $N_1,N_2$ -bis(2,4-dichloro-1,3,5-triazin-6-yl)- $N_1,N_2$ -diethylethane-1,2-diamine (CDEDC).

$^{13}\text{C}$  NMR (300 MHz, acetone- $d_6$ , ppm): 169.78, 169.39, 164.92, 44.61, 43.31, 11.51.

In  $^{13}\text{C}$  NMR spectrum (**Figure 3.25**), signals of aliphatic diamine moieties are observable at high field. Signals at 44.61 ppm and at 43.31 ppm are attributable to carbons in  $\alpha$  position to the nitrogen while the signal at 11.51 ppm is assignable to ( $\text{NCH}_2\text{CH}_3$ ) carbon.

Triazine carbons signals are observable at low-field of the spectrum, the signal at 164.92 ppm is attributable to C-N carbon, while the two close signals at 169.78 ppm and 169.39 ppm are assignable to C-Cl carbons. Halogenated atoms do not have the same resonance frequencies probably due to restricted rotation around the Triazine-N bond, with a mechanism similar to what has been explained previously.<sup>[36,41]</sup> (**Chapter 3.1.3**)

In order to confirm the restricted bond rotation, in place of cyanuric chloride, 2-chloro-4,6-dimethoxy-1,3,5-triazine (CDMT) has been used. The synthesis of  $N_1,N_2$ -bis(2,4-dimethoxy-1,3,5-triazin-6-yl)- $N_1,N_2$ -diethylethane-1,2-diamine (DDEDD) has been carried out in acetone for 24 hours. (**Scheme 3.19**)



**Scheme 3.19:** Synthesis of  $N_1,N_2$ -bis(2,4-dimethoxy-1,3,5-triazin-6-yl)- $N_1,N_2$ -diethylethane-1,2-diamine (DDEDD).

$^1\text{H}$  NMR,  $^{13}\text{C}$  NMR and FT-IR spectra confirmed the desired product isolation, DDEDD, with 90% of yield (purity 97%).

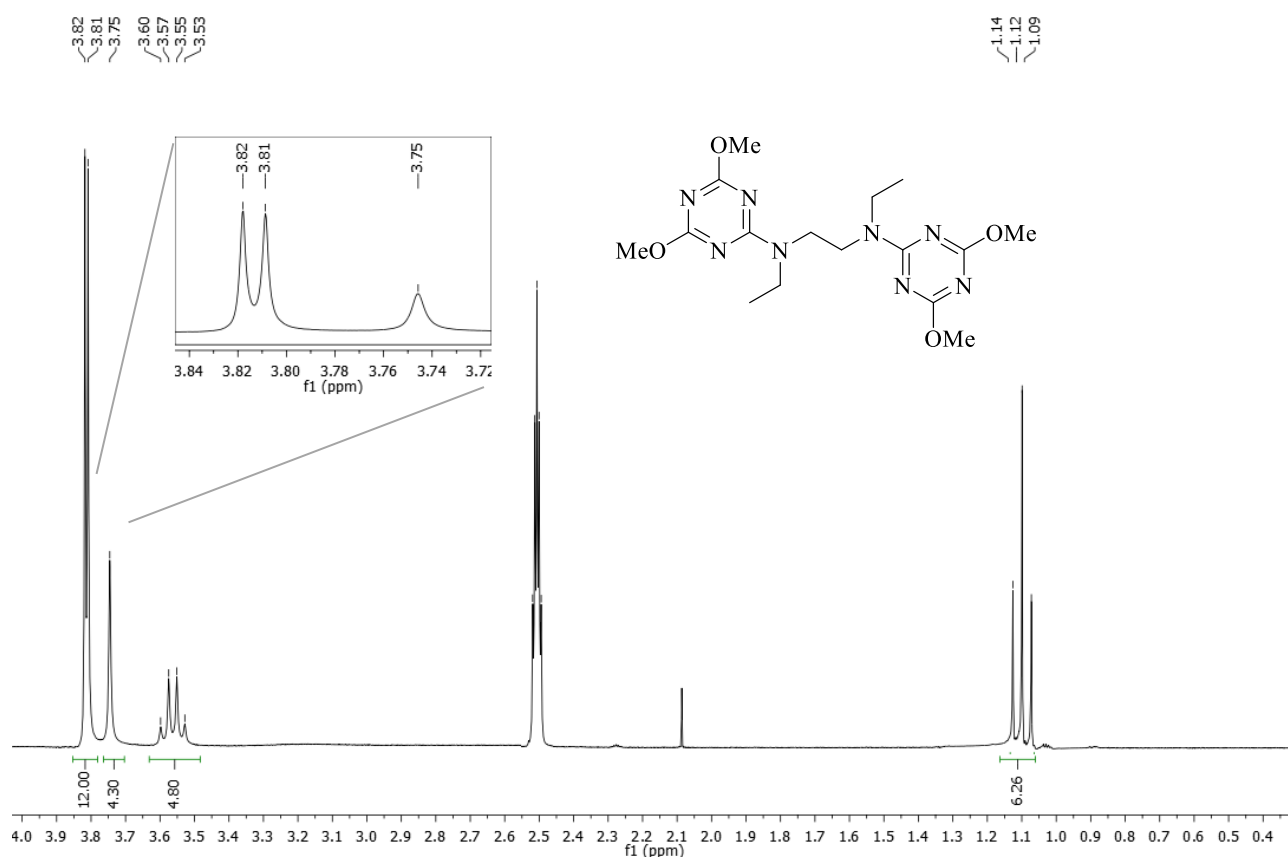


**Figure 3.26:**  $^1\text{H}$  NMR spectrum (DMSO- $d_6$ ) of  $N_1,N_2$ -bis(2,4-dimethoxy-1,3,5-triazin-6-yl)- $N_1,N_2$ -diethylethane-1,2-diamine (DDEDD) at 298 K.

$^1\text{H}$  NMR (300 MHz, DMSO- $d_6$ , ppm): 3.82-3.81 (12H, s,  $\text{OCH}_3$ ), 3.75 (4H, s,  $\text{NCH}_2\text{CH}_2\text{N}$ ), 3.57 (4H, q,  $\text{NCH}_2\text{CH}_3$ ), 1.12 (6H, t,  $\text{NCH}_2\text{CH}_3$ ).

In  $^1\text{H}$  NMR spectrum (**Figure 3.26**), it is possible to give signals attributions similar to CDEDC: ethylene bridge signal is observable at 3.75 ppm, while ethyl protons signals are observable at 3.57 ppm and at 1.12 ppm, respectively for  $\text{NCH}_2\text{CH}_3$  and  $\text{NCH}_2\text{CH}_3$  protons. Two signals at 3.82-3.81 ppm are assignable to methoxy groups protons. These atoms do not possess the same frequencies

due to the restricted bond rotation around Triazine-N bond. When DDEDD is heated at 338 K, it is possible to observe the two signals coalesce into one. (**Figure 3.27**)

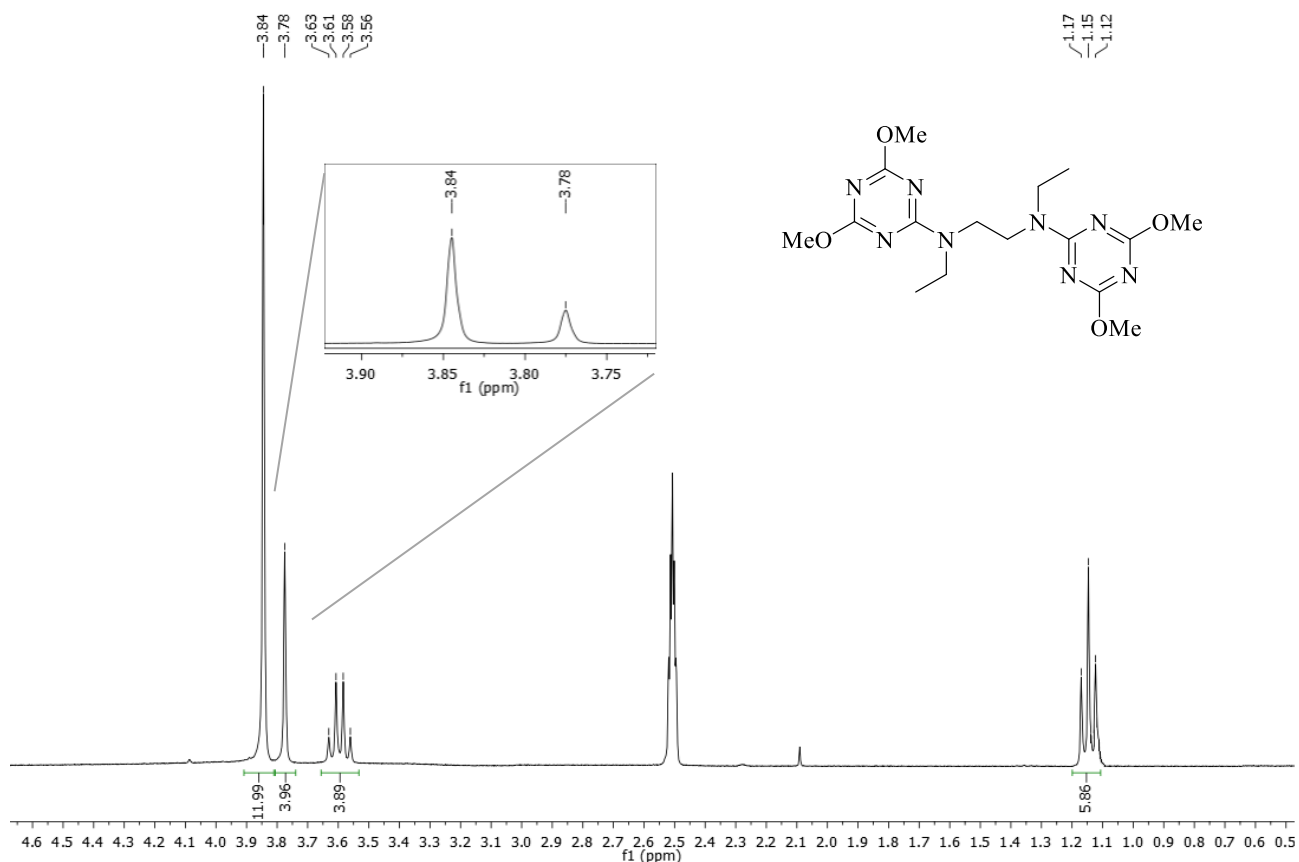


**Figure 3.27:**  $^1\text{H}$  NMR spectrum (DMSO- $d_6$ ) of  $N_1,N_2$ -bis(2,4-dimethoxy-1,3,5-triazin-6-yl)- $N_1,N_2$ -diethylethane-1,2-diamine (DDEDD) at 338 K.

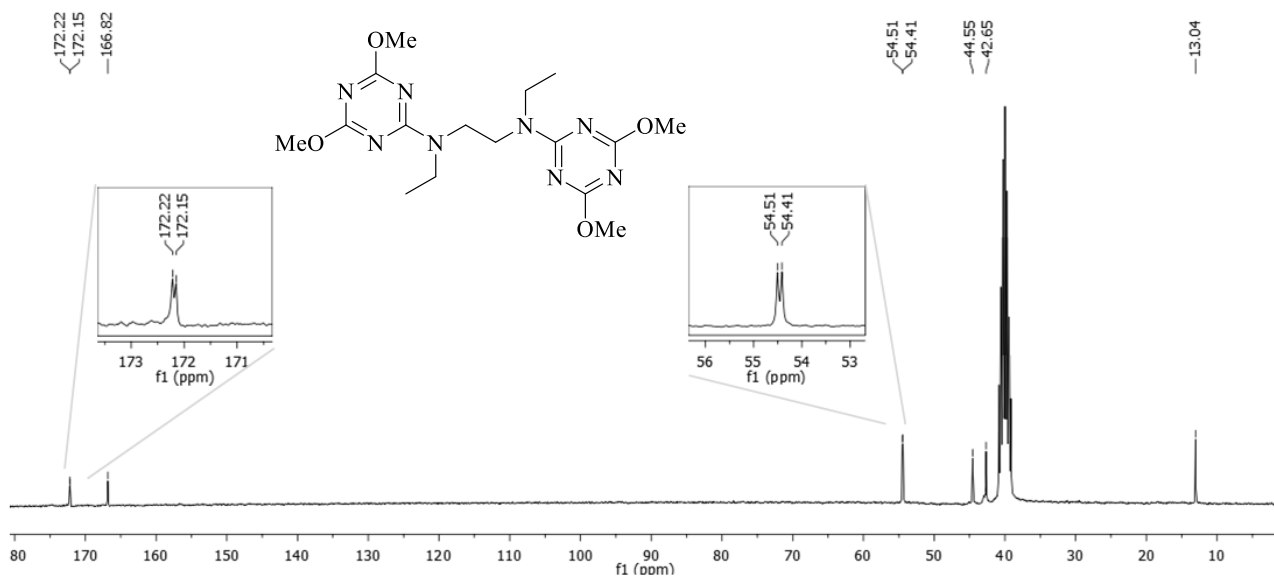


**Figure 3.28:**  $^{13}\text{C}$  NMR spectrum (DMSO- $d_6$ ) of  $N_1,N_2$ -bis(2,4-dimethoxy-1,3,5-triazin-6-yl)- $N_1,N_2$ -diethylethane-1,2-diamine (DDEDD) at 298 K.

$^{13}\text{C}$  NMR (300 MHz, DMSO- $d_6$ , ppm): 172.22, 172.15, 166.82, 54.51, 54.41, 44.55, 42.65, 13.04.

In  $^{13}\text{C}$  NMR spectrum (**Figure 3.28**), it is possible to observe signals of diamine moieties at low field of the spectrum, between 44.55 ppm and 13.04 ppm, very similar to CDEDC signals (**Figure 3.25**). Triazine ring carbons are observable at high field of the spectrum, while methoxy groups can be assigned to the couple of signal at 54.51-54.41 ppm.

$^{13}\text{C}$  NMR spectroscopy further confirm barrier to rotation around Triazine-N bond, indeed, it is observed that methoxy groups of each triazine do not possess the same frequencies due to a different spatial arrangement. (**Figure 3.29**)

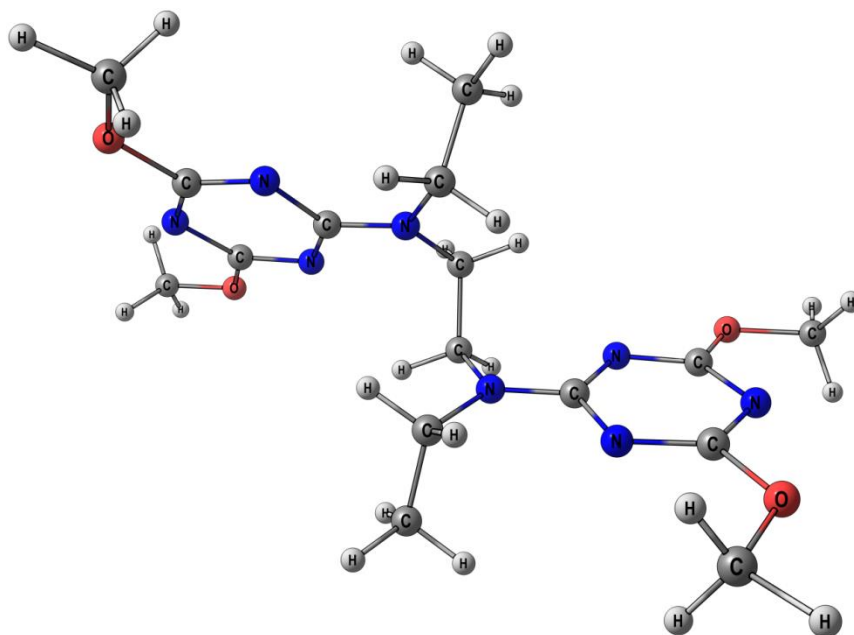


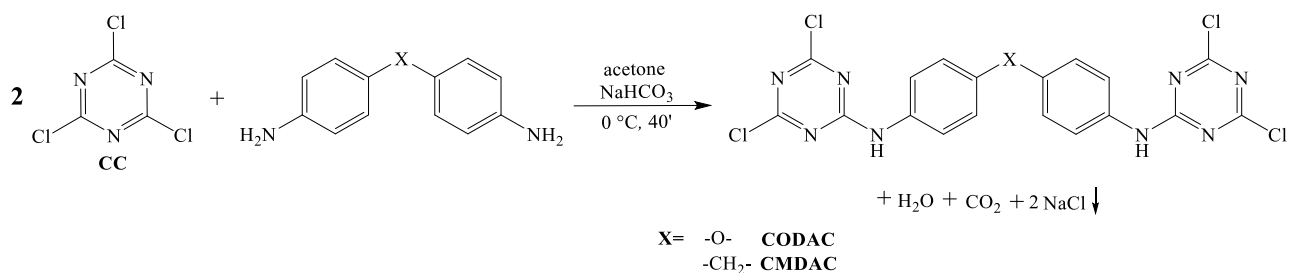
**Figure 3.29:** Spatial arrangement supposed for  $N_1,N_2$ -bis(2,4-dimethoxy-1,3,5-triazin-6-yl)- $N_1,N_2$ -diethylethane-1,2-diamine (DDEDD).

Finally,  $N_1,N_2$ -bis(2,4-dichloro-1,3,5-triazin-6-yl)- $N_1,N_2$ -diethylethane-1,2-diamine (CDEDC) has been used for the synthesis of a tetrakis-ammonium salt and reported later in this work. (**Chapter 3.3.4**)

### 3.2.5 Syntheses of $N,N'$ -(oxybis(4,1-phenylene))bis(2,4-dichloro-1,3,5-triazin-6-amine) (CODAC) and $N,N'$ -(methylenebis(4,1-phenylene))bis(2,4-dichloro-1,3,5-triazin-6-amine) (CMDAC)

As reported previously (**Chapters 3.1.4 and 3.1.5**), triazine substituted by anilino-derivatives are of great interest in many fields.<sup>[42,44,45]</sup> Kusano *et al.* and Yuan *et al.* reported the synthesis of compounds with 4,4'-oxydianiline (ODA) and 4,4'-methyldianiline (MDA) acting as bridges between two 2,4-dichloro-6-substituted-1,3,5-triazines used for the studies on calixarenes.<sup>[47,48]</sup> Hence, compounds based on ODA and MDA were investigated for the synthesis of ammonium salts precursors with two triazine rings and four reactive sites.

Syntheses of CODAC and CMDAC have been carried out by the reaction between cyanuric chloride and respectively 4,4'-oxydianiline or 4,4'-methyldianiline in the presence of an inorganic base. The yield is quantitative without the need to use an excess of dianiline, indeed, para-aryl substituted aniline derivatives possess a pKa ca. 4.2 and do not compete with an inorganic base for HCl scavenging.<sup>[49]</sup> Moreover, in order to avoid oligomerization by the second substitution of the triazine ring, the reaction has been carried out at 0 °C. (**Scheme 3.20**).



**Scheme 3.20:** Synthesis of *N,N'*-(oxybis(4,1-phenylene))bis(2,4-dichloro-1,3,5-triazin-6-amine) (CODAC) and *N,N'*-(methylenebis(4,1-phenylene))bis(2,4-dichloro-1,3,5-triazin-6-amine) (CMDAC).

The reactions were monitored by gas-chromatographic analyses and led to complete conversion in 40 minutes. <sup>1</sup>H NMR, <sup>13</sup>C NMR and FT-IR spectra confirmed the isolation of the desired products with yields above 84% (purity >96%). NMR spectra of CODAC are reported as example of characterization of the two compounds.

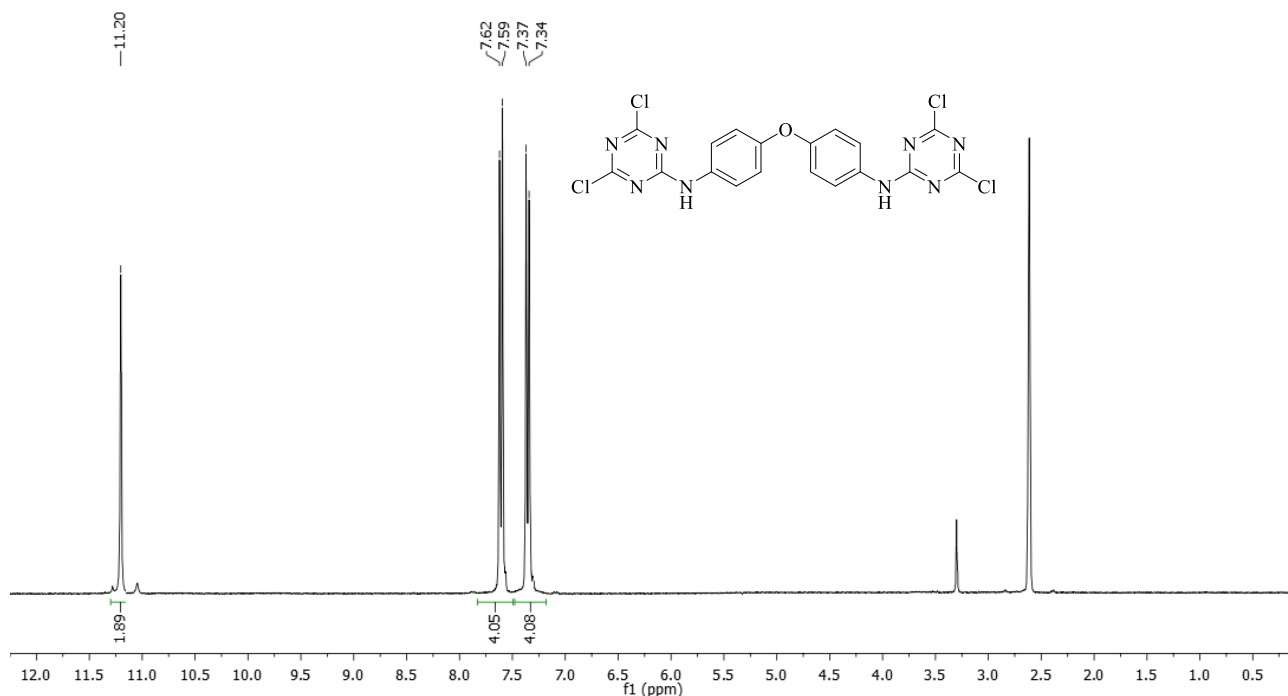


**Figure 3.30:** <sup>1</sup>H NMR spectrum (DMSO-d<sub>6</sub>) of *N,N'*-(oxybis(4,1-phenylene))bis(2,4-dichloro-1,3,5-triazin-6-amine) (CODAC).

$^1\text{H}$  NMR (300 MHz, DMSO- $d_6$ , ppm): 11.20 (2H, s, NH), 7.62 (4H, m, NCC $\mathbf{H}$ CHCO), 7.37 (4H, m, NCC $\mathbf{H}$ CHCO).

In  $^1\text{H}$  NMR spectrum (**Figure 3.30**), typical aromatic proton signals are observable between 7.62 ppm and 7.34 ppm. Signal at 11.20 ppm is attributable to NH protons. As explained before (**Chapters 3.1.4 and 3.1.5**), the lone pair of the nitrogens conjugates with the  $\pi$  aromatic system to create a partial double bond, shifting amino protons signal to low field of the spectrum.<sup>[50,51]</sup> Differently from MODAM and MMDAM, the two rotamers are not observable due to the presence of two equals substituents in position 2 and 4 of the triazine rings.

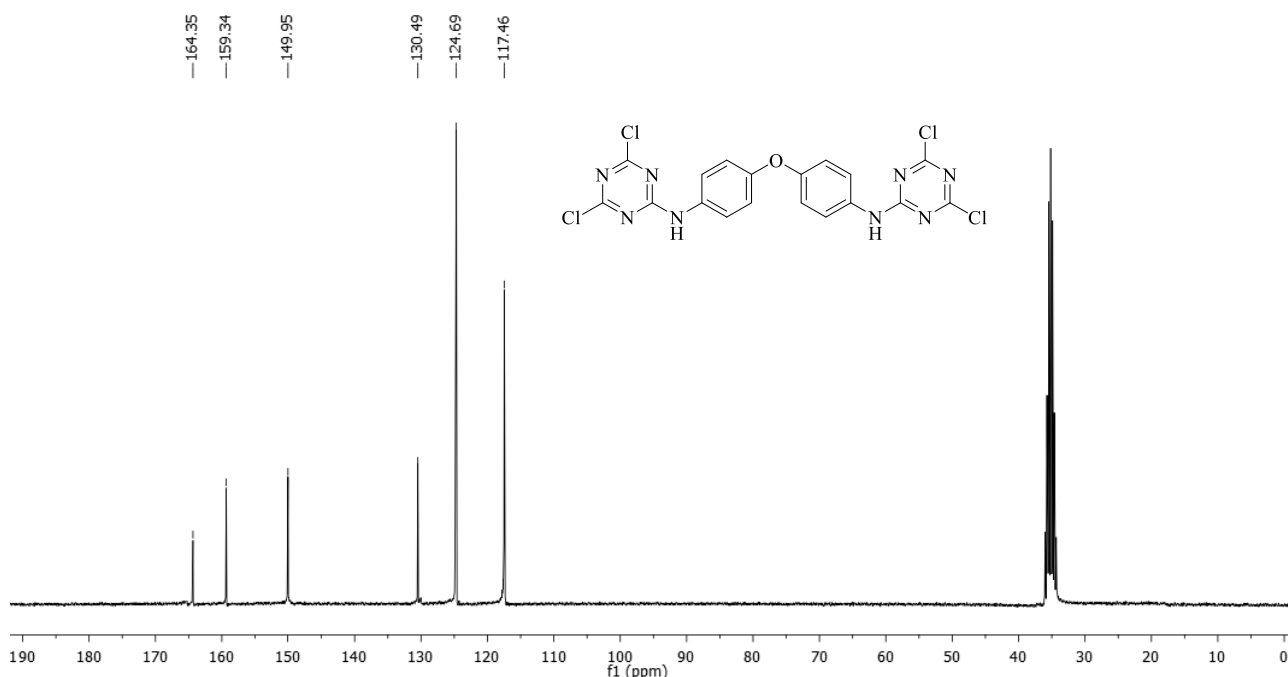


**Figure 3.31:**  $^{13}\text{C}$  NMR spectrum (DMSO- $d_6$ ) of *N,N'*-(oxybis(4,1-phenylene))bis(2,4,-dichloro-1,3,5-triazin-6-amine) (CODAC).

$^{13}\text{C}$  NMR (300 MHz, DMSO- $d_6$ , ppm): 164.35, 159.34, 149.95, 130.49, 124.69, 117.46.

In  $^{13}\text{C}$  NMR spectrum (**Figure 3.31**), the signals at 164.35 ppm and 159.34 ppm are attributable to triazine ring carbons, while aromatic carbon signals are observable between 149.95 ppm and 117.46 ppm. These attributions are in accord with the resonance frequencies of  $^{13}\text{C}$  NMR spectrum of MODAM. (**Chapter 3.1.4**) Similar results have been achieved in characterization of CMDAC, reported below:

$^1\text{H}$  NMR (300 MHz, DMSO- $d_6$ , ppm): 11.10 (2H, s, NH), 7.49 (4H, m, NCC $\mathbf{H}$ CHCO), 7.24 (4H, m, NCC $\mathbf{H}$ CHCO), 3.91 (2H, s,  $\mathbf{CH}_2$ ).

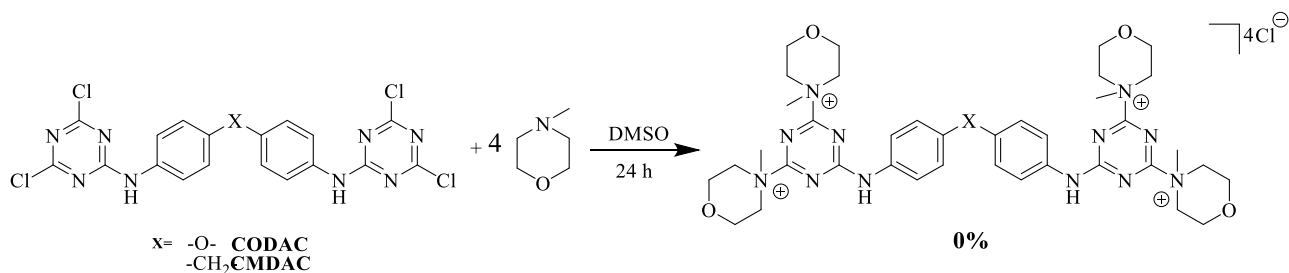
$^{13}\text{C}$  NMR (300 MHz, DMSO- $d_6$ , ppm): 169.14, 164.13, 138.50, 135.28, 129.48, 122.25, 40.43.



Syntheses of *N,N'*-(oxybis(4,1-phenylene))bis(2,4-dichloro-1,3,5-triazin-6-amine) (CODAC) and *N,N'*-(methylenebis(4,1-phenylene))bis(2,4-dichloro-1,3,5-triazin-6-amine) (CMDAC) have been investigated also in a study by Azarifar *et al.*<sup>[35]</sup> Nevertheless, experimental data are not in agreement with this study, where NMR characterizations of the two compounds in CDCl<sub>3</sub> has been reported.

Both CODAC and CMDAC did not show any solubility in halogenated or organic solvents with the exception of dimethyl sulfoxide and thus, it was necessary to carry out NMR spectra in DMSO-d<sub>6</sub>. Moreover, in <sup>1</sup>H NMR spectrum reported by Azarifar *et al.*, nitrogen protons were attributed to signal at 7.46-7.55 ppm, very close to aromatic signals. This attribution is not in agreement with experimental data gathered and it may be possible that, NMR spectra gathered by Azarifar *et al.*, were not wide enough to appreciate resonance frequencies of protons bonded to partially sp<sup>2</sup> hybridized nitrogens.<sup>[50,51]</sup>

Finally, CODAC and CMDAC have been employed for synthesis of the quaternary ammonium salts by reaction with of *N*-methyl morpholine in DMSO. (**Scheme 3.21**)



**Scheme 3.21:** Synthesis of quaternary ammonium salts derived from the reaction *N*-methyl morpholine with CODAC and CMDAC.

Despite long reaction times no product was isolated. It may be supposed that this behaviour is attributable to the extra stability granted by sp<sup>2</sup> hybridization of amine nitrogens, that deactivate halogenated carbons toward nucleophilic substitution by a tertiary amine.

Hence, considering the lack of reactivity showed by product synthesized by 4,4'-oxydianiline (ODA) and 4,4'-methyldianiline (MDA) it has been decided to do not investigate further anilino substituted triazines.

### 3.3 Synthesis of quaternary multi-ammonium salts derived from 2,4-dichloro-6-substituted-1,3,5-triazine

A study by Kunishima *et al.* investigated the reaction of CDMT with tertiary amine different from *N*-methylmorpholine to create a "library" of amidation agents similar to DMTMM.<sup>[21]</sup> Similarly, 2,4-dichloro-6-substituted-1,3,5-triazines have been used as reagents for the syntheses of quaternary bis-ammonium salts by the reaction with eight possible tertiary amines: *N*-methylmorpholine (MM, I), *N*-ethylmorpholine (EM, II), *N*-methylpiperidine (MP, III), *N*-ethylpiperidine (EP, IV), *N*-methylpyrrolidine (MPD, V), *N*-methylimidazole (MI, VI), trimethylamine (TMA, VII) and triethylamine (TEA, VIII). (**Figure 3.32**)

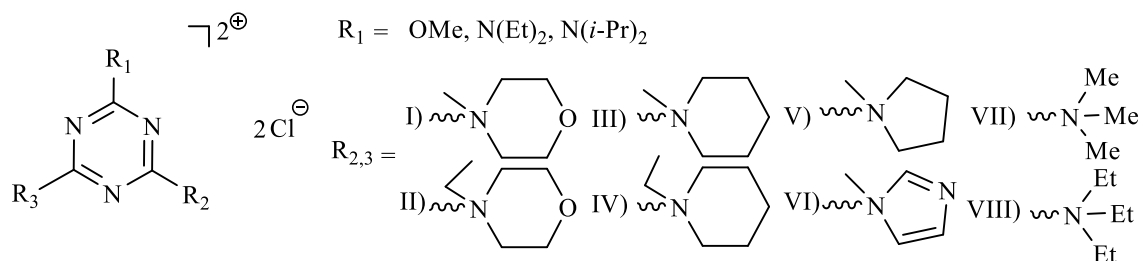


**Figure 3.32:** General formula of bis-ammonium salts derived from 2,4-dichloro-6-substituted-1,3,5-triazines.

Moreover, the study for the synthesis of a tetrakis-ammonium salt derived from *N*<sub>1</sub>,*N*<sub>2</sub>-bis(2,4-dichloro-1,3,5-triazin-6-yl)-*N*<sub>1</sub>,*N*<sub>2</sub>-diethylethane-1,2-diamine (CDEDC) is reported. (**Chapter 3.3.4**) The activity of these compounds as condensation agents for amide bonds formation will be described later in this thesis. (**Chapter 3.4**)

#### 3.3.1 Synthesis of quaternary bis-ammonium salts derived from 2,4-dichloro-6-methoxy-1,3,5-triazine (MMT)

2,4-dichloro-6-methoxy-1,3,5-triazine has been known as possible precursor of ammonium quaternary salts since 2000,<sup>[29]</sup> but the use of its quaternary ammonium salt as amidation agent has never been exploited or studied. In literature, only two cases of bis-ammonium salts derived by 2,4-dichloro-6-methoxy-1,3,5-triazine are reported:

- an untranslated french-belgian patent published by Sandoz Ltd. (now Novartis International AG) for antifouling and antitumoral applications.<sup>[55]</sup> In this work, the syntheses of bis-ammonium salts made from the reaction between 2,4-dichloro-6-methoxy-1,3,5-triazine and trimethylamine, pyridine or *N*-methyl heterocycles such as morpholine, piperidine and pyrrolidine are reported. All these compounds are synthesized in dioxane (with low yields)

or in benzene, a known human carcinogen,<sup>[63,64]</sup> with reaction times up to a week long. Many experimental data gathered in this thesis are in disagreement with results or characterizations reported in the patent, as it will be explained in each case below.

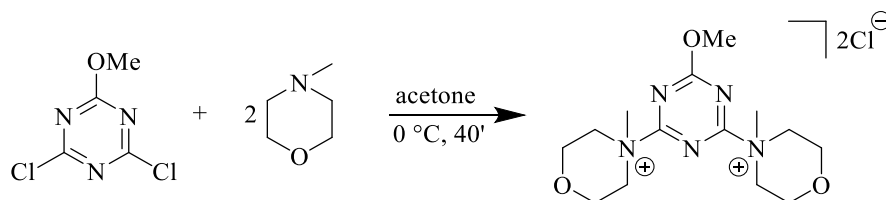
- A study by Chesnkiuk *et al.* about nucleophilic substitutions reactions,<sup>[65]</sup> where methylammonium salts synthesized by 2-chloro-4,6-disubstituted-1,3,5-triazine are investigated and a bis-trimethylammonium salt derived by MMT is reported to be highly unstable.

All the syntheses of bis-ammonium salts of MMT have been carried out reacting 2,4-dichloro-6-methoxy-1,3,5-triazine with an appropriate *N*-ethyl or *N*-methyl substituted tertiary amine.

In literature, Kunishima *et al.* reported the decomposition mechanism by demethylation or deethylation of quaternary ammonium triazine salts at *r.t.* in organic solvent.<sup>[19]</sup> Thus, all the syntheses have been carried out at 0°C in order to avoid decomposition processes.

### 3.3.1.1 Synthesis of quaternary bis-ammonium salt of 2,4-dichloro-6-methoxy-1,3,5-triazine in the presence of *N*-methylmorpholine (MMTMM)

MMTMM has been synthesized by the reaction, at 0 °C, of MMT in acetone solution with *N*-methylmorpholine. (Scheme 3.22)



Scheme 3.22: Synthesis of MMTMM.

<sup>1</sup>H NMR and FT-IR spectra confirmed the isolation of MMTMM, with a yield of 87% (purity 94%).

MMTMM demonstrated to be highly reactive and to quickly undergo decomposition processes in solution, preventing the characterization by <sup>13</sup>C NMR. Supposed decomposition process is similar to the one reported by Borke *et al.* for DMTMM, with formation of *N*-methylmorpholinium chloride and hydroxy-substituted-1,3,5-triazine.<sup>[66]</sup>

Determination of melting point led to the product decomposition at 73 °C, differently from what reported in the patent of Sandoz Ltd., which estimates a m.p. of 173 °C.<sup>[55]</sup>

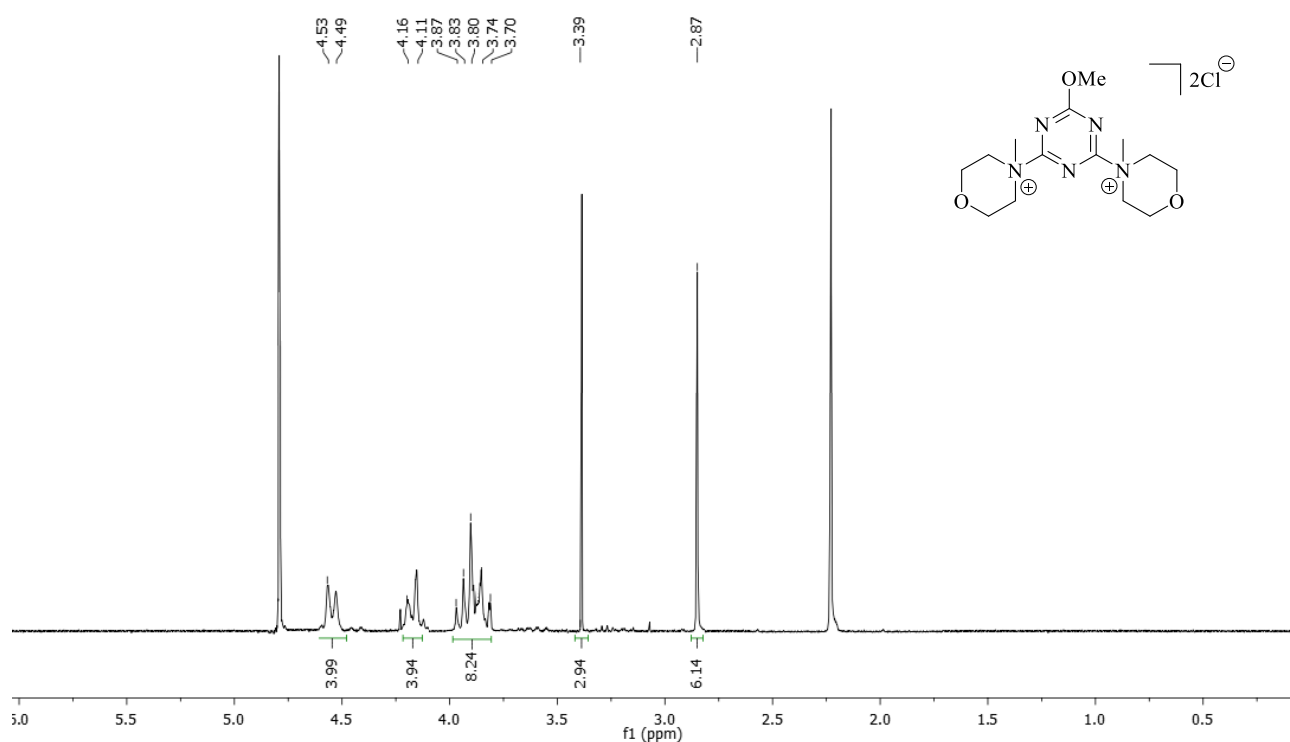


**Figure 3.33:**  $^1\text{H}$  NMR spectrum ( $\text{D}_2\text{O}$ ) of MMTMM.

$^1\text{H}$  NMR (300 MHz,  $\text{D}_2\text{O}$ , ppm): 4.53 (4H, m,  $\text{N}^+\text{CH}_2\text{CH}_2\text{O}$ ), 4.16 (4H, m,  $\text{N}^+\text{CH}_2\text{CH}_2\text{O}$ ), 3.87 (8H, m,  $\text{N}^+\text{CH}_2\text{CH}_2\text{O}$ ), 3.39 (3H, s,  $\text{OCH}_3$ ), 2.87 (6H, s,  $\text{N}^+\text{CH}_3$ ).

$^1\text{H}$  NMR spectrum (**Figure 3.33**) has been gathered few minutes after the filtration of MMTMM in order to avoid decomposition processes and, for this reason, an intense peak of acetone solvent is present at 2.22 ppm. Two singlets at 3.39 ppm and at 2.97 ppm are attributable respectively to protons of methoxy and ammonium-bonded methyl groups.

Protons in meta positions of the morpholine ring are observable as a multiplet at 3.85 ppm, while two separate signals at 4.53 ppm and at 4.15 ppm are attributable to protons in ortho positions. These do not possess the same resonance frequencies due to conformational arrangement of the molecule. Indeed, as reported by Kaminski and Kunishima,<sup>[32,21]</sup> triazine heterocyclic salts exist as two possible conformers with triazine ring in axial or in equatorial position. (**Figure 3.34**)

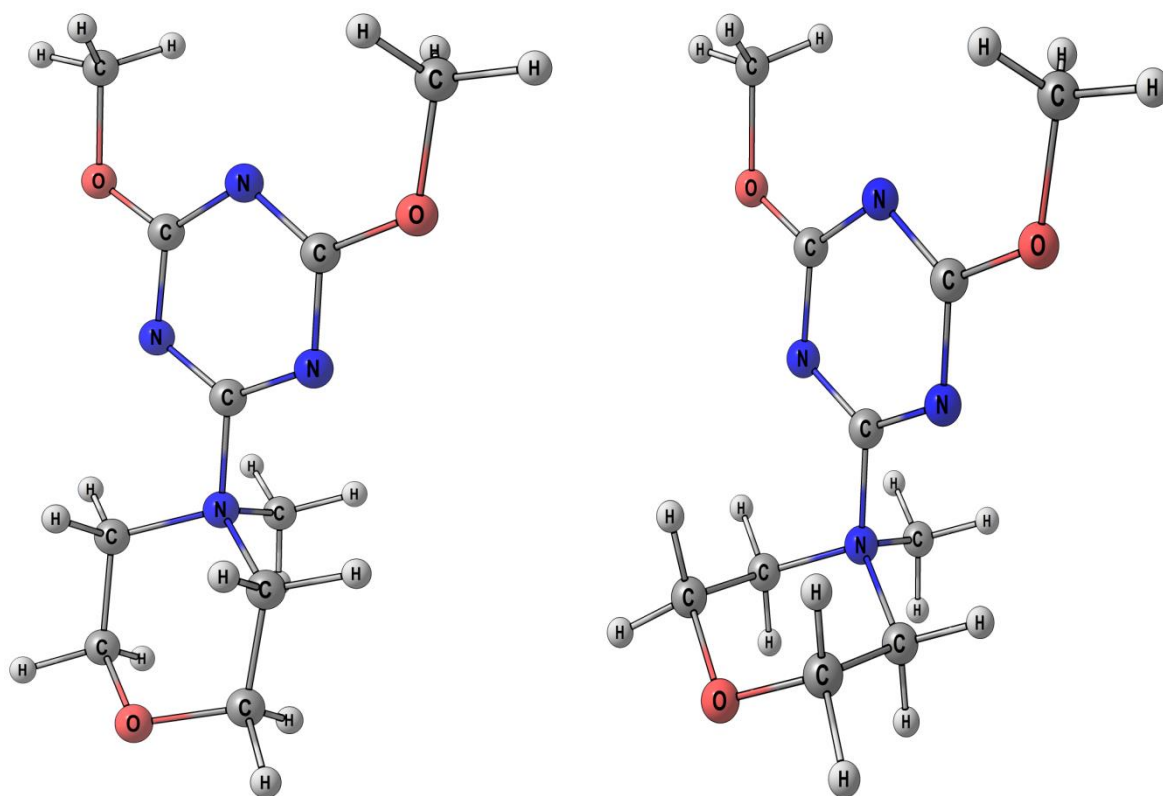
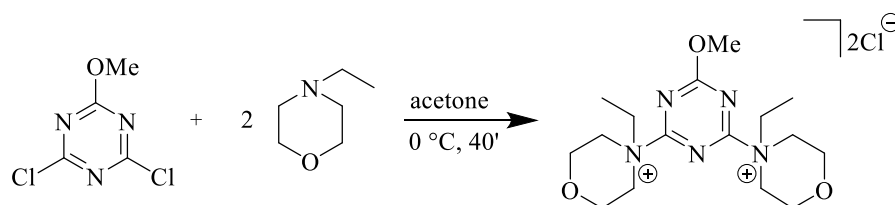


**Figure 3.34:** DMTMM possible conformers with triazine in equatorial position (left) and axial position (right) to morpholine ring.

For *N*-methylmorpholine in DMTMM, Kaminski reported that the stablest conformer is with the triazine in axial position.<sup>[32]</sup> (**Figure 3.34**) Kunishima *et al.* reported that the most stable conformer depends on the nature of the heterocycle bonded to the triazine ring and identifiable thanks to <sup>13</sup>C NMR spectroscopy. Unfortunately, it has not been possible to record a <sup>13</sup>C NMR spectrum of MMTMM due to its reactivity but, regardless of the heterocycle favorite conformation, the separation into two distinct peaks by the protons in ortho position is symptomatic of the quaternary ammonium salt formation.

### 3.3.1.2 Synthesis of quaternary bis-ammonium salt of 2,4-dichloro-6-methoxy-1,3,5-triazine in the presence of *N*-ethylmorpholine (MMTEM)

MMTEM has been isolated by reaction between MMT, dissolved in acetone at 0 °C, with *N*-ethylmorpholine. (**Scheme 3.23**)



**Scheme 3.23:** Synthesis of MMTEM.

$^1\text{H}$  NMR,  $^{13}\text{C}$  NMR and FT-IR confirmed the synthesis of MMTEM with yield of 89% (purity 93%).

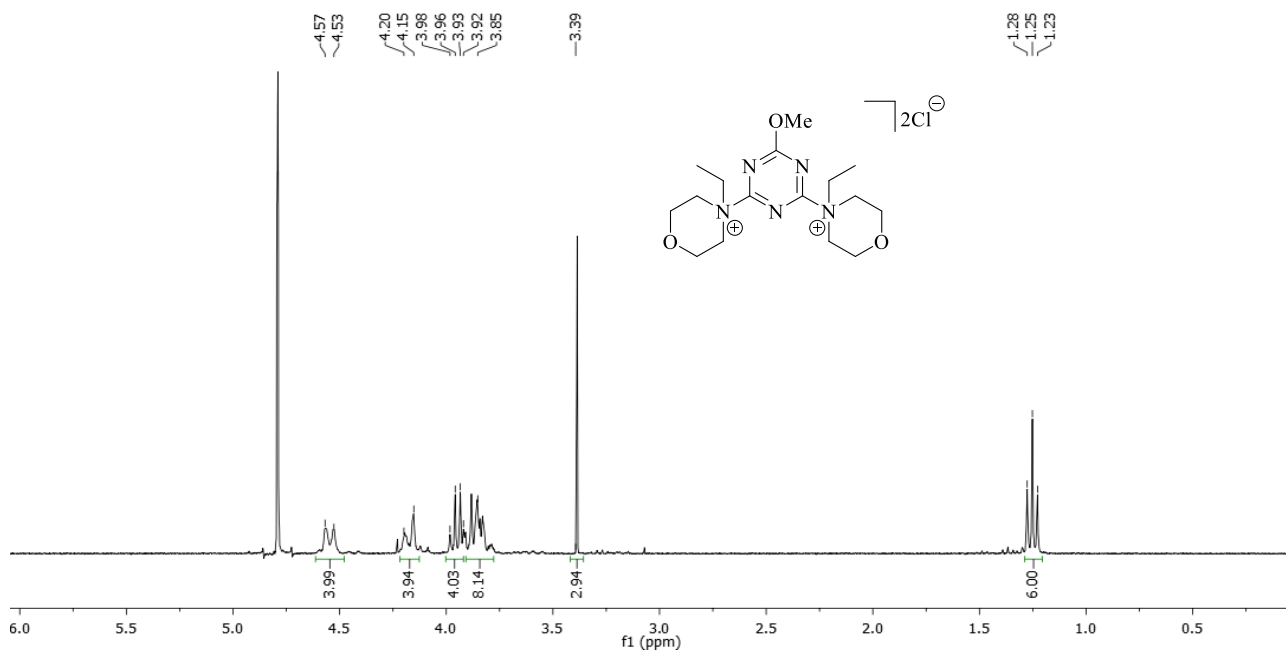


**Figure 3.35:**  $^1\text{H}$  NMR spectrum ( $\text{D}_2\text{O}$ ) of MMTEM.

$^1\text{H}$  NMR (300 MHz,  $\text{D}_2\text{O}$ , ppm): 4.57 (4H, d,  $\text{N}^+\text{CH}_2\text{CH}_2\text{O}$ ), 4.20 (4H, d,  $\text{N}^+\text{CH}_2\text{CH}_2\text{O}$ ), 3.96 (4H, q,  $\text{N}^+\text{CH}_2\text{CH}_3$ ), 3.85 (8H, m,  $\text{N}^+\text{CH}_2\text{CH}_2\text{O}$ ), 3.39 (3H, s,  $\text{OCH}_3$ ), 1.25 (6H, t,  $\text{N}^+\text{CH}_2\text{CH}_3$ ).

In  $^1\text{H}$  NMR (**Figure 3.35**), multiplet at 3.85 ppm is attributable to protons in para position of morpholine ring, while signals of protons in ortho position are observable as two doublets at 4.57 ppm and at 4.20 ppm, as explained before. (**Chapter 3.3.1.1**) The quartet at 3.96 ppm and the triplet at 1.25 ppm are attributable respectively to ( $\text{N}^+\text{CH}_2\text{CH}_3$ ) and ( $\text{N}^+\text{CH}_2\text{CH}_3$ ) protons of ethyl group. Finally, signal at 3.39 ppm is assignable to methoxy group protons.

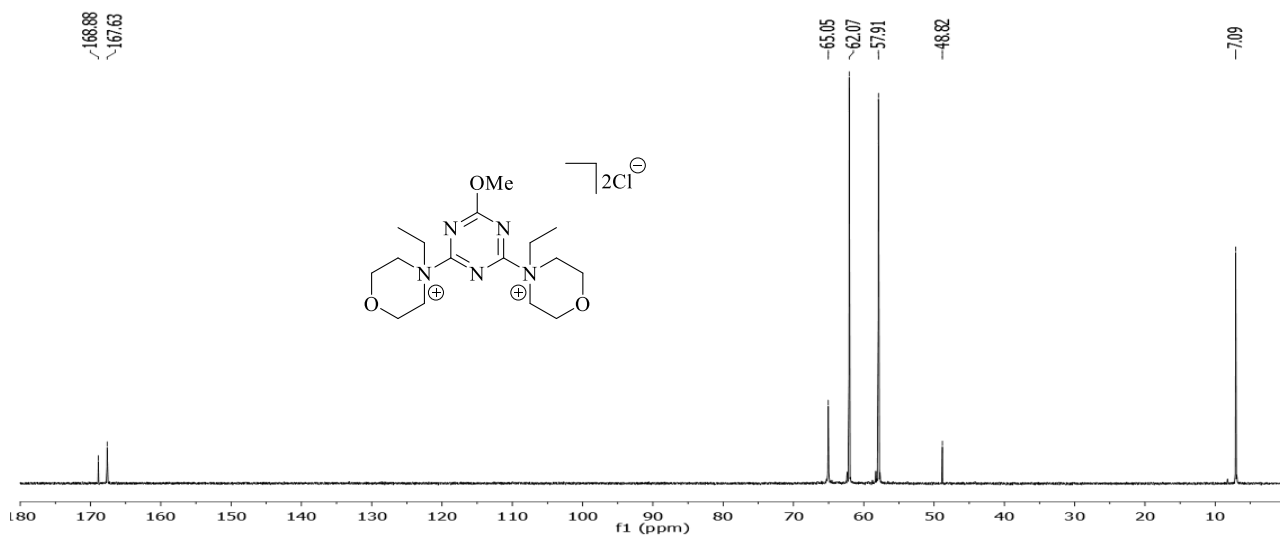


**Figure 3.36:**  $^{13}\text{C}$  NMR spectrum ( $\text{D}_2\text{O}$ ) of MMTEM.

$^{13}\text{C}$  NMR (300 MHz,  $\text{D}_2\text{O}$ , ppm): 168.88, 167.63, 65.05, 62.07, 57.91, 48.82, 7.09.

In  $^{13}\text{C}$  NMR (**Figure 3.36**), signals at 168.88 ppm and at 167.88 ppm are attributable to triazine carbons, respectively bonded to oxygen and to ammonium nitrogen. Signals at 65.05 ppm and at 7.09 ppm are assignable respectively to secondary and primary carbons of ethyl groups. Morpholine ring carbon are observable at 62.07 ppm, for ortho position, and at 57.91 ppm for meta position. Finally, signal at 48.82 ppm is attributable to methoxy group carbon.

Kunishima *et al.* reported a study on conformational arrangement of triazine quaternary ammonium salts by  $^{13}\text{C}$  NMR, later supported by X-ray structural analyses.<sup>[21]</sup> Kunishima asserted that thanks to resonance frequencies of *N*-alkyl substituent in the heterocycle, it is possible to identify the dominant conformer of the molecule: higher resonance (>60 ppm) are attributable to alkyl substituents in equatorial position, while axial positions are characterized by lower frequencies (<60 ppm). In this study Kunishima confirmed conformational arrangement given by Kaminski for DMTMM.<sup>[32]</sup> In the case of 4-(4,6-dimethoxy-1,3,5-triazin-2-yl)-4-ethyl-morpholinium chloride (DMTEM), he reported a  $\delta=66$  ppm for the secondary carbon of *N*-ethyl group and asserted the axial conformation for the triazine ring.

Thanks to  $^{13}\text{C}$  NMR of MMTEM (**Figure 3.36**), it is possible to attribute the signal at 65.05 ppm to the  $\text{NCH}_2\text{CH}_3$  carbon and thus it may be assumed that, in MMTEM as well, both the heterocycles have the triazine ring in axial position. (**Figure 3.37**)

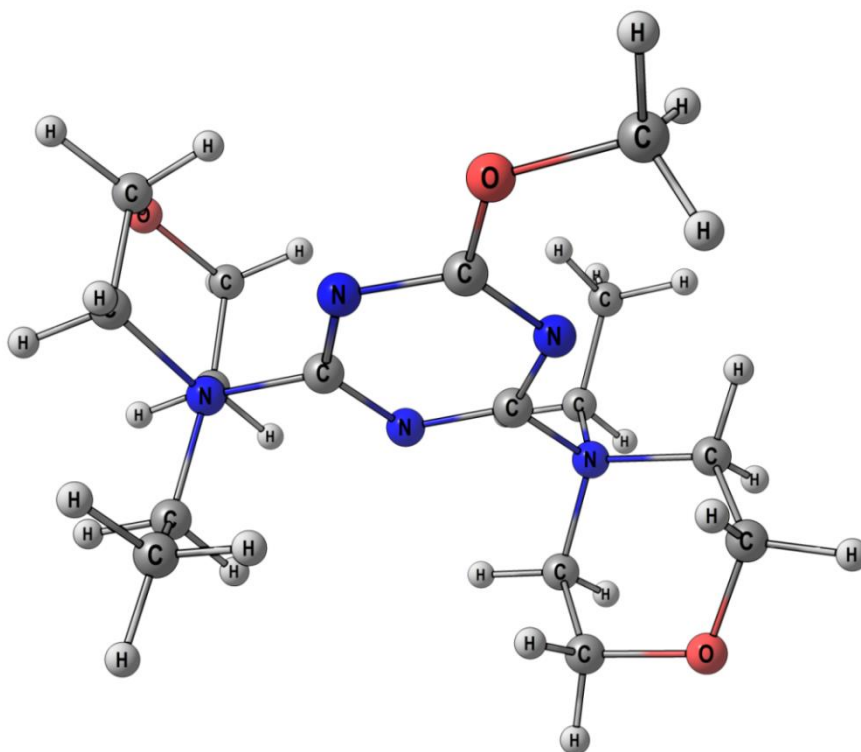
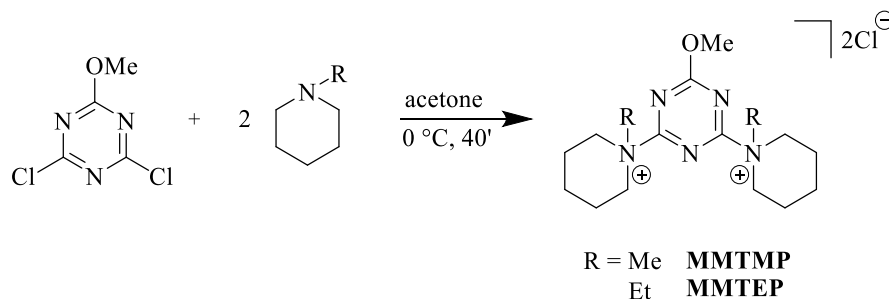


**Figure 3.37:** Estimated conformer of MMTEM.

### 3.3.1.3 Synthesis of quaternary bis-ammonium salts of 2,4-dichloro-6-methoxy-1,3,5-triazine in the presence of *N*-methylpiperidine (MMTMP) and of *N*-ethylpiperidine (MMTEP)

Syntheses of MMTMP and MMTEP have been investigated by the reaction, at 0 °C, between an acetone solution of MMT and the desired *N*-alkylpiperidine. (**Scheme 3.24**)



**Scheme 3.24:** Synthesis of MMTMP and MMTEP.

$^1\text{H}$  NMR,  $^{13}\text{C}$  NMR and FT-IR spectra confirmed the synthesis of MMTEP with a yield of 94% (purity 90%).

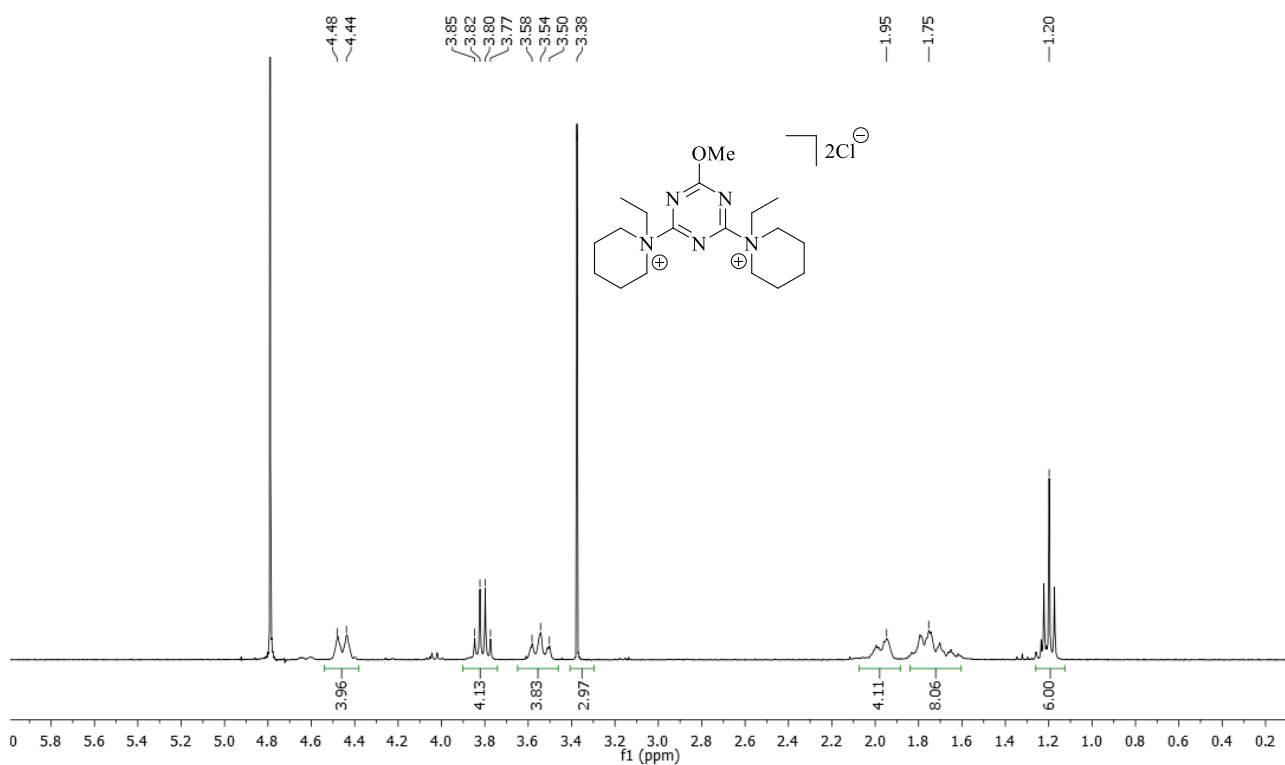


**Figure 3.38:**  $^1\text{H}$  NMR spectrum (D<sub>2</sub>O) of MMTEP.

$^1\text{H}$  NMR (300 MHz, D<sub>2</sub>O, ppm): 4.48 (4H, d, N<sup>+</sup>CH<sub>2</sub>CH<sub>2</sub>CH<sub>3</sub>), 3.82 (4H, q, N<sup>+</sup>CH<sub>2</sub>CH<sub>3</sub>), 3.54 (4H, t, N<sup>+</sup>CH<sub>2</sub>CH<sub>2</sub>CH<sub>3</sub>), 3.38 (3H, s, OCH<sub>3</sub>), 1.95 (4H, m, N<sup>+</sup>CH<sub>2</sub>CH<sub>2</sub>CH<sub>3</sub>), 1.75 (8H, m, N<sup>+</sup>CH<sub>2</sub>CH<sub>2</sub>CH<sub>3</sub>), 1.20 (6H, t, N<sup>+</sup>CH<sub>2</sub>CH<sub>3</sub>).



In  $^1\text{H}$  NMR spectrum (**Figure 3.38**), signals of piperidine ring protons can be observed as a doublet at 4.48 ppm and as a triplet at 3.54 ppm, for hydrogens in ortho position. Multiplets at 1.95 ppm and at 1.75 ppm are assignable respectively to para and meta position of the heterocycle. The quartet at 3.82 ppm and the triplet at 1.20 ppm are attributable to ( $\text{N}^+\text{CH}_2\text{CH}_3$ ) and ( $\text{N}^+\text{CH}_2\text{CH}_3$ ) protons of ammonium ethyl substituents. Finally, signal of methoxy group are observed at 3.38 ppm.

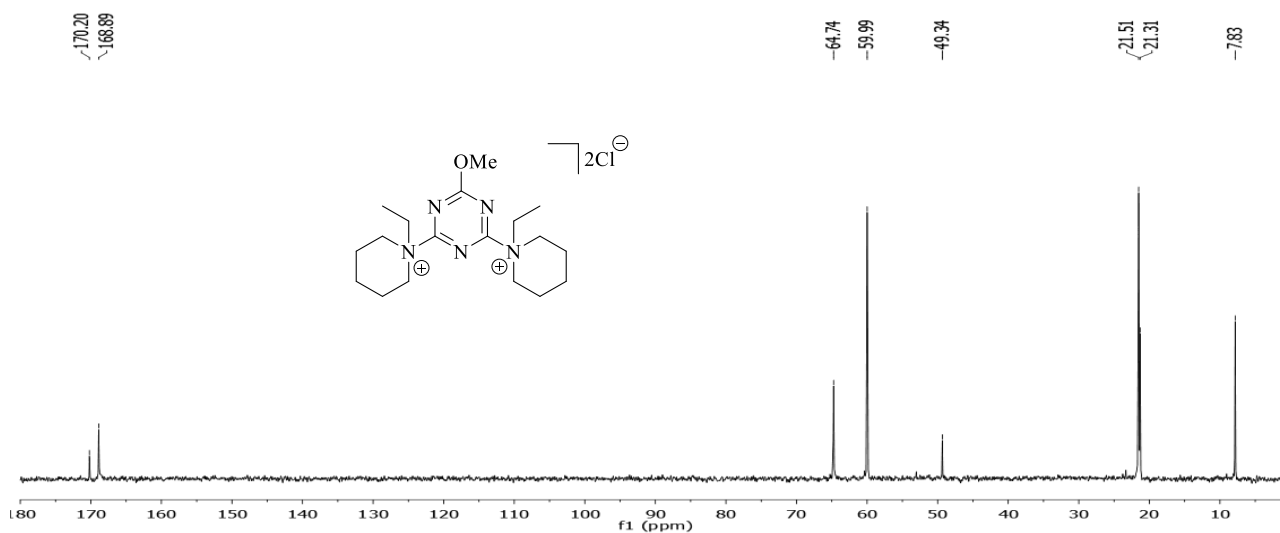


**Figure 3.39:**  $^{13}\text{C}$  NMR spectrum ( $\text{D}_2\text{O}$ ) of MMTEP.

$^{13}\text{C}$  NMR (300 MHz,  $\text{D}_2\text{O}$ , ppm): 170.20, 168.89, 64.74, 59.99, 49.34, 21.51, 21.31, 7.83.

In  $^{13}\text{C}$  NMR spectrum (**Figure 3.39**), signals at 170.26 ppm and at 168.89 ppm are attributable respectively to oxygen- and ammonium nitrogen-substituted triazine carbons. Ammonium ethyl substituents signals are observed at 64.74 ppm and at 7.83 ppm, respectively for secondary and primary carbons. Piperidine rings carbons can be attributed to signals at 55.99 ppm, at 21.51 ppm and at 21.31 ppm. Finally, methoxy group signal is observable at 49.34 ppm.

In the study about triazine heterocycle conformers, 4-(4,6-dimethoxy-1,3,5-triazin-2-yl)-4-ethylpiperidinium chloride (DMTEP) is investigated as well by Kunishima.<sup>[21]</sup> (**Chapter 3.3.1.2**) He reported that DMTEP secondary carbon of *N*-ethyl group is in equatorial position due to signal attribution at  $\delta=66$  ppm in  $^{13}\text{C}$  NMR spectrum.

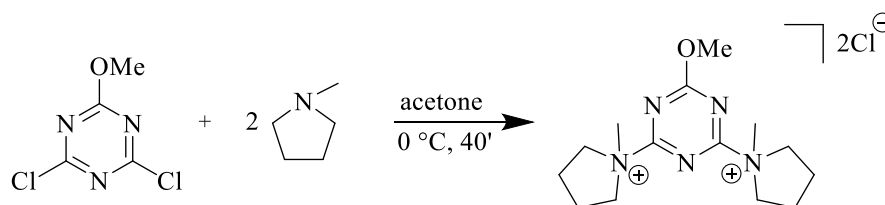
Thanks to the signal at 64.74 ppm, in  $^{13}\text{C}$  NMR spectrum (**Figure 3.19**), attributable to  $\text{NCH}_2\text{CH}_3$  carbons, it is possible to assume that, similarly to DMTEP, also MMTEP has the triazine ring in axial position of both its heterocycles.

Unfortunately, when *N*-methylpiperidine was used, the reaction led to the formation of an orange compound insoluble in most used solvents for NMR analysis. A possible explanation about this behaviour, is that, as reported in literature for CDMT,<sup>[19]</sup> quaternary ammonium salts obtained by reaction between methoxy substituted 1,3,5-triazines and *N*-methylpiperidine are not stable and undergo demethylation decomposition processes as reported before. (**Chapter 3.1**)

Despite experimental data gathered, in the patent published by Sandoz Ltd.,<sup>[55]</sup> MMTMP is reported to be isolable, nevertheless no synthesis methodology or characterization is reported.

### 3.3.1.4 Synthesis of quaternary bis-ammonium salt of 2,4-dichloro-6-methoxy-1,3,5-triazine in the presence of *N*-methylpyrrolidine (MMTMPD)

MMTMPD has been synthesized by the reaction between a solution of MMT, dissolved in acetone at 0 °C, and *N*-methylpyrrolidine. (**Scheme 3.25**)



**Scheme 3.25:** Synthesis of MMTMPD.

<sup>1</sup>H NMR, <sup>13</sup>C NMR and FT-IR spectra confirmed the synthesis of MMTMPD with a yield of 73% (purity 94%).

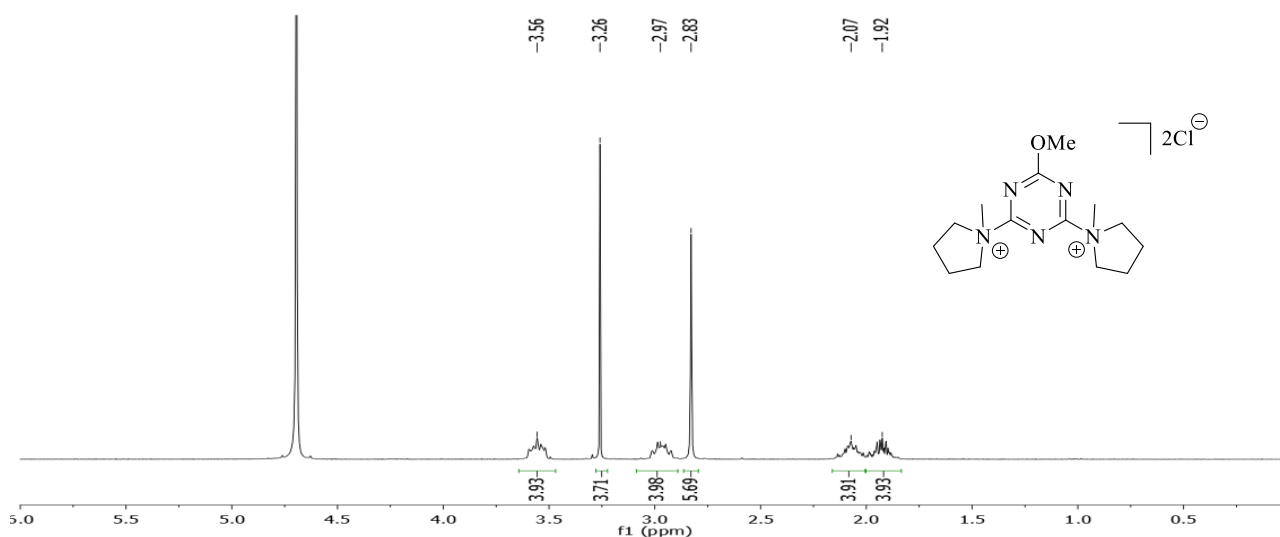


**Figure 3.40:** <sup>1</sup>H NMR spectrum (D<sub>2</sub>O) of MMTMPD.

$^1\text{H}$  NMR (300 MHz,  $\text{D}_2\text{O}$ , ppm): 3.56 (4H, m,  $\text{N}^+\text{CH}_2\text{CH}_2$ ), 3.26 (3H, s,  $\text{OCH}_3$ ), 2.97 (4H, m,  $\text{N}^+\text{CH}_2\text{CH}_2$ ), 2.83 (6H, s,  $\text{N}^+\text{CH}_3$ ), 2.07 (4H, m,  $\text{N}^+\text{CH}_2\text{CH}_2$ ), 1.92 (4H, m,  $\text{N}^+\text{CH}_2\text{CH}_2$ ).

In  $^1\text{H}$  NMR spectrum (**Figure 3.40**), *N*-methyl substituent singlet can be observed at 2.83 ppm, while signal at 3.26 ppm is attributed to the methoxy group. Signals of pyrrolidine rings protons are observed as multiplets at 3.56 ppm and at 2.97 ppm, for atoms in positions 2-5, and at 2.07 ppm and at 1.97 ppm for positions 3-4.

Kunishima *et al.* reported the synthesis of 4-(4,6-dimethoxy-1,3,5-triazin-2-yl)-1-methylpyrrolidinium as a perchlorate salt (DMTMPD[ $\text{ClO}_4$ ]), but its characterization is not commented.<sup>[21]</sup>

$^1\text{H}$  NMR of (DMTMPD[ $\text{ClO}_4$ ]) is reported:

$^1\text{H}$  NMR (400 MHz,  $\text{D}_2\text{O}$ , ppm): 4.42–4.52 ppm (2H, m,  $\text{N}^+\text{CH}_2\text{CH}_2$ ), 4.16 (6H, s,  $\text{OCH}_3$ ), 3.82–3.92 (4H, m,  $\text{N}^+\text{CH}_2\text{CH}_2$ ), 3.55 (3H, s,  $\text{N}^+\text{CH}_3$ ), 2.19 (2H, m,  $\text{N}^+\text{CH}_2\text{CH}_2$ ), 2.42 (2H, m,  $\text{N}^+\text{CH}_2\text{CH}_2$ )

Regardless of the counterion nature, both DMTMPD[ $\text{ClO}_4$ ] and MMTMPD present  $\text{CH}_2$  protons in position 2-5 and 3-4 with different resonance frequencies, probably due to the blocked conformation of five membered rings.<sup>[67]</sup>

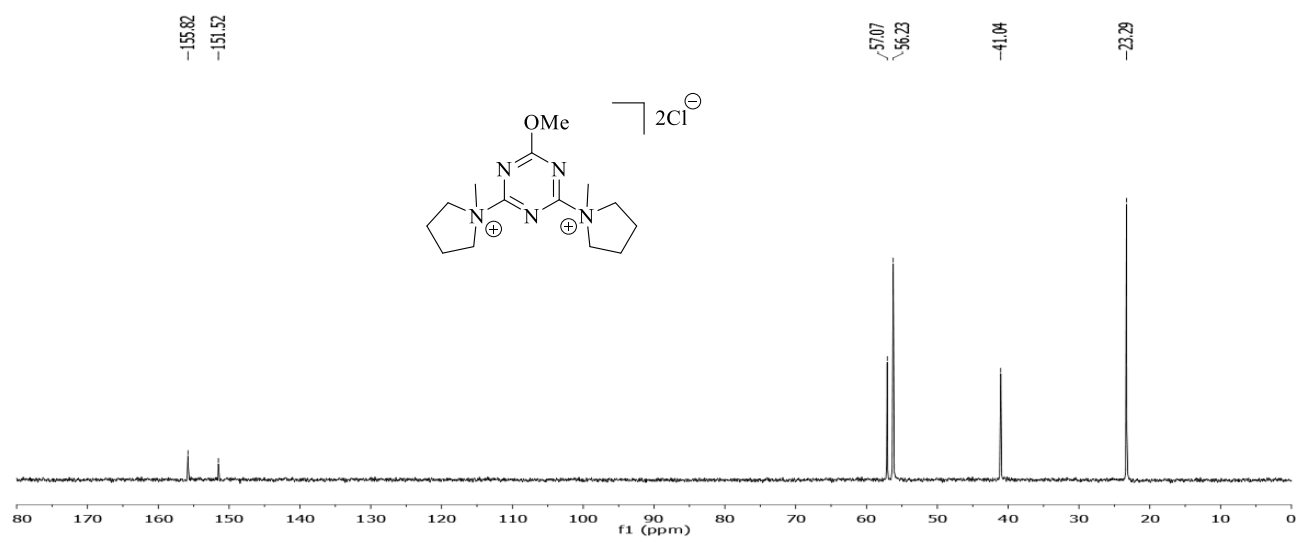


**Figure 3.41:**  $^{13}\text{C}$  NMR spectrum ( $\text{D}_2\text{O}$ ) of MMTMPD.

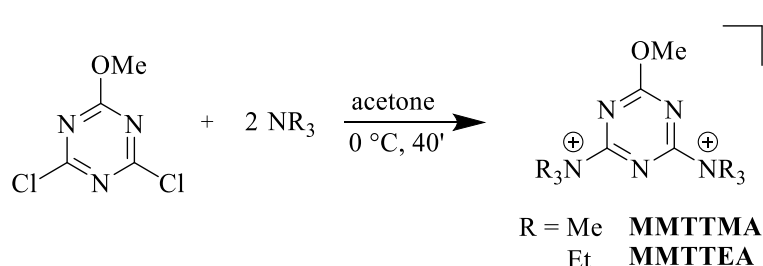
$^{13}\text{C}$  NMR (300 MHz,  $\text{D}_2\text{O}$ , ppm): 155.82, 151.52, 57.07, 56.23, 41.04, 23.29.

In  $^{13}\text{C}$  NMR spectrum (**Figure 3.41**), signals at 155.82 ppm and at 151.52 ppm can be attributed respectively to ammonium nitrogen- and to methoxy-substituted carbons of the triazine ring. Methoxy group signal is observable at 57.07 ppm. Pyrrolidine rings carbons are assignable to signals at 56.23 ppm and 23.29 ppm respectively for position 2-5 and 3-4.

Finally, ammonium methyl group signal is observed at 41.04 ppm. According to the study of Kunishima *et al.* reported before (**Chapter 3.3.1.2**), *N*-alkyl substituents in axial position are characterized by frequencies lower than 60 ppm.<sup>[21]</sup> Therefore, it may be supposed that, in MMTMPD, triazine ring is in equatorial position to both pyrrolidine cycles, in opposition to what has been previously observed for other MMT heterocycled ammonium salts.

### 3.3.1.5 Synthesis of quaternary bis-ammonium salts of 2,4-dichloro-6-methoxy-1,3,5-triazine in the presence of trimethylamine (MMTTMA) and triethylamine (MMTTEA)

Syntheses of MMTTMA and MMTTEA have been investigated by reaction, under vigorous stirring at 0 °C, between an acetone solution of MMT and the desired trialkylamine. (**Scheme 3.26**)



**Scheme 3.26:** Synthesis of MMTTMA and MMTTEA.

For the synthesis of MMTMA, a water solution 45% in weight of trimethylamine has been used and a white solid has been isolated and characterized by <sup>1</sup>H NMR.

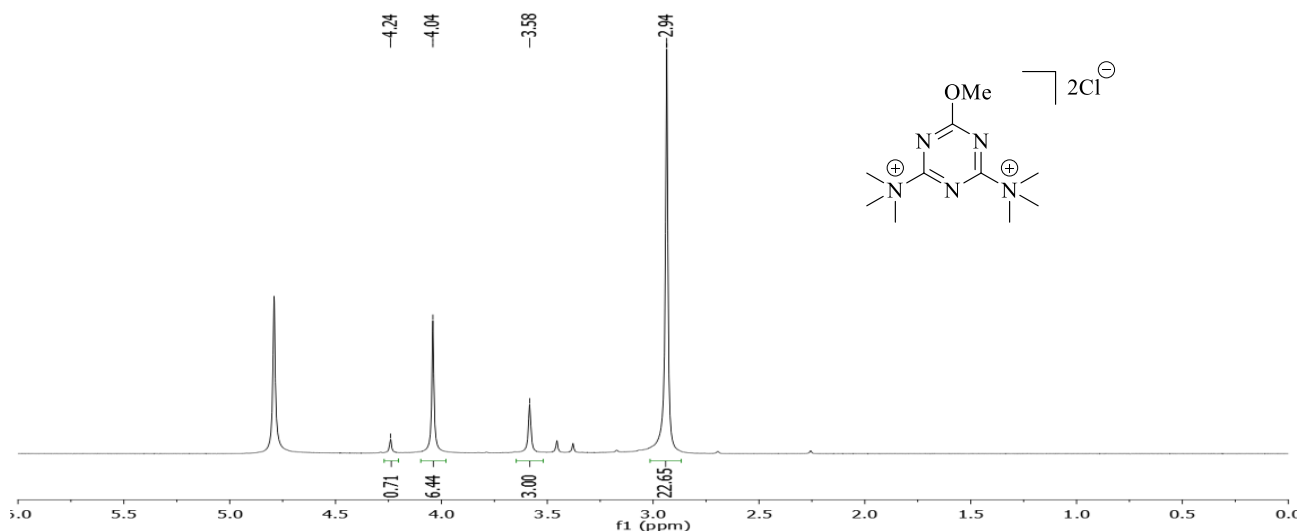


**Figure 3.42:** <sup>1</sup>H NMR spectrum (D<sub>2</sub>O) of MMTTMA.

In <sup>1</sup>H NMR spectrum (**Figure 3.42**), it is possible to observe the presence of at least two species. Characterization by NMR spectroscopy proved to be difficult, due to the presence in the molecule of only methyl group protons that do not couple with other signals.

In literature are present many studies that report the quick demethylation of trimethylammonium salts in solution.<sup>[21,26]</sup> Chesniuk *et al.* reported that the great majority of trimethylammonium salts (MMTTMA included) resulted to be highly unstable leading to demethylation processes.<sup>[65]</sup>

Due to the use of water solution of trimethylamine, the synthesis of MMTTMA has been carried out at alkaline pH (trimethylamine pKa= 9.76).<sup>[37]</sup> It is possible that the mixture of species, observable in <sup>1</sup>H NMR spectrum (**Figure 3.42**), is composed of triazine rings substituted by any combination of trimethylammonium salts, dimethylamine and/or hydroxy groups.

In the patent published by Sandoz Ltd.,<sup>[55]</sup> MMTTMA is reported to be isolable, nevertheless no synthesis methodology or characterization is reported. Other synthesis routes has been tried, but in all cases a complex mixture of products has been obtained.

The mixture of species, reported for simpleness as MMTTMA<sup>(\*)</sup>, proved to be highly reactive in solution and to decompose rapidly, thus it was not possible to gather a <sup>13</sup>C NMR spectrum. Nevertheless, the mixture of species (MMTTMA<sup>(\*)</sup>) has been tested as amidation agent for condensation reaction. (**Chapter 3.5**)

Unfortunately in the synthesis of MMT with triethylamine, the precipitation of a white solid has been observed, but this quickly turned into a yellowish oily precipitate. Other similar attempts have confirmed this behavior and it was therefore not possible to isolate a solid product in any case.

### **3.3.2 Synthesis of quaternary bis-ammonium salts derived from 2,4-dichloro-6-diisopropylamino-1,3,5-triazine (MIAT)**

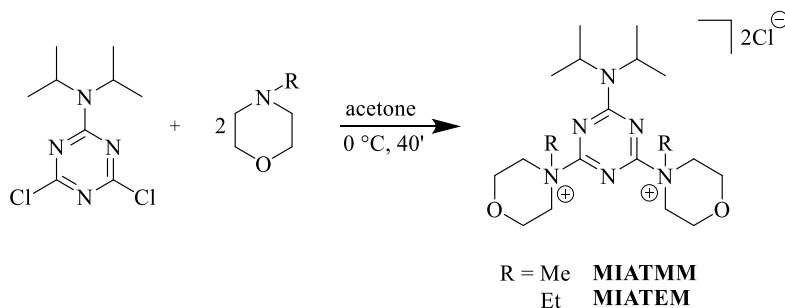
In literature few cases are reported about ammonium salts derived from nitrogen substituted triazine. About amidation agents of this kind, the only researches reported are recent studies by Kunishima *et al.* on amido- or imido-substituted triazines for synthesis and application of ammonium quaternary salts.<sup>[33,34]</sup>

An untraslated french-belgian patent, published by Sandoz Ltd., claims the synthesis of bis-ammonium salts derived by reaction between monoalkylamino substituted triazines and pyridine or *N*-methylheterocycles for antifouling and antitumoral applications.<sup>[55]</sup> The only case of a disubstituted amino triazine salt is attributable to Rushton *et al.* for the synthesis of a “heptamethylmelamine salt” ((4-6-bis-dimethylamino-1,3,5-triazin-2-yl)-trimethylammonium chloride) as a possible antitumor agent.<sup>[26]</sup>

Similarly to what previously reported for the quaternary bis-ammonium salts derived from MMT, all syntheses regarding quaternary bis-ammonium salts with MIAT have been carried out by reacting a solution of 2,4-dichloro-6-diisopropylamino-1,3,5-triazine with the appropriate tertiary amine, methyl or ethyl substituted. Also in this case, all the syntheses presented below were conducted at 0 ° C in order to avoid the possible decomposition of ammonium salts.<sup>[19]</sup>

### 3.3.2.1 Synthesis of quaternary bis-ammonium salts of 2,4-dichloro-6-diisopropylamino-1,3,5-triazine in the presence of *N*-methylmorpholine (MIATMM) and *N*-ethylmorpholine (MIATEM)

MIATMM and MIATEM have been investigated by the reaction at 0 °C of an acetone solution of MIAT and the desired *N*-alkylmorpholine. (Scheme 3.27)



**Scheme 3.27:** Synthesis of MIATMM and MIATEM.

<sup>1</sup>H NMR, <sup>13</sup>C NMR and FT-IR spectra confirmed the synthesis of MIATMM with a yield of 88% (purity 94%).

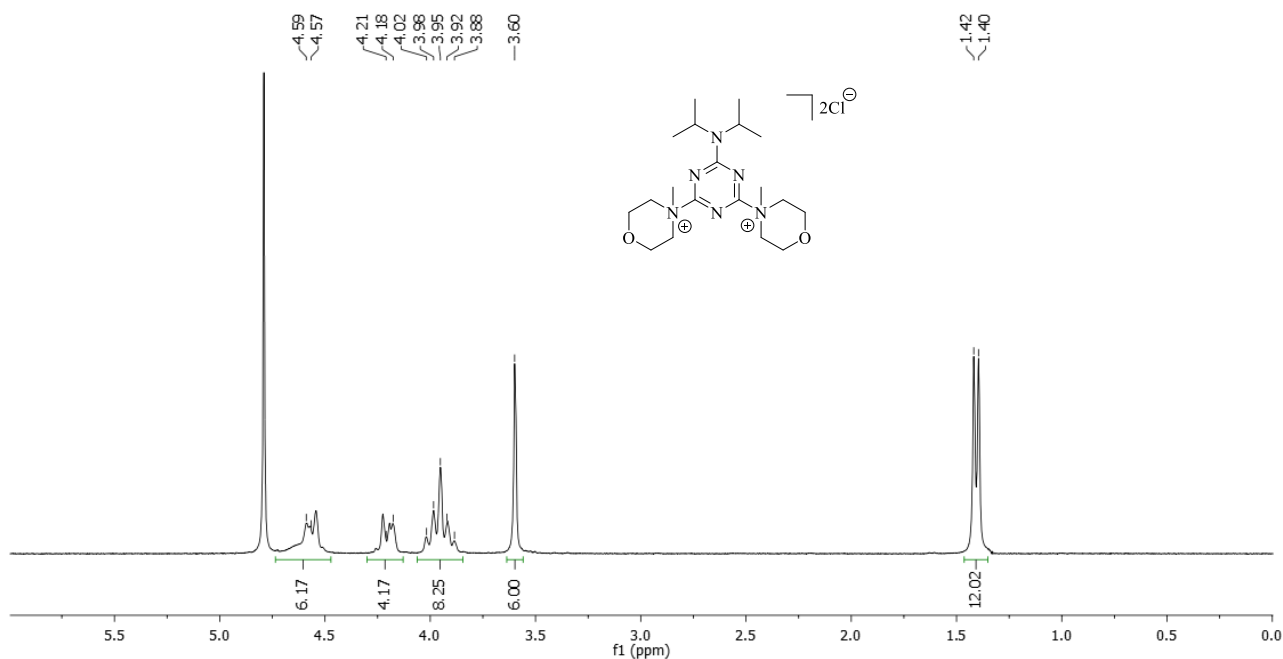


**Figure 3.43:** <sup>1</sup>H NMR spectrum (D<sub>2</sub>O) of MIATMM.

$^1\text{H}$  NMR (300 MHz,  $\text{D}_2\text{O}$ , ppm): 4.59 (2H, m broad,  $\text{NCH}(\text{CH}_3)_2$ ), 4.59 (4H, m,  $\text{N}^+\text{CH}_2\text{CH}_2\text{O}$ ), 4.21 (4H, d,  $\text{N}^+\text{CH}_2\text{CH}_2\text{O}$ ), 3.95 (8H, m,  $\text{N}^+\text{CH}_2\text{CH}_2\text{O}$ ), 3.60 (6H, s,  $\text{N}^+\text{CH}_3$ ), 1.42 (12H, d,  $\text{NCH}(\text{CH}_3)_2$ ).

In  $^1\text{H}$  NMR spectrum (**Figure 3.43**), it is possible to observe signals of isopropyl substituents protons as a doublet at 1.42 ppm and as a multiplet at 4.59 ppm. The latter signal, attributable to the two  $\text{CH}(\text{CH}_3)_2$  atoms, is overlying one of the signals of morpholine protons in ortho position, observable as two distinct peaks at 4.59 ppm and at 4.21 ppm due to conformational structure of the morpholine ring, as explained before. (**Chapter 3.3.1.1**) Finally, signals of morpholine protons in meta position are observable at 3.95 ppm, while the singlet at 3.60 ppm is attributable to methyl substituent of ammonium nitrogens.

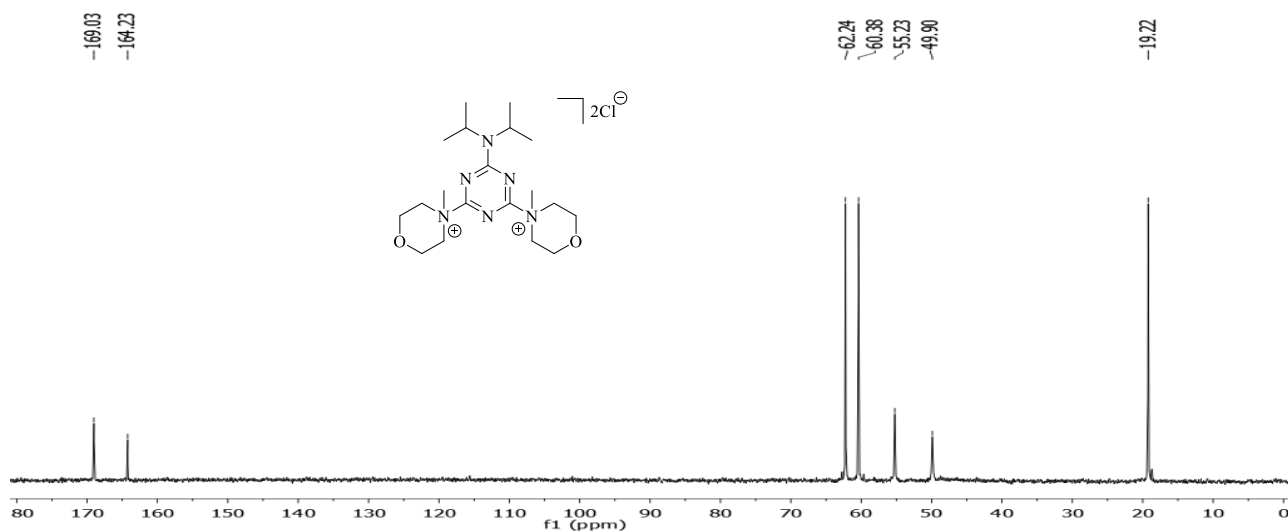


**Figure 3.44:**  $^{13}\text{C}$  NMR spectrum ( $\text{D}_2\text{O}$ ) of MIATMM.

$^{13}\text{C}$  NMR (300 MHz,  $\text{D}_2\text{O}$ , ppm): 169.03, 164.23, 62.24, 60.38, 55.23, 49.90, 19.22.

In  $^{13}\text{C}$  NMR spectrum (**Figure 3.44**), signals at 169.03 ppm and at 164.23 ppm can be attributed to quaternary carbons of the triazine ring, respectively to quaternary ammonium and isopropylamino-substituted carbons. Signals of diisopropylamino substituent are observed at 49.90 ppm for tertiary carbons and at 19.25 ppm for primary carbons. Finally, the signals of morpholine rings are observed at 62.24 ppm for carbons in ortho position and at 60.38 ppm for meta position, while the signal at 55.23 ppm is attributed to methyl groups of quaternary ammonium nitrogens.

As explained before (**Chapter 3.3.1.2**), Kunishima *et al.* reported a study on conformational arrangement of triazine quaternary ammonium salts by  $^{13}\text{C}$  NMR.<sup>[21]</sup> According to this study, *N*-alkyl substituents in axial position are characterized by frequencies lower than 60 ppm. In  $^{13}\text{C}$  NMR spectrum (**Figure 3.44**), MIATMM ammonium methyl groups signal is observable at 55.23 ppm.

Therefore, it may be supposed that triazine ring is in equatorial position to both morpholine cycles (**Figure 3.45**), in opposition to what has been previously observed for MMT morpholinium salts. Nevertheless, X-ray structural analysis will be carried out to confirm the proposed explanation.

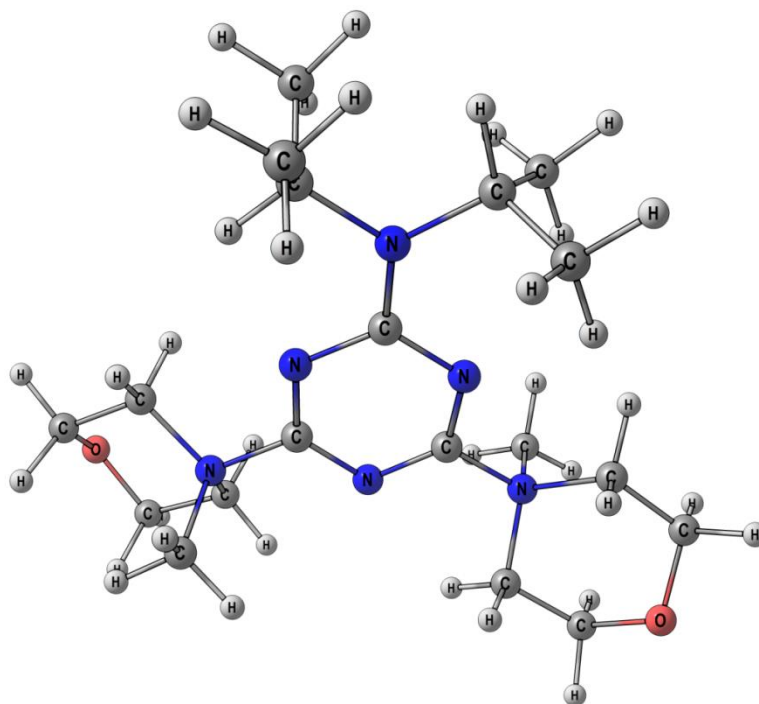
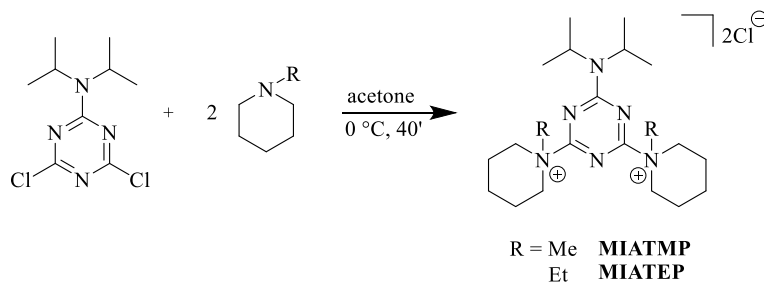


**Figure 3.17:** Estimated conformer of MIATMM.

Unfortunately, when *N*-ethylmorpholine was added to the MIAT acetone solution, no precipitation of product has been observed even after 24 hours of reaction at room temperature. Other similar attempts have confirmed this behavior, it was not possible to isolate a solid product in any case.

### 3.3.2.2 Synthesis of quaternary bis-ammonium salts of 2,4-dichloro-6-diisopropylamino-1,3,5-triazine in the presence of *N*-methylpiperidine (MIATMP) and of *N*-ethylpiperidine (MIATEP)

MIATMP and MIATEP have been investigated by the reaction at 0 °C of an acetone solution of MIAT and the desired *N*-alkylpiperidine. (**Scheme 3.28**)



**Scheme 3.28:** Synthesis of MIATMP and MIATEP.



$^1\text{H}$  NMR,  $^{13}\text{C}$  NMR and FT-IR spectra confirmed the synthesis of MIATMP with a yield of 85% (purity 92%).

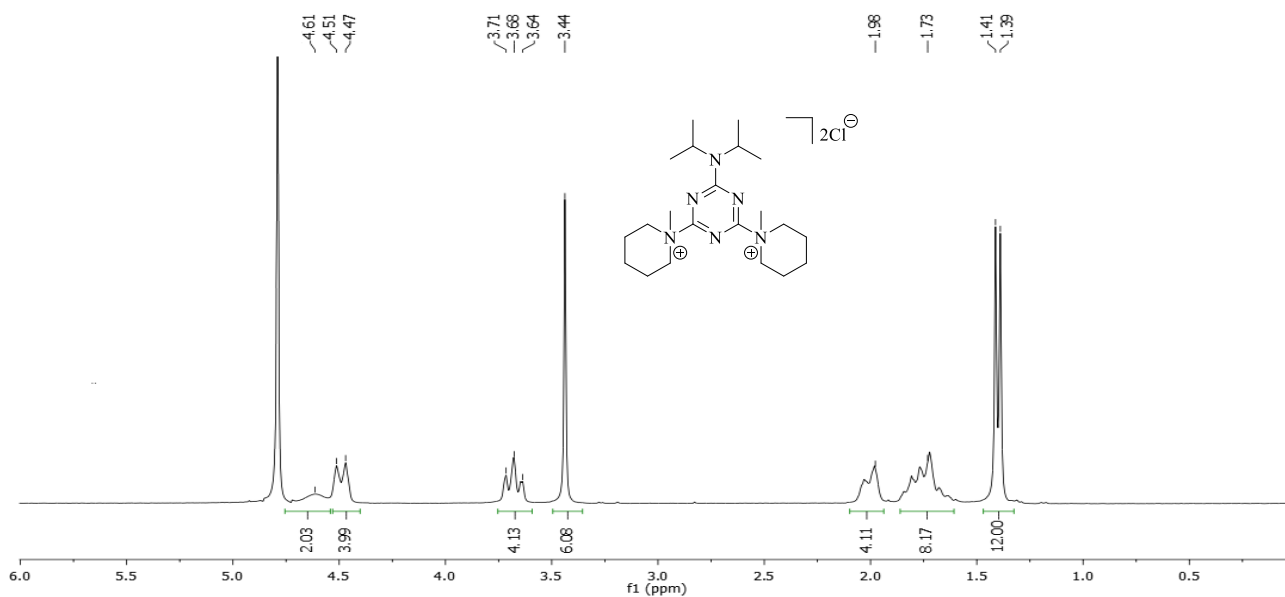


**Figure 3.46:**  $^1\text{H}$  NMR spectrum (D<sub>2</sub>O) of MIATMP.

$^1\text{H}$  NMR (300 MHz, D<sub>2</sub>O, ppm): 4.61 (2H, m broad, NCH(CH<sub>3</sub>)<sub>2</sub>), 4.51 (4H, d, N<sup>+</sup>CH<sub>2</sub>CH<sub>2</sub>CH<sub>3</sub>), 3.68 (4H, t, N<sup>+</sup>CH<sub>2</sub>CH<sub>2</sub>CH<sub>2</sub>), 3.44 (6H, s, CH<sub>3</sub>), 1.98 (4H, m, N<sup>+</sup>CH<sub>2</sub>CH<sub>2</sub>CH<sub>2</sub>), 1.73 (8H, m, N<sup>+</sup>CH<sub>2</sub>CH<sub>2</sub>CH<sub>3</sub>), 1.41 (12H, d, NCH(CH<sub>3</sub>)<sub>2</sub>).

In  $^1\text{H}$  NMR (**Figure 3.46**), the broad singlet at 4.61 ppm and the doublet at 1.41 ppm are attributable to protons of isopropylamino groups, respectively to [NCH(CH<sub>3</sub>)<sub>2</sub>] and [NCH(CH<sub>3</sub>)<sub>2</sub>]. Signals of piperidine rings protons are observable at 4.51 ppm and at 3.68 ppm for ortho position, as explained before (**Chapter 3.3.1.1**), while multiplets at 1.98 ppm and 1.73 ppm are attributable respectively to para and meta position. Finally, methyl ammonium protons are attributed to the singlet at 3.44 ppm.

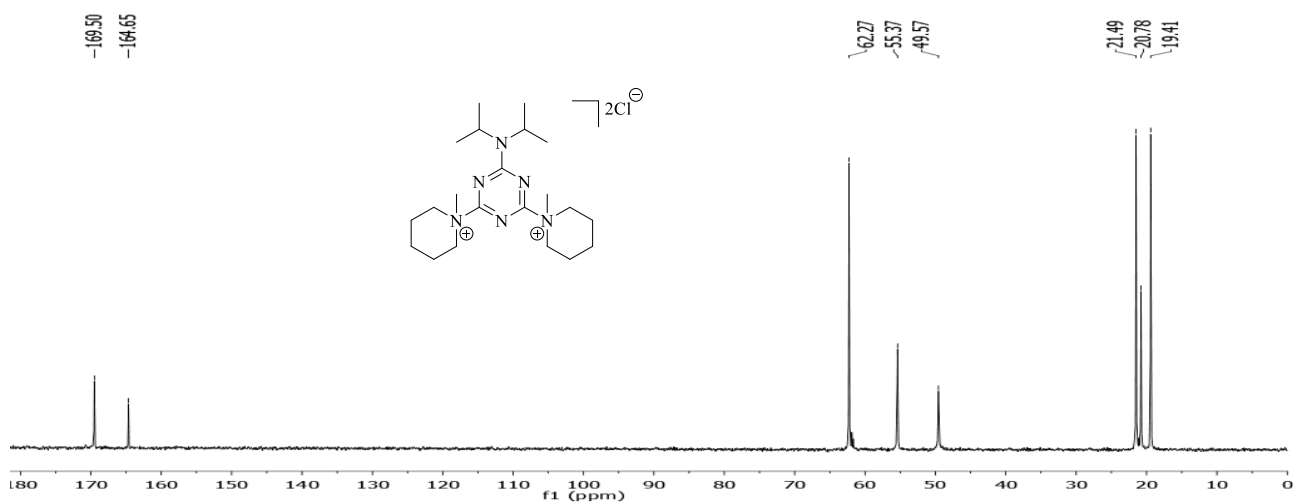


**Figure 3.47:**  $^{13}\text{C}$  NMR spectrum (D<sub>2</sub>O) of MIATMP.

$^{13}\text{C}$  NMR (300 MHz,  $\text{D}_2\text{O}$ , ppm): 169.50, 164.65, 62.27, 55.37, 49.57, 21.49, 20.78, 19.41.

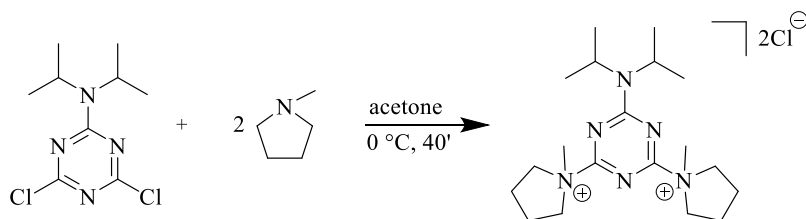
In  $^{13}\text{C}$  NMR spectrum (**Figure 3.47**), signals of triazine ring carbons can be observed at 169.50 ppm, for ammonium-substituted, and at 164.65 ppm, for diisopropylamino-substituted. Signals at 49.57 ppm and 19.41 ppm are attributed to tertiary and primary carbons of diisopropylamino group. Piperidine rings signals can be assigned to the carbons in ortho, para and meta position respectively at 62.27 ppm, at 21.49 ppm and at 20.78 ppm.

Finally, methyl substituents signal of ammonium groups is observed at 55.37 ppm. According to the study of Kunishima *et al.* reported before (**Chapter 3.3.1.2**), *N*-alkyl substituents in axial position are characterized by frequencies lower than 60 ppm.<sup>[21]</sup> Therefore, it may be supposed that, in MIATMP, triazine ring is in equatorial position to both piperidine cycles. Nevertheless, X-ray structural analysis will be carried out to confirm the proposed explanation.

Unfortunately, when *N*-ethylpiperidine was added to the MIAT acetone solution, no precipitation of product has been observed even after 24 hours of reaction at room temperature. Other similar attempts have confirmed this behavior, it was not possible to isolate a solid product in any case.

### 3.3.2.3 Synthesis of quaternary bis-ammonium salt of 2,4-dichloro-6-diisopropylamino-1,3,5-triazine in the presence of *N*-methylpyrrolidine (MIATMPD)

MIATMPD has been synthesized by the reaction at 0 °C in an acetone solution of MIAT and *N*-methylpyrrolidine. (**Scheme 3.29**)



**Scheme 3.29:** Synthesis of MIATMPD.

$^1\text{H}$  NMR,  $^{13}\text{C}$  NMR and FT-IR spectra confirmed the synthesis of MIATMPD with a yield of 72% (purity 93%).

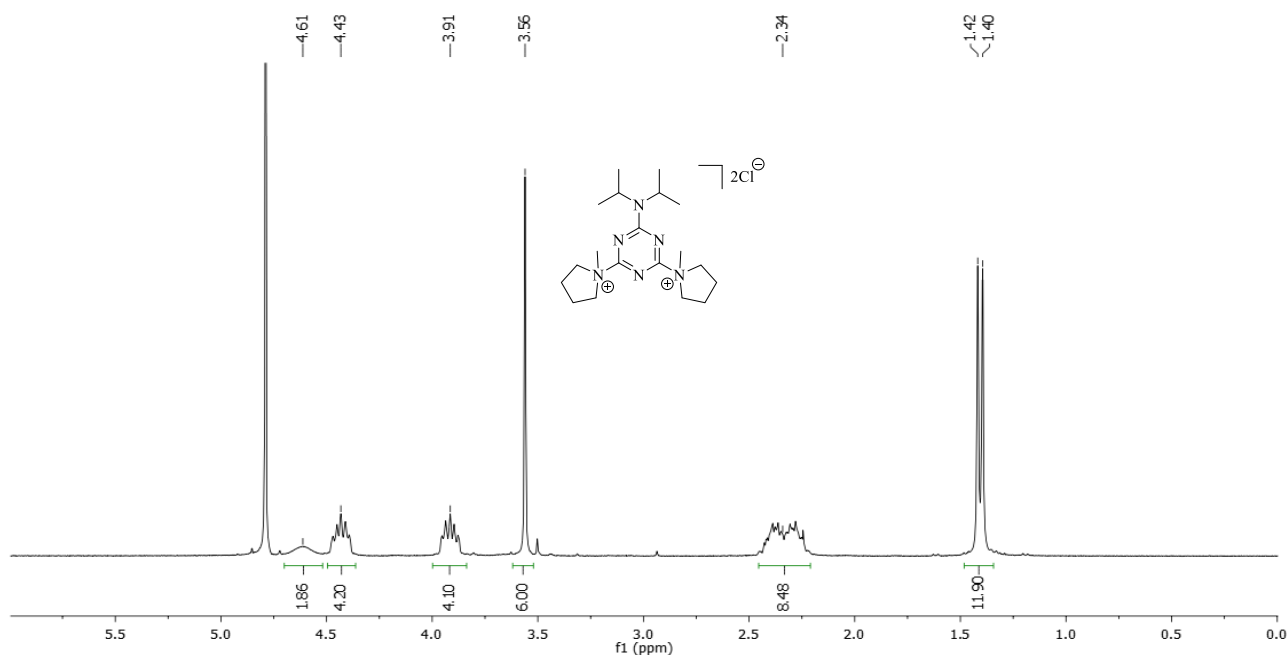


**Figure 3.48:**  $^1\text{H}$  NMR spectrum ( $\text{D}_2\text{O}$ ) of MIATMPD.

$^1\text{H}$  NMR (300 MHz,  $\text{D}_2\text{O}$ , ppm): 4.61 (2H, m broad,  $\text{NCH}(\text{CH}_3)_2$ ), 4.43 (4H, m,  $\text{N}^+\text{CH}_2\text{CH}_2$ ), 3.91 (4H, d,  $\text{N}^+\text{CH}_2\text{CH}_2$ ), 3.56 (6H, s,  $\text{N}^+\text{CH}_3$ ), 2.34 (8H, m,  $\text{N}^+\text{CH}_2\text{CH}_2$ ), 1.42 (12H, d,  $\text{NCH}(\text{CH}_3)_2$ ).

In  $^1\text{H}$  NMR spectrum (**Figure 3.48**), signals of isopropylamino [ $\text{NCH}(\text{CH}_3)_2$ ] and [ $\text{NCH}(\text{CH}_3)_2$ ] protons are observed respectively at 4.61 ppm, as a broad singlet, and at 1.42 ppm, as a doublet. Multiplets at 4.43 ppm and at 3.91 ppm are attributed to pyrrolidine rings protons in ortho position, while two close multiplets at 2.34 ppm are assigned to the protons in meta position. Atoms in position 2-5 and 3-4 show different resonance frequencies probably due to the blocked conformation of five membered rings, as explained before.<sup>[67]</sup> (**Chapter 3.3.1.4**) Finally, signal of methyl groups bonded to ammonium nitrogens is observed at 3.56 ppm.

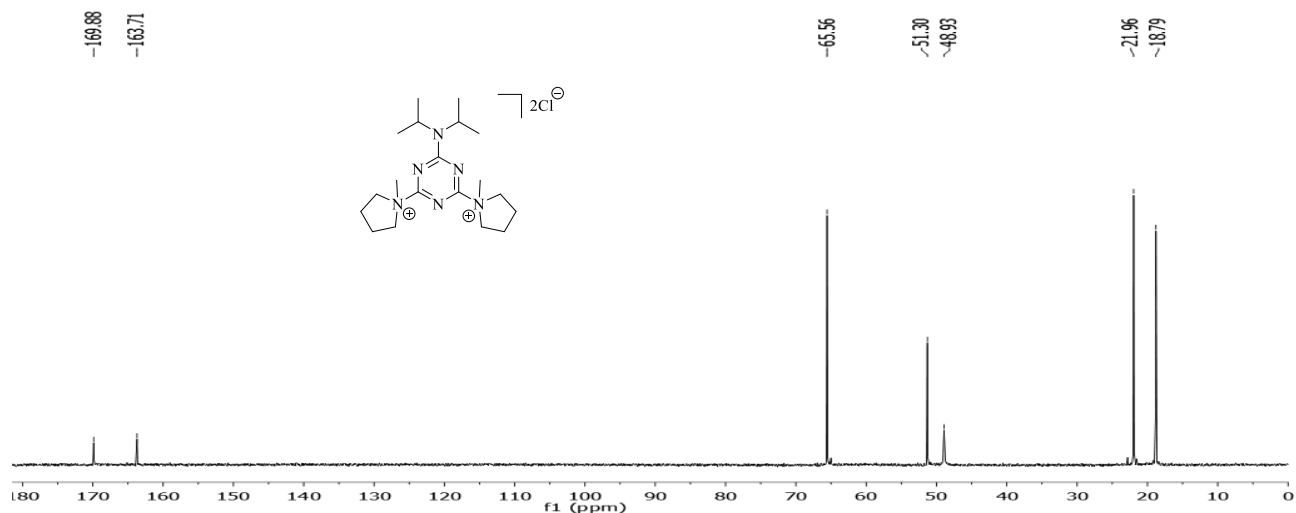


**Figure 3.49:**  $^{13}\text{C}$  NMR spectrum ( $\text{D}_2\text{O}$ ) of MIATMPD.

$^{13}\text{C}$  NMR (300 MHz,  $\text{D}_2\text{O}$ , ppm): 169.88, 163.71, 65.56, 51.30, 48.93, 21.96, 18.79.

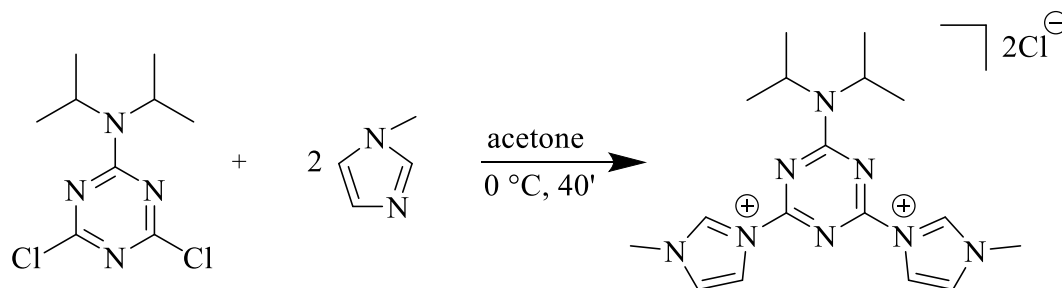
In  $^{13}\text{C}$  NMR spectrum (**Figure 3.49**), it is possible to observe triazine ring signals of ammonium-bonded carbons at 169.88 ppm and of diisopropylamino-substituted carbon at 163.71 ppm. Diisopropylamino group signals are observed at 48.93 ppm for tertiary carbons and at 18.79 ppm for primary carbons. Signals at 65.56 ppm and at 21.96 ppm are attributed to pyrrolidine rings carbons, respectively in position 2-5 and 3-4.

Finally, signal at 51.30 ppm is assigned to methyl groups bonded to quaternary nitrogen. According to the study of Kunishima *et al.* (**Chapter 3.3.1.2**), *N*-alkyl substituents in axial position are characterized by frequencies lower than 60 ppm.<sup>[21]</sup> Thus, as observed before for pyrrolidinium salts (**Chapter 3.3.1.5**), it may be supposed that triazine ring is in equatorial position to both pyrrolidine cycles. X-ray structural analysis will be carried out to confirm the proposed explanation.

#### 3.3.2.4 Synthesis of quaternary bis-ammonium salt of 2,4-dichloro-6-diisopropylamino-1,3,5-triazine in the presence of *N*-methylimidazole (MIATMI)

With 2,4-dichloro-6-diisopropylamino-1,3,5-triazine (MIAT) has been carried out a test with *N*-methylimidazole in order to study the reactivity of *N*-methylimidazolium salts. Similarly to what has been reported by Kunishima *et al.*,<sup>[21]</sup> quaternary imidazolium salts are isolable and stable, but they are not reactive as activators of amidation reaction. This behaviour has been confirmed by experimental data and thus, the same reaction with 2,4-dichloro-6-methoxy-1,3,5-triazine (MMT) and 2,4-dichloro-6-diethylamino-1,3,5-triazine (MEAT) has not been investigated.

MIATMI has been synthesized by addition of *N*-methylimidazole to an acetone solution of MIAT at 0 °C. (**Scheme 3.30**)



**Scheme 3.30:** Synthesis of MIATMI.

$^1\text{H}$  NMR,  $^{13}\text{C}$  NMR and FT-IR spectra confirmed the synthesis of MIATMI with a yield of 78% (purity 95%).

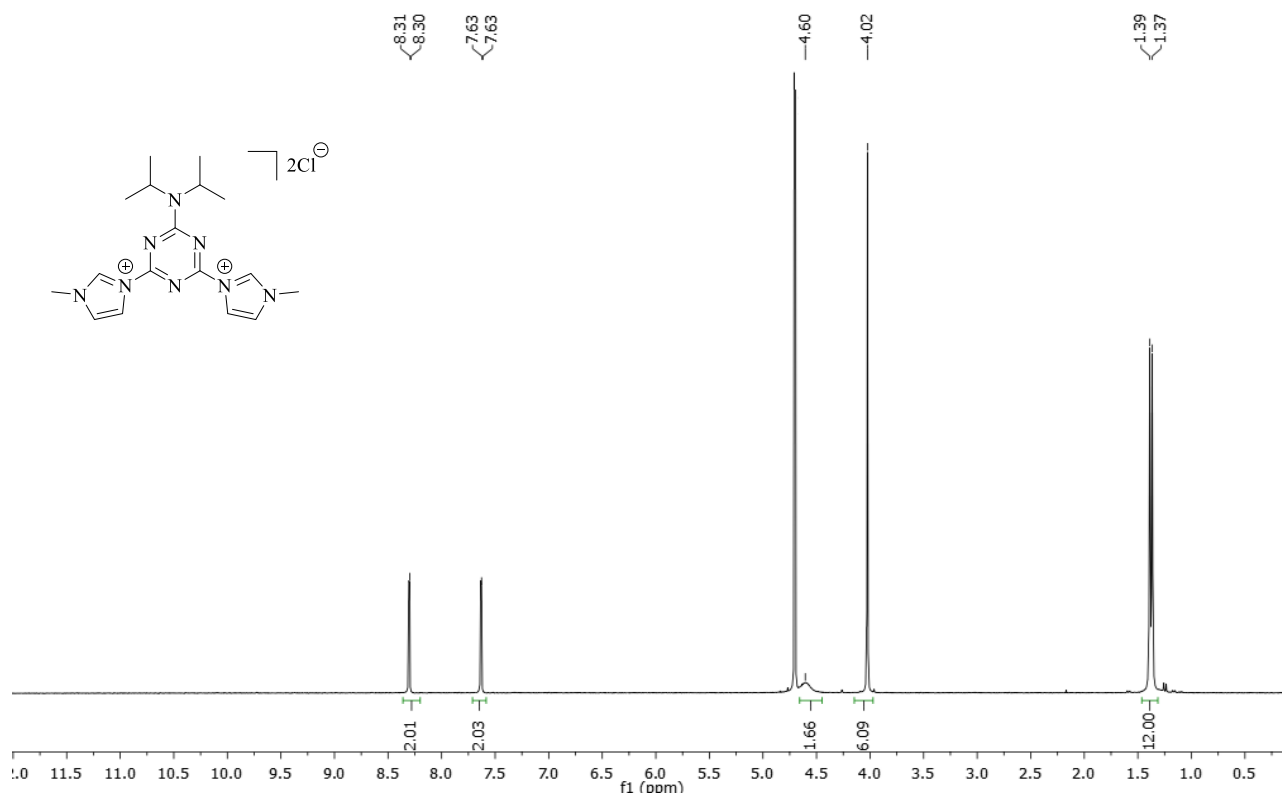


**Figure 3.50:**  $^1\text{H}$  NMR spectrum ( $\text{D}_2\text{O}$ ) of MIATMI.

In  $^1\text{H}$  NMR spectrum (**Figure 3.50**), it is possible to observe a broad signal at 4.61 ppm and a doublet at 1.40 ppm typical of  $[\text{NCH}(\text{CH}_3)_2]$  and  $[\text{NCH}(\text{CH}_3)_2]$  diisopropylamino group protons. Signal at 4.02 ppm is attributable to methyl substituents of imidazole rings. Thanks to COSY NMR (**Figure 3.51**), signals at 8.30 ppm and 7.63 ppm are assignable to protons of the heterocycle rings.

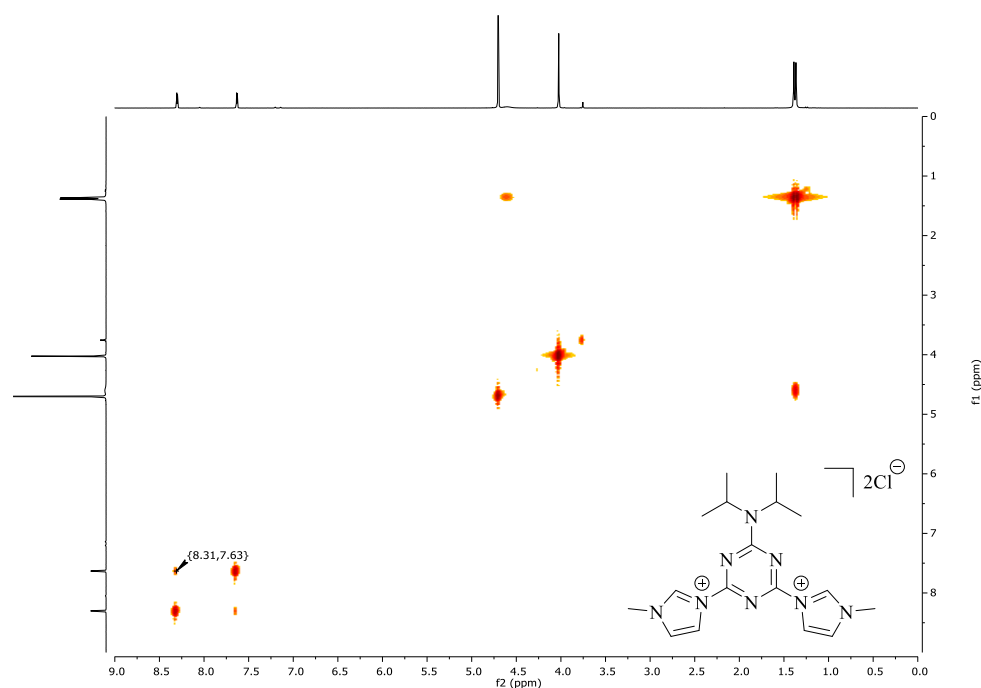


**Figure 3.51:** COSY NMR spectrum ( $\text{D}_2\text{O}$ ) of MIATMI.

In COSY NMR (**Figure 3.51**), it is possible to observe the coupling between the signals at 8.31 ppm and 7.63 ppm, both attributable to (NCH=CHN) protons of the imidazole rings.

Katritzky and Riduan reported that (NCHN) imidazole proton is acidic and therefore is not observable by  $^1\text{H}$  NMR in  $\text{D}_2\text{O}$  due to solvent exchange.<sup>[68,69]</sup> For this reason,  $^1\text{H}$  NMR spectrum in  $\text{DMSO-d}_6$  has been carried out for a full characterization of the sample. (**Figure 3.52**)

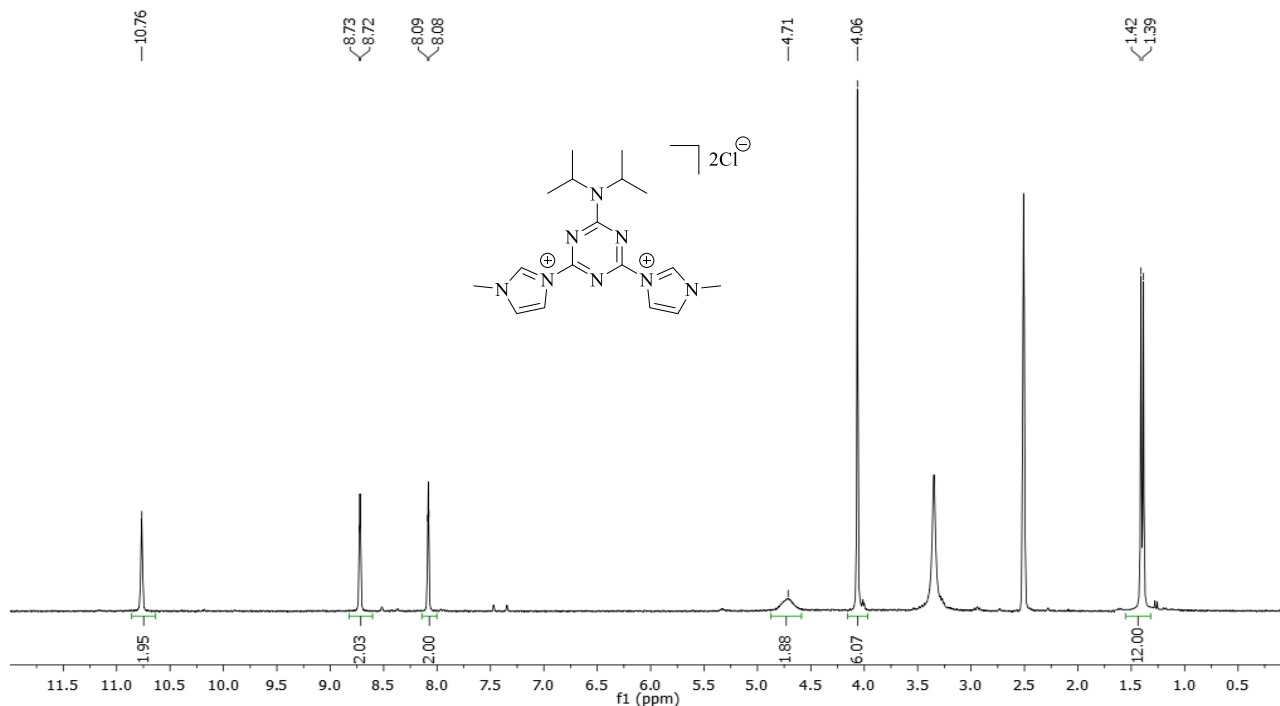


**Figure 3.52:**  $^1\text{H}$  NMR spectrum ( $\text{DMSO-d}_6$ ) of MIATMI.

$^1\text{H}$  NMR (300 MHz,  $\text{DMSO-d}_6$ , ppm): 10.76 (2H, s, NCHN), 8.73 (2H, s,  $\text{N}^+\text{CH=CHN}$ ), 8.09 (2H, s,  $\text{N}^+\text{CH=CHN}$ ), 4.71 (2H, m broad,  $\text{NCH}(\text{CH}_3)_2$ ), 4.06 (6H, s,  $\text{NCH}_3$ ), 1.42 (12H, d,  $\text{NCH}(\text{CH}_3)_2$ ).

Thanks to  $^1\text{H}$  NMR spectrum in  $\text{DMSO-d}_6$  (**Figure 3.52**), it is possible to observe the presence of (NCHN) protons of the imidazole rings at 10.76 ppm. Due to the presence of two nitrogen atoms in the cycle, *N*-methylimidazole can react in position 1 or 3, leading to the formation of two possible isomers. (**Figure 3.53**)

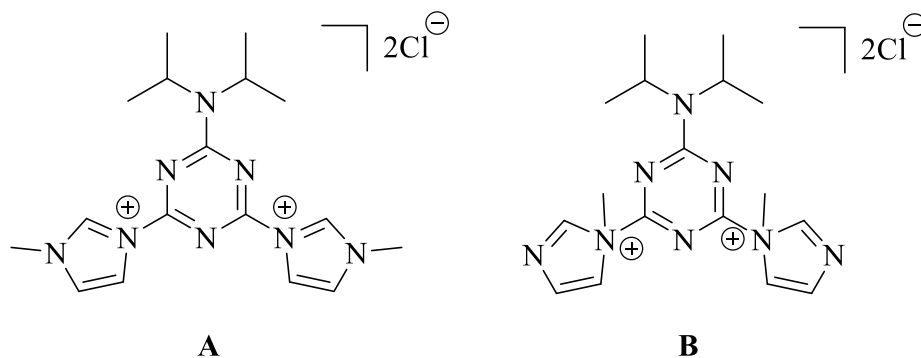


**Figure 3.53:** Possible isomers of MIATMI.

Hoffman reported that *N*-alkylimidazoles in addition reactions with an electrophile for the synthesis of dialkylimadazolium salts, follow a mechanism that leads to the formation of 1,3-dialkylimadazolium rather than 1,1-dialkylimadazolium salts.<sup>[70]</sup>

Therefore, it may be assumed that MIATMI is only present in the form of isomer A. (**Figure 3.53**) In consideration of this, it is interesting to notice that *N*-methyl groups of MIATMI imidazolium cycle have a resonance frequency of  $\delta=4.02$  ppm, with a shift to low field of 0.57 ppm compared to *N*-methylimidazole reagent counterpart ( $\delta=3.52$  ppm).

<sup>1</sup>H NMR spectrum data of *N*-methylimidazole are reported below.

<sup>1</sup>H NMR (300 MHz, D<sub>2</sub>O, ppm): 7.42 (1H, s, NCHN), 6.91 (1H, s, NCH=CHN), 6.85 (1H, s, NCH=CHN), 3.52 (3H, s, N-CH<sub>3</sub>).

Otherwise, *N*-methylmorpholine (MM) presents a wider shift of 1.44 ppm for *N*-methyl group when salified into MIATMM (**Chapter 3.3.2.1**): specifically from  $\delta=2.16$  ppm for MM to  $\delta=3.60$  ppm for the derived salt. Other *N*-methylheterocycles studied present similar behaviours for salts derived from 2,4-dichloro-6-diisopropylamino-1,3,5-triazine (MIAT). Therefore, it can be supposed that, in MIATMI, the *N*-methyl groups of imidazolium salt undergo a lesser electron withdrawing effect, because the nitrogen atom is not directly bonded to the triazine as observable in other *N*-methylheterocycles studied, in agreement with what reported by Hoffman.<sup>[70]</sup>

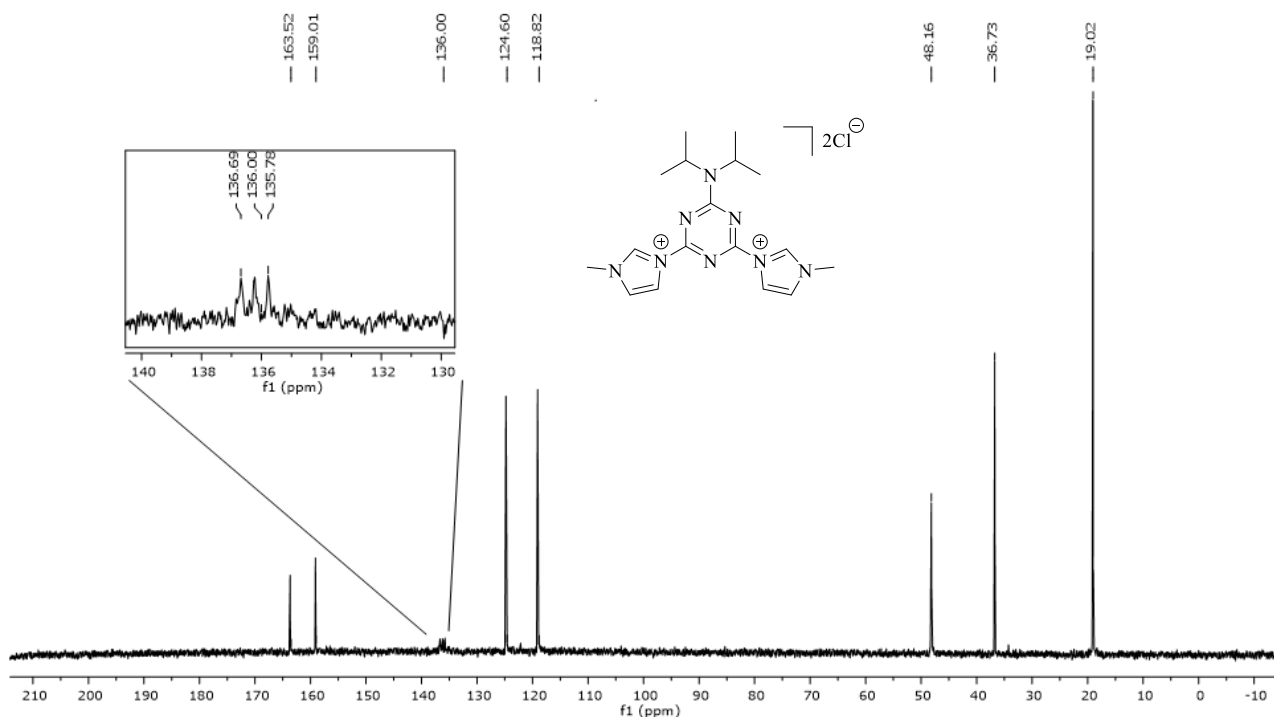


**Figure 3.54:** <sup>13</sup>C NMR spectrum (D<sub>2</sub>O) of MIATMI.

In  $^{13}\text{C}$  NMR spectrum (**Figure 3.54**), it is possible to observe signals of the triazine ring carbons at 163.52 ppm and 159.01 ppm. Diisopropylamino group signals are observed at 48.16 ppm for tertiary carbons and at 19.02 ppm for primary carbons. Methyl substituents of imidazole rings are observable at 36.73 ppm, while ( $\text{N}^+\text{CH}=\text{CHN}$ ) carbons are observable at 124.60 ppm and 118.82 ppm, respectively for position 4 and 5. Finally, at 136.00 ppm it is possible to observe a triplet of intensity 1:1:1, that is attributable to the coupling C-D of ( $\text{NCN}$ ) imidazole carbon. In literature, the substitution of imidazole ( $\text{NCHN}$ ) proton with deuterium in  $\text{D}_2\text{O}$  is well known.<sup>[71-73]</sup> Indeed, the deuterium nucleus has a different nuclear spin compared to  $^1\text{H}$  and undergoes resonance at different frequencies than either the proton or  $^{13}\text{C}$  nucleus. For this reasons spin-spin coupling between the  $^{13}\text{C}$  and the deuterium is not eliminated during proton decoupling and gives rise to the mentioned triplet.

To confirm this behavior  $^{13}\text{C}$  NMR in  $\text{DMSO-d}_6$  has been registered for a full characterization of the sample. (**Figure 3.55**)

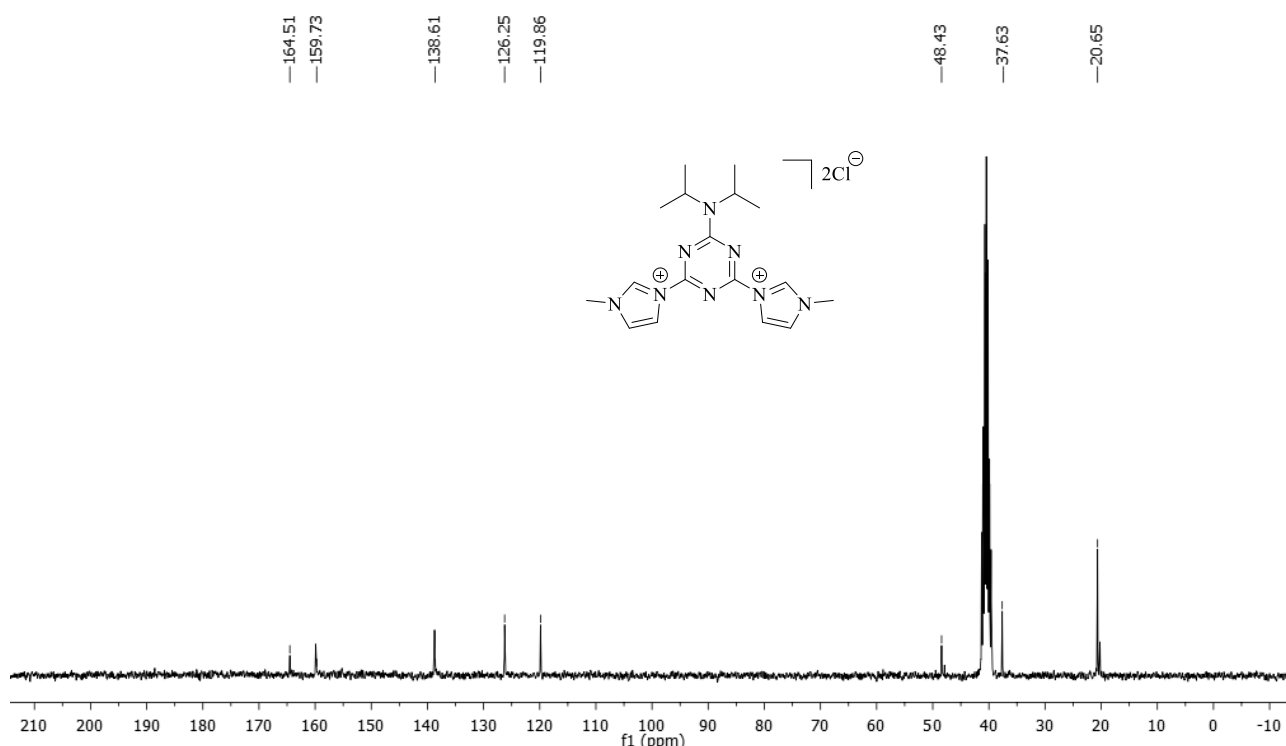


**Figure 3.55:**  $^{13}\text{C}$  NMR spectrum ( $\text{DMSO-d}_6$ ) of MIATMI.

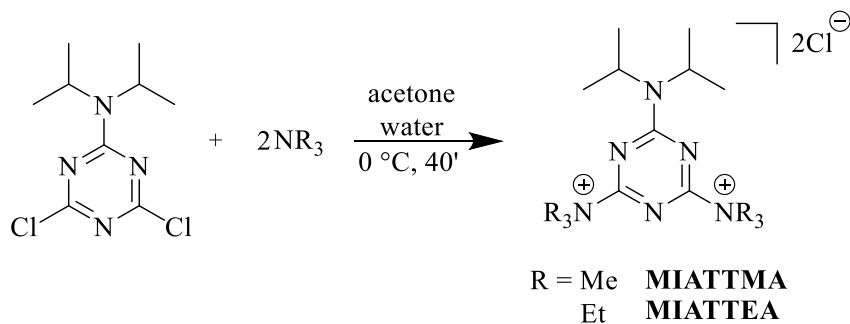
$^{13}\text{C}$  NMR (300 MHz,  $\text{DMSO-d}_6$ , ppm): 164.51, 159.73, 138.61, 126.25, 119.86, 48.43, 37.63, 20.65.

Thanks to  $^{13}\text{C}$  NMR spectrum in  $\text{DMSO-d}_6$  (**Figure 3.55**), it is possible to observe the presence of ( $\text{NCN}$ ) imidazole carbon at 138.61 ppm.



### 3.3.2.5 Synthesis of quaternary bis-ammonium salts of 2,4-dichloro-6-diisopropylamino-1,3,5-triazine in the presence of trimethylamine (MIATTMA) and triethylamine (MIATTEA)

MIATTMA and MIATTEA have been investigated by the reaction, at 0 °C, in an acetone solution of MIAT and the desired trialkylamine. (Scheme 3.31)



**Scheme 3.31:** Synthesis of MIATTMA and MIATTEA.

<sup>1</sup>H NMR, <sup>13</sup>C NMR and FT-IR spectra confirmed the synthesis of MIATTMA with a yield of 70% (purity 95%).

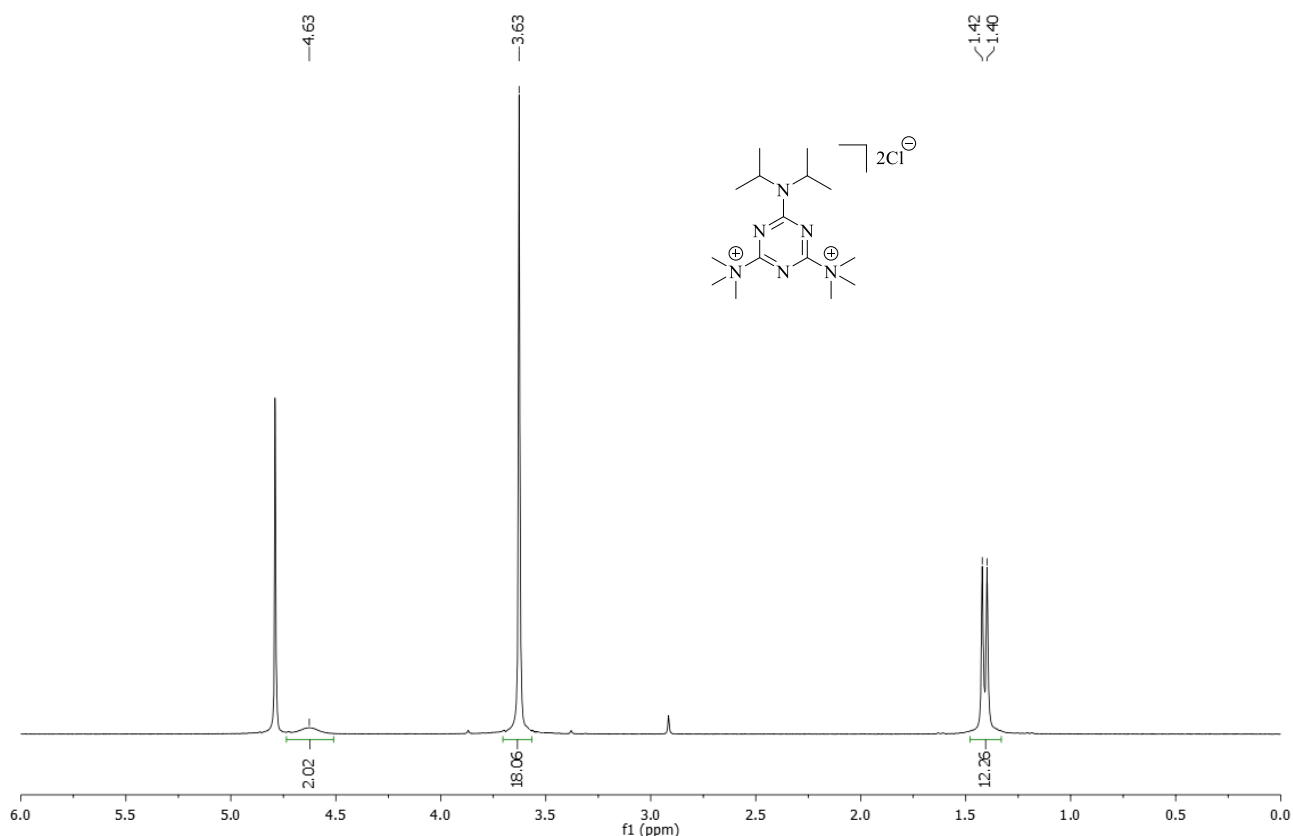


**Figure 3.56:** <sup>1</sup>H NMR spectrum (D<sub>2</sub>O) of MIATTMA.

<sup>1</sup>H NMR (300 MHz, D<sub>2</sub>O, ppm): 4.63 (2H, m broad, NCH(CH<sub>3</sub>)<sub>2</sub>), 3.63 (18H, s, CH<sub>3</sub>), 1.42 (12H, d, NCH(CH<sub>3</sub>)<sub>2</sub>).

In  $^1\text{H}$  NMR spectrum (**Figure 3.56**), the broad signal at 4.61 ppm and the doublet at 1.40 ppm are attributable respectively to diisopropylamino  $[\text{NCH}(\text{CH}_3)_2]$  and  $[\text{NCH}(\text{CH}_3)_2]$  protons. Methyl substituents of quaternary ammonium groups are observable in the singlet at 3.63 ppm.

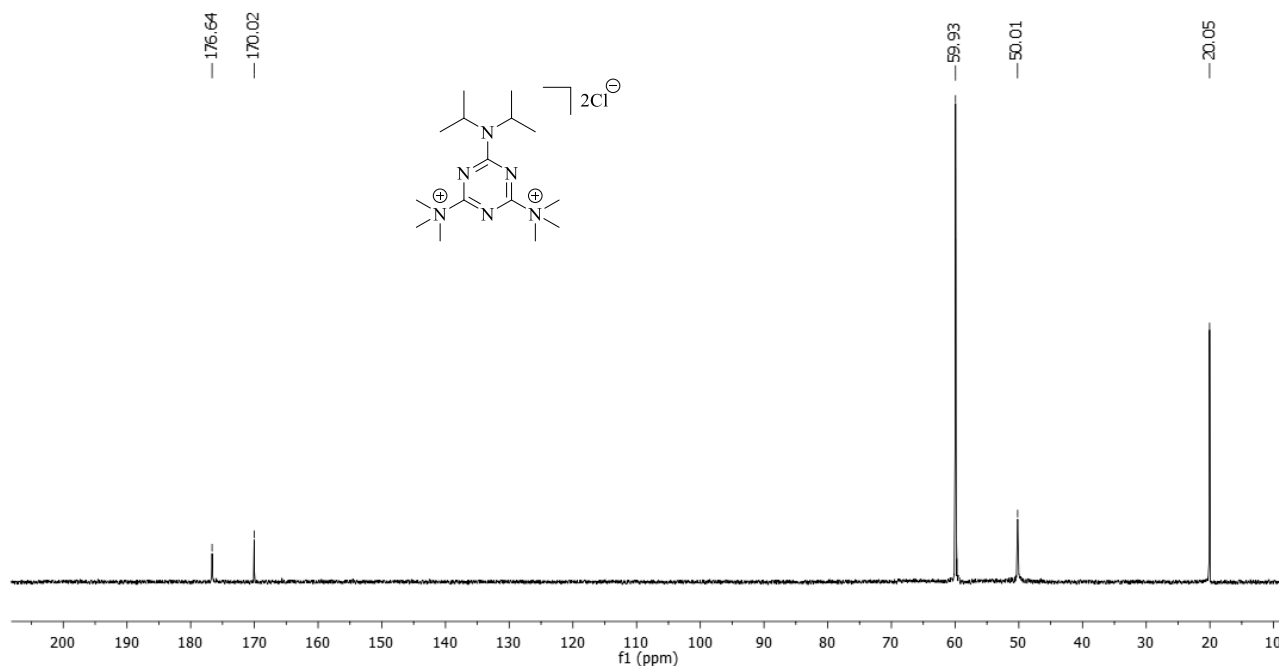


**Figure 3.57:**  $^{13}\text{C}$  NMR spectrum ( $\text{D}_2\text{O}$ ) of MIATTMA.

$^{13}\text{C}$  NMR (300 MHz,  $\text{D}_2\text{O}$ , ppm): 176.64, 170.02, 59.93, 50.01, 20.05.

In  $^{13}\text{C}$  NMR spectrum (**Figure 3.57**), signals at 176.64 ppm and at 170.02 ppm are attributable respectively to the diisopropylamino- and ammonium-bonded carbons of the triazine ring. Primary carbon signals of trimethylammonium groups are observable at 59.93 ppm, while signals at 50.01 ppm and 20.05 ppm are assignable to tertiary and primary carbons of the diisopropylamino group.

Unfortunately, when triethylamine was added to the MIAT acetone solution, no precipitation of product has been observed even after 24 hours of reaction at room temperature. Other similar attempts have confirmed this behavior, it was not possible to isolate a solid product in any case.

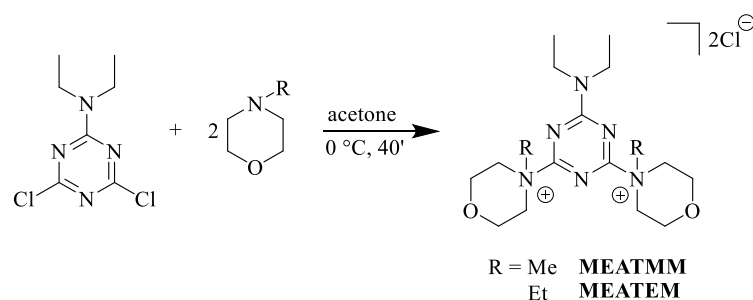
### 3.3.3 Synthesis of quaternary bis-ammonium salts derived from 2,4-dichloro-6-diethylamino-1,3,5-triazine (MEAT)

As reported previously (**Chapter 3.3.2**), few examples about ammonium salts of nitrogen substituted triazine exist in literature.<sup>[26,33,34,55]</sup> Similarly to what has been done for the quaternary bis-ammonium salts of MMT and MIAT, synthesis reactions of MEAT quaternary bis-ammonium

salts were carried out by the reaction of an acetone solution of 2,4-dichloro-6-diethylamino-1,3,5-triazine with an appropriate tertiary amine, methyl or ethyl substituted. Also in this case, all the following reactions were carried out by previously cooling the system at 0 °C with a water and ice bath, in order to avoid possible decomposition of the desired ammonium salts.<sup>[19]</sup>

### 3.3.3.1 Synthesis of quaternary bis-ammonium salts of 2,4-dichloro-6-diethylamino-1,3,5-triazine in the presence of *N*-methylmorpholine (MEATMM) and *N*-ethylmorpholine (MEATEM)

MEATMM and MEATEM have been investigated by the reaction, at 0 °C, in an acetone solution of MEAT and the desired *N*-alkylmorpholine. (**Scheme 3.32**)



**Scheme 3.32:** Synthesis of MEATMM and MEATEM.

<sup>1</sup>H NMR, <sup>13</sup>C NMR and FT-IR spectra confirmed the synthesis of MEATMM with a yield of 90% (purity 92%).

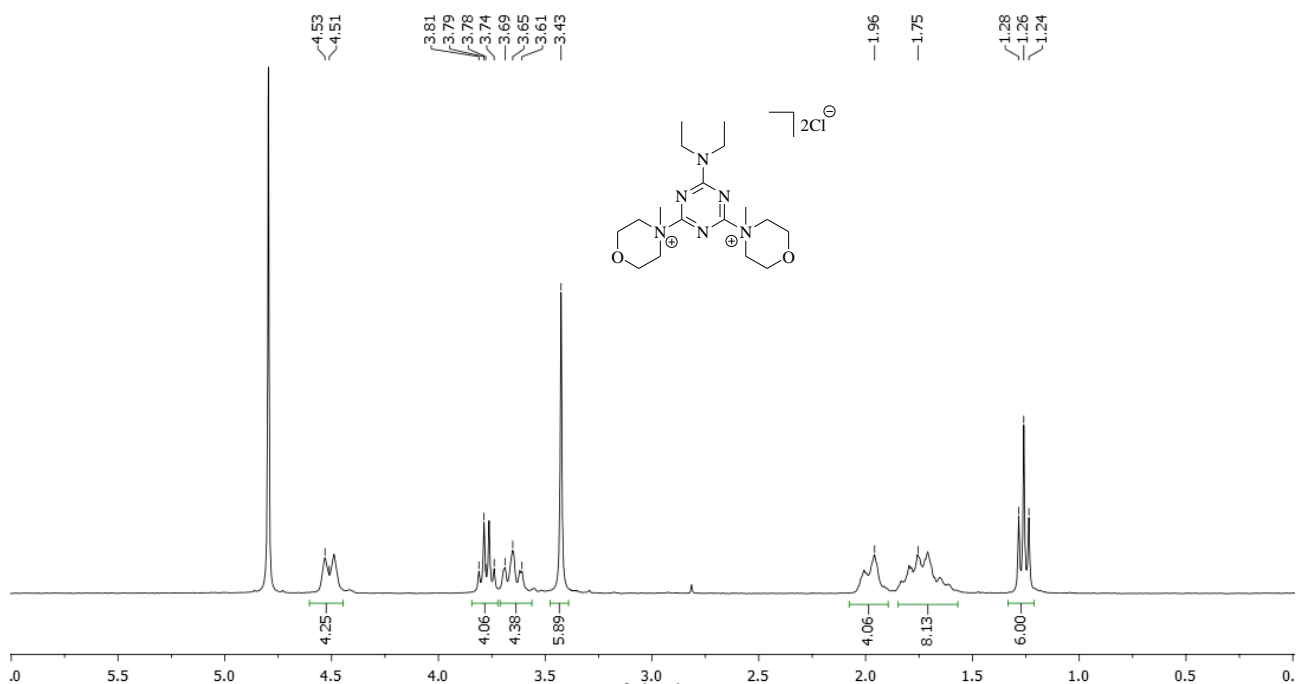


**Figure 3.58:** <sup>1</sup>H NMR spectrum (D<sub>2</sub>O) of MEATMM.

$^1\text{H}$  NMR (300 MHz,  $\text{D}_2\text{O}$ , ppm): 4.49 (4H, d,  $\text{N}^+\text{CH}_2\text{CH}_2\text{O}$ ), 4.10 (4H, d,  $\text{N}^+\text{CH}_2\text{CH}_2\text{O}$ ), 3.82 (8H, qi,  $\text{N}^+\text{CH}_2\text{CH}_2\text{O}$ ), 3.70 (4H, q,  $\text{N}^+\text{CH}_2\text{CH}_3$ ), 3.48 (6H, s,  $\text{N}^+\text{CH}_3$ ) 1.16 (6H, t,  $\text{N}^+\text{CH}_2\text{CH}_3$ ).

In  $^1\text{H}$  NMR spectrum (**Figure 3.58**), signals of the morpholine rings protons are observable as a multiplet at 3.82 ppm, for protons in meta position, and as two separated doublets at 4.49 ppm and at 4.10 ppm, for ortho position. This is in agreement with what explained before (**Chapter 3.3.1.1**) about conformational structure of the morpholine ring. Methyl groups bonded to quaternary ammonium nitrogens are attributable to the singlet at 3.48 ppm. Finally, the quartet at 3.70 ppm and the triplet at 1.16 ppm are assignable respectively to ethylamino ( $\text{N}^+\text{CH}_2\text{CH}_3$ ) and ( $\text{N}^+\text{CH}_2\text{CH}_3$ ) protons.

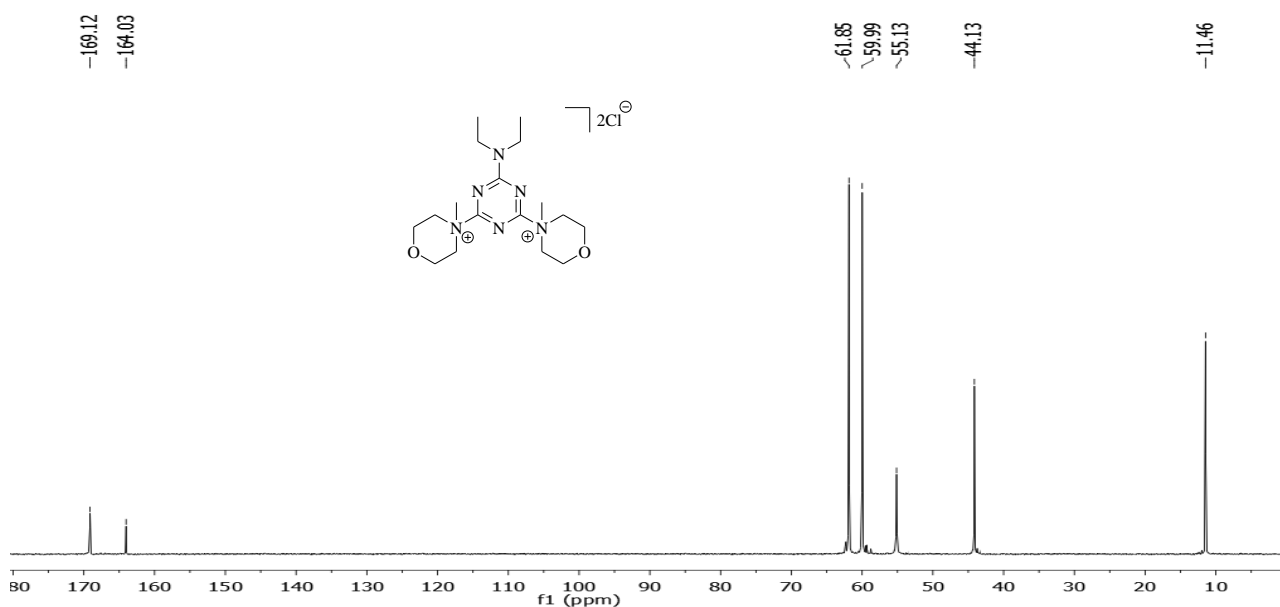


**Figure 3.59:**  $^{13}\text{C}$  NMR spectrum ( $\text{D}_2\text{O}$ ) of MEATMM.

$^{13}\text{C}$  NMR (300 MHz,  $\text{D}_2\text{O}$ , ppm): 169.12, 164.03, 61.85, 59.99, 55.13, 44.13, 11.46.

In  $^{13}\text{C}$  NMR spectrum (**Figure 3.59**), signals at 169.12 ppm and at 164.03 ppm are attributable to the triazine ring carbons, respectively to ammonium- and diethylamino-substituted carbons. Diethylamino group signals are observed at 44.13 ppm and at 11.46 ppm, respectively for secondary and primary carbons.

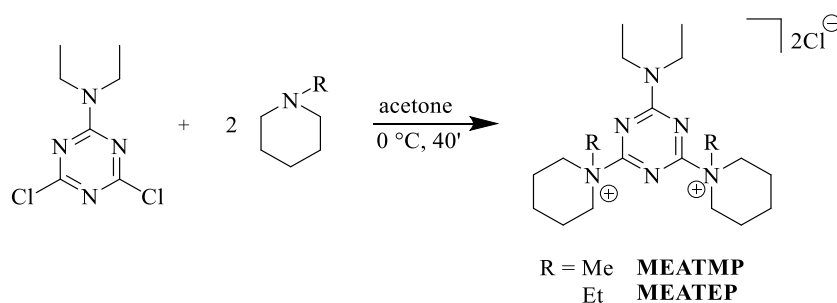
Signals at 61.82 ppm and at 59.99 ppm are assignable to the morpholine rings carbons in ortho and para positions. Finally, primary carbon signal of methyl groups is observable at 55.13 ppm. As observed for MIATMM (**Chapter 3.3.2.1**), it may be supposed that, in MEATMM as well, triazine ring is in equatorial position to both morpholine cycles. According to Kunishima's study where it is

reported that *N*-alkyl substituents in axial position are characterized by frequencies lower than 60 ppm.<sup>[21]</sup> X-ray structural analysis will be carried out to confirm the proposed explanation.

Unfortunately, when *N*-ethylmorpholine was added to the MEAT acetone solution, no precipitation of product has been observed even after 24 hours of reaction at room temperature. Other similar attempts have confirmed this behavior, it was not possible to isolate a solid product in any case.

### 3.3.3.2 Synthesis of quaternary bis-ammonium salts of 2,4-dichloro-6-diethylamino-1,3,5-triazine in the presence of *N*-methylpiperidine (MEATMP) and *N*-ethylpiperidine (MEATEP)

MEATMP and MEATEP have been investigated by the reaction, at 0 °C, in an acetone solution of MEAT and the desired *N*-alkylpiperidine. (Scheme 3.33)



Scheme 3.33: Synthesis of MEATMP and MEATEP.

<sup>1</sup>H NMR, <sup>13</sup>C NMR and FT-IR spectra confirmed the synthesis of MEATMP with a yield of 78% (purity 90%).

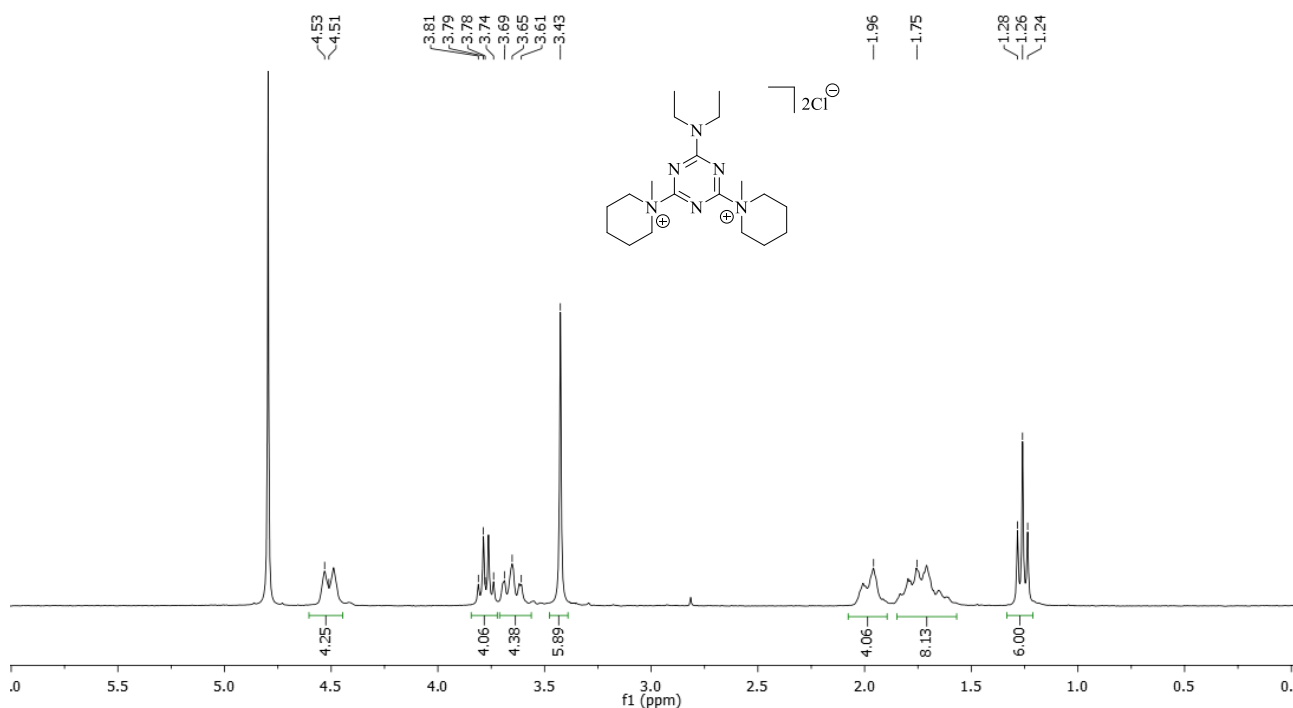


Figure 3.60: <sup>1</sup>H NMR spectrum (D<sub>2</sub>O) of MEATMP.

$^1\text{H}$  NMR (300 MHz,  $\text{D}_2\text{O}$ , ppm): 4.53 (4H, d,  $\text{N}^+\text{CH}_2\text{CH}_2\text{CH}_2$ ), 3.79 (4H, q,  $\text{N}^+\text{CH}_2\text{CH}_3$ ), 3.65 (4H, t,  $\text{N}^+\text{CH}_2\text{CH}_2\text{CH}_2$ ), 3.43 (6H, s,  $\text{N}^+\text{CH}_3$ ), 1.96 (4H, m,  $\text{N}^+\text{CH}_2\text{CH}_2\text{CH}_2$ ), 1.75 (8H, m,  $\text{N}^+\text{CH}_2\text{CH}_2\text{CH}_2$ ), 1.26 (6H, t  $\text{N}^+\text{CH}_2\text{CH}_3$ ).

In  $^1\text{H}$  NMR spectrum (**Figure 3.60**), signals of the piperidine rings protons are attributed to:

- ortho position, the doublet at 4.51 ppm and the triplet at 3.78 ppm
- para position, the multiplet at 1.98 ppm
- meta position, the multiplet at 1.73 ppm

Signal of methyl groups bonded to quaternary ammonium nitrogens are observable at 3.43 ppm. Finally, diethylamino group is attributable to the signals at 3.78 ppm and at 1.26 ppm, respectively for ( $\text{N}^+\text{CH}_2\text{CH}_3$ ) and ( $\text{N}^+\text{CH}_2\text{CH}_3$ ) protons.

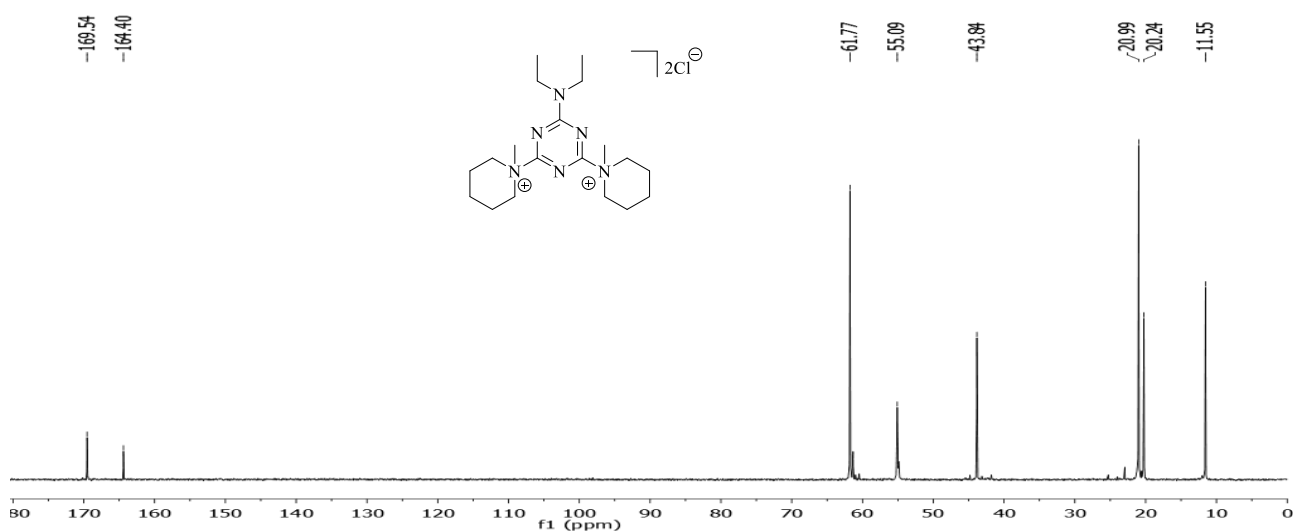


**Figure 3.61:**  $^{13}\text{C}$  NMR spectrum ( $\text{D}_2\text{O}$ ) of MEATMP.

$^{13}\text{C}$  NMR (300 MHz,  $\text{D}_2\text{O}$ , ppm): 169.54, 164.40, 61.17, 55.09, 43.84, 20.99, 20.24, 11.55.

In  $^{13}\text{C}$  NMR spectrum (**Figure 3.61**), signal of the triazine ring carbons bonded to quaternary ammonium nitrogens is observable at 169.54 ppm, while the diethylamino-substituted carbon is attributable to signal at 164.40 ppm.

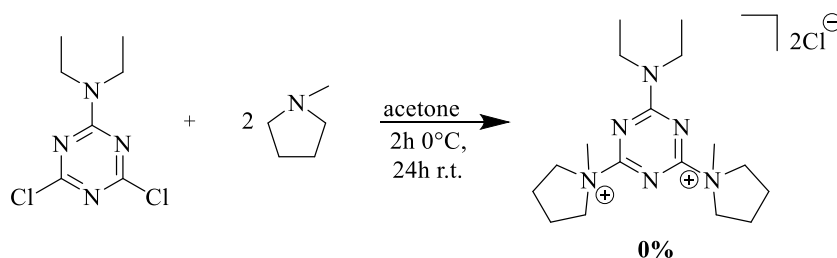
Diethylamino group signals are observed at 43.84 ppm and at 11.85 ppm, respectively for secondary and primary carbons. Signals at 61.77 ppm, at 20.99 ppm and at 20.24 ppm are assignable to the piperidine rings carbons in ortho, para and meta positions. Primary carbons signal of methyl groups bonded to quaternary ammonium nitrogens is observable at 55.09 ppm. Also in this case, it may be supposed that in MEATMP the triazine ring is in equatorial position to both piperidine cycles, in agreement with what reported by Kunishima about *N*-alkyl substituents in axial

position, characterized by frequencies lower than 60 ppm.<sup>[21]</sup> X-ray structural analysis will be carried out to confirm the proposed explanation.

Unfortunately, when *N*-piperidine was added to the MEAT acetone solution, no precipitation of product has been observed even after 24 hours of reaction at room temperature. Other similar attempts have confirmed this behavior, it was not possible to isolate a solid product in any case.

### 3.3.3.3 Study of quaternary bis-ammonium salt of 2,4-dichloro-6-diethylamino-1,3,5-triazine in the presence of *N*-methylpyrrolidine (MEATMPD)

MEATMPD has been investigated by reaction, at 0 °C, in an acetone solution of MEAT and *N*-methylpyrrolidine. (Scheme 3.34)

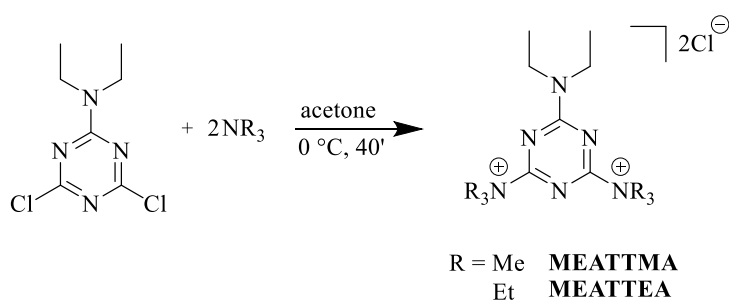


**Scheme 3.34:** Synthesis of MEATMPD.

Contrary to what has been previously observed for MIATMPD (**Chapter 3.3.2.3**), once the tertiary amine has been added, no precipitation of product has been observed. Even after that the reaction has been carried out at *r.t.* and left under stirring for 24 hours, no product could be isolated.

### 3.3.3.4 Synthesis of quaternary bis-ammonium salts of 2,4-dichloro-6-diethylamino-1,3,5-triazine in the presence of trimethylamine (MEATTMA) and triethylamine (MEATTEA)

MEATTMA and MEATEA have been investigated by the reaction between MEAT and the desired trialkylamine in an acetone solution at 0 °C. (Scheme 3.35)



**Scheme 3.35:** Synthesis of MEATTMA and of MEATTEA.

$^1\text{H}$  NMR,  $^{13}\text{C}$  NMR and FT-IR spectra confirmed the synthesis of MEATTMA with a yield of 96% (purity 90%). Experimentally, it has been verified that reaction times longer than 40 minutes lead to the formation of a yellowish oil.

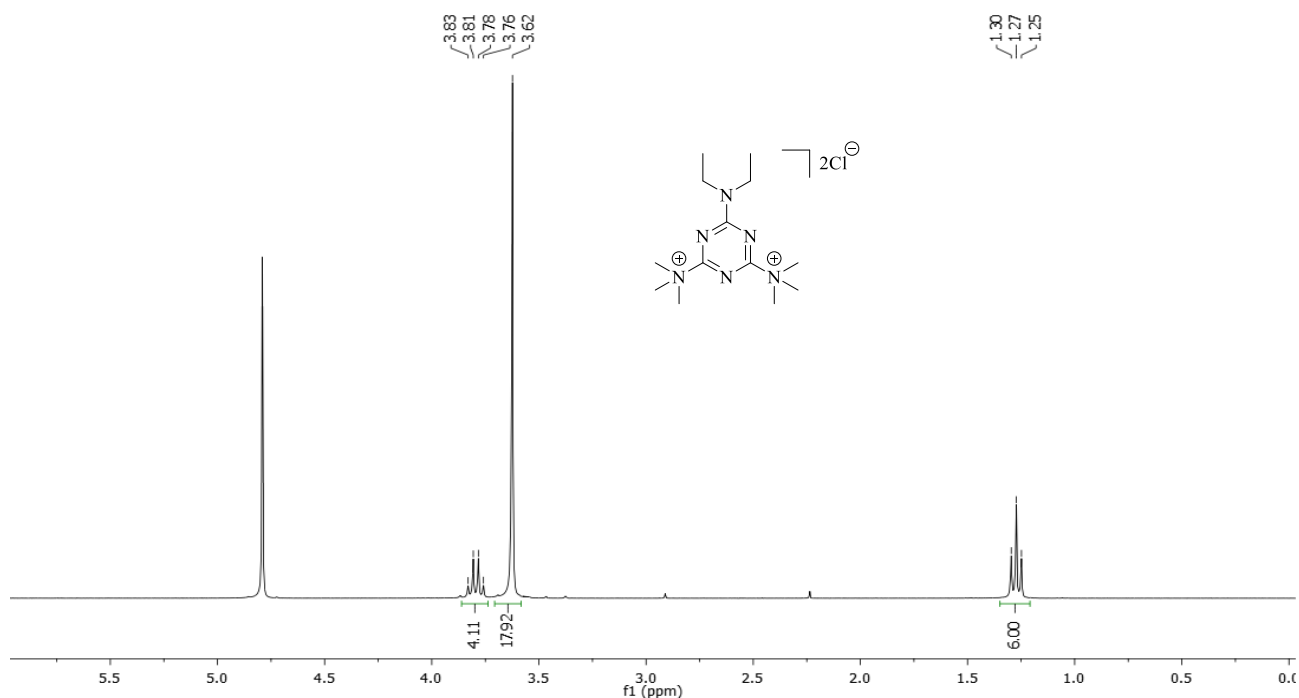


**Figure 3.62:**  $^1\text{H}$  NMR spectrum ( $\text{D}_2\text{O}$ ) of MEATTMA.

$^1\text{H}$  NMR (300 MHz,  $\text{D}_2\text{O}$ , ppm): 3.81 (4H, q,  $\text{N}^+\text{CH}_2\text{CH}_3$ ), 3.62 (18H, s,  $\text{N}^+\text{CH}_3$ ), 1.27 (6H, t,  $\text{N}^+\text{CH}_2\text{CH}_3$ ).

In  $^1\text{H}$  NMR spectrum (**Figure 3.62**), the quartet at 3.81 ppm and the triplet at 1.27 ppm are attributable respectively to ( $\text{N}^+\text{CH}_2\text{CH}_3$ ) and ( $\text{N}^+\text{CH}_2\text{CH}_3$ ) protons of diethylamino group. While, methyl substituents of quaternary ammonium nitrogens are observable at 3.62 ppm as a singlet.

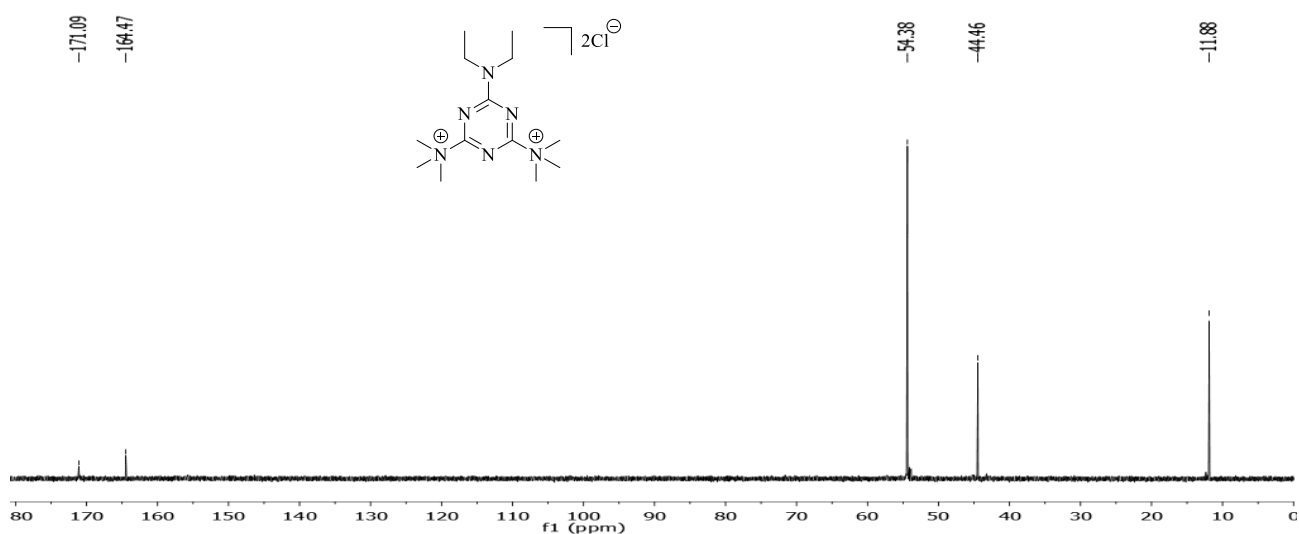


**Figure 3.63:**  $^{13}\text{C}$  NMR spectrum ( $\text{D}_2\text{O}$ ) of MEATTMA.



$^{13}\text{C}$  NMR (300 MHz,  $\text{D}_2\text{O}$ , ppm): 171.09, 164.47, 54.38, 44.46, 11.08.

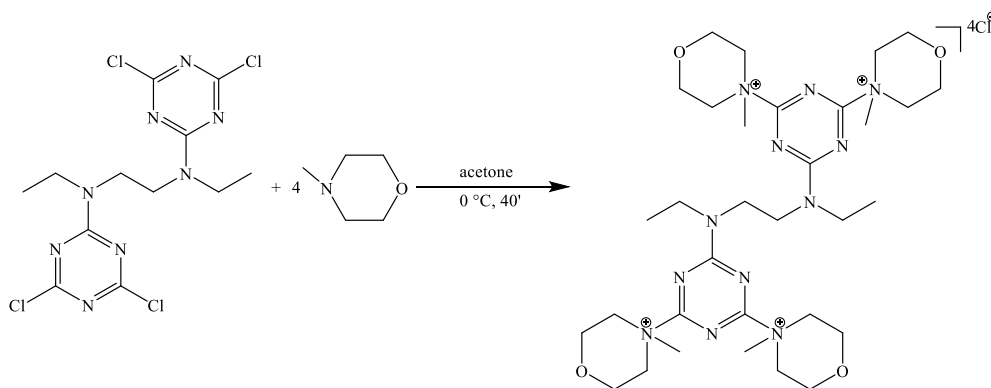
In  $^{13}\text{C}$  NMR spectrum (**Figure 3.63**), signals at 171.09 ppm and at 164.47 ppm are attributable respectively to diethylamino- and ammonium-bonded carbons of the triazine ring. Primary carbons signal of trimethylammonium groups is observable at 54.38 ppm. Finally, signals at 44.46 ppm and at 11.08 ppm are assignable to secondary and primary carbons of diethylamino group.

Unfortunately, when triethylamine was added to the MEAT acetone solution, no precipitation of product has been observed even after 24 hours of reaction at room temperature. Other similar attempts have confirmed this behavior, it was not possible to isolate a solid product in any case.

### 3.3.4 Study of quaternary tetrakis-ammonium salts derived from $N_1,N_2$ -bis(2,4-dichloro-1,3,5-triazin-6-yl)- $N_1,N_2$ -diethylethane-1,2-diamine in the presence of $N$ -methylmorpholine (MMDEDMM)

As reported before (**Chapter 3.2.4**), alkyldiamines are usually studied with 1,3,5-triazines for the synthesis of polyguanamines by polycondensation.<sup>[59,60]</sup> Austin *et al.* investigated the quaternization to bis-ammonium salts by alkylation of tertiary diamine moieties, rather than by tertiary amine substitution on the triazine rings.<sup>[61]</sup> To the best of our knowledge, no studies about ammonium salts derived by compounds similar to  $N_1,N_2$ -bis(2,4-dichloro-1,3,5-triazin-6-yl)- $N_1,N_2$ -diethylethane-1,2-diamine (CDEDC) are reported in literature.

Only one tetrakis-ammonium quaternary salt derived by CDEDC has been investigated using  $N$ -methylmorpholine (MM) as tertiary amine. For the synthesis, a similar protocol to what has been previously reported for 2,4-dichloro-6-substituted-1,3,5-triazines has been used. The reaction (**Scheme 3.36**) has been carried out by the addition of MM to an acetone solution of CDEDC. Also in this case, the synthesis was carried out by previously cooling the system at  $0^\circ\text{C}$  with a water and ice bath, in order to avoid possible decomposition of the desired ammonium salt.<sup>[19]</sup>



**Scheme 3.36:** Synthesis of MMDEDMM.

The isolated powder, has been characterized by  $^1\text{H}$  NMR,  $^{13}\text{C}$  NMR and FT-IR spectroscopy.

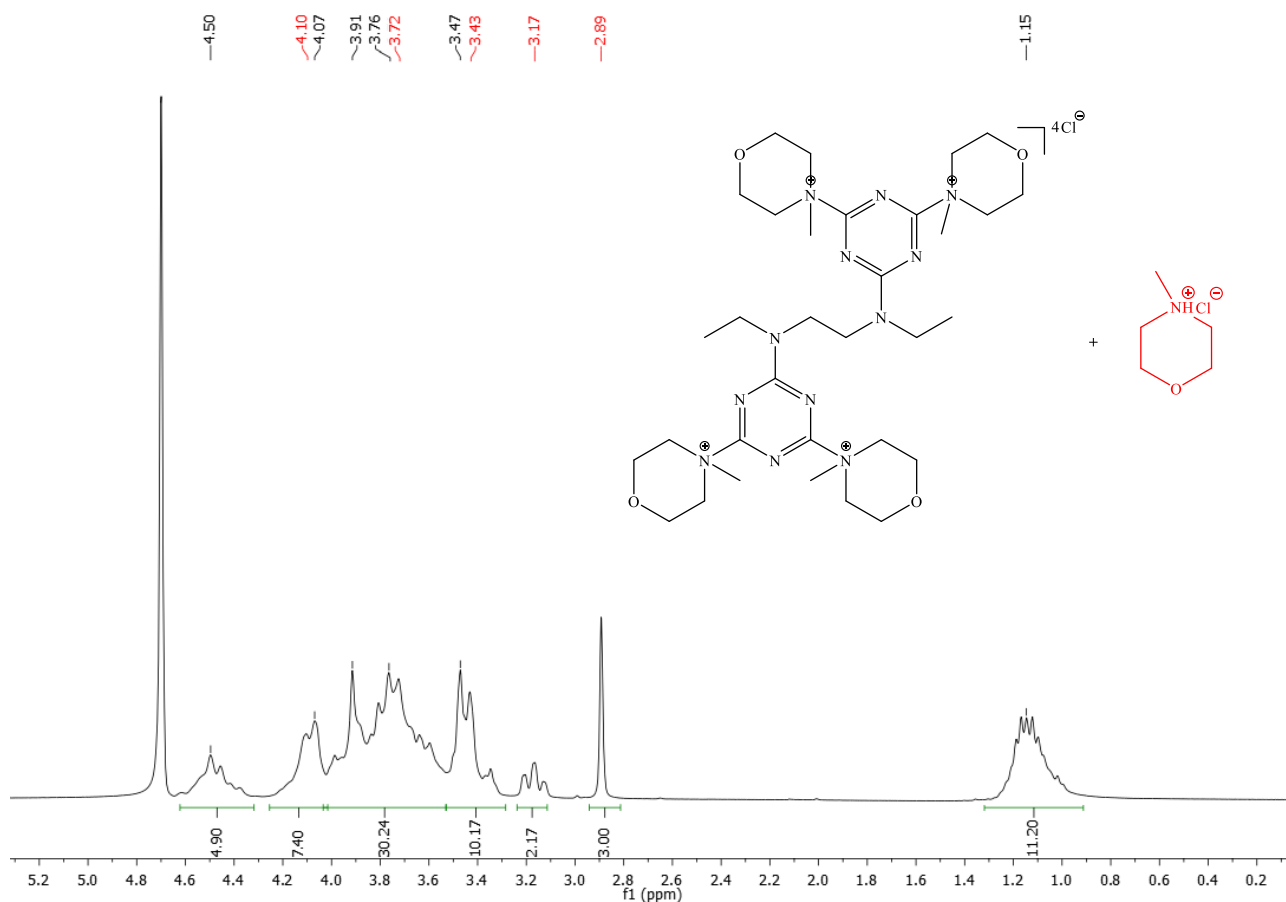


**Figure 3.64:**  $^1\text{H}$  NMR spectrum ( $\text{D}_2\text{O}$ ) of MMDEDMM.

$^1\text{H}$  NMR spectroscopy presented a complex spectrum probably due to the presence of different species in the product, in addition to molecule characteristics that may further influence the spectrum:

- restricted rotation around triazines-diamine bond explained before (**Chapter 3.2.4**)
- axial or equatorial conformational arrangements of *N*-methylmorpholinium rings investigated previously (**Chapter 3.3.1.1**)
- the presence of four possible morpholinium cycles in the molecule that may create steric hindrance issues.

In order to better understand  $^1\text{H}$  NMR spectrum (**Figure 3.64**), it has been necessary to gather a COSY NMR, reported below. (**Figure 3.65**)

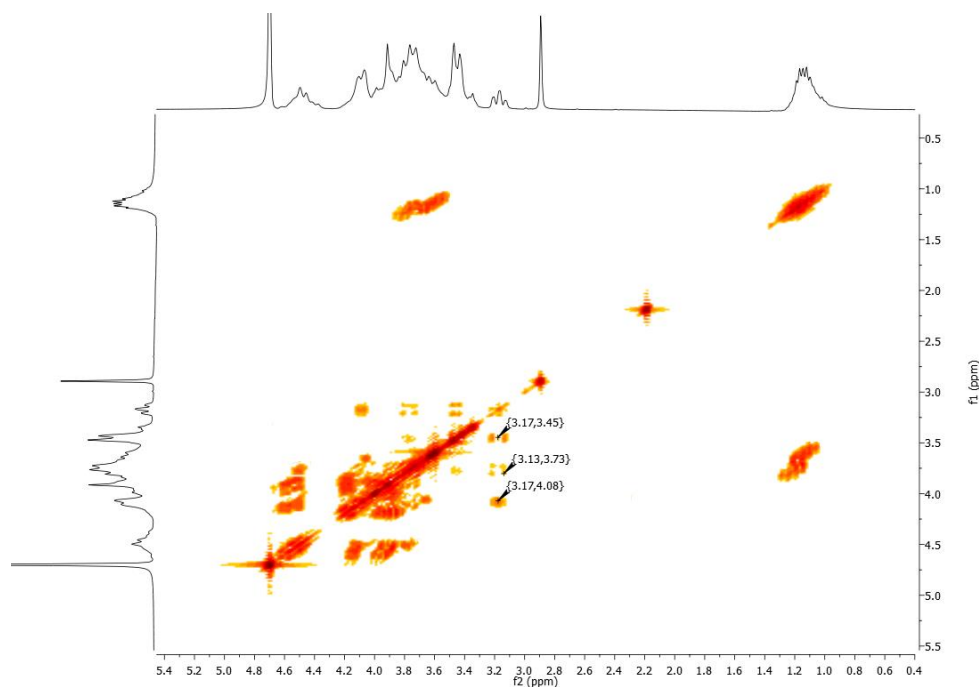


**Figure 3.65:** COSY NMR spectrum ( $D_2O$ ) of MMDEDMM.

In  $^1H$  NMR spectrum (**Figure 3.64**), it is possible to observe a triplet at 3.17 ppm and a singlet at 2.89 ppm, these signals can be attributed to *N*-methylmorpholinium chloride formed as byproduct of the reaction (reported in red in the spectrum for a better readability). Due to conformational arrangement of *N,N'*-disubstituted heterocycles,<sup>[32,21]</sup> protons of *N*-methylmorpholinium chloride do not possess the same resonance frequencies. In COSY NMR spectrum (**Figure 3.65**) it is possible to observe the coupling between the signal at 3.17 ppm with peaks at 3.43 ppm, at 3.72 ppm and at 4.10 ppm, assigning them to the byproduct.

In  $^1H$  NMR spectrum (**Figure 3.64**), multiplet at 1.15 ppm is attributable to ethyl substituent primary protons ( $NCH_2CH_3$ ) of the diamine moiety. In COSY NMR spectrum (**Figure 3.65**), this signal couples with ( $NCH_2CH_3$ ) ethyl protons at 3.76 ppm.

Protons in ortho position of the morpholine rings are observable at 4.50 ppm and at 4.07 ppm (**Figure 3.64**), as two distinct peaks due to conformational arrangements of the morpholine rings. In COSY NMR spectrum (**Figure 3.65**), it is possible to notice the coupling of ortho protons with the signal at 3.91 ppm, attributable to atoms in meta position.

It may be assumed that signals of ( $NCH_2CH_2N$ ) and *N*-methyl protons are present at resonance frequencies paragonable to those of similar compounds previously studied. (**Chapter 3.2.4** and **Chapter 3.3.3.1**)

Due to the presence of *N*-methylmorpholinium chloride it is possible that MMDEDMM may be a mixture of bis-, tris- or tetrakis *N*-methylmorpholinium salts. It is possible that the triazine substitution with two or three heterocycles is enough to let the molecule precipitate from the solution. The transition to heterogenous phase may slow down the reaction enough to allow the formation of *N*-methylmorpholinium chloride. Considering  $^1\text{H}$  NMR spectrum (**Figure 3.64**), this possibility is supported by the fact that relative intensities of the peaks attributable to MMDEDMM do not have the values expected. For this reasons the product is considered a mixture of species, reported for simpleness as MMDEDMM<sup>(\*)</sup>.

$^{13}\text{C}$  NMR spectrum it has proven to be too complicated for characterization of MMDEDMM<sup>(\*)</sup>, this may be caused by the presence of different species in the product and possibly due to restricted bond rotations as previously explained in this chapter.

### 3.4 Summary table of synthesized agents and their stability in aqueous solution and inert atmosphere

Below, a table (**Table 3.1**) is reported summarizing the yield and stability data up to 30 weeks for each of the synthesized compounds in solid phase or in solution.

**Table 3.1:** Yield and stability data over time of synthesized compounds

Condensation Agent	Chapter	Yield (%)	Stability in solution	Stability in solid form under N <sub>2</sub> atmosphere
DIAT	3.1.1	73	n.a. <sup>(a)</sup>	n.a. <sup>(a)</sup>
DEAT	3.1.2	79	n.a. <sup>(a)</sup>	n.a. <sup>(a)</sup>
MAT	3.1.3	74	> 30 weeks (acetone-d <sub>6</sub> )	> 30 weeks
MODAM	3.1.4	86	4 weeks (DMSO-d <sub>6</sub> )	> 30 weeks
MMDAM	3.1.5	94	5 weeks (DMSO-d <sub>6</sub> )	> 30 weeks
MMT	3.2.1	97	38% decomposed in 30 weeks (acetone-d <sub>6</sub> )	> 34 weeks
MIAT	3.2.2	95	> 30 weeks (acetone-d <sub>6</sub> )	> 30 weeks
MEAT	3.2.3	92	8% decomposed in 30 weeks (acetone-d <sub>6</sub> )	> 30 weeks
CEDC	3.2.4	97	1 day (acetone-d <sub>6</sub> )	n.a. <sup>(a)</sup>
CODAC	3.2.5	84	3 days (DMSO-d <sub>6</sub> )	15 weeks
CMDAC	3.2.5	85	5 days (DMSO-d <sub>6</sub> )	20 weeks
MMTMM	3.3.1.1	87	< 30 minutes (D <sub>2</sub> O)	< 2 days
MMTEM	3.3.1.2	89	10 weeks (D <sub>2</sub> O)	20 weeks
MMTMP	3.3.1.3	n.i. <sup>(b)</sup>	n.i. <sup>(b)</sup>	n.i. <sup>(b)</sup>
MMTEP	3.3.1.3	94	8 weeks (D <sub>2</sub> O)	10 weeks
MMTMPD	3.3.1.4	73	12 days (D <sub>2</sub> O)	3 weeks
MMTTMA <sup>(*)</sup>	3.3.1.5	n.a. <sup>(a)</sup>	< 1 day (D <sub>2</sub> O)	< 2 days
MMTTEA	3.3.1.5	n.i. <sup>(b)</sup>	n.i. <sup>(b)</sup>	n.i. <sup>(b)</sup>
MIATMM	3.3.2.1	88	20 weeks (D <sub>2</sub> O)	15 weeks
MIATEM	3.3.2.1	n.i. <sup>(b)</sup>	n.i. <sup>(b)</sup>	n.i. <sup>(b)</sup>
MIATMP	3.3.2.2	85	9 weeks (D <sub>2</sub> O)	10 weeks
MIATEP	3.3.2.2	n.i. <sup>(b)</sup>	n.i. <sup>(b)</sup>	n.i. <sup>(b)</sup>
MIATMPD	3.3.2.3	72	8 days (D <sub>2</sub> O)	16 days
MIATMI	3.3.2.4	78	8 days (D <sub>2</sub> O)	6 weeks
MIATTMA	3.3.2.5	70	1 day (D <sub>2</sub> O)	8 weeks
MIATTEA	3.3.2.5	n.i. <sup>(b)</sup>	n.i. <sup>(b)</sup>	n.i. <sup>(b)</sup>
MEATMM	3.3.3.1	90	19 days (D <sub>2</sub> O)	13 week
MEATEM	3.3.3.1	n.i. <sup>(b)</sup>	n.i. <sup>(b)</sup>	n.i. <sup>(b)</sup>
MEATMP	3.3.3.2	78	7 days (D <sub>2</sub> O)	26 week
MEATEP	3.3.3.2	n.i. <sup>(b)</sup>	n.i. <sup>(b)</sup>	n.i. <sup>(b)</sup>
MEATMPD	3.3.3.3	n.i. <sup>(b)</sup>	n.i. <sup>(b)</sup>	n.i. <sup>(b)</sup>
MEATTMA	3.3.3.4	96	1 day (D <sub>2</sub> O)	23% decomposed in 23 weeks
MEATTEA	3.3.3.4	n.i. <sup>(b)</sup>	n.i. <sup>(b)</sup>	n.i. <sup>(b)</sup>
MMDEDMM <sup>(*)</sup>	3.3.4	n.a. <sup>(a)</sup>	1 day (D <sub>2</sub> O)	n.a. <sup>(a)</sup>

(a) data not available, (b) it was not possible to isolate quaternary bis-ammonium salt, (\*) mixture of different species

### 3.5 Amidation reactions by use of quaternary bis-ammonium salts

DMTMM is a well known activator of carboxylic groups promoting the synthesis of amide bonds in condensation reactions when amines are used.<sup>[19,20]</sup> The synthesis of 2,4-dichloro-6-substituted-1,3,5-triazines (MMT, MIAT and MEAT), reported before, has been investigated in order to verify if the presence of two chloride atoms bonded to the triazine ring could lead to the formation of a “double active ester”, allowing the reduction of amidation agent used.

The reactivity of bis-ammonium salts has been tested in amidation reactions, both with aromatic and aliphatic carboxylic acids, to evaluate the performances.

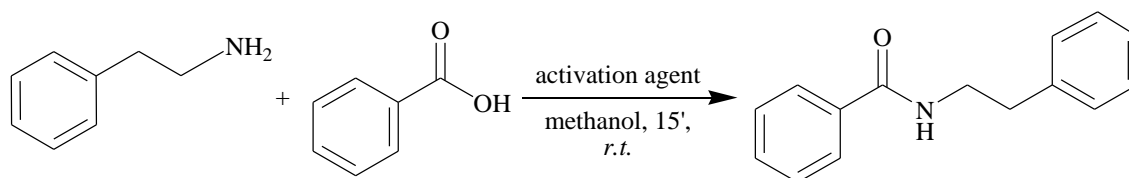
These condensation reactions have been carried out using amidation agents obtained with two different protocols, identified as “*isolated product procedure*” (*IPP*) and “*in situ*”.

By using the term “*IPP*” protocol, it is meant that an active solid amidation agent is used by a simply addition to the reaction solution.

By using the term “*in situ*” protocol, it is meant that the amidation agent is synthesized in its active form directly in the reaction solution.

#### 3.5.1 Amidation reactions with benzoic acid and phenylethylamine

Amidation of benzoic acid with phenylethylamine has been studied to obtain *N*-phenylethyl-benzamide. (**Scheme 3.37**)



**Scheme 3.37:** Synthesis of *N*-phenylethyl-benzamide.

Yield data have been obtained by gaschromatography using a calibration line made with isolated *N*-phenylethyl-benzamide (**Appendix 6.1**) and using tetraethylene-glycol-dimethyl-ether (tetraglyme) as internal standard.

Below are reported the yields in *N*-phenylethyl-benzamide obtained by the application of bis-ammonium quaternary salts with a substrate:amidation agent ratio of 2:1.

The data obtained are shown below. (**Table 3.2**)

**Table 3.2:** Yields in *N*-phenylethyl-benzamide by use of different bis-ammonium quaternary salts.

IPP	Yield <sup>(a)</sup> (%)	<i>in situ</i> <sup>(b)</sup>	Yield <sup>(a)</sup> (%)
MMTMM	71	MMT + MM	52
MMTEM	23	MMT + EM	50
MMTMP	n.i. <sup>(c)</sup>	MMT + MP	55
MMTEP	6	MMT + EP	8
MMTMPD	57	MMT + MPD	87
MMTTMA <sup>(*)</sup>	57	MMT + TMA	34
MMTTEA	n.i. <sup>(c)</sup>	MMT + TEA	9
MIATMM	51	MIAT + MM	33
MIATEM	n.i. <sup>(c)</sup>	MIAT + EM	12
MIATMP	33	MIAT + MP	20
MIATEP	n.i. <sup>(c)</sup>	MIAT + EP	5
MIATMPD	42	MIAT + MPD	51
MIATMI	0	MIAT + MI	0
MIATTMA	47	MIAT + TMA	20
MIATTEA	n.i. <sup>(c)</sup>	MIAT + TEA	7
MEATMM	44	MEAT + MM	40
MEATEM	n.i. <sup>(c)</sup>	MEAT + EM	18
MEATMP	57	MEAT + MP	28
MEATEP	n.i. <sup>(c)</sup>	MEAT + EP	6
MEATMPD	n.i. <sup>(c)</sup>	MEAT + MPD	47
MEATTMA	46	MEAT + TMA	19
MEATTEA	n.i. <sup>(c)</sup>	MEAT + TEA	8

Reaction conditions: tetraglyme 0.6 mmoles (standard), benzoic acid 1.2 mmoles, phenylethylamine 1.2 mmoles, at *r.t.* for 15 minutes;

*IPP* protocol: amidation agent 0.6 mmoles, 6 mL of methanol;

*In situ* protocol: premixing of a 2,4-dichloro-6-substituted-1,3,5-triazine (0.6 mmoles) and a tertiary amine (1.2 mmoles) in 2 mL of methanol, (total volume of solvent for reaction 6 mL);

(a) yield is calculated by gaschromatography, analysis conditions: isotherm at 50 °C for 4 minutes; heating cycle from 50 °C to 230 °C at 20 °C/min; isotherm at 230 °C for 30 minutes;

(b) tertiary amines used are: *N*-methylmorpholine (MM), *N*-ethylmorpholine (EM), *N*-methylpiperidine (MP), *N*-ethylpiperidine (EP), *N*-methylpyrrolidine (MPD), *N*-methylimidazole (MI), trimethylamine (TMA), triethylamine (TEA);

(c) quaternary bis-ammonium salt has not been isolated;

(\*) MMTTMA resulted to be a mixture of different species as explained in **Chapter 3.3.1.5**.

From data in **Table 3.2**, it is possible to observe:

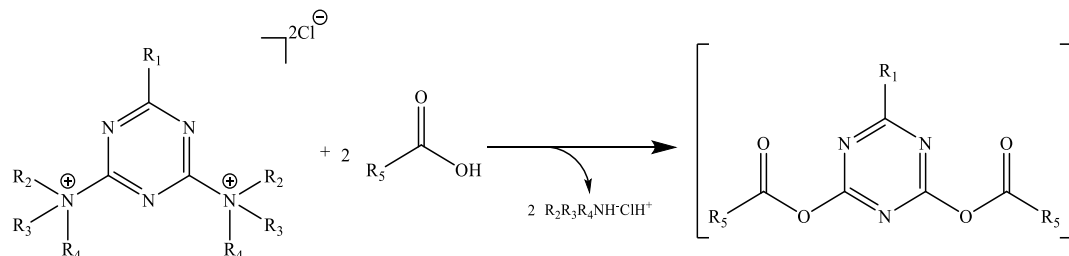
- Reactions carried out in the presence of quaternary bis-ammonium salts derived from MMT show, generally, higher yields in *N*-phenylethyl-benzamide compared to relative salts derived from MIAT and MEAT;
- MIATMI, both with *IPP* and *in situ* protocols, has proven to be completely inactive as condensing agent in amidation reactions, this results are in agreement with what reported in literature,<sup>[21]</sup>
- Considering reactions carried out with *IPP* protocol, highest yield has been obtained using MMTMM, with yield of 71%;
- *In situ* protocol has proven to be active for amidation reaction in all tested cases (with exception of MIAT+MI), with yields between 5% and 87%. Therefore, it can be considered preferable to *IPP* protocol;
- For what concerns *in situ* protocol, the highest yield has been obtained using MMT+MPD with yield of 87%;
- Although it was not possible to isolate some compounds, such as MMTMP and MEATMPD, the amidation reactions with their *in situ* protocol counterparts led to good yields in amide (respectively 55% and 47%), suggesting that the agent is able to activate the carboxylic acid in the solution, even if its salt could not be isolated.
- Reactions carried out in the presence of quaternary bis-ammonium salts derived from *N*-ethyl tertiary amines (MMTEM, MMTEP, MMTTEA), always led to yields lower than the ones obtained using salts derived by their *N*-methyl counterparts.

It is important to notice that the amidation reactions carried out in the presence of DMTMM needs at least the same molecular amount of ammonium salt in order to activate the carboxylic acid group.<sup>[21]</sup> Kunishima *et al.* report a yield in *N*-phenylethyl-benzamide of 81% (in THF)<sup>[20]</sup> or 90% (MeOH)<sup>[33]</sup> using DMTMM as amidation agent. In order to make a comparative test, an amidation reaction has been carried out using DMTMM with both *IPP* and *in situ* protocols with a substrate:DMTMM ratio of 2:1. In these conditions, the yields in desired amide were respectively of 47% and 45%

As reported above (**Table 3.2**), in many cases yields are higher than 50%. Moreover, the amidation reactions have been carried out with a substrate:amidation agent ratio of 2:1. Considering these factors, it can be assumed that bis-ammonium salts derived by 2,4-dichloro-6-substituted-1,3,5-triazine proved in many cases to have better performances than DMTMM.

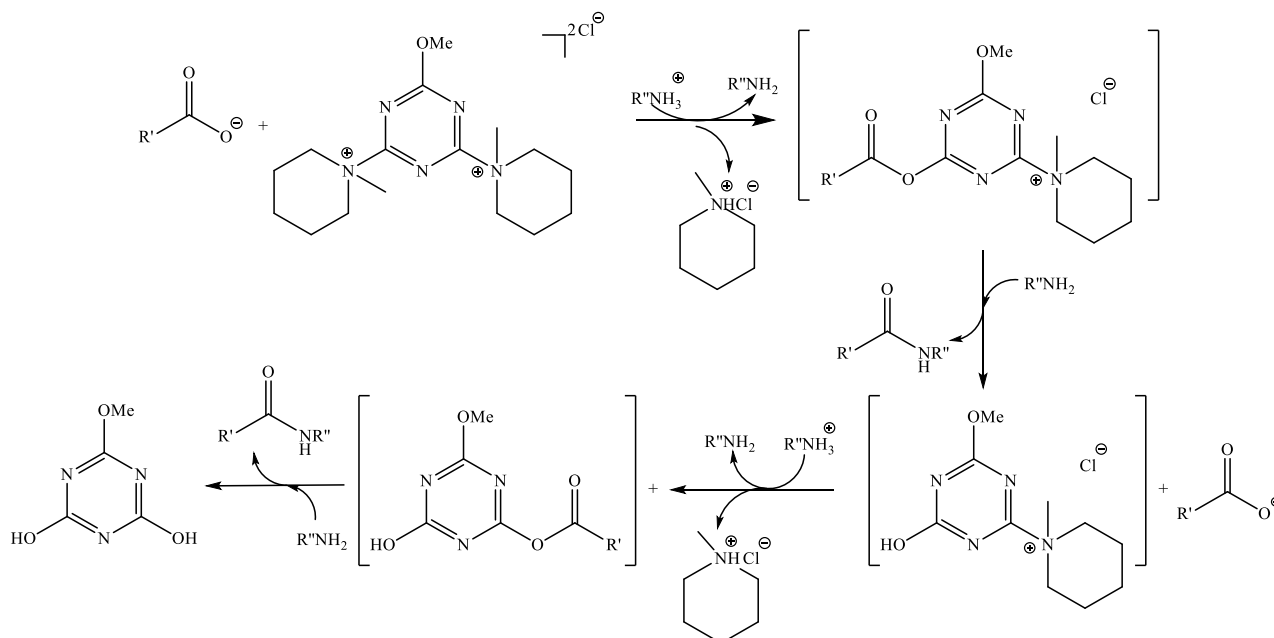


It may be supposed that the use of bis-ammonium salts derived from 2,4-dichloro-6-substituted-1,3,5-triazine led to the formation of an active intermediate diester (2,4-diacyloxy-6-substituted-1,3,5-triazine) (**Scheme 3.38**), that allow to halve the quantity of active agent needed for the reaction.



**Scheme 3.38:** Supposed formation of a general intermediate 2,4-diacyloxy-6-substituted-1,3,5-triazine (active diester) in an amidation reaction.

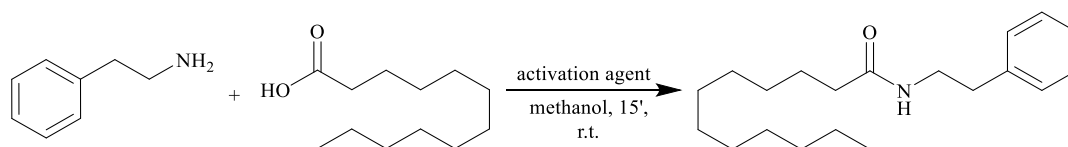
Kaminsky reported that 2,4-diacyloxy-6-substituted-1,3,5-triazine (active diester) is isolable at low temperatures and quickly undergoes decomposition processes at room temperature.<sup>[29]</sup> In this study suppositions are made about the mechanism involved for amidation reaction and it is considered improbable that the reaction undergoes a one step mechanism, but rather two independent subsequent stages, as shown below, using MMTMM for better readability. (**Scheme 3.39**)



**Scheme 3.39:** Supposed amidation mechanism involving a bis-ammonium salt, in this case MMTMM.

### 3.5.2 Amidation reactions with dodecanoic acid and phenylethylamine

Amidation reaction of dodecanoic acid with phenylethylamine has been studied in order to synthesize *N*-phenylethyl-dodecanamide. (**Scheme 3.40**)



**Scheme 3.40:** Synthesis reaction of *N*-phenylethyl-dodecanamide.

Yield data have been obtained by gaschromatography using a calibration line made with isolated *N*-phenylethyl-dodecanamide (**Appendix 6.2**) and using tetraethylene-glycol-dimethyl-ether (tetraglyme) as internal standard.

Below are reported the yields in *N*-phenylethyl-dodecanamide obtained by the application of bis-ammonium quaternary salts with a substrate:amidation agent ratio of 2:1.

The data obtained are shown below. (**Table 3.3**)

**Table 3.3:** Yields of *N*-phenylethyl-dodecanamide of amidation reactions by different bis-ammonium quaternary salts.

IPP	Yield <sup>(a)</sup> (%)	<i>in situ</i> <sup>(b)</sup>	Yield <sup>(a)</sup> (%)
MMTMM	63	MMT + MM	46
MMTEM	24	MMT + EM	29
MMTMP	n.i. <sup>(c)</sup>	MMT + MP	41
MMTEP	11	MMT + EP	27
MMTMPD	32	MMT + MPD	27
MMTTMA <sup>(*)</sup>	43	MMT + TMA	21
MMTTEA	n.i. <sup>(c)</sup>	MMT + TEA	17
MIATMM	39	MIAT + MM	27
MIATEM	n.i. <sup>(c)</sup>	MIAT+EM	9
MIATMP	19	MIAT + MP	34
MIATEP	n.i. <sup>(c)</sup>	MIAT+EP	4
MIATMPD	48	MIAT + MPD	13
MIATMI	0	MIAT + MI	0
MIATTMA	39	MIAT + TMA	13
MIATTEA	n.i. <sup>(c)</sup>	MIAT+TEA	11
MEATMM	49	MEAT + MM	36
MEATEM	n.i. <sup>(c)</sup>	MEAT+EM	11
MEATMP	42	MEAT + MP	26
MEATEP	n.i. <sup>(c)</sup>	MEAT+EP	5
MEATMPD	n.i. <sup>(c)</sup>	MEAT + MPD	22
MEATTMA	41	MEAT + TMA	18
MEATTEA	n.i. <sup>(c)</sup>	MEAT+TEA	11

Reaction conditions: tetraglyme 0.6 mmoles (standard), dodecanoic acid 1.2 mmoles, phenylethylamine 1.2 mmoles, at *r.t.* for 15 minutes;

*IPP* protocol: amidation agent 0.6 mmoles, 6 mL of methanol;

*In situ* protocol: premixing of a 2,4-dichloro-6-substituted-1,3,5-triazine (0.6 mmoles) and a tertiary amine (1.2 mmoles) in 2 mL of methanol, (total volume of solvent for reaction 6 mL);

(a) yield is calculated by gaschromatography, analysis conditions: isotherm at 50 °C for 4 minutes; heating cycle from 50 °C to 230 °C at 20 °C/min; isotherm at 230 °C for 30 minutes;

(b) tertiary amines used are: *N*-methylmorpholine (MM), *N*-ethylmorpholine (EM), *N*-methylpiperidine (MP), *N*-ethyl piperidine (EP), *N*-methylpiperolidine (MPD), *N*-methylimidazole (MI), trimethylamine (TMA), triethylamine (TEA);

(c) quaternary bis-ammonium salt has not been isolated;

(\*) MMTMA resulted to be a mixture of different species as explained in **Chapter 3.3.1.5**.

From data in **Table 3.3**, it is possible to observe:

- Reactions carried out in the presence of quaternary bis-ammonium salts derived from MMT show, generally, yields in *N*-phenylethyl-dodecanamide comparable to the yields obtained using salts derived from MIAT and MEAT;
- MIATMI, both with *IPP* and *in situ* protocols, has proven to be completely inactive as condensing agent in amidation reactions. These results are in agreement with other experimental data (**Table 3.2**) and with what have been reported in literature;<sup>[21]</sup>
- Considering reactions carried out with *IPP* protocol, yields obtained are generally higher compared to what observed by the application of *in situ* protocol. The highest yield has been obtained using MMTMM, with yield of 63%;
- *In situ* protocol has proven to be active for amidation reaction in all tested cases (with exception of MIAT+MI), with yields between 4% and 46%. Therefore, it can be considered preferable to *IPP* protocol;
- Amidation reaction with *in situ* protocol of MMT+MP led to good yields (41%) in amide even if it was not possible to isolate some compounds, suggesting that the agent is able to activate the carboxylic acid in the solution, even if its salt could not be isolated.
- Reactions carried out in the presence of quaternary bis-ammonium salts derived from *N*-ethyl tertiary amines (MMTEM, MMTEP, MMTTEA), always led to yields lower than the ones obtained using salts derived by their *N*-methyl counterparts.

To the best of our knowledge, only one study about amidation of saturated aliphatic carboxylic acid (hexanoic acid) exists in literature. Kunishima *et al.* reported a yield in *N*-phenylethyl-hexanamide of 83% in a reaction carried overnight in the presence of stoichiometric DMTMM using THF as

solvent.<sup>[20]</sup> Experimental data demonstrated that reaction in methanol with another saturated aliphatic carboxylic, such as dodecanoic acid, led to similar results to what reported by Kunishima. Reaction yield in *N*-phenylethyl-dodecanamide at different time were: 78% for overnight reaction and 74% after 15 minutes. In order to make a comparative test, an amidation reaction has been carried out using DMTMM with both *IPP* and *in situ* protocols with a substrate:DMTMM ratio of 2:1. In these conditions, yields in desired amide after 15 minutes were respectively of 45% and 39%. As reported above (**Table 3.3**), in many cases yields of amidation reaction activated by the application of bis-ammonium quaternary salts are comparable or higher to results obtained with DMTMM. As explained in **Chapter 3.5.1.1**, it may be supposed that amidation reaction are enhanced by the formation of an an active intermediate diester (2,4-diacyloxy-6-substituted-1,3,5-triazine), that allow to halve the quantity of active agent needed for the reaction.

## **CHAPTER 4**

### **CONCLUSIONS**

### **SYNTHESIS OF AMIDATION AGENTS AND THEIR REACTIVITY IN COUPLING REACTIONS**

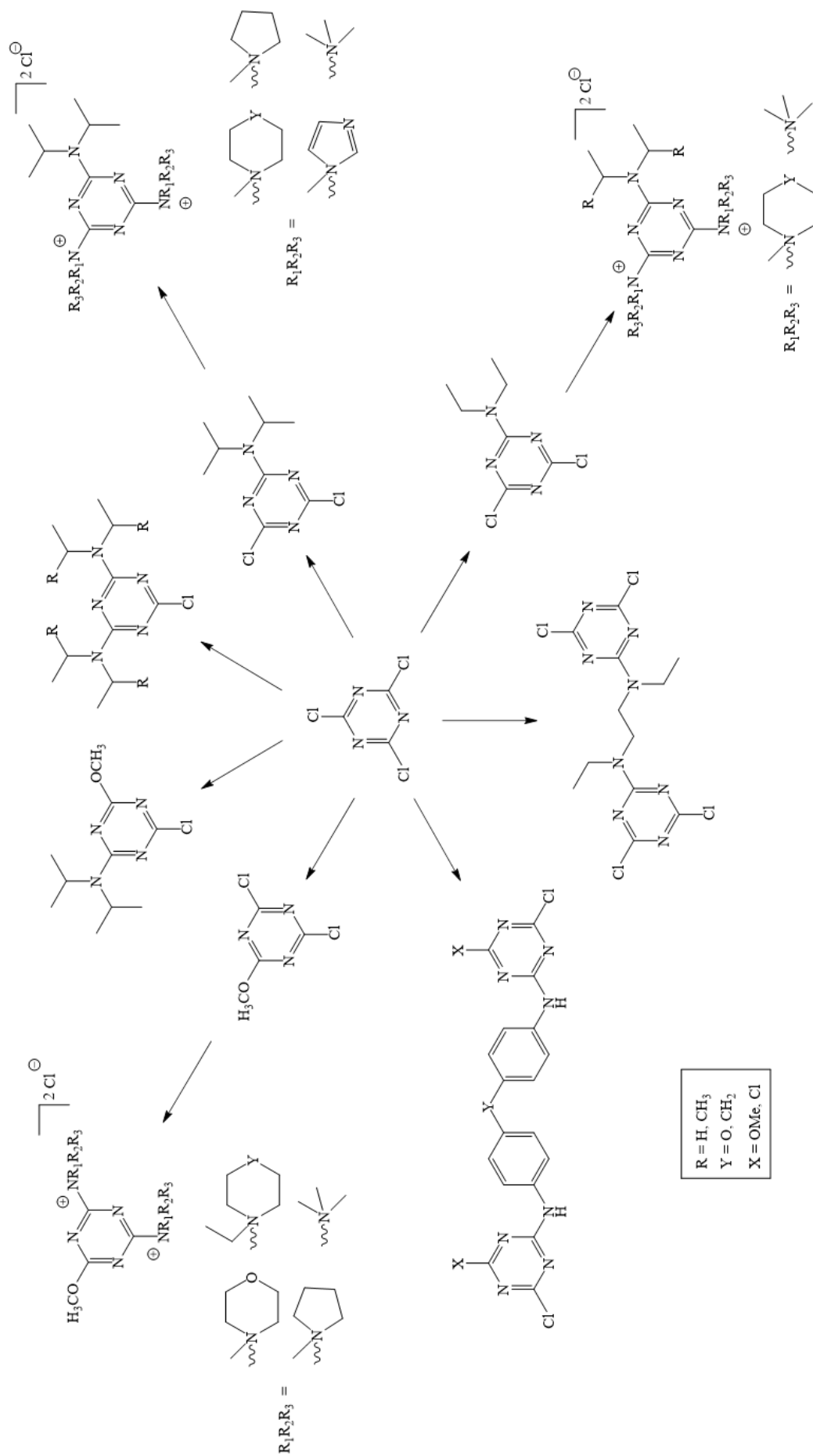
The research carried out in this part of the PhD thesis has focused on the development of a new library of quaternary ammonium salts derived from 1,3,5-triazine-based compounds. (**Scheme 4.1**) Moreover, a study concerning their reactivity as amidation agents has been carried out.

The main results achieved are:

- Identification of a standard synthesis procedure for the preparation of MMT, MIAT and MEAT which allows to obtain, under mild reaction conditions, 2,4-dichloro-6-substituted-1,3,5-triazine with high yields (in all cases above 92%). Products have been characterized by  $^1\text{H}$  NMR,  $^{13}\text{C}$  NMR, FT-IR and m.p.;
- Identification of a standard synthesis procedure for the preparation of MODAM, MMDAM, CDEDC, CODAC and CMDAC which led to the isolation of 2-chloro-4,6-disubstituted- or 2,4-dichloro-6-substituted-1,3,5-triazine compounds with triazine rings (yield between 75% and 90%). Products have been characterized by  $^1\text{H}$  NMR,  $^{13}\text{C}$  NMR, FT-IR and m.p.;
- 2,4-dichloro-6-substituted-1,3,5-triazine have been used for the synthesis of the derivated quaternary ammonium salts obtained by reaction with *N*-methylmorpholine, *N*-ethylmorpholine, *N*-methylpiperidine, *N*-ethylpiperidine, *N*-methylpyrrolidine, *N*-methylimidazole, trimethylamine and triethylamine. All products have been characterized by  $^1\text{H}$  NMR,  $^{13}\text{C}$  NMR, FT-IR and m.p.;
- The quaternary ammonium salts with a *N*-ethyl moiety resulted to be less reactive in amidation reaction compared to their *N*-methyl substituted counterparts;
- The *In situ* protocol proved to be preferable compared to *IPP* protocol, leading to the activation of carboxylic acids even when the corresponding quaternary ammonium salt was not isolable;
- Quaternary bis-ammonium salts of the 2,4-dichloro-6-substituted-1,3,5-triazines have been tested as amidation agents for condensation reactions in the presence of aromatic or aliphatic carboxylic acids and phenylethylamine. A substrate:amidation agent ratio of 2:1 has been used and yields higher than 50% are obtained with the use of several ammonium salts. Hence, it is possible to assume that the formation of an intermediate active diester occurs, allowing to reduce the amount of amidation agent required by half. In order to demonstrate this hypothesis, a comparative test using DMTMM has been carried out in the same reaction conditions.

This study led to the draft of two patents:

1. V. Beghetto, L. Agostinis, PCT/EP2017/064720, **2017**
2. V. Beghetto, V. Gatto, L. Agostinis, 102016000064898, **2016**



**Scheme 4.1:** New 1,3,5-triazine and derivated multi-ammonium salts synthesized.

## **CHAPTER 5**

### **EXPERIMENTAL SECTION**

### **SYNTHESIS OF AMIDATION AGENTS AND THEIR REACTIVITY IN COUPLING REACTIONS**



## 5.1 General methods

All chemicals were commercially available and procured from Sigma Aldrich, Merck, Alfa Aesar and Fluka with high grade of purity.

Solvents were of analytical grade and used without further purification.

NMR spectra were recorded with a Bruker Avance 300 model spectrometer. The chemical shifts were reported as parts per million (ppm) downfield from TMS (Me<sub>4</sub>Si) with <sup>1</sup>H resonant frequency of 300.13 MHz and <sup>13</sup>C resonant frequency of 75.4 MHz for the carbon spectrum.

Deuterated solvents used for the NMR analyses were the following: CDCl<sub>3</sub>, acetone-d<sub>6</sub>, DMSO-d<sub>6</sub> and D<sub>2</sub>O and procured by Euriso-Top and Sigma Aldrich. The purity of 1,3,5-triazine compounds and their derivated ammonium salts was calculated by integrating the signals present in the <sup>1</sup>H NMR spectrum.

Spectra in the region of middle infrared (4000-450 cm<sup>-1</sup>) were recorded using a Perkin-Elmer Spectrum-One spectrophotometer using KBr disks.

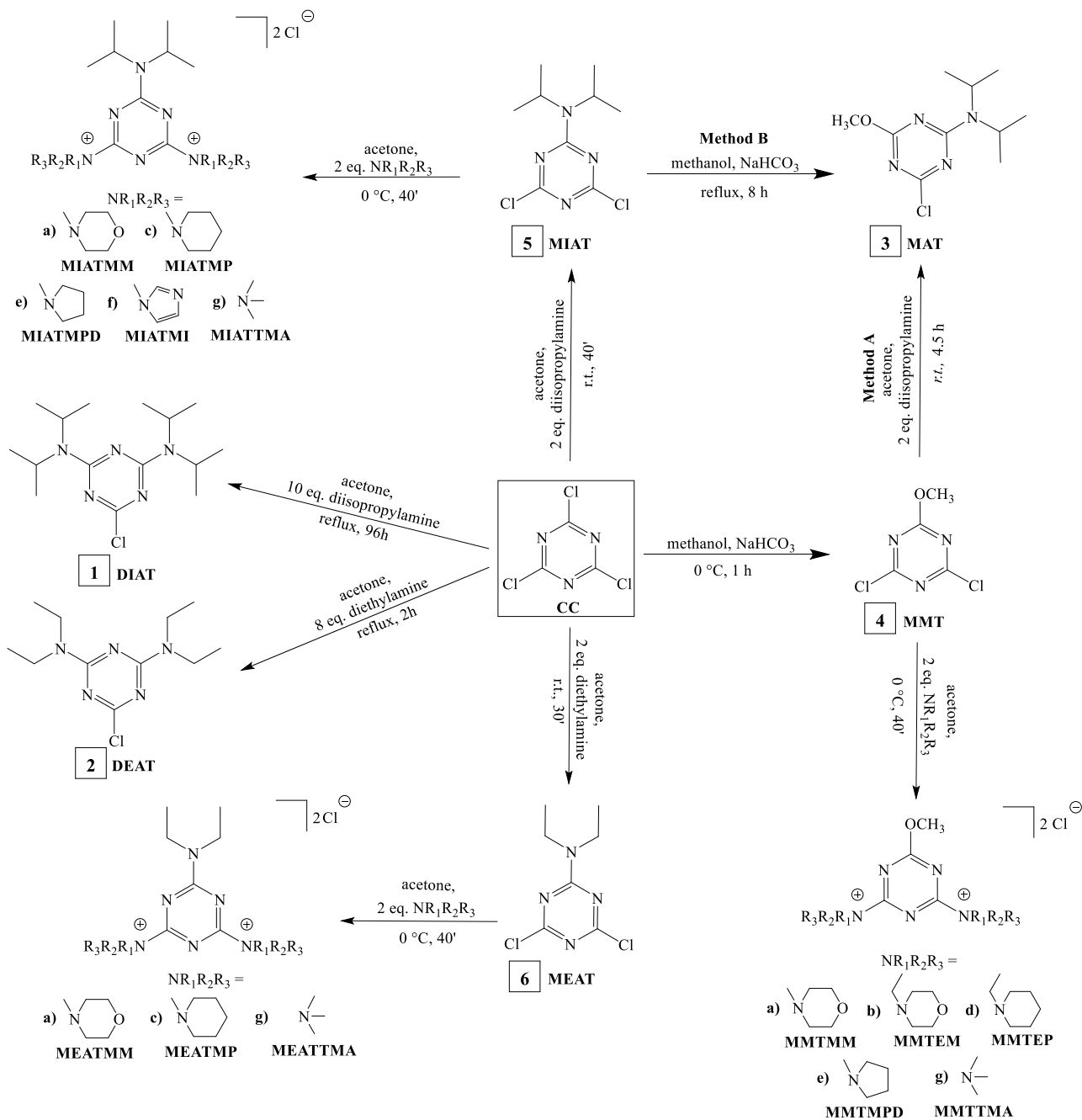
Gas-chromatography analysis were recorded with an Agilent Technologies 6850 gas chromatograph equipped with FID detector and capillary column HP-5 (cross-linked 5% phenylmethylsilicone) or HP-1 (100% dimethylsiloxane). Analyses were registered with following temperature ramps:

- HP-1 column: Ti: 50 °C x 1 min., rate: 20 °C/min., Tf: 230 °C x 35 min.
- HP-5 column: Ti: 50 °C x 4 min., rate: 20 °C/min., Tf: 230 °C x 30 min.

Finally, melting points were determined in open capillaries on a Buchi 235 model.

## 5.2 Synthesis of mono-1,3,5-triazine compounds and their derived ammonium salts

A general scheme for the synthesis of mono-1,3,5 triazine compounds is reported below, where numbers are assigned to 2-chloro-4,6-disubstituted-1,3,5-triazine and 2,4-dichloro-6-substituted-1,3,5-triazine and letters to each tertiary amine of their derived bis-ammonium salts. (**Scheme 5.1**)

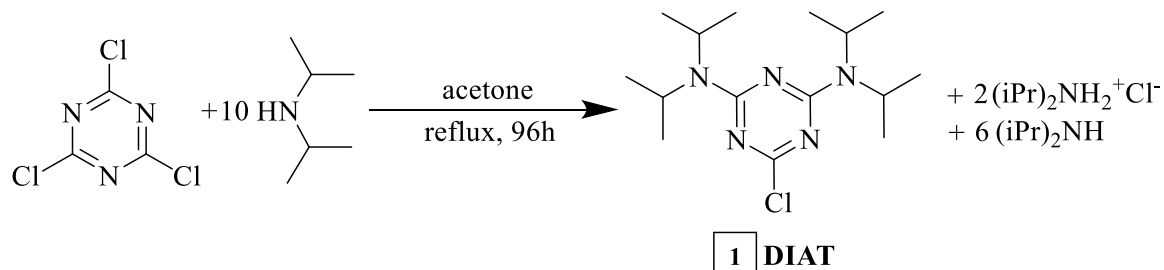


**Scheme 5.1:** Syntheses of mono-1,3,5-triazine precursors and their salts.

## 5.2.1 Preparation of 2-chloro-4,6-disubstituted-1,3,5-triazine

### 5.2.1.1 Synthesis of 2-chloro-4,6-bis-diisopropylamino-1,3,5-triazine (DIAT)

Synthesis of DIAT has been carried out following a method proposed by Katritzky *et al.*<sup>[36]</sup>



**Scheme 5.2:** Synthesis of 2-chloro-4,6-diisopropylamino-1,3,5-triazine (DIAT).

In a two-necked 100 mL flask equipped with magnetic stirrer and bubble condenser, 1 g of cyanuric chloride (CC, 5.42 mmoles) is added in 30 mL of acetone. The system is cooled to 0 °C and 30 mL of an acetone solution with 7.6 mL (54.20 mmoles) of diisopropylamine are added. The solution is heated to reflux and left under stirring for 96 hours while being monitored by gas-chromatography. Every 24 hours, 10 mL of acetone are added. Later on, the precipitate is filtered by gooch and mother liquors are evaporated to dryness. Finally, in order to remove unreacted amine, the obtained oil is washed and dried with 4 aliquotes of CH<sub>2</sub>Cl<sub>2</sub>. The yellowish solid is characterized by <sup>1</sup>H NMR, <sup>13</sup>C NMR, FT-IR and m.p.

Yield is 80% and purity 98%.

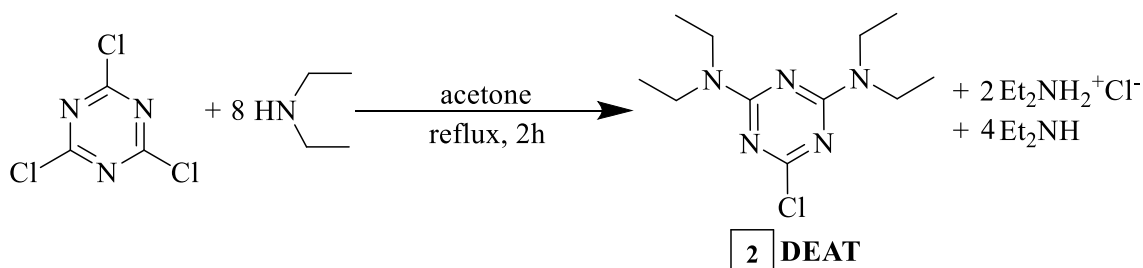
Characterization:

**1** DIAT:

- **m.p.:** 111 ° C.
- **<sup>1</sup>H NMR** (300 MHz, CDCl<sub>3</sub>, ppm): 4.38 (4H, m broad, CH(CH<sub>3</sub>)<sub>2</sub>), 1.33 (24H, d, CH(CH<sub>3</sub>)<sub>2</sub>).
- **<sup>13</sup>C NMR** (300 MHz, CDCl<sub>3</sub>, ppm): 167.43, 163.69, 45.76, 20.57, 20.26.
- **FT-IR** (KBr, cm<sup>-1</sup>): 1521, 1330, 1236, 810.

### 5.2.1.2 Synthesis of 2-chloro-4,6-bis-diethylamino-1,3,5-triazine (DEAT)

Synthesis of DEAT has been carried out following a method similar to what reported by Katritzky *et al.*<sup>[36]</sup>



**Scheme 5.3:** Synthesis of 2-chloro-4,6-diethylamino-1,3,5-triazine (DEAT).

In a two-necked 100 mL flask equipped with magnetic stirrer and bubble condenser, 1 g of cyanuric chloride (CC, 5.42 mmoles) is added in 30 mL of acetone. The system is cooled to 0 °C and 30 mL of an acetone solution with 4.5 mL (43.36 mmoles) of diethylamine are slowly added. The solution is heated to reflux and left under stirring for 2 hours while being monitored by gas-chromatography. Later on, the precipitate is filtered by gooch and mother liquors are evaporated to dryness. Finally, in order to remove unreacted amine, the obtained oil is washed and dried with 4 aliquotes of CH<sub>2</sub>Cl<sub>2</sub>. The brownly oil is characterized by <sup>1</sup>H NMR, <sup>13</sup>C NMR and FT-IR.

Yield is 80% and purity 94%.

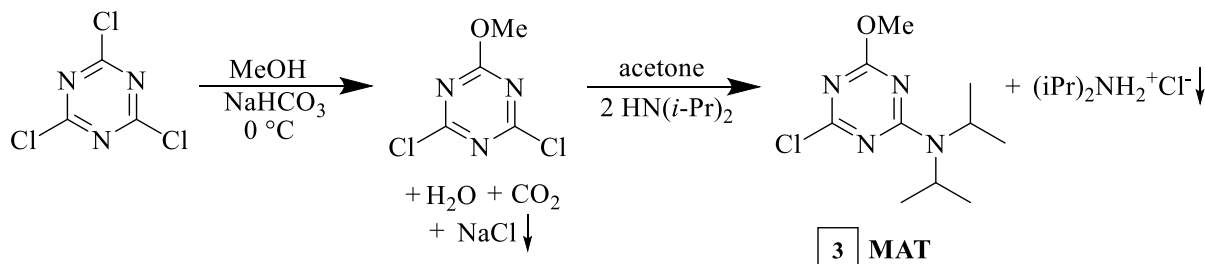
Characterization:

**2** DEAT:

- <sup>1</sup>H NMR (300 MHz, CDCl<sub>3</sub>, ppm): 3.52 (8H, qi, CH(CH<sub>3</sub>)<sub>2</sub>), 1.14 (12H, t, CH(CH<sub>3</sub>)<sub>2</sub>).
- <sup>13</sup>C NMR (300 MHz, CDCl<sub>3</sub>, ppm): 168.99, 164.03, 41.60, 41.36, 13.33, 12.79.
- FT-IR (KBr, cm<sup>-1</sup>): 1519, 1334, 1231, 813.

### 5.2.1.3 Synthesis of 2-chloro-4-alkoxy-6-diisopropylamino-1,3,5-triazine (MAT)

Method 1:

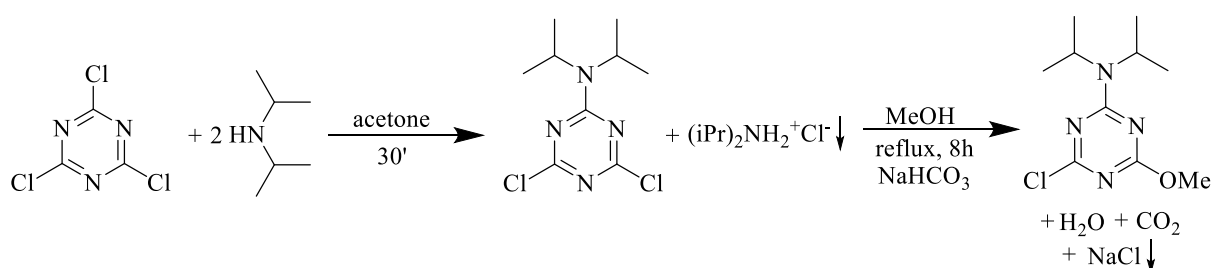


**Scheme 5.4:** Synthesis of 2-chloro-4-methoxy-6-diisopropylamino-1,3,5-triazine (MAT) (Method 1).

In a 100 mL flask, equipped with magnetic stirrer, 0.23 g (2.71 mmoles) of NaHCO<sub>3</sub> are added in 30 mL of methanol. Thus, the system is cooled to 0 °C and 0.5 g of cyanuric chloride (CC, 2.71 mmoles) are slowly added. The solution is left under stirring for 1 hour while being monitored by gas-chromatography. Later on, solvent is removed by reduced pressure evaporation, then 30 mL of acetone are added and the suspension obtained is filtered of NaCl subproduct. Thus, 0.76 mL (5.42 mmoles) of diisopropylamine are added to the solution and the reaction is left under stirring at *r.t.* for 3.5 hours. Finally, the suspension is filtered and mother liquors are evaporated to dryness. The white solid obtained is characterized by <sup>1</sup>H NMR, <sup>13</sup>C NMR, FT-IR and m.p.

Yield is 66% and purity 98%.

#### Method 2:



**Scheme 5.5:** Synthesis of 2-chloro-4-methoxy-6-diisopropylamino-1,3,5-triazine (MAT) (Method 2).

In a two-necked 100 mL flask, equipped with magnetic stirrer and bubble condenser, 0.5 g of cyanuric chloride (CC, 2.71 mmoles) are added in 30 mL of acetone. Then, 0.76 mL (5.42 mmoles) of diisopropylamine is added to the solution. The reaction is left under stirring at *r.t.* for 30' and monitored by gas-chromatography. Later on, diisopropylammonium chloride is removed by filtration and mother liquors are dried by reduced pressure evaporatotion. The obtained solid is dissolved in 20 mL of methanol and 0.23 g (2.71 mmoles) of NaHCO<sub>3</sub> are added. The reaction is refluxed for 8 h and monitored by GC. The suspended NaCl byproduct is removed by filtration and the mother liquors are finally taken to dryness. The obtained solid is characterized by <sup>1</sup>H NMR, <sup>13</sup>C NMR, FT-IR and m.p. Yield is 74% and purity 95%.

Characterization:

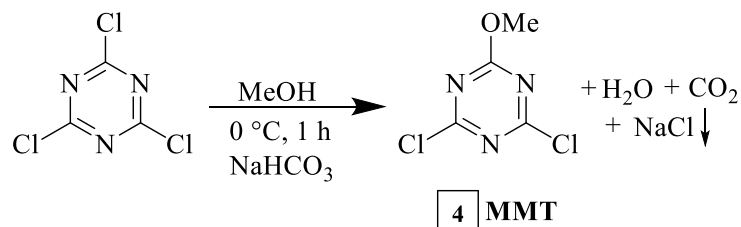
#### 3 MAT:

- **m.p.:** 81 ° C.
- **<sup>1</sup>H NMR** (300 MHz, acetone-d<sub>6</sub>, ppm): 4.61-4.39 (2H, m broad, NCH(CH<sub>3</sub>)<sub>2</sub>), 3.93 (3H, s, OCH<sub>3</sub>), 1.38-1.31 (12H, d, NCH(CH<sub>3</sub>)<sub>2</sub>).
- **<sup>13</sup>C NMR** (300 MHz, acetone-d<sub>6</sub>, ppm): 170.85, 170.01, 165.51, 54.82, 47.15, 46.84, 19.76, 19.69.
- **FT-IR** (KBr, cm<sup>-1</sup>): 1521, 1336, 1261, 1232, 803.

## 5.2.2 Preparation of 2,4-dichloro-6-substituted-1,3,5-triazines

### 5.2.2.1 Synthesis of 2,4-dichloro-6-methoxy-1,3,5-triazine (MMT)

Synthesis of MMT has been carried out following a method proposed by Kaminski.<sup>[29]</sup>



**Scheme 5.6:** Synthesis of 2,4-dichloro-6-methoxy-1,3,5-triazine (MMT).

In a 100 mL flask, equipped with magnetic stirrer, 0.91 g (10.8 mmoles) of NaHCO<sub>3</sub> are added in 30 mL of methanol. The suspension is then cooled to 0 °C with an ice-cold water bath. Afterwards, 2.0 g of cyanuric chloride (CC, 10.8 mmoles) are slowly added. The reaction is left under stirring at 0 °C for 1 hour, monitored by GC, and the solvent is removed by reduced pressure evaporation.

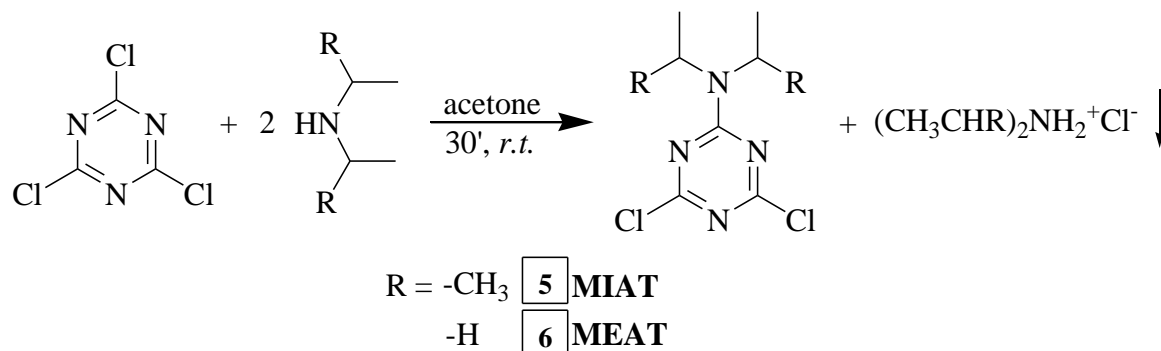
Then, 30 mL of acetone are added to solubilize the white solid and the suspension is filtered to remove NaCl by-product. Mother liquors are finally taken to dryness and the white solid obtained is characterized by <sup>1</sup>H NMR, <sup>13</sup>C NMR, FT-IR and m.p. Yield is 97% and purity 98%.

Characterization:

**4** DIAT:

- **m.p.:** 88 °C.
- **<sup>1</sup>H NMR** (300 MHz, acetone-d<sub>6</sub>, ppm): 4.17 (3H, s, OCH<sub>3</sub>).
- **<sup>13</sup>C NMR** (300 MHz, acetone-d<sub>6</sub>, ppm): 172.76, 172.71, 57.40.
- **FT-IR** (KBr, cm<sup>-1</sup>): 1528, 1258, 815.

### 5.2.2.2 Synthesis of 2,4-dichloro-6-diisopropylamino-1,3,5-triazine (MIAT) and 2,4-dichloro-6-diethylamino-1,3,5-triazine (MEAT)



**Scheme 5.7:** Synthesis of 2,4-dichloro-6-diisopropylamino-1,3,5-triazine (MIAT) 2,4-dichloro-6-diethylamino-1,3,5-triazine (MEAT).

In a 100 mL flask, equipped with magnetic stirrer, 2.0 g of cyanuric chloride (CC, 10.8 mmol) are added in 20 mL of acetone. Then, 2 equivalents of the desired amine (21.6 mmol) are dripped to the solution, the reaction is left under stirring at *r.t.* for 30' and monitored by GC. The suspension is filtered of the ammonium chloride byproduct and mother liquors are taken to dryness. The obtained solid is characterized by  $^1\text{H}$  NMR,  $^{13}\text{C}$  NMR, FT-IR and m.p.

Characterization:

**5** MIAT: R = CH<sub>3</sub>

Yield 95% (purity 96%)

- **m.p.:** 103 °C.
- **$^1\text{H}$  NMR** (300 MHz, acetone-d<sub>6</sub>, ppm): 4.51 (2H, m broad, NCH(CH<sub>3</sub>)<sub>2</sub>), 1.39 (12H, d, NCH(CH<sub>3</sub>)<sub>2</sub>).
- **$^{13}\text{C}$  NMR** (300 MHz, acetone-d<sub>6</sub>, ppm): 169.16, 164.19, 47.73, 19.41.
- **FT-IR** (KBr, cm<sup>-1</sup>): 1525, 1333, 1229, 808.

**6** MEAT: R = H

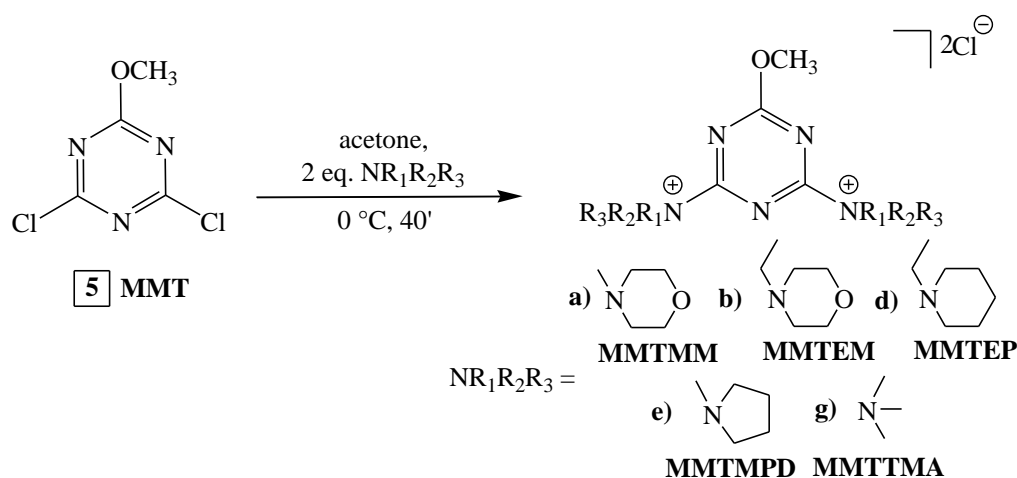
Yield 92% (purity 97%)

- **m.p.:** 77 °C.
- **$^1\text{H}$  NMR** (300 MHz, acetone-d<sub>6</sub>, ppm): 3.71 (4H, q, NCH<sub>2</sub>CH<sub>3</sub>), 1.22 (6H, t, NCH<sub>2</sub>CH<sub>3</sub>).
- **$^{13}\text{C}$  NMR** (300 MHz, acetone-d<sub>6</sub>, ppm): 169.16, 164.19, 47.73, 19.41.
- **FT-IR** (KBr, cm<sup>-1</sup>): 1521, 1336, 1235, 811.

### 5.2.3 Preparation of quaternary bis-ammonium salts derived from 2,4-dichloro-6-substituted 1,3,5-triazine

Quaternary bis-ammonium salts have been synthesized from 2,4-dichloro-6-substituted-1,3,5-triazine precursors identified as MMT [4], MIAT [5] and MEAT [6] and the opportune tertiary amine: *N*-methylmorpholine (MM) [a], *N*-ethylmorpholine (EM) [b], *N*-methylpiperidine (MP) [c], *N*-ethylpiperidine (EP) [d], *N*-methylpyrrolidine (MPD) [e], *N*-methylimidazole (MI) [f] and trimethylamine (TMA) [g]. (Scheme 5.1)

#### 5.2.3.1 Synthesis of quaternary bis-ammonium salts derived from 2,4-dichloro-6-methoxy-1,3,5-triazine (MMT)



**Scheme 5.8:** Syntheses of quaternary bis-ammonium salts derivatived by 2,4-dichloro-6-methoxy-1,3,5-triazine (MMT).

In a 50 mL flask, equiped with magnetic stirrer, 0.5 g of 2,4-dichloro-6-methoxy-1,3,5-triazine (MMT, 2.7 mmoles) are added in 20 mL of acetone. Thus, the solution is cooled to 0 °C and two equivalents of the desired amine (5.4 mmoles) are slowly added (in the case of TMA a 45% wt. water solution is used). The reaction is left under stirring for 40', then the precipitate is filtered and dried under vacuum. The solid product obtained is characterized by <sup>1</sup>H NMR, FT-IR and m.p., when possible <sup>13</sup>C NMR spectrum has been gather as well.

Characterization:



Yield 87% (purity 94%)

- **m.p.:** product decomposition observed at 73 °C.
- **<sup>1</sup>H NMR** (300 MHz, D<sub>2</sub>O, ppm): 4.53 (4H, m, N<sup>+</sup>CH<sub>2</sub>CH<sub>2</sub>O), 4.16 (4H, m, N<sup>+</sup>CH<sub>2</sub>CH<sub>2</sub>O), 3.87 (8H, m, N<sup>+</sup>CH<sub>2</sub>CH<sub>2</sub>O), 3.39 (3H, s, OCH<sub>3</sub>), 2.87 (6H, s, N<sup>+</sup>CH<sub>3</sub>).
- **FT-IR** (KBr, cm<sup>-1</sup>): 1521, 1336, 1288, 1261, 1129.



**4b** MMTEM NR<sub>1</sub>R<sub>2</sub>R<sub>3</sub>= EM

Yield 89% (purity 93%)

- **m.p.:** product decomposition observed at 87 °C.
- **<sup>1</sup>H NMR** (300 MHz, D<sub>2</sub>O, ppm): 4.57 (4H, d, N<sup>+</sup>CH<sub>2</sub>CH<sub>2</sub>O), 4.20 (4H, d, N<sup>+</sup>CH<sub>2</sub>CH<sub>2</sub>O), 3.96 (4H, q, N<sup>+</sup>CH<sub>2</sub>CH<sub>3</sub>), 3.85 (8H, m, N<sup>+</sup>CH<sub>2</sub>CH<sub>2</sub>O), 3.39 (3H, s, OCH<sub>3</sub>), 1.25 (6H, t, N<sup>+</sup>CH<sub>2</sub>CH<sub>3</sub>).
- **<sup>13</sup>C NMR** (300 MHz, D<sub>2</sub>O, ppm): 168.88, 167.63, 65.05, 62.07, 57.91, 48.82, 7.09.
- **FT-IR** (KBr, cm<sup>-1</sup>): 1571, 1370, 1288, 1263, 1135.

**4d** MMTEP NR<sub>1</sub>R<sub>2</sub>R<sub>3</sub>= EP

Yield 94% (purity 90%)

- **m.p.:** product decomposition observed at 73 °C.
- **<sup>1</sup>H NMR** (300 MHz, D<sub>2</sub>O, ppm): 4.48 (4H, d, N<sup>+</sup>CH<sub>2</sub>CH<sub>2</sub>CH<sub>3</sub>), 3.82 (4H, q, N<sup>+</sup>CH<sub>2</sub>CH<sub>3</sub>), 3.54 (4H, t, N<sup>+</sup>CH<sub>2</sub>CH<sub>2</sub>CH<sub>3</sub>), 3.38 (3H, s, OCH<sub>3</sub>), 1.95 (4H, m, N<sup>+</sup>CH<sub>2</sub>CH<sub>2</sub>CH<sub>3</sub>), 1.75 (8H, m, N<sup>+</sup>CH<sub>2</sub>CH<sub>2</sub>CH<sub>3</sub>), 1.20 (6H, t, N<sup>+</sup>CH<sub>2</sub>CH<sub>3</sub>).
- **<sup>13</sup>C NMR** (300 MHz, D<sub>2</sub>O, ppm): 170.20, 168.89, 64.74, 59.99, 49.34, 21.51, 21.31, 7.83.
- **FT-IR** (KBr, cm<sup>-1</sup>): 1579, 1371, 1288, 1259.

**4e** MMTMPD NR<sub>1</sub>R<sub>2</sub>R<sub>3</sub>= MPD

Yield 73% (purity 94%)

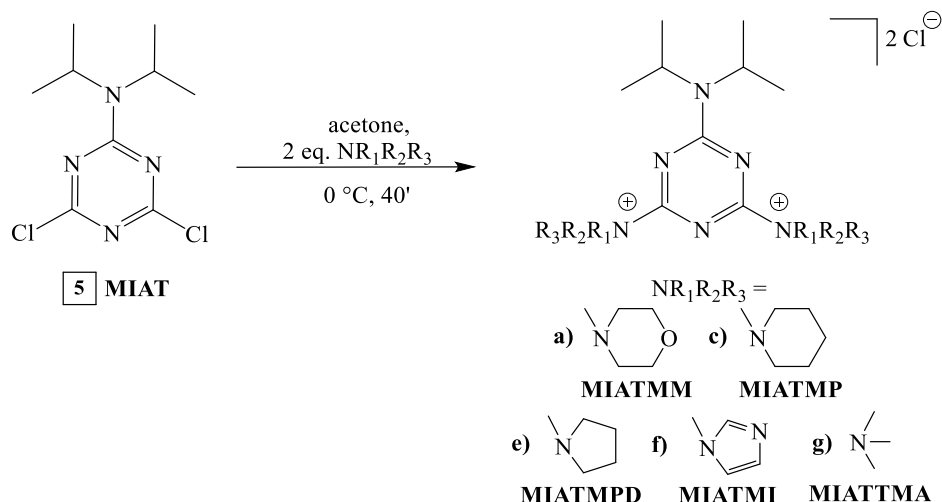
- **m.p.:** product decomposition observed at 69 °C.
- **<sup>1</sup>H NMR** (300 MHz, D<sub>2</sub>O, ppm): 3.56 (4H, m, N<sup>+</sup>CH<sub>2</sub>CH<sub>2</sub>), 3.26 (3H, s, OCH<sub>3</sub>), 2.97 (4H, m, N<sup>+</sup>CH<sub>2</sub>CH<sub>2</sub>), 2.83 (6H, s, N<sup>+</sup>CH<sub>3</sub>), 2.07 (4H, m, N<sup>+</sup>CH<sub>2</sub>CH<sub>2</sub>), 1.92 (4H, m, N<sup>+</sup>CH<sub>2</sub>CH<sub>2</sub>).
- **<sup>13</sup>C NMR** (300 MHz, D<sub>2</sub>O, ppm): 155.82, 151.52, 57.07, 56.23, 41.04, 23.29.
- **FT-IR** (KBr, cm<sup>-1</sup>): 1551, 1343, 1289, 1275.

**4g** MMTTMA<sup>(\*)</sup> NR<sub>1</sub>R<sub>2</sub>R<sub>3</sub>= TMA

<sup>(\*)</sup>Data are not available because the product is a mixture of species.

In-depth analysis is reported in **Chapter 3.3.1.5**.

### 5.2.3.2 Synthesis of quaternary bis-ammonium salts derived from 2,4-dichloro-6-diisopropyl-1,3,5-triazine (MIAT)



**Scheme 5.9:** Syntheses of quaternary bis-ammonium salts derived from 2,4-dichloro-6-diisopropylamino-1,3,5-triazine (MIAT).

In a 50 mL flask, equipped with magnetic stirrer, 0.5 g of 2,4-dichloro-6-diisopropylamino-1,3,5-triazine (MIAT, 2.0 mmoles) are dissolved in 20 mL of acetone. Then, the solution is cooled to 0 °C and two equivalents of the desired amine (4.0 mmoles) are slowly added (in the case of TMA a 45% wt. water solution is used). The reaction is left under stirring for 40', thus the precipitate is filtered and dried under vacuum. The solid product obtained is characterized by  $^1\text{H}$  NMR,  $^{13}\text{C}$  NMR, FT-IR and m.p.

Characterization:



Yield 88% (purity 94%)

- **m.p.:** product decomposition observed at 68 °C.
- $^1\text{H}$  NMR (300 MHz,  $\text{D}_2\text{O}$ , ppm): 4.59 (2H, m broad,  $\text{NCH}(\text{CH}_3)_2$ ), 4.59 (4H, m,  $\text{N}^+\text{CH}_2\text{CH}_2\text{O}$ ), 4.21 (4H, d,  $\text{N}^+\text{CH}_2\text{CH}_2\text{O}$ ), 3.95 (8H, m,  $\text{N}^+\text{CH}_2\text{CH}_2\text{O}$ ), 3.60 (6H, s,  $\text{N}^+\text{CH}_3$ ), 1.42 (12H, d,  $\text{NCH}(\text{CH}_3)_2$ ).
- $^{13}\text{C}$  NMR (300 MHz,  $\text{D}_2\text{O}$ , ppm): 169.03, 164.23, 62.24, 60.38, 55.23, 49.90, 19.22.
- **FT-IR** (KBr,  $\text{cm}^{-1}$ ): 1518, 1341, 1271, 1231, 1134.



Yield 85% (purity 92%)

- **m.p.:** product decomposition observed at 70 °C.

- $^1\text{H NMR}$  (300 MHz,  $\text{D}_2\text{O}$ , ppm): 4.61 (2H, m broad,  $\text{NCH}(\text{CH}_3)_2$ ), 4.51 (4H, d,  $\text{N}^+\text{CH}_2\text{CH}_2\text{CH}_3$ ), 3.68 (4H, t,  $\text{N}^+\text{CH}_2\text{CH}_2\text{CH}_2$ ), 3.44 (6H, s,  $\text{CH}_3$ ), 1.98 (4H, m,  $\text{N}^+\text{CH}_2\text{CH}_2\text{CH}_2$ ), 1.73 (8H, m,  $\text{N}^+\text{CH}_2\text{CH}_2\text{CH}_3$ ), 1.41 (12H, d,  $\text{NCH}(\text{CH}_3)_2$ ).
- $^{13}\text{C NMR}$  (300 MHz,  $\text{D}_2\text{O}$ , ppm): 169.50, 164.65, 62.27, 55.37, 49.57, 21.49, 20.78, 19.41.
- **FT-IR** (KBr,  $\text{cm}^{-1}$ ): 1532, 1351, 1267, 1222.

**5e** **MIATMPD**  $\text{NR}_1\text{R}_2\text{R}_3 = \text{MPD}$

Yield 72% (purity 93%)

- **m.p.:** product decomposition observed at 68 °C.
- $^1\text{H NMR}$  (300 MHz,  $\text{D}_2\text{O}$ , ppm): 4.61 (2H, m broad,  $\text{NCH}(\text{CH}_3)_2$ ), 4.43 (4H, m,  $\text{N}^+\text{CH}_2\text{CH}_2$ ), 3.91 (4H, d,  $\text{N}^+\text{CH}_2\text{CH}_2$ ), 3.56 (6H, s,  $\text{N}^+\text{CH}_3$ ), 2.34 (8H, m,  $\text{N}^+\text{CH}_2\text{CH}_2$ ), 1.42 (12H, d,  $\text{NCH}(\text{CH}_3)_2$ ).
- $^{13}\text{C NMR}$  (300 MHz,  $\text{D}_2\text{O}$ , ppm): 169.88, 163.71, 65.56, 51.30, 48.93, 21.96, 18.79.
- **FT-IR** (KBr,  $\text{cm}^{-1}$ ): 1540, 1345, 1279, 1215.

**5f** **MIATMI**  $\text{NR}_1\text{R}_2\text{R}_3 = \text{MI}$

Yield 78% (purity 95%)

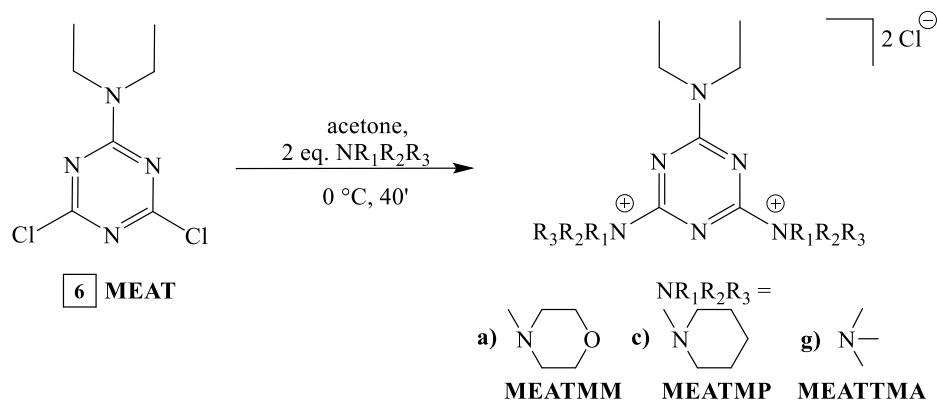
- **m.p.:** product decomposition observed at 102 °C.
- $^1\text{H NMR}$  (300 MHz,  $\text{DMSO-d}_6$ , ppm): 10.76 (2H, s,  $\text{NCHN}$ ), 8.73 (2H, s,  $\text{N}^+\text{CH}=\text{CHN}$ ), 8.09 (2H, s,  $\text{N}^+\text{CH}=\text{CHN}$ ), 4.71 (2H, m broad,  $\text{NCH}(\text{CH}_3)_2$ ), 4.06 (6H, s,  $\text{NCH}_3$ ), 1.42 (12H, d,  $\text{NCH}(\text{CH}_3)_2$ ).
- $^{13}\text{C NMR}$  (300 MHz,  $\text{DMSO-d}_6$ , ppm): 164.51, 159.73, 138.61, 126.25, 119.86, 48.43, 37.63, 20.65.
- **FT-IR** (KBr,  $\text{cm}^{-1}$ ): 1575, 1486, 1361, 1210.

**5g** **MIATTMA**  $\text{NR}_1\text{R}_2\text{R}_3 = \text{TMA}$

Yield 70% (purity 95%)

- **m.p.:** product decomposition observed at 73 °C.
- $^1\text{H NMR}$  (300 MHz,  $\text{D}_2\text{O}$ , ppm): 4.63 (2H, m broad,  $\text{NCH}(\text{CH}_3)_2$ ), 3.63 (18H, s,  $\text{CH}_3$ ), 1.42 (12H, d,  $\text{NCH}(\text{CH}_3)_2$ ).
- $^{13}\text{C NMR}$  (300 MHz,  $\text{D}_2\text{O}$ , ppm): 176.64, 170.02, 59.93, 50.01, 20.05.
- **FT-IR** (KBr,  $\text{cm}^{-1}$ ): 1540, 1340, 1271, 1211.

### 5.2.3.3 Synthesis of quaternary bis-ammonium salts derived from 2,4-dichloro-6-diethyl-1,3,5-triazine (MEAT)



**Scheme 5.10:** Syntheses of quaternary bis-ammonium salts derived from 2,4-dichloro-6-diethylamino-1,3,5-triazine (MEAT).

In a 50 mL flask, equipped with magnetic stirrer, 0.5 g of 2,4-dichloro-6-diethylamino-1,3,5-triazine (MEAT, 2.3 mmol) are dissolved in 20 mL of acetone. Thus, the solution is cooled to 0 °C and two equivalents of the desired amine (4.6 mmol) are slowly added (in the case of TMA a 45% wt. water solution is used). The reaction is left under stirring for 40', then the precipitate is filtered and dried under vacuum. The solid product obtained is characterized by  $^1\text{H}$  NMR,  $^{13}\text{C}$  NMR, FT-IR and m.p.

Characterization:



Yield 90% (purity 92%)

- **m.p.:** product decomposition observed at 86 °C.
- $^1\text{H}$  NMR (300 MHz,  $\text{D}_2\text{O}$ , ppm): 4.49 (4H, d,  $\text{N}^+\text{CH}_2\text{CH}_2\text{O}$ ), 4.10 (4H, d,  $\text{N}^+\text{CH}_2\text{CH}_2\text{O}$ ), 3.82 (8H, qi,  $\text{N}^+\text{CH}_2\text{CH}_2\text{O}$ ), 3.70 (4H, q,  $\text{N}^+\text{CH}_2\text{CH}_3$ ), 3.48 (6H, s,  $\text{N}^+\text{CH}_3$ ) 1.16 (6H, t,  $\text{N}^+\text{CH}_2\text{CH}_3$ ).
- $^{13}\text{C}$  NMR (300 MHz,  $\text{D}_2\text{O}$ , ppm): 169.12, 164.03, 61.85, 59.99, 55.13, 44.13, 11.46.
- **FT-IR** (KBr,  $\text{cm}^{-1}$ ): 1531, 1361, 1268, 1219, 1130.

**6c** MEATMP NR<sub>1</sub>R<sub>2</sub>R<sub>3</sub>= MP

Yield 78% (purity 90%)

- **m.p.:** product decomposition observed at 86 °C.
- **<sup>1</sup>H NMR** (300 MHz, D<sub>2</sub>O, ppm): 4.53 (4H, d, N<sup>+</sup>CH<sub>2</sub>CH<sub>2</sub>CH<sub>2</sub>), 3.79 (4H, q, N<sup>+</sup>CH<sub>2</sub>CH<sub>3</sub>), 3.65 (4H, t, N<sup>+</sup>CH<sub>2</sub>CH<sub>2</sub>CH<sub>2</sub>), 3.43 (6H, s, N<sup>+</sup>CH<sub>3</sub>), 1.96 (4H, m, N<sup>+</sup>CH<sub>2</sub>CH<sub>2</sub>CH<sub>2</sub>), 1.75 (8H, m, N<sup>+</sup>CH<sub>2</sub>CH<sub>2</sub>CH<sub>2</sub>), 1.26 (6H, t N<sup>+</sup>CH<sub>2</sub>CH<sub>3</sub>).
- **<sup>13</sup>C NMR** (300 MHz, D<sub>2</sub>O, ppm): 169.54, 164.40, 61.17, 55.09, 43.84, 20.99, 20.24, 11.55.
- **FT-IR** (KBr, cm<sup>-1</sup>): 1542, 1359, 1261, 1215.

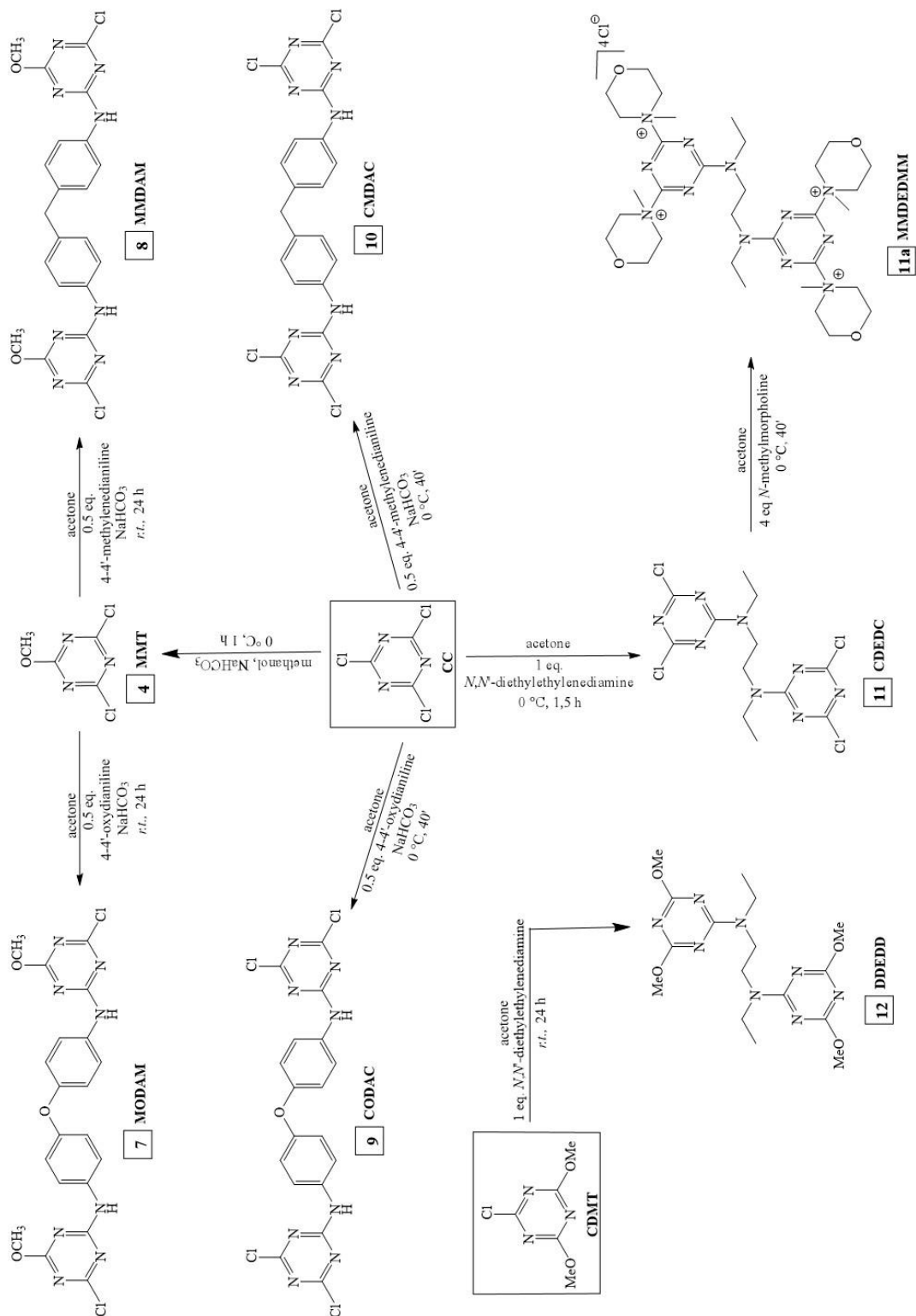
**6g** MEATTMA NR<sub>1</sub>R<sub>2</sub>R<sub>3</sub>= TMA

Yield 96% (purity 90%)

- **m.p.:** product decomposition observed at 72 °C.
- **<sup>1</sup>H NMR** (300 MHz, D<sub>2</sub>O, ppm): 3.81 (4H, q, NCH<sub>2</sub>CH<sub>3</sub>), 3.62 (18H, s, N<sup>+</sup>CH<sub>3</sub>), 1.27 (6H, t, NCH<sub>2</sub>CH<sub>3</sub>).
- **<sup>13</sup>C NMR** (300 MHz, D<sub>2</sub>O, ppm): 171.09, 164.47, 54.38, 44.46, 11.08.
- **FT-IR** (KBr, cm<sup>-1</sup>): 1563, 1368, 1268, 1215.

### 5.3 Synthesis of bis-1,3,5-triazine compounds and their derived ammonium salts

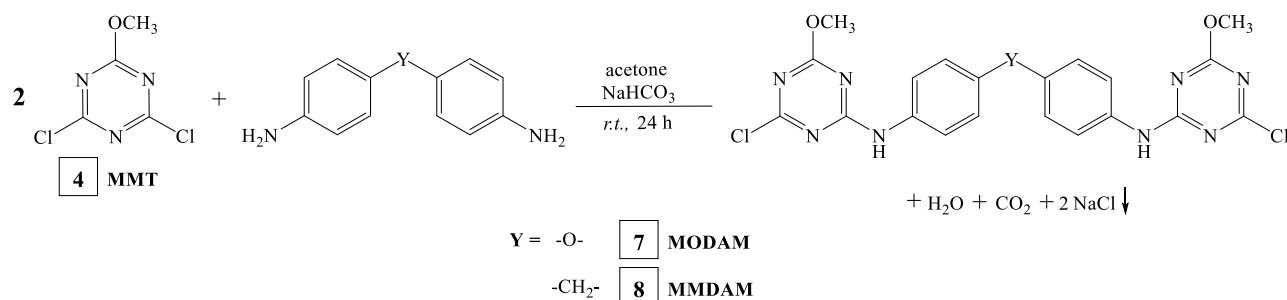
A general scheme for the synthesis of bis-1,3,5 triazine compounds is reported below, where numbers are assigned to identify each product isolated and letters for tertiary amine used to synthesize tetrakis-ammonium salt. (**Scheme 5.11**)



**Scheme 5.11:** Syntheses of bis-1,3,5-triazine precursors and their salts.

### 5.3.1 Preparation of 2,4-disubstituted-6-anilino-bis-1,3,5-triazine with chloro or methoxy groups

#### 5.3.1.1 Synthesis of *N,N'*-(oxybis(4,1-phenylene))bis(2-chloro-4-methoxy-1,3,5-triazin-6-amine) (MODAM) and *N,N'*-(methylenebis(4,1-phenylene))bis(2-chloro-4-methoxy-1,3,5-triazin-6-amine) (MMDAM)



**Scheme 5.12:** Synthesis of *N,N'*-(oxybis(4,1-phenylene))bis(2-chloro-4-methoxy-1,3,5-triazin-6-amine) (MODAM) and *N,N'*-(methylenebis(4,1-phenylene))bis(2-chloro-4-methoxy-1,3,5-triazin-6-amine) (MMDAM).

In a 50 mL flask, equipped with magnetic stirrer, 0.5 g of 2,4-dichloro-6-methoxy-1,3,5-triazine (MMT, 2.8 mmoles) are dissolved in 20 mL of acetone. Then, a 10 mL water solution with the desired dianiline (1.4 mmoles) and 292 mg (3.5 mmoles) of NaHCO<sub>3</sub> are slowly added. The reaction is left under stirring for 24 hours. Finally, the precipitate is filtered, washed with clean water and dried under vacuum. The solid product obtained is characterized by <sup>1</sup>H NMR, <sup>13</sup>C NMR, FT-IR and m.p.

Characterization:

**7** MODAM: Y = O

Yield 86% (purity 91%)

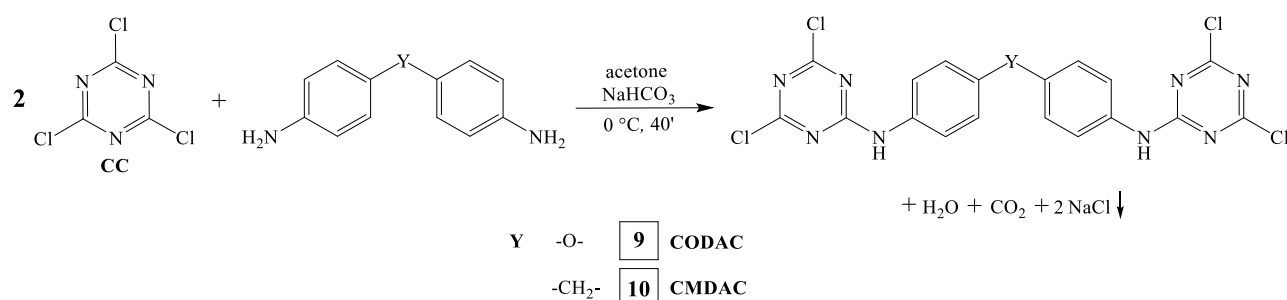
- **m.p.:** 228 °C.
- **<sup>1</sup>H NMR** (300 MHz, DMSO-d<sub>6</sub>, ppm): 10.64 (2H, m, NH), 7.71-7.58 (4H, dd, NCCHCHCO), 7.05-7.00 (4H, dt, NCCHCHCO), 3.94 (6H, s, OCH<sub>3</sub>).
- **<sup>13</sup>C NMR** (300 MHz, DMSO-d<sub>6</sub>, ppm): 171.42, 169.85, 165.23, 165.02, 153.46, 133.86, 123.61, 122.93, 119.21, 55.83.
- **FT-IR** (KBr, cm<sup>-1</sup>): 3414, 1564, 1520, 1341, 1271, 1258, 812.

**8** MMDAM: Y = CH<sub>2</sub>

Yield 94% (purity 96%)

- **m.p.:** 230 °C.
- **<sup>1</sup>H NMR** (300 MHz, DMSO-d<sub>6</sub>, ppm): 10.58 (2H, m, NH), 7.62-7.48 (4H, dd, NCCHCHCO), 7.22-7.19 (4H, d, NCCHCHCO), 3.93 (6H, s, OCH<sub>3</sub>), 3.38 (2H, s, CH<sub>2</sub>).
- **<sup>13</sup>C NMR** (300 MHz, DMSO-d<sub>6</sub>, ppm): 171.40, 169.84, 165.16, 165.00, 137.58, 137.40, 136.35, 129.33, 121.98, 121.30, 55.79, 40.39.
- **FT-IR** (KBr, cm<sup>-1</sup>): 3449, 1571, 1518, 1339, 1260, 809.

### 5.3.1.2 Synthesis of *N,N'*-(oxybis(4,1-phenylene))-bis(2,4-dichloro-1,3,5-triazin-6-amine) (CODAC) and *N,N'*-(methylenebis(4,1-phenylene))-bis(2,4-dichloro-1,3,5-triazin-6-amine) (CMDAC).



**Scheme 5.13:** Synthesis of *N,N'*-(oxybis(4,1-phenylene))bis(2,4-dichloro-1,3,5-triazin-6-amine) (CODAC) and *N,N'*-(methylenebis(4,1-phenylene))bis(2,4-dichloro-1,3,5-triazin-6-amine) (CMDAC).

In a 50 mL flask, equipped with magnetic stirrer, 0.5 g of cyanuric chloride (CC, 2.71 mmoles) are dissolved in 20 mL of acetone. The system is cooled to 0 °C, then a 10 mL water solution with the desired dianiline (1.35 mmoles) and 284 mg (3.4 mmoles) of NaHCO<sub>3</sub> are slowly added. The reaction is left under stirring for 40 minutes. Finally, the precipitate is filtered, washed with clean water and dried under vacuum. The solid product obtained is characterized by <sup>1</sup>H NMR, <sup>13</sup>C NMR, FT-IR and m.p. Characterization:

**9** CODAC: Y = O

Yield 84% (purity 96%)

- **m.p.:** 230 °C.
- **<sup>1</sup>H NMR** (300 MHz, DMSO-d<sub>6</sub>, ppm): 11.20 (2H, s, NH), 7.62 (4H, m, NCCHCHCO), 7.37 (4H, m, NCCHCHCO).
- **<sup>13</sup>C NMR** (300 MHz, DMSO-d<sub>6</sub>, ppm): 164.35, 159.34, 149.95, 130.49, 124.69, 117.46.
- **FT-IR** (KBr, cm<sup>-1</sup>): 3429, 1561, 1525, 1343, 1275, 811.



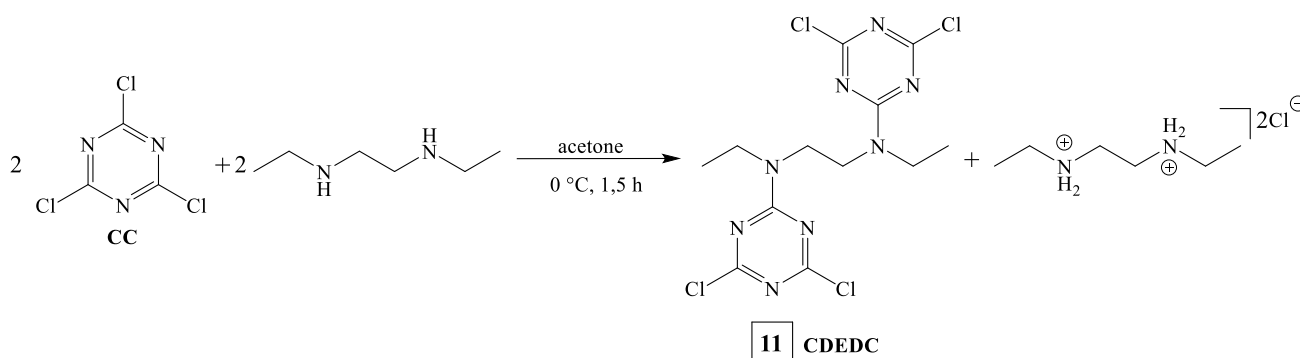
**10** CMDAC: Y = CH<sub>2</sub>

Yield 85% (purity 97%)

- **m.p.:** 234 °C.
- **<sup>1</sup>H NMR** (300 MHz, DMSO-d<sub>6</sub>, ppm): 11.10 (2H, s, **NH**), 7.49 (4H, m, **NCCHCHCO**), 7.24 (4H, m, **NCCHCHCO**), 3.91 (2H, s, **CH<sub>2</sub>**).
- **<sup>13</sup>C NMR** (300 MHz, DMSO-d<sub>6</sub>, ppm): 169.14, 164.13, 138.50, 135.28, 129.48, 122.25, 40.43.
- **FT-IR** (KBr, cm<sup>-1</sup>): 3452, 1569, 1520, 1345, 811.

### 5.3.2 Preparation of 2,4-disubstituted-6-amino-bis-1,3,5-triazine derived from *N,N'*-diethylethylenediamine

#### 5.3.2.1 Synthesis of *N*<sub>1</sub>,*N*<sub>2</sub>-bis(2,4-dichloro-1,3,5-triazin-6-yl)-*N*<sub>1</sub>,*N*<sub>2</sub>-diethylethane-1,2-diamine (CDEDC).



**Scheme 5.14:** Synthesis of *N*<sub>1</sub>,*N*<sub>2</sub>-bis(2,4-dichloro-1,3,5-triazin-6-yl)-*N*<sub>1</sub>,*N*<sub>2</sub>-diethylethane-1,2-diamine (CDEDC).

In a 50 mL flask, equipped with magnetic stirrer, 1 g of cyanuric chloride (CC, 5.4 mmol) is added to 25 mL of acetone. The system is cooled to 0 °C and then a 10 mL acetone solution with 0.77 mL of *N,N'*-diethylethylenediamine (DED, 5.4 mmol) are added in two aliquotes at 30 minutes distance. The reaction is monitored by gas-chromatography. After 1.5 hours, the precipitate is filtered and mother liquors are taken to dryness. Finally, the yellowish powder is dried under vacuum and characterized by <sup>1</sup>H-NMR, <sup>13</sup>C-NMR, FT-IR and m.p.

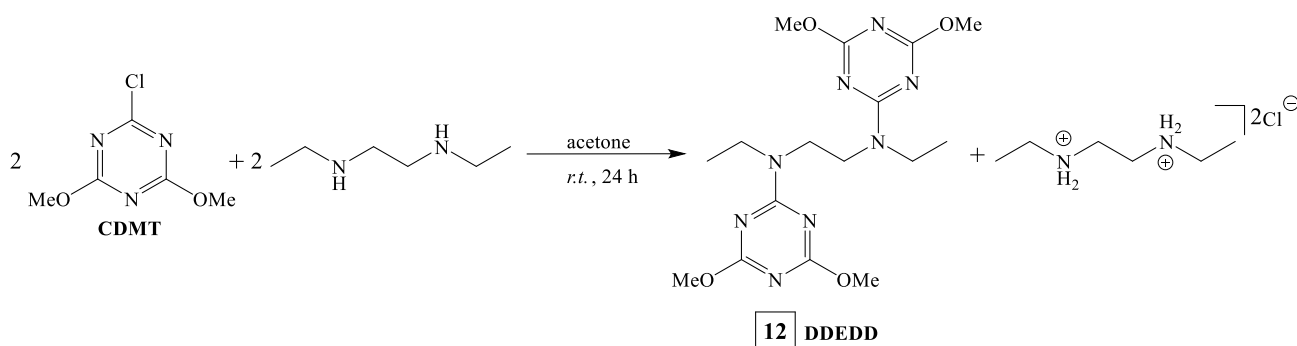
Characterization:

**11** CDEDC:

Yield 97% (purity 98%)

- **m.p.:** 102 °C.
- **<sup>1</sup>H NMR** (300 MHz, acetone-d<sub>6</sub>, ppm): 3.98 (4H, m s, NCH<sub>2</sub>CH<sub>2</sub>N), 3.73 (4H, q, NCH<sub>2</sub>CH<sub>3</sub>), 1.23 (6H, t, NCH<sub>2</sub>CH<sub>3</sub>).
- **<sup>13</sup>C NMR** (300 MHz, acetone-d<sub>6</sub>, ppm): 169.78, 169.39, 164.92, 44.61, 43.31, 11.51.
- **FT-IR** (KBr, cm<sup>-1</sup>): 1520, 1335, 1230, 809.

### 5.3.2.2 Synthesis of *N*<sub>1</sub>,*N*<sub>2</sub>-bis(2,4-dimethoxy-1,3,5-triazin-6-yl)-*N*<sub>1</sub>,*N*<sub>2</sub>-diethylethane-1,2-diamine (DDEDD):



**Scheme 3.15:** Synthesis of *N*<sub>1</sub>,*N*<sub>2</sub>-bis(2,4-dimethoxy-1,3,5-triazin-6-yl)-*N*<sub>1</sub>,*N*<sub>2</sub>-diethylethane-1,2-diamine (DDEDD).

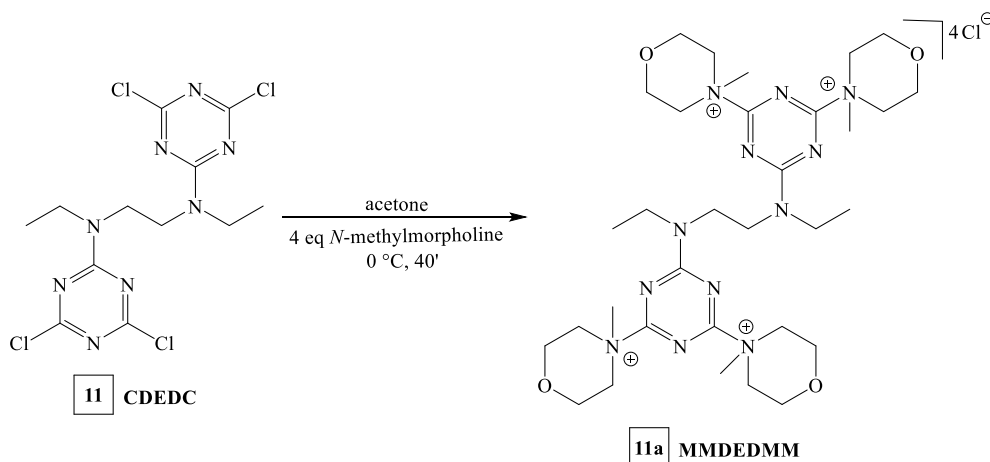
In a 50 mL flask, equipped with magnetic stirrer, 0.3 g of 2-chloro-4,6-dimethoxy-1,3,5-triazine (CDMT, 1.8 mmol) are added to 25 mL of acetone. Thus, a 5 mL acetone solution with 0.24 mL of *N,N'*-diethylethylenediamine (DED, 1.8 mmol) is added and the reaction is monitored by gas-chromatography. After 24 hours, the precipitate is filtered and mother liquors are taken to dryness. The white powder is finally dried under vacuum and characterized by <sup>1</sup>H-NMR, <sup>13</sup>C-NMR, FT-IR and m.p. Characterization:

**12** DDEDD:

Yield 90% (purity 97%)

- **m.p.:** 93 °C.
- **<sup>1</sup>H NMR** (300 MHz, DMSO-d<sub>6</sub>, ppm): 3.82-3.81 (12H, s, OCH<sub>3</sub>), 3.75 (4H, s, NCH<sub>2</sub>CH<sub>2</sub>N), 3.57 (4H, q, NCH<sub>2</sub>CH<sub>3</sub>), 1.12 (6H, t, NCH<sub>2</sub>CH<sub>3</sub>).
- **<sup>13</sup>C NMR** (300 MHz, DMSO-d<sub>6</sub>, ppm): 172.22, 172.15, 166.82, 54.51, 54.41, 44.55, 42.65, 13.04.
- **FT-IR** (KBr, cm<sup>-1</sup>): 1520, 1335, 1258, 1230.

### 5.3.3 Study of quaternary tetrakis-morpholinium salt derived from $N_1,N_2$ -bis(2,4-dichloro-1,3,5-triazin-6-yl)- $N_1,N_2$ -diethylethane-1,2-diamine (MMDEDMM)



**Scheme 3.16:** Synthesis of quaternary tetrakis-morpholinium salt derived from  $N_1,N_2$ -bis(2,4-dichloro-1,3,5-triazin-6-yl)- $N_1,N_2$ -diethylethane-1,2-diamine (MMDDEDMM<sup>(\*)</sup>).

In a 100 mL flask, equipped with magnetic stirrer, 0.3 g of  $N_1,N_2$ -bis(2,4-dichloro-1,3,5-triazin-6-yl)- $N_1,N_2$ -diethylethane-1,2-diamine (CDEDC, 0.7 mmol) are added to 60 mL of acetone. The system is cooled to 0 °C, thus a 10 mL acetone solution with 0.31 mL of *N*-methylmorpholine (MM, 2.8 mmol) is slowly added. Precipitation of a solid is observed and the reaction is left under stirring for 40 minutes, then the precipitate is filtered. The yellow powder is dried under vacuum and characterized by  $^1\text{H-NMR}$ ,  $^{13}\text{C-NMR}$ , FT-IR and m.p.

Characterization:

**11a** MMDDEDMM<sup>(\*)</sup>:

<sup>(\*)</sup> Data are not available because the product is a mixture of species.

In-depth analysis is reported in **Chapter 3.3.4**.

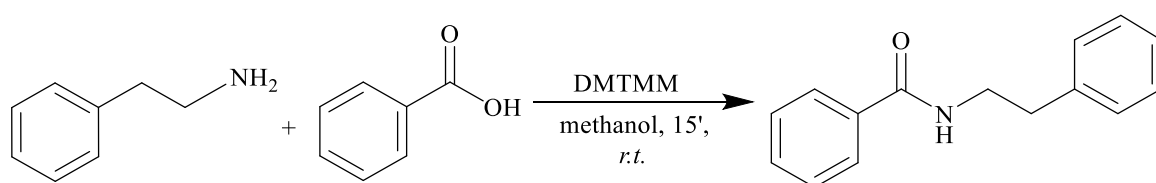
## 5.4 Application of amidation agents in condensation reactions

In this work, bis-ammonium salts have been tested with both “*isolated product procedure*” (*IPP*) and “*in situ*”.

By using the term “*IPP*” protocol, it is meant that an active solid amidation agent is used by a simply addition to the reaction solution.

By using the term “*in situ*” protocol, it is meant that the amidation agent is synthesized in its active form directly in the reaction solution.

### 5.4.1 Isolation of *N*-phenylethyl-benzamide



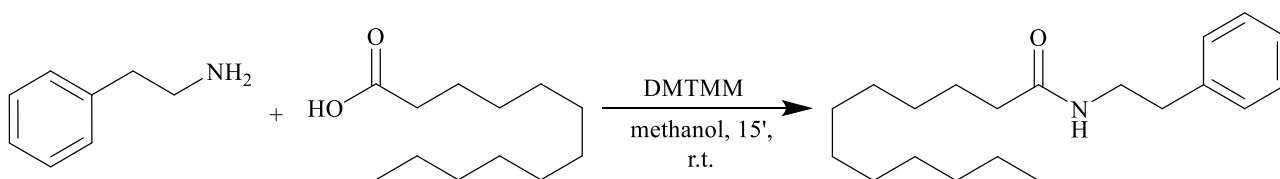
**Scheme 5.17:** Condensation reaction of *N*-phenylethyl-benzamide.

In a 50 mL flask, equipped with magnetic stirrer, 731 mg of phenylethylamine (6.0 mmoles) are added in 30 mL of methanol. Thus, 733 mg of benzoic acid (6.0 mmoles) and 1.641 g of 4-(4,6-dimethoxy-1,3,5-triazin-2-yl)-4-methyl-morpholinium chloride (DMTMM, 6.0 mmoles) are added to the solution. The reaction is monitored by gas-chromatographic analysis. After 15 minutes, the solution is dried by reduced pressure evaporation. The solid obtained is washed with 30 mL water solution (10% wt. NaHCO<sub>3</sub>). Finally, the product is filtered, dried under vacuum and characterized by <sup>1</sup>H NMR.

Yield 69% (purity 92%)

<sup>1</sup>H NMR (300 MHz, CDCl<sub>3</sub>, ppm): 7.73-7.25 (10H, m, CH<sub>arom</sub>), 6.20 (1H, s broad, NH), 3.76 (2H, q, NHCH<sub>2</sub>CH<sub>2</sub>), 2.96 (2H, t, NHCH<sub>2</sub>CH<sub>2</sub>).

### 5.4.2 Isolation of *N*-phenylethyl-dodecanamide



**Scheme 5.18:** Condensation reaction of *N*-phenylethyl-dodecanamide.

In a 50 mL flask, equipped with magnetic stirrer, 731 mg of phenylethylamine (6.0 mmoles) are added in 30 mL of methanol. Thus, 1.322 g of dodecanoic acid (6.0 mmoles) and 1.641 g of 4-(4,6-dimethoxy-1,3,5-triazin-2-yl)-4-methyl-morpholinium chloride (DMTMM, 6.0 mmoles) are added to the solution. The reaction is monitored by gas-chromatographic analysis. After 15 minutes, the solution is dried by reduced pressure evaporation. The oil obtained is washed with 30 mL water solution (10% wt. NaHCO<sub>3</sub>) and extracted with 3 aliquotes of 15 mL of CH<sub>2</sub>Cl<sub>2</sub>. Finally, the solution is taken to dryness and the obtained solid is characterized by <sup>1</sup>H NMR.

Yield 55% (purity 95%)

<sup>1</sup>H NMR (300 MHz, CDCl<sub>3</sub>, ppm): 7.36-7.20 (5H, m, CH<sub>arom</sub>), 5.43 (1H, s broad, NH), 3.56 (2H, q, NHCH<sub>2</sub>CH<sub>2</sub>C<sub>6</sub>H<sub>5</sub>), 2.84 (2H, t, NHCH<sub>2</sub>CH<sub>2</sub>C<sub>6</sub>H<sub>5</sub>), 2.13 (2H, t, COCH<sub>2</sub>CH<sub>2</sub>(CH<sub>2</sub>)<sub>8</sub>CH<sub>3</sub>), 1.60 (4H, qi, COCH<sub>2</sub>CH<sub>2</sub>(CH<sub>2</sub>)<sub>8</sub>CH<sub>3</sub>), 1.28 (16 H, m, COCH<sub>2</sub>CH<sub>2</sub>(CH<sub>2</sub>)<sub>8</sub>CH<sub>3</sub>), 0.90 (3H, t, COCH<sub>2</sub>CH<sub>2</sub>(CH<sub>2</sub>)<sub>8</sub>CH<sub>3</sub>).

#### 5.4.3 Synthesis of an amide in the presence of quaternary ammonium salts with IPP protocol

Into a 10 mL flask, equipped with magnetic stirrer, 133 mg of tetraethylene-glycol-dimethyl-ether (tetraglyme, 0.6 mmoles) and 146 mg of phenylethylamine (1.2 mmoles) are weighed and dissolved in 6 mL of methanol. Thus, 1.2 mmoles of the desired carboxylic acid and 0.6 mmoles of the appropriate preformed amidation agent are added to the solution.

The reaction is monitored by gas-chromatographic analysis. Yield is calculated by calibration line, reported in **Chapter 6.1** and **Chapter 6.2**, respectively for *N*-phenylethyl-benzamide and *N*-phenylethyl-dodecanamide.

GC temperature programme: T<sub>i</sub>: 50 °C x 4 min rate: 20 °C/min T<sub>f</sub>: 230 °C x 30 min

#### 5.4.4 Synthesis of an amide in the presence of quaternary ammonium salts with *in situ* protocol

Into a 10 mL flask, equipped with magnetic stirrer, 133 mg of tetraethylene-glycol-dimethyl-ether (tetraglyme, 0.6 mmoles) and 146 mg of phenylethylamine (1.2 mmoles) are weighed and dissolved in 4 mL of methanol. Thus, 1.2 mmoles of the desired carboxylic acid are added to the solution.

In a second 5 mL flask, 0.6 mmoles of the desired 2,4-dichloro-6-substituted-1,3,5-triazine and 1.2 mmol of the chosen tertiary amine are dissolved in 2 mL of methanol and added to the first solution. The reaction is monitored by gas-chromatographic analysis. Yield is calculated by calibration line, reported in **Chapter 6.1** and **Chapter 6.2**, respectively for *N*-phenylethyl-benzamide and *N*-phenylethyl-dodecanamide.

GC temperature programme: T<sub>i</sub>: 50 °C x 4 min rate: 20 °C/min T<sub>f</sub>: 230 °C x 30 min

## **CHAPTER 6**

### **ATTACHMENT**

#### **SYNTHESIS OF AMIDATION AGENTS AND THEIR REACTIVITY IN COUPLING REACTIONS**

## 6.1 Calibration line for synthesis of *N*-phenylethyl-benzamide

The data reported in this work for yields in *N*-phenylethyl-benzamide have been obtained by gas-chromatography using a calibration line based on the product synthesized by the procedure previously described. (**Chapter 5.4.1**)

The  $^1\text{H}$  NMR spectrum of the isolated product is shown below. (**Figure 6.1**)

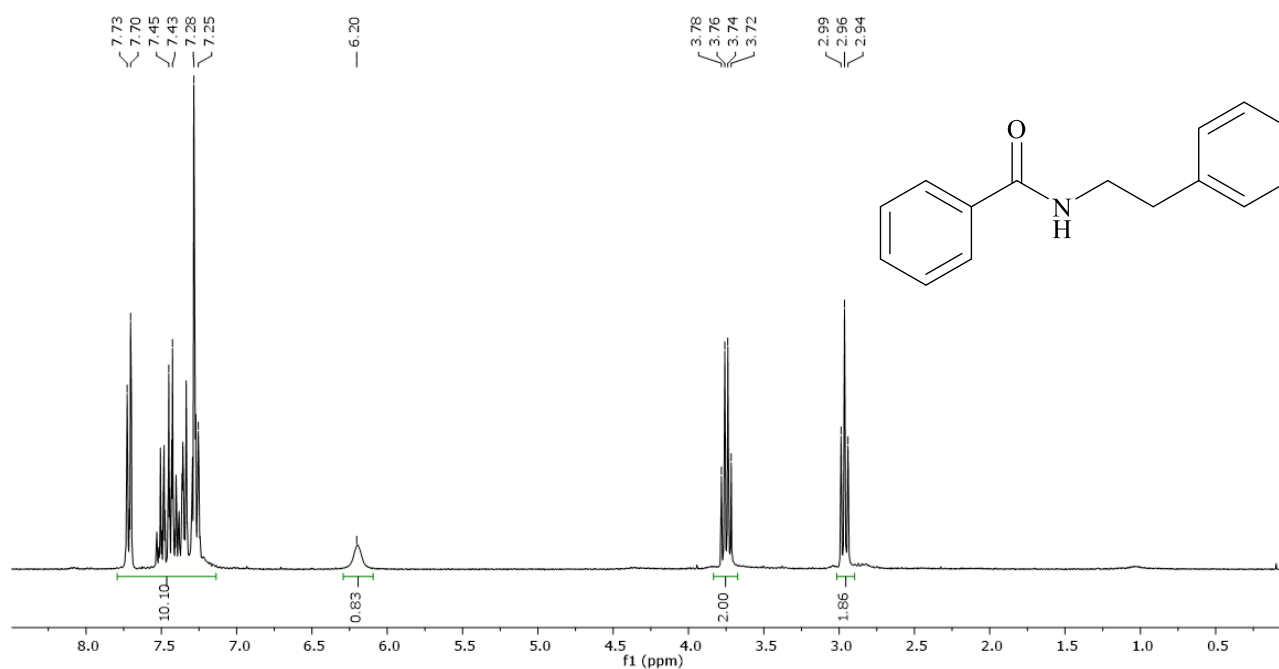


**Figure 6.1:**  $^1\text{H}$  NMR spectrum ( $\text{CDCl}_3$ ) of *N*-phenylethyl-benzamide.

$^1\text{H}$  NMR (300 MHz,  $\text{CDCl}_3$ , ppm): 7.73-7.25 (10H, m,  $\text{CH}_{\text{arom}}$ ), 6.20 (1H, s broad,  $\text{NH}$ ), 3.76 (2H, q,  $\text{NHCH}_2\text{CH}_2$ ), 2.96 (2H, t,  $\text{NHCH}_2\text{CH}_2$ ).

The calibration line (**Figure 6.2**) of *N*-phenylethyl-benzamide has been prepared using an Agilent Technologies 6850 Network Gas-Chromatograph equipped with an HP-5 column.

GC temperature programme:  $T_i$ : 50 °C x 4 min rate: 20 °C/min  $T_f$ : 230 °C x 30 min

Tetraethylene-glycol-dimethyl-ether (tetraglyme) has been used as internal standard.

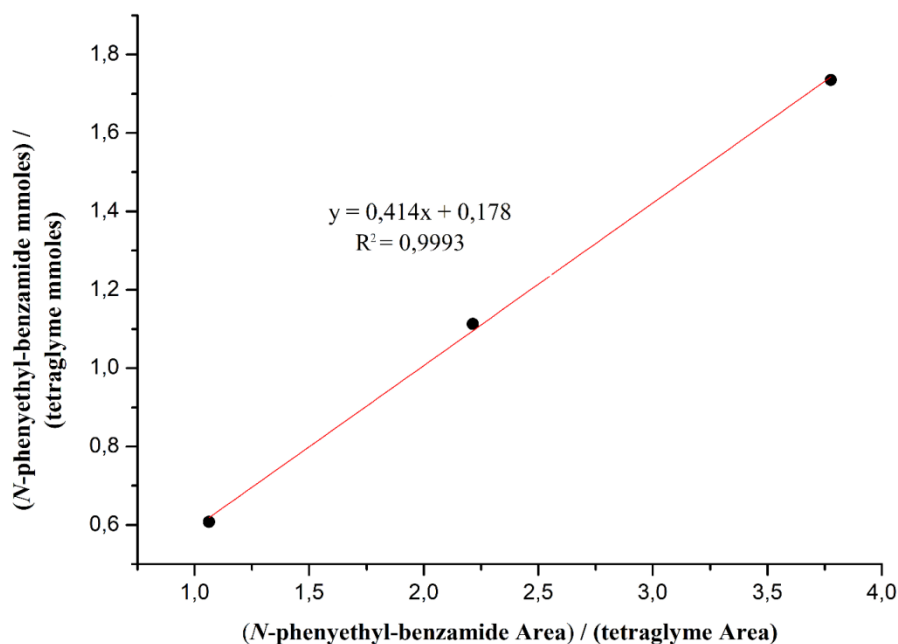


Figure 6.2: Calibration line for *N*-phenylethyl-benzamide yield.

## 6.2 Calibration line for synthesis of *N*-phenylethyl-dodecanamide

The data reported in this work for yields in *N*-phenylethyl-dodecanamide have been obtained by gas-chromatography using a calibration line based on the product synthesized by the procedure previously described. (Chapter 5.4.2)

The  $^1\text{H}$  NMR spectrum of the isolated product is shown below. (Figure 6.3)

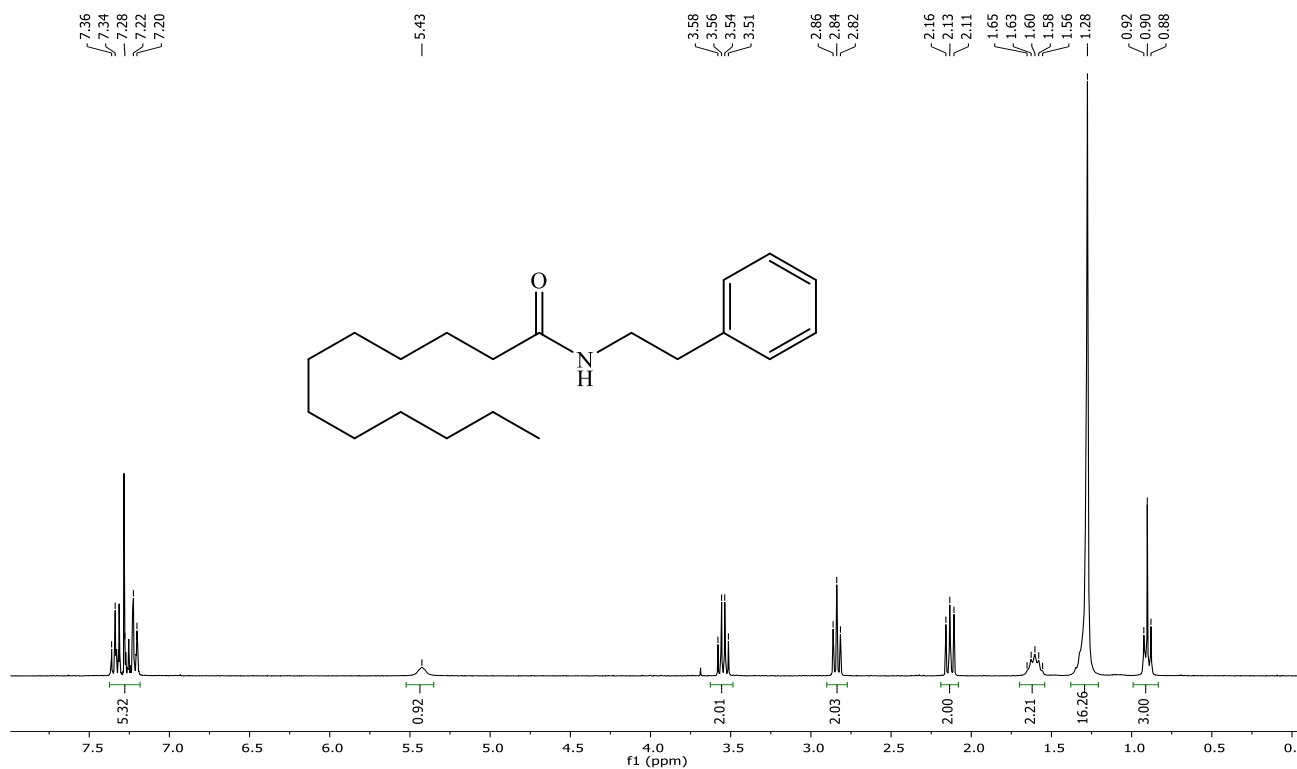


Figure 6.3:  $^1\text{H}$  NMR spectrum ( $\text{CDCl}_3$ ) of *N*-phenylethyl-dodecanamide.



<sup>1</sup>H-NMR (300 MHz, CDCl<sub>3</sub>, ppm): 7.36-7.20 (5H, m, CH<sub>arom</sub>), 5.43 (1H, s broad, NH), 3.56 (2H, q, NHCH<sub>2</sub>CH<sub>2</sub>C<sub>6</sub>H<sub>5</sub>), 2.84 (2H, t, NHCH<sub>2</sub>CH<sub>2</sub>C<sub>6</sub>H<sub>5</sub>), 2.13 (2H, t, COCH<sub>2</sub>CH<sub>2</sub>(CH<sub>2</sub>)<sub>8</sub>CH<sub>3</sub>), 1.60 (4H, qi, COCH<sub>2</sub>CH<sub>2</sub>(CH<sub>2</sub>)<sub>8</sub>CH<sub>3</sub>), 1.28 (16 H, m, COCH<sub>2</sub>CH<sub>2</sub>(CH<sub>2</sub>)<sub>8</sub>CH<sub>3</sub>), 0.90 (3H, t, COCH<sub>2</sub>CH<sub>2</sub>(CH<sub>2</sub>)<sub>8</sub>CH<sub>3</sub>).

The calibration line (**Figure 6.4**) of *N*-phenylethyl-dodecanamide has been prepared using an Agilent Technologies 6850 Network Gas-Chromatograph, equipped with an HP-5 column.

GC temperature programme: T<sub>i</sub>: 50 °C x 4 min rate: 20 °C/min T<sub>f</sub>: 230 °C x 30 min

Tetraethylene-glycol-dimethyl-ether (tetraglyme) has been used as internal standard.

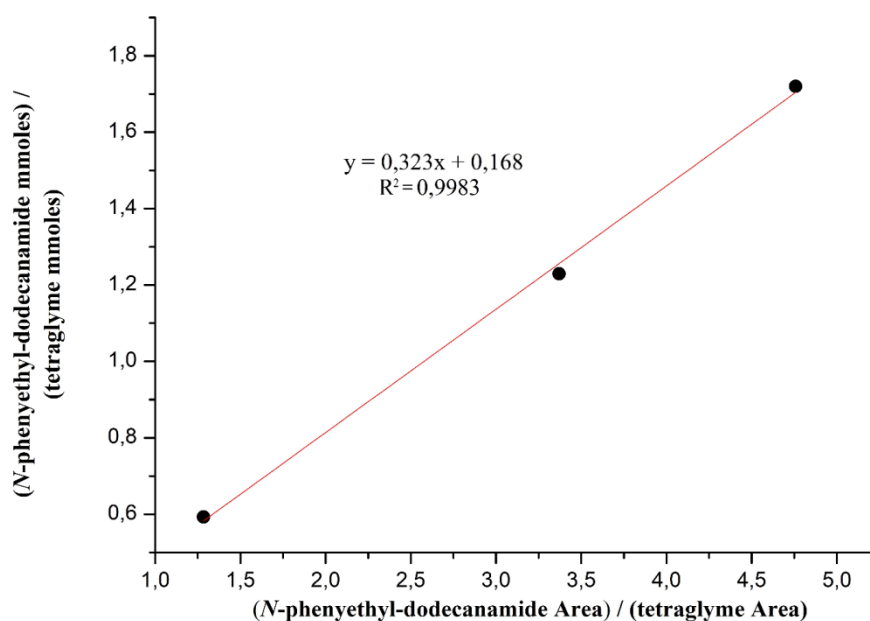


**Figure 6.4:** Calibration line for *N*-phenylethyl-dodecanamide yield.

## **APPLICATION OF AMIDATION AGENTS**

### **COLLAGEN CROSS-LINKING**

## **CHAPTER 7**

### **INTRODUCTION COLLAGEN CROSS-LINKING**

## 7.1 Collagen

The term ‘collagen’ is used to identify the main structural protein in connective tissues such as skin, bones, tendons or cartilages. This polypeptide forms elongated fibrils that provide mechanical stability to connective tissues,<sup>[74]</sup> collagen is regarded as one of the most useful biopolymers, used in a wide range of disciplines. Thanks to its excellent biocompatibility and biodegradability,<sup>[75,76]</sup> many studies are reported for its use in several biomedical applications, such as: wound care,<sup>[77]</sup> drug delivery systems,<sup>[75]</sup> or engineering for organic tissues reconstruction (tendons, cartilages, corneal tissues, etc.)<sup>[78-80]</sup> However, some disadvantages in the use of collagen-based systems may arise from their poor mechanical strength, fast biodegradation and low thermal stability. Cross-linking is a well-known technique to improve stability of collagen matrices, although physical treatments may be employed, such as ultraviolet irradiation or thermal dehydration treatments,<sup>[81-83]</sup> chemical reticulation is the most widely employed method for collagen stabilization.<sup>[84,85]</sup>

### 7.1.1 Structure of collagen

Collagen is a generic name used to identify a kind of at least 28 different biopolymer chains, each serving different function in vertebrates, mainly as connective tissues.<sup>[86]</sup> The so-called “type I” collagen is the most common biopolymer chain in mammals, thus when the terms “collagen” is used, if not differently specified, it refers to type I collagen.

Collagen  $\alpha$ -chains are constituted generally of 1050 amino acids and the chemical composition of each collagen type is easily accessible in the literature.<sup>[75,87,88]</sup> These polypeptides are unusually rich in glycine (Gly), proline (Pro) and hydroxyproline (Hyp) and their chains, known as  $\alpha$ -chains, are constituted of two sequences of amino acids: Gly-Pro-X and Gly-Y-Hyp triplets. Glycine occupies always the same position, while X and Y positions can be occupied by any aminoacid, with the exception of tryptophan (Trp), not present in any collagen structure.<sup>[89]</sup>

Among the amino acids that are components of the collagen structure, it is important to mention: aspartic acid (Asp), glutamic acid (Glu), lysine (Lys), hydroxylysine (Hyl) and arginine (Arg). When part of the  $\alpha$ -chain, these amino acids still possess free carboxylic group or primary amino groups not involved in peptidic bonds.

Collagen is composed of three polypeptidic chains organized in a right handed triple-helix, held together by intermolecular N-H $\cdots$ O=C hydrogen bonds between adjacent strands. (**Figure 7.1**)

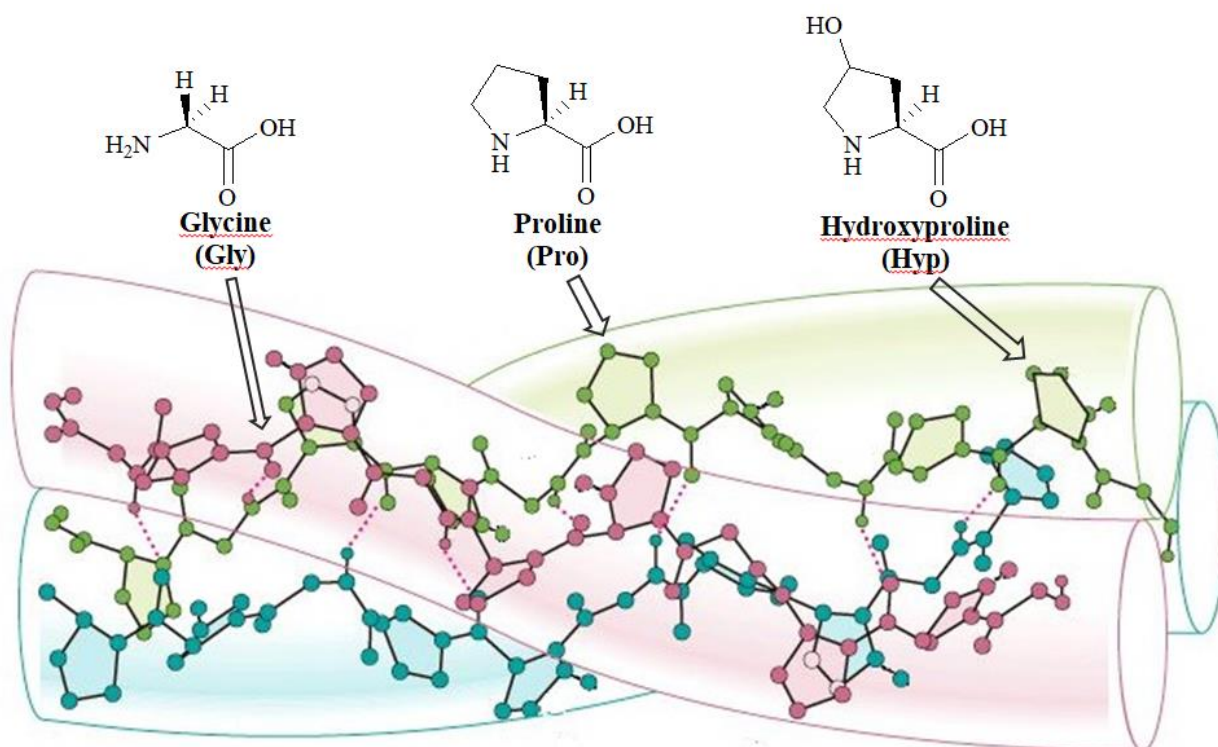


**Figure 7.1:** Collagen triple helix.

The type of collagen depends, besides other factors, on the amino acids composition of  $\alpha$ -chains and on the kind of  $\alpha$ -chains constituting the triple helix. Indeed, helical structures may present equals  $\alpha$ -chains and be homotrimeric, as the majority of collagen helices, or heterotrimeric, such as in the case of type I collagen, constituted by two identical chains and one different.<sup>[87,90]</sup>

### 7.1.2 Role of water in collagen

Water has been found to be essential in the maintenance of collagen in its native conformation. Thanks to the fibrous structure and the large concentration of hydrophilic groups (C=O, N-H, COOH, OH, etc.), water can be considered an integral part of the collagen structure.<sup>[91]</sup>

According to Privalov,<sup>[92]</sup> hydroxyproline and, to a less extent, proline residues assume a role as initiators for an extended network of water bound to the triple helix. Model studies have confirmed that the triple helix is indeed surrounded by water molecules, with hydroxyproline as the center of nucleation.<sup>[93]</sup> Nevertheless, these models just highlight that water is directly involved in interactions with collagen; it must be taken into account that bound water interacts with other water molecules as well, creating layers of water structures, that may be considered a supramolecular solvent sheath.

Collagen hydration is capable to influence thermodynamic properties.<sup>[94]</sup> Besides being important for collagen stabilization, the presence of water is fundamental for cross-linking reactions in this

matrix, because it occupies the collagen regions where these reactions occur. Anyhow, it has been demonstrated that not all water molecules interact with the matrix in the same way and can be divided in four groups:<sup>[91,94]</sup>

1. Water directly bound to collagen by two H bonds, known as “unfreezable water”, poorly influenced by reticulation;
2. Water linked by one H bond, associated with an increase of denaturation enthalpy. The greater is the reticulation, the smaller is the amount of this kind of water;
3. Water bound to side-chains and peptide links, its presence does not influence the denaturation enthalpy but leads to a decrease in denaturation temperature. The amount of this kind of water increases with reticulation of collagen;
4. Bulk Water, causing swelling. It is interstitial within the fiber structure and does not affect the thermodynamic properties of collagen.

### 7.1.3 Denaturation process of collagen

Hydrothermal stability is the main property used for collagen characterization. This thermodynamic property is defined as the effect of wet heat on the material integrity and it is known as shrinkage temperature, due to the tendency of collagenic matrices to shrink when denaturated.<sup>[91,95]</sup>

Another name used to refer to this temperature is Temperature of Gelatinization (Tg), due to the process of gelatinization of the collagen fibers when the transition occurs.<sup>[96]</sup>

Hydrothermal stability may be investigated by many techniques such as: Microthermal Analysis, Atomic Force Microscopy (AFM) or Nuclear Magnetic Resonance (NMR),<sup>[96,97]</sup> but Differential Scanning Calorimetry (DSC) is the most common and used.<sup>[98]</sup>

Collagen denaturation is referred to as the transition from triple helix structure to a random coil and may be traced back to breakage of H bonds, as a result of heat treatment. This can be considered an irreversible process, though reversibility is reported to be viable in the very early stages of the process.<sup>[99,100]</sup> As reported before (**Chapter 7.1.2**), differences in collagen hydration are associated to changes in denaturation temperature and in enthalpy variation for the transition.<sup>[94,97]</sup>

In native collagen, shrinkage temperature is commonly observable between 60 and 65 °C, depending on the matrix source (animal species, age, nutriment etc.) and on the test conditions.

As further demonstration of the H bonds role in denaturation processes, it is known that if collagen is analyzed by DSC after treatment with lithium bromide, a known H-bond breaker, denaturation transition is no more observable.<sup>[91,101]</sup>

Moreover, by DSC it is possible to observe that the shrinking transition is not the only hydrothermal process, since at higher temperature another transition occurs around 110-130 °C, unaffected by

LiBr treatment. It is not clear which reactions are responsible for this process. Various assumptions refer to breaking of structures associated with protein sidechains or to amide links decomposition in the peptide chains.<sup>[91]</sup>

From a mechanical or thermodynamical standpoint, the denaturation process is the same for native or reticulated collagen. Nevertheless, it is well known that shrinkage transition for cross-linked matrices occurs at higher temperatures. This behaviour may be related to at least two factors:<sup>[102]</sup>

- Reduction of possible molecular configurations, thanks to an increase of covalent bonds among  $\alpha$ -chains, with a decrease in entropy;
- Reduction of collagen hydration and therefore closer binding among  $\alpha$ -chains, with consequent lowering of the space available for H-bonds.<sup>[102,103]</sup>

Dehydration caused by cross-linking leads to an increased temperature stability. It has been demonstrated that fibres reticulated using different agents have exactly the same denaturation temperature and enthalpy if measured with the same water content.<sup>[102]</sup>

## **7.2 Chemical cross-linking of collagen**

As explained before, cross-linking of collagen causes changes in the matrix in terms of rise in denaturation temperature, resistance to putrefaction by microorganisms and in macroscopic aspects (touch, smell and appearance).<sup>[91]</sup> Chemical cross-linking is by far the most used technique for collagen reticulation, exploiting the functional groups granted by the different amino acids of the  $\alpha$ -chains. It has been calculated that in sequences of 1000 amino acids are present ca. 120 carboxylic acid groups and ca. 30 primary amines.<sup>[104,105]</sup> Depending on the kind of cross-linking agent used, different functional groups and chemical bonds are involved.

There are five main families of cross-linking agents:<sup>[91]</sup>

- Mineral: based on the use of metals, it involves the formation of coordinative bonds with carboxylate groups;
- Vegetable: based on the use of polyphenolic biomolecules, it involves H bonds and dipole-dipole interactions;
- Aldehydic: it is based on the formation of covalent bonds by reacting di-aldehydes with the amine groups of  $\alpha$ -chains;
- Zero-length: actually used only on laboratory scale, it involves the application of activation agents to create amide bonds among  $\alpha$ -chains;
- Inorganic: of secondary importance, it involves the use of  $\text{SiO}_2$  or phosphates. This family will be no longer considered in this work.

The study of collagen cross-linking agents is a large and spread topic that exceeds the purpose of this work. A short presentation in terms of chemistry, benefits and drawbacks of the most important collagen cross-linking agents is reported below. For a further investigation other sources are recommended.<sup>[91]</sup>

### 7.2.1 Mineral cross-linking agents

The most used technique for reticulation of collagen, the mineral cross-linking may involve different metals such as aluminium, iron, zirconium or titanium, but 90% of tanning in the world is based on the use of chrome. Cr(III) salts are known as excellent reticulation agents and nowadays no other cross-linking agent is comparable in terms of versatility. Used as reagent in the form of  $\text{Cr}_2(\text{SO}_4)_3$ , chrome cross-linking shows many advantages compared to other agents:<sup>[91]</sup>

- High hydrothermal stability, shrinkage temperature may reach 110 °C;
- High process speed, reaction time is lower than 24 hours;
- Low quantity of agent required, normally less than 5% wt. is used.

Bjerrum has proposed a possible interaction between chrome and collagen that is commonly accepted:<sup>[106]</sup>  $\text{Cr}_2(\text{SO}_4)_3$  dissolves in water and undergoes a process called chromium-olation, to give polychromium(III) compounds that links  $\alpha$ -chains through carboxylate groups.<sup>[107]</sup> (**Figure 7.2**)

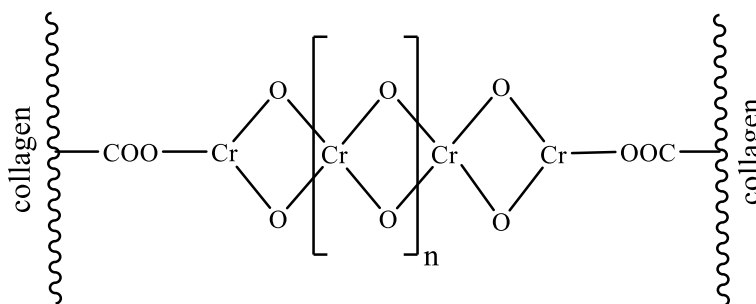


**Figure 7.2:** Collagen cross-linking by chromium-olation.

In industrial processes, chrome tanning presents a very strong environmental impact, in terms of contaminated wastewater and chromium sludges, that are mainly entombed. Various international organizations published data that estimated the released tannery contaminated water in 17 millions  $\text{m}^3$ , with an incisive chrome content.<sup>[108,109]</sup> Finally, under heating Cr(III) may give rise to Cr(VI), whose toxicity and carcinogenicity to humans and animals is widely known.<sup>[110,111]</sup>



## 7.2.2 Vegetable and aldehydic cross-linking agents

Vegetable and aldehydic cross-linking agents are, currently, the main alternatives to chrome and metals used in industry for reticulation of collagen. Aldehydic cross-linking agents used are mainly formaldehyde or glutaraldehyde,<sup>[104,112,113]</sup> while vegetable cross-linking agents are polyphenolic biomolecules with polycondensed structure, known as tannins.<sup>[114,115]</sup>

The nature of interaction with collagen matrix is different between the two types of cross-linking agents. Thanks to the presence of phenolic hydroxyl moieties, tannins are capable to interact with carboxylic group of  $\alpha$ -chains via H bonds.<sup>[91]</sup> On the other hand aldehydes interact with  $\text{NH}_2$  groups of collagen arginine, lysine and hydroxylysine to start an aldol polycondensation.<sup>[116]</sup> (**Figure 7.3**)

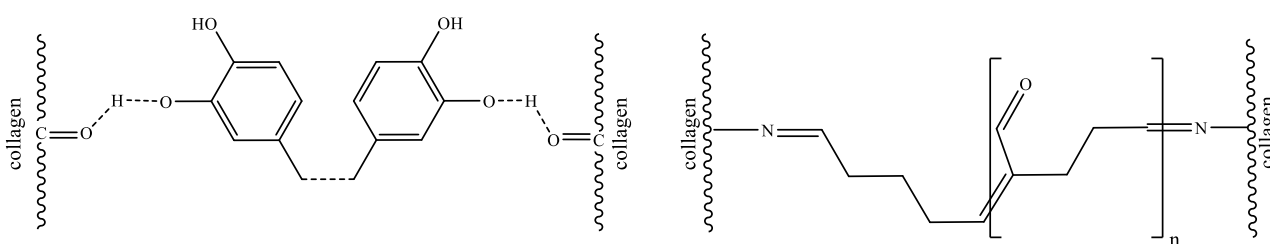


**Figure 7.3:** Collagen cross-link by tannins (left) and glutaraldehyde (right).

Vegetable and aldehydic cross-linking agents lead to physical and mechanical characteristics of collagen significantly lower than chrome. Moreover, their application does not solve environmental impact or toxicity issues, since carcinogenicity (formaldehyde) or cytotoxicity (phenols and glutaraldehyde) have been proven.<sup>[117-119]</sup>

## 7.2.3 Zero-length cross-linking agents

Recently, cross-linking methods based on application of agents able to activate carboxylic groups towards amidation reaction have been tested for reticulation of collagen. Indeed, aspartic acid (Asp), glutamic acid (Glu), lysine (Lys), hydroxylysine (Hyl) and arginine (Arg) are among the aminoacids present in collagen  $\alpha$ -chains and possess carboxylic and primary amino groups not involved in peptide bonds.<sup>[75,87,88]</sup> Thus, direct polypeptide chains reticulation can occur, resulting in the formation of amide bonds, the reaction follows the same mechanism reported previously in this work. (**Chapter 1**) No cross-linking agent is present in the reticulated collagen structure acting as bridge between the chains, hence the name “zero-length” cross-linking.

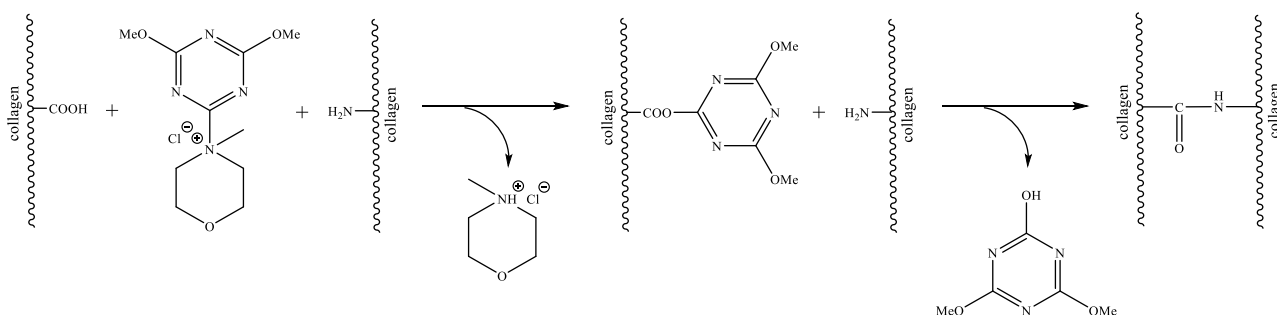
The first application of amidation agents on collagen is attributable to Petite *et al.* in a study about cross-linking of pericardium, where the comparison between glutaraldehyde and acyl azides is reported.<sup>[120]</sup> Despite interesting results in collagen reticulation and lower cytotoxicity compared to aldehydic cross-linking agents, acyl azides require a long multistep reaction in presence of alcohols.

An alternative to acyl azides was proposed first by van Luyn *et al.* and more recently by Davidenko *et al.*,<sup>[104,121]</sup> based on the application of *N*-(3-dimethylaminopropyl)-*N'*-ethylcarbodiimide (EDC) and *N*-hydroxysuccinimide (NHS) for collagen cross-linking.

Treatment of collagen with EDC led to materials with an increased shrinkage temperature and a decreased content in the matrix free amino groups, indicating that cross-linking occurred. As previously explained (**Chapter 1.6**), application of NHS as additive avoids intermediate rearrangements, resulting in an increased rate of cross-linking and higher Tg values (until 83 °C).

4-(4,6-dimethoxy-1,3,5-triazin-2-yl)-4-methylmorpholinium chloride (DMTMM) is an unexploited amidation agent used mainly for peptide synthesis,<sup>[1,5,122]</sup> but known also for application with biopolymers. Farkas *et al.* reported a study about activation of carboxyl acids in polysaccharides by DMTMM,<sup>[123]</sup> while more recently, D'este *et al.* reported a comparison between EDC/NHS and DMTMM for the grafting of amines to hyaluronan (HA) in water.<sup>[124]</sup> According to the authors, DMTMM appears superior to EDC/NHS for grafting HA in water since it does not require buffering of the reaction mixture and a smaller quantity of coupling agent is employed.

Finally, DMTMM has been used as cross-linking agent by Beghetto *et al.* for cross-linking of collagen both in laboratory and industrial scales.<sup>[125,126]</sup> Activation mechanism of carboxyl groups by DMTMM has been previously explained in this work. (**Chapter 1.7**), Beghetto reported that cross-linking may be achieved using DMTMM as a preformed agent (**Scheme 7.1**) or by a process called “*in situ*”, which provides the synthesis of the agent directly in the reaction environment.<sup>[126]</sup>



**Scheme 7.1:** Collagen cross-linking by DMTMM.

In Beghetto's patents, it is reported that DMTMM appears to be an efficient and active cross-linking agent, able to lead high rate of cross-linking and high Tg values (84 °C). Moreover, the use of this agent results in reduction of chemical and water consumption.

Triazine multi-ammonium salts developed in this work are unexploited compounds for cross-linking of collagen, which may lead to a further reduction in chemical agents needed for the process, having showed better performance compared to DMTMM. (**Chapter 3.5**)

## **CHAPTER 8**

### **SCOPE OF THE WORK COLLAGEN CROSS-LINKING**

The scope of this part of the PhD thesis is to develop a protocol for the cross-linking of dermal collagen by the use of triazine quaternary bis-ammonium salts, previously synthesized in this work, in order to obtain cross-linked collagen without the presence of metals or other toxic compounds (aldehydes, polyphenols) into the matrix. Collagen cross-linked by use of different quaternary bis-ammonium salts will be characterized by studies of hydrothermal stability to compare these amidation agents with those actually reported in literature.<sup>[125-126]</sup>

Finally, a second protocol for collagen cross-linking will be tested by formation of the active species “*in situ*” starting from chloro-triazines and a tertiary amine, this results of particular interest because it allows a cost reduction for application in industrial sector thanks to a reduced number of synthesis steps.

The objectives of this thesis are to optimize the cross-linking process with triazine quaternary ammonium salts and will be carried out as follows:

1. Optimize the previously reported process of collagen cross-linking using 4-(4,6-dimethoxy-1,3,5-triazin-2-yl)-4-methylmorpholinium chloride (DMTMM);
2. Perform cross-linking of collagen with the most efficient quaternary bis-ammonium salts synthesized in this work;
3. Perform cross-linking of collagen by protocol with “*in situ*” formed species;
4. Perform hydrothermal stability characterization to individuate the most active amidation agents for cross-linking.

## **CHAPTER 9**

### **RESULTS AND DISCUSSION COLLAGEN CROSS-LINKING**

Collagen is a biopolymers with a proteic structure constituted by three  $\alpha$ -chains generally composed by a sequence of 1050 amino acids.<sup>[75,87,88]</sup> On the study of collagen cross-linking, there are some amino acids present in these sequences that are worthy of mention: aspartic acid (Asp), glutamic acid (Glu), lysine (Lys), hydroxylysine (Hyl) and arginine (Arg). These amino acids are important because they present free carboxylic or primary amino groups not involved in the peptidic bonds when part of the  $\alpha$ -chains. (**Figure 9.1**)

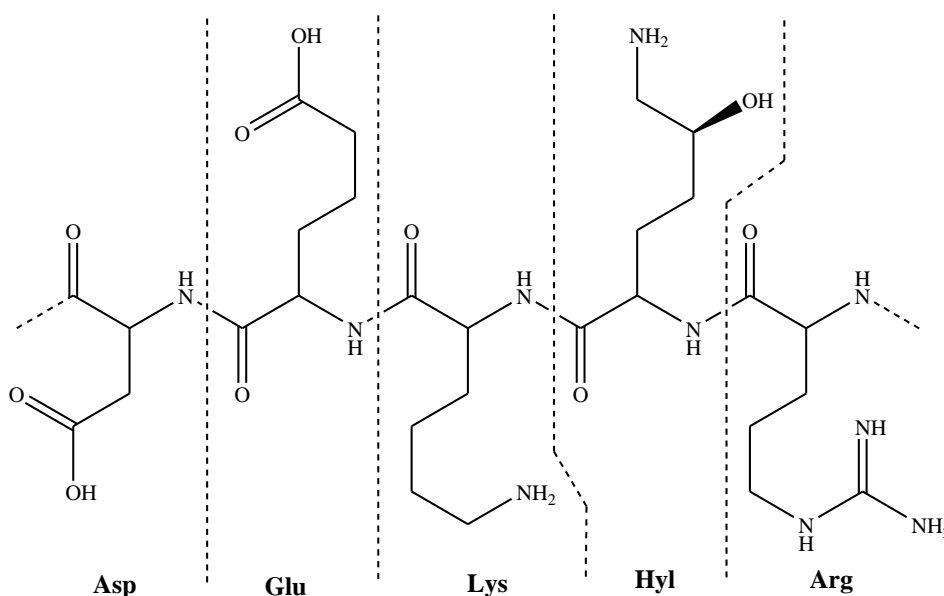


**Figure 9.1:** A peptidic sequence Asp-Glu-Lys-Hyl-Arg.

Many studies report that these amino acids are capable to interact with cross-linking agents, leading to collagen reticulation thanks to the interaction between carboxylic groups and metals,<sup>[107]</sup> by the reaction between primary amino groups and aldehydic compounds<sup>[116]</sup> or by the H bond interaction with polyphenolic macromolecules.<sup>[91]</sup> (**Chapter 7.2**) For this reason, in literature are reported studies about amino acid composition of  $\alpha$ -chains of each type of collagen.<sup>[75,87,88]</sup> Damink *et al.* reported that for 1 gram of type I collagen are present 1.2 mmoles of free carboxylic groups.<sup>[104,116]</sup> Recently, Petite and Damink have demonstrated that it is possible to activate collagen carboxylic acids to amidation reaction for direct cross-linking of  $\alpha$ -chains, leading to a direct amide bonds within collagen fibers.<sup>[104,120]</sup> This kind of cross-linking is known as “zero-length”.<sup>[79]</sup> In two patents by Beghetto *et al.*, it is reported the possibility to use 4-(4,6-dimethoxy-1,3,5-triazin-2-yl)-4-methylmorpholinium chloride (DMTMM) (**Figure 9.2**) as a water soluble amidation agent for collagen cross-linking, in particular Beghetto focused on tanning of animal hides.<sup>[125,126]</sup> Collagen cross-linking mechanism by DMTMM has been previously described (**Chapter 7.2.3**).

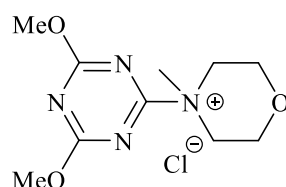


**Figure 9.2:** Chemical formula of 4-(4,6-dimethoxy-1,3,5-triazin-2-yl)-4-methylmorpholinium chloride (DMTMM).

## 9.1 Optimization of cross-linking process with 1,3,5-triazine salts

Beghetto *et al.* reported that DMTMM shows activity for collagen cross-linking in the pH range from 5.5 to 8.5, with the best value at pH 8.<sup>[125,126]</sup> In this work cross-linking tests have been carried out with a starting pH of 8, that decreases as the reaction progresses and settles at pH 5.5, due to the formation of the slightly acid byproduct 2-hydroxy-4,6-dimethoxy-1,3,5-triazine (DMTOH).<sup>[21]</sup>

In a study about collagen cross-linking by EDC/NHS, Damink identifies the best ratio between collagen carboxylic groups and amidation agent as 2:1.<sup>[104]</sup> The same value for DMTMM has been used by Beghetto as well and confirmed in preliminary tests on laboratory scale. Otherwise, for an industrial process, it is reported that cross-linking agent are used preferably 5 - 5.5% of animal hides weight.<sup>[91,125,126]</sup>

Finally, to the best of our knowledge, no study is reported to identify the best concentration of amidation agents (AA) in the solvent. Preliminary tests have shown that not only the ratio between AA and collagen influences the rate of cross-linking, but also an increase of DMTMM concentration leads to higher shrinkage temperatures ( $T_s$ ). Thus, influence of amidation agent concentration on  $T_s$  has been investigated comparing values of tests carried out both in laboratory and industrial scale. (**Table 9.1** and **Figure 9.3**)

**Table 9.1:** Shrinkage temperature as function of amidation agent (AA) concentration.

Run	Collagen ( $10^{-3} n_{\text{COOH}}$ )	AA ( $10^{-3} n_{\text{AA}}$ )	H <sub>2</sub> O (mL)	AA % wt.	[AA] ( $10^{-3} \text{ M}$ )	$T_s$ (°C)
1 ■	0.3	0.15	50	16.6	3	69 <sup>(a)</sup>
2 ■	0.3	0.15	25	16.6	6	73 <sup>(a)</sup>
3 ■	0.3	0.15	6	16.6	25	76 <sup>(a)</sup>
4 ■	1.2	0.6	14	16.6	40	78 <sup>(a)</sup>
5 ■	120	19.9	300	5.5	66	83 <sup>(a,b)</sup>
6 ■	$12 \cdot 10^3$	$19.9 \cdot 10^3$	$10 \cdot 10^3$	5.5	198	84 <sup>(b)</sup>

Reaction conditions: collagen (1.2 mmoles of COOH groups per gram)<sup>[104]</sup> and amidation agent (DMTMM) in water at *r.t.* for 4 hours;

(a) shrinkage temperature is calculated by DSC, analysis conditions: sample ca. 10 mg. Temperature programme: isotherm at 25 °C for 1 minute; heating cycle from 25 °C to 150 °C at 10 °C/min;

(b) shrinkage temperature is calculated by EN ISO 3380 method.<sup>[127]</sup>

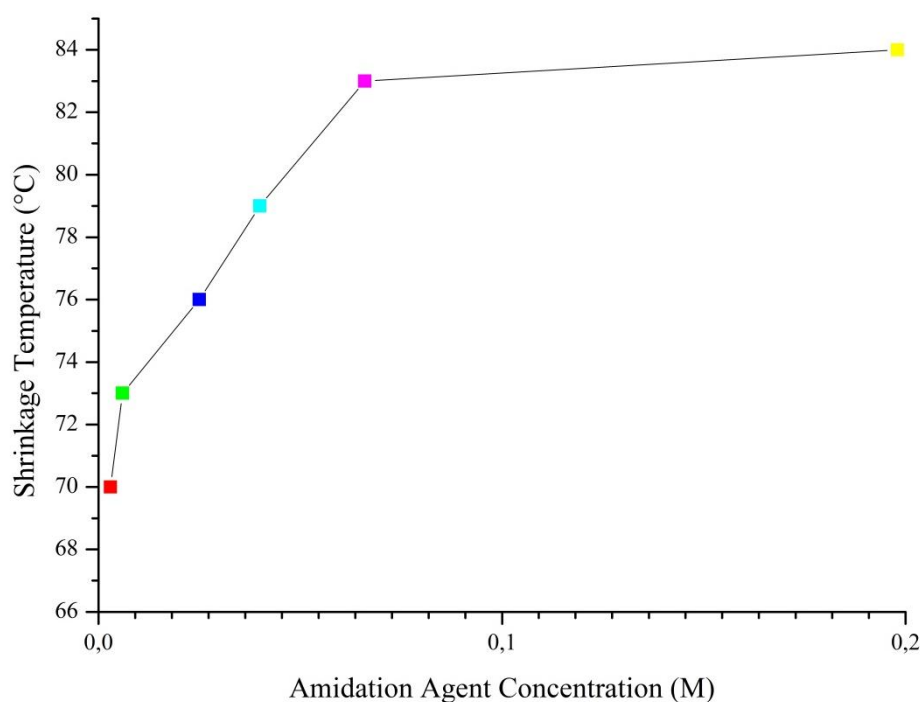


**Figure 9.3:** Shrinkage temperature vs. Amidation Agent (AA) Concentration.

In **Figure 9.3** and in Runs from 1 to 4 (**Table 9.1**), it is possible to observe a direct correlation between the shrinkage temperature and the amidation agent concentration, with a constant collagen:DMTMM ratio. Moreover, in Run 5 and 6 (**Table 9.1**) the quantity of AA used is reduced while the concentration is still increased. The difference of shrinkage temperature between Runs 5 and 6 is very small, thus it is possible to assume that further increases in concentration lead to a plateau value, as observable above. (**Figure 9.3**) The laboratory scale tests do not allow cross-linking rate optimization compared to a industrial process. Considering that the shrinkage temperatures of Run 1 and Run 6 (**Table 9.1**) present a difference of 15 °C, the Ts data reported below in this work may possibly present higher values if carried out in an industrial protocol. Moreover, this thesis has investigated the performances bis-ammonium salts compared to DMTMM, focusing on collagen:amidation agent ratio. It should be considered that bis-ammonium salts synthesized in this work present two sites capable to activate carboxylic groups for amidation reaction and thus the quantity used for collagen cross-linking tests is reduced to one half compared to DMTMM, consequently also their concentration is therefore reduced.

Finally, for laboratory scale the highest Ts value is achieved in Run 4 (**Table 9.1**), nevertheless the protocol of Run 3 has been favoured, presenting small differences in Ts values but requiring a much smaller amount of reagents.



## 9.2 Collagen cross-linking with 1,3,5-triazine quaternary bis-ammonium salts

The synthesis of 2,4-dichloro-6-substituted-1,3,5-triazines (MMT, MIAT and MEAT) and their derivated salts, reported before (**Chapter 3**), has been investigated in order to verify if the presence of two reactive sites in the triazine ring lead to high shrinkage temperatures in cross-linked collagen. After performance tests in condensation reaction (**Chapter 3.5**), only the compounds that presented interesting values in amide yields have been tested for collagen cross-linking.

Kaminski reported that is possible to activate carboxylic acids for synthesis of amides, without the need to use preformed DMTMM, by the reaction between 2-chloro-4,6-dimethoxy-1,3,5-triazine (CDMT) and *N*-methylmorpholine.<sup>[29]</sup> With this protocol, called “*in situ*”, it is possible to synthesize the ammonium salt directly in the reaction environment where it acts as an intermediate for carboxylic groups activation. Beghetto reported that application of the *in situ* protocol allows to activate collagen COOH moieties as well, leading to interesting results in shrinkage temperatures.<sup>[126]</sup>

For this reason, in this work, bis-ammonium salt have been tested with both “*isolated product procedure*” (*IPP*) and “*in situ*” protocols.

By using the term “*IPP*” protocol, it is meant that an active solid amidation agent is used by a simply addition to the reaction solution.

By using the term “*in situ*” protocol, it is meant that the amidation agent is synthesized in its active form directly in the reaction solution.

The shrinkage temperature of native collagen typically occurs at ca. 60 °C, depending on animal source and test conditions.<sup>[101]</sup> As references for performance of quaternary bis-ammonium salts derived from 2,4-dichloro-6-substituted-1,3,5-triazines, collagen has been cross-linked by DMTMM with both *IPP* and *in situ* protocols, with a COOH<sub>collagen</sub>:DMTMM ratio of 2:1. The shrinkage temperatures of cross-linked collagen obtained were respectively 76 °C and 74 °C.

The data below (**Table 9.2**) report the shrinkage temperatures of cross-linked collagen obtained by the application of bis-ammonium quaternary salts with a COOH<sub>collagen</sub>:amidation agent ratio of 4:1.

**Table 9.2:** Shrinkage temperature of collagen cross-linking by different bis-ammonium quaternary salts.

<i>IPP</i>	T <sub>g</sub> (°C) <sup>(a)</sup>	<i>in situ</i> <sup>(b)</sup>	T <sub>g</sub> (°C) <sup>(a)</sup>
MMTMM	68	MMT + MM	70
MMTMP	n.i. <sup>(c)</sup>	MMT + MP	80
MMTMPD	62	MMT + MPD	66
MMTTMA <sup>(*)</sup>	68	MMT + TMA	63
MIATMM	75	MIAT + MM	65
MIATMP	64	MIAT + MP	67
MIATMPD	63	MIAT + MPD	63
MIATTMA	74	MIAT + TMA	68
MEATMM	79	MEAT + MM	71
MEATMP	65	MEAT + MP	64
MEATMPD	n.i. <sup>(c)</sup>	MEAT + MPD	66
MEATTMA	77	MEAT + TMA	70

Reaction conditions: collagen 250 mg (0.3 mmoles COOH)<sup>[104]</sup>, at *r.t.* for 4 hours;

*IPP* protocol: amidation agent 0.075 mmoles, 6 mL water

*In situ* protocol: 4 mL water and parallel premix of a 2,4-dichloro-6-substituted-1,3,5-triazine (0.075 mmoles) and a tertiary amine (0.150 mmoles) in 1 mL of water (plus 1 mL of methanol if MIAT or MEAT are used or 1 mL of water if MMT is used);

(a) shrinkage temperature is calculated by DSC, analysis conditions: sample ca. 10 mg. Temperature programme: isotherm at 25 °C for 1 minute; heating cycle from 25 °C to 150 °C at 10 °C/min;

(b) 2,4-dichloro-6-substituted-1,3,5-triazines used are: 2,4-dichloro-6-methoxy-1,3,5-triazine (MMT), 2,4-dichloro-6-diisopropylamino-1,3,5-triazine (MIAT), 2,4-dichloro-6-diethylamino-1,3,5-triazine (MEAT). Tertiary amines used are: *N*-methylmorpholine (MM), *N*-methylpiperidine (MP), *N*-methylpyrrolidine (MPD) or trimethylamine (TMA);

(c) quaternary bis-ammonium salt has not been isolated for *IPP* protocol.

(\*) MMTTMA resulted to be a mixture of different species as explained in **Chapter 3.3.1.5**.

From data in **Table 9.2**, it is possible to observe:

- Collagen cross-linked by quaternary bis-ammonium salts derived by amino-substituted-1,3,5-triazine (MIAT and MEAT) show, generally, higher shrinkage temperatures compared to salts derived from MMT;
- Quaternary bis-ammonium salts derived by MEAT show generally better performances compared to relative salts derived from MIAT in terms of cross-linked collagen T<sub>s</sub>;

- *In situ* protocol has proven to be active for cross-linking reaction in all tested cases, with shrinkage temperatures between 63 °C and 80 °C. Therefore, it may be considered preferable to *IPP* protocol;
- Considering cross-linking carried out with *IPP* protocol, highest shrinkage temperature has been obtained using MEATMM, with a  $T_s$  of 79 °C;
- For what concerns *in situ* protocol, the highest shrinkage temperature has been obtained using MMT+MP with  $T_s$  of 80 °C;
- Although it was not possible to isolate some compounds, such as MMTMP and MEATMPD, cross-linking reactions with their *in situ* protocol counterparts led to high  $T_s$  values, especially for MMT+MP which was the highest value obtained. It is therefore possible to assume that the agent is able to activate carboxylic acid moieties in collagen, even if its salt could not be isolated.

It is important to notice that DMTMM presents one site capable to activate carboxylic groups, while quaternary bis-ammonium salts derived from 2,4-dichloro-6-substituted-1,3,5-triazines, reported above (**Table 9.2**), present two sites. Moreover, both *IPP* and *in situ* protocols for quaternary bis-ammonium salts have been carried out with a  $\text{COOH}_{\text{collagen}}:\text{amidation agent}$  ratio of 4:1.

In order to make a comparative test, collagen has been cross-linked using DMTMM with both *IPP* and *in situ* protocols with the same  $\text{COOH}_{\text{collagen}}:\text{DMTMM}$  ratio (4:1), leading to  $T_s$  values respectively of 71 °C and 68 °C.

As reported above (**Table 9.2**), in many cases shrinkage temperatures are comparable or higher to  $T_s$  values obtained with DMTMM, both for *IPP* and *in situ* protocols. Therefore, it may be supposed that quaternary bis-ammonium salts of 1,3,5-triazine proved in many cases to have better performances than DMTMM. As explained previously (**Chapter 3.5.1**), their use leads to the formation of an active intermediate capable to activate two carboxylic groups, allowing to reduce to 1 half the quantity of active agent needed for the cross-linking.

## **CHAPTER 10**

### **CONCLUSIONS COLLAGEN CROSS-LINKING**

The research of this part of the PhD thesis has focused on the development of a protocol for the cross-linking of collagen without the use of metals or other commonly used toxic compounds, such as aldehydes or polyphenols. The protocol provides the use of 1,3,5-triazine-based amidation agents previously synthesized in this work (**Chapter 3**) with a reduced amount compared to what reported in literature.<sup>[104,125,126]</sup>

The main results achieved are:

- A systematic study concerning the influence of the amidation agents concentration for efficiency in collagen cross-linking;
- Development of a protocol for the production of metal-free atoxic cross-linked collagen with reduced use of chemical products;
- The *In situ* protocol proved to be preferable compared to *IPP* protocol, leading to collagen cross-linking even when the quaternary ammonium salt is not isolable;
- The quaternary ammonium salts with a 6-amino-substituent resulted to have better performances in collagen cross-linking compared to their 6-methoxy-substituted counterparts;
- Cross-linking of collagen performed by use of bis ammonium salts has been carried out with a molar ratio between collagen carboxylic groups and amidation agents of 4:1, resulting in shrinkage temperature in many cases higher compared to those obtained in the same conditions in the presence of DMTMM (71 °C), allowing, in best conditions, to reduce the amount of amidation agent required by half.

These findings encourage further studies to investigate the optimization of bis-ammonium salts concentration in cross-linking of collagen as well as tests about their application on industrial scale.

This study led to the draft of one patents:

1. V. Beghetto, L. Agostinis, PCT/EP2017/064720, **2017**

## **CHAPTER 11**

### **EXPERIMENTAL SECTION COLLAGEN CROSS-LINKING**

## 11.1 General methods

All chemicals were commercially available and procured from Sigma Aldrich, Merck, Alfa Aesar and Fluka with high grade of purity. Solvents were of analytical grade and used without further purification.

Collagen dermal skin powder has been procured by Research Institute of Leather and Plastic Sheeting - Filk. Bovine hides were obtained from tanneries of the Santa Croce sull'Arno Leather District. Degree of cross-linking of collagen samples has been evaluated by measures of shrinkage temperature according to DSC analysis or EN ISO 3380 method.

DSC analyses were recorded in a Perkin Elmer DSC 7 combined with a Perkin Elmer TAC 7/DX. Sealed aluminium pans were used and for the analysis the sample pan were deposited in a platinum pan. Analyses were run in a 20 mL/min N<sub>2</sub> flow, using an empty Al pan as standard.

NMR spectra were recorded with a Bruker Avance 300 model spectrometer. The chemical shifts were reported as parts per million (ppm) downfield from TMS (Me<sub>4</sub>Si) with <sup>1</sup>H resonant frequency of 300.13 MHz and <sup>13</sup>C resonant frequency of 75.4 MHz for the carbon spectrum.

Deuterated solvents used for the NMR analyses were the following: acetone-d<sub>6</sub> and D<sub>2</sub>O, procured by Sigma Aldrich. The purity of synthesized compounds was calculated by integrating the signals present in the <sup>1</sup>H NMR spectrum.

Spectra in the region of middle infrared (4000-450 cm<sup>-1</sup>) were recorded using a Perkin-Elmer Spectrum-One spectrophotometer using KBr disks.

Gas-chromatography analysis were recorded with a Agilent Technologies 6850 gas chromatograph equipped with FID detector and capillary column HP-1 (100% dimethylsiloxane). Analyses were registered with following temperature ramp:

GC temperature programme: T<sub>i</sub>: 50 °C x 1 min rate: 20 °C/min T<sub>f</sub>: 230 °C x 35 min

Finally, melting points were determined in open capillaries on a Buchi 235 model.

## 11.2 Synthesis and Characterization

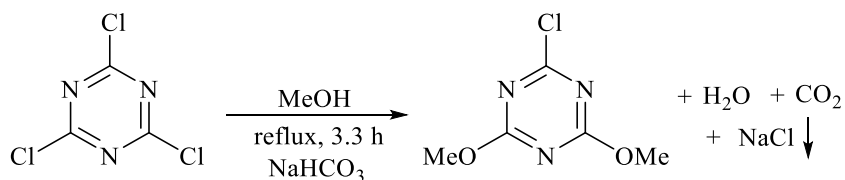
### 11.2.1 Preparation of 1,3,5-triazine precursors and quaternary ammonium salts

Quaternary bis-ammonium salts have been synthesized from 2,4-dichloro-6-substituted-1,3,5-triazine precursors identified as 2,4-dichloro-6-methoxy-1,3,5-triazine (MMT), 2,4-dichloro-6-diisopropyl-1,3,5-triazine (MIAT) and 2,4-dichloro-6-diethyl-1,3,5-triazine (MEAT). These were reacted with opportune tertiary amines: *N*-methylmorpholine (MM), *N*-methylpiperidine (MP), *N*-methylpyrrolidine (MPD) and trimethylamine (TMA). Quaternary bis-ammonium salts and their precursors have been synthesized as previously reported in this work. (**Chapter 5**)

Synthesis of 2-chloro-4,6-dimethoxy-1,3,5-triazine (CDMT) and 4-(4,6-dimethoxy-1,3,5-triazin-2-yl)-4-methylmorpholinium chloride (DMTMM) have been carried out in order to be used as reference amidation agents.<sup>[125,126]</sup>

#### 11.2.1.1 Synthesis of 2-chloro-4,6-dimethoxy-1,3,5-triazine (CDMT)

Synthesis of CDMT has been carried out following the method proposed by Kaminski.<sup>[29]</sup> (**Scheme 11.1**)



**Scheme 11.1:** Synthesis of 2-chloro-4,6-dimethoxy-1,3,5-triazine (CDMT).

In a 250 mL flask, equipped with magnetic stirrer and bubble condenser, 16 g (190.45 mmoles) of NaHCO<sub>3</sub> are added in 100 mL of methanol. Afterwards, 10 g of cyanuric chloride (CC, 54.23 mmoles) are slowly added to the suspension. The reaction is left under stirring for 40' and then heated to reflux for 2 hour and 40 minutes. The process is monitored by GC. Finally, the suspension is filtered, the white solid obtained is washed with four aliquotes of distilled water (50 mL) and dried under vacuum. White solid obtained is characterized by <sup>1</sup>H NMR and m.p.

Yield 95% (purity 96%).

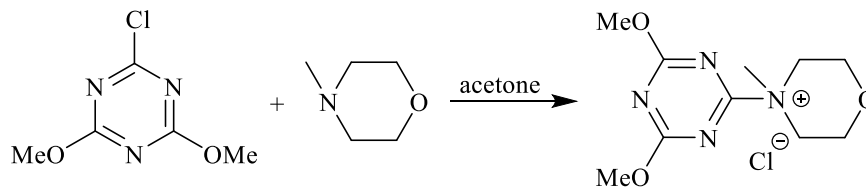
Characterization:

- **m.p.:** 73 °C.
- **<sup>1</sup>H NMR** (300 MHz, acetone-d<sub>6</sub>, ppm): 4.14 (6H, s, OCH<sub>3</sub>).



### 11.2.1.2 Synthesis of 4-(4,6-dimethoxy-1,3,5-triazin-2-yl)-4-methylmorpholinium chloride (DMTMM)

Synthesis of DMTMM has been carried out following the method proposed by Kaminski.<sup>[32]</sup> (Scheme 11.2)



**Scheme 11.2:** Synthesis of 4-(4,6-dimethoxy-1,3,5-triazin-2-yl)-4-methylmorpholinium chloride (DMTMM).

In a 100 mL flask, equipped with magnetic stirrer, 5 g of 2-chloro-4,6-dimethoxy-1,3,5-triazine (CDMT, 28.48 mmol) are added in 50 mL of acetone. Thus, the solution is cooled to 0 °C and 3.14 mL of *N*-methylmorpholine (MM, 28.48 mmol) are slowly added. The reaction is left under stirring for 40', then the precipitate is filtered and dried under vacuum. The solid product obtained is characterized by <sup>1</sup>H NMR. Yield 92% (purity 95%)

Characterization:

- <sup>1</sup>H NMR (300 MHz, D<sub>2</sub>O, ppm): 4.59 (2H, m, N<sup>+</sup>CH<sub>2</sub>CH<sub>2</sub>O), 4.12 (6H, s, OCH<sub>3</sub>), 4.09 (2H, m, N<sup>+</sup>CH<sub>2</sub>CH<sub>2</sub>O), 3.83 (4H, m, N<sup>+</sup>CH<sub>2</sub>CH<sub>2</sub>O), 3.50 (3H, s, N<sup>+</sup>CH<sub>3</sub>).

### 11.2.2 Collagen cross-linking by 1,3,5-triazine quaternary ammonium salts

In this work, bis-ammonium salt have been tested with both “*isolated product procedure*” (*IPP*) and “*in situ*”.

By using the term “*IPP*” protocol, it is meant that an active solid amidation agent is used by a simply addition to the reaction solution.

By using the term “*in situ*” protocol, it is meant that the amidation agent is synthesized in its active form directly in the reaction solution.

#### 11.2.2.1 Collagen cross-linking in the presence of quaternary ammonium salts with *IPP* protocol

Into a 10 mL flask, equipped with magnetic stirrer, 250 mg of collagen (0.3 mmol of COOH groups)<sup>[104]</sup> are dispersed in 6 mL of water. The suspension is left under stirring for 15 minutes to ensure that the collagen is adequately moisturized, thus pH is adjusted to 8. Then, 0.075 mmol of the desired preformed amidation agent (0.15 mmol if DMTMM is used) are added to the solution. The reaction is left under stirring for 4 h, then collagen is filtered and washed with 3 x 5 mL aliquotes of distilled water. Cross-linked collagen is then characterized by DSC.

### 11.2.2.2 Collagen cross-linking in the presence of quaternary ammonium salts with *in situ* protocol

Into a 10 mL flask, equipped with magnetic stirrer, 250 mg of collagen (0.3 mmol of COOH groups)<sup>[104]</sup> are dispersed in 4 mL of water. Suspension is left under stirring for 15 minutes to ensure that the collagen is adequately moisturized, thus pH is adjusted to 8. In a second 5 mL flask, 0.075 mmoles of the desired precursor (0.15 mmoles if CDMT is used) are dispersed in 1 mL of water. Thus, in order to help solubilization, another 1 mL of solvent is added, based on the precursor used:

- 1 mL of water for 2,4-dichloro-6-methoxy-1,3,5-triazine (MMT) and 2-chloro-4,6-dimethoxy-1,3,5-triazine (CDMT);
- 1 mL of methanol for 2,4-dichloro-6-diisopropyl-1,3,5-triazine (MIAT) and 2,4-dichloro-6-diethyl-1,3,5-triazine (MEAT).

Then, 0.15 mmol of the desired tertiary amine are added and the solution is slowly dripped to collagen suspension. The reaction is left under stirring for 4 hours, thus collagen is filtered, washed with 3 x 5 mL aliquotes of distilled water. Cross-linked collagen is then characterized by DSC.

### 11.2.2.3 Collagen cross-linking in tanning process with DMTMM

The pelts are received after standard beamhouse operations.<sup>[91]</sup> In a drum, the soaked bovine hide (50% wt. water) is mixed together with a water solution (50% wt.) of 5% wt. DMTMM. The tanning is carried out for 4h, then the water is discharged and the hide is washed with 100% wt. water for 10 min. Finally, the hide is characterized by DSC analysis and/or by EN ISO 3380 method.

### 11.2.3 Shrinkage temperature characterization

The degree of collagen cross-linking is related to an increase of shrinkage temperature ( $T_s$ ).<sup>[95,116]</sup>  $T_s$  values of cross-linked and unreticulated collagen are determined by DSC analyses and/or by EN ISO 3380 method. The samples are prepared as reported below:

#### DSC analysis:

Collagen sample is hydrated for at least 30 minutes. In an aluminium pan, 10 mg of wet collagen are weighed and then the pan is sealed. The sample is analyzed by DSC analysis and the onset of shrinkage transition is recorded as  $T_s$ . Finally, the pan is weighed again to record water loss.

DSC temperature programme:  $T_i$ : 25 °C x 1 min rate: 10 °C/min  $T_f$ : 150 °C

#### EN ISO 3380 method:

A tanned leather sample is suspended vertically in water, and the rate of heating is maintained at  $2 \pm 0.2$  °C/min. The  $T_s$  is the temperature at which the leather shrinks 1/3 of its original length.<sup>[127]</sup>

## **APPLICATION OF AMIDATION AGENTS**

### **POLYMER GRAFTING**

Supervisors:

**Dr. Belén Monje Martínez**

**Dr. Lorena Rodríguez Garrido**

**Dr. María Dolores Gómez Jiménez**

**Dr. Alba María Ortiz Álvarez**

---

In collaboration with:



**AIMPLAS**

INSTITUTO TECNOLÓGICO  
DEL PLÁSTICO

## **CHAPTER 12**

### **INTRODUCTION POLYMER GRAFTING**

## 12.1 Polymers modification

Nowadays, the trend in modern culture is to gradually replace natural materials with partially modified natural or fully synthetic products. Polymers find their application in every aspect of human life: medication, nutrition, communication, transportation, irrigation, packaging, clothing, recording, buildings, highways, etc.<sup>[128]</sup> In recent developing, the common procedure is to modify the properties of a polymer according to its final application and different procedures are known to achieve the desired modifications in polymers:<sup>[129]</sup>

- Blending
- Curing
- Grafting

This work focuses on polymer modification by grafting technique and a short presentation of the other different techniques is reported below for greater clarity.

### 12.1.1 Polymers blends

In a similar way to metal alloys, polymers blends are a class of materials composed by at least two different polymers to give a new product with different physical properties.<sup>[130]</sup> (**Figure 12.1**)

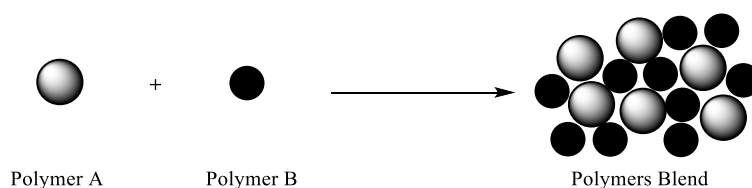


**Figure 12.1:** Schematic representation of polymer blending.

The blending modification of the polymers is always of physical nature and not chemical,<sup>[130]</sup> it leads to materials with different properties from the original ones of which they are composed. An example can be given by polystyrene, known for its brittle nature: when rubber is included in its structure a tough material with still good stiffness is produced.

### 12.1.2 Curing process

The term “curing” involves the irreversible transformation of a monomer layer covering a polymer’s surface into a network of oligomers by use of energy or chemical initiators.<sup>[131,132]</sup> (**Figure 12.2**)

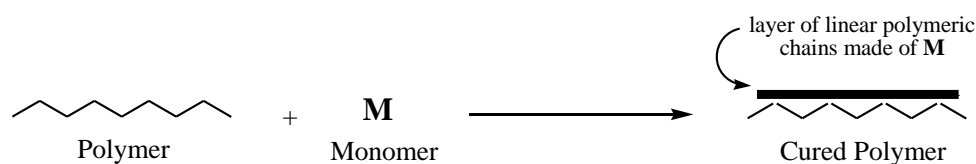


**Figure 12.2:** Schematic representation of curing process.

Monomers are turned into a solid, insoluble and infusible layer. The conversion requires the melting of monomers into a gel state followed by vitrification of the oligomers network.

Curing can involve different approaches:

- Use of curing agents, such as aldehydes or acid anhydrides;<sup>[133,134]</sup>
- Radiation exposure (gamma ray, x-ray, ultraviolet, accelerated electron beams);<sup>[131]</sup>
- Thermal processes (heating by convection, conduction, ultrasonic or with thermal additives).<sup>[131,135]</sup>

Nowadays, the most widespread curing processes for polymer modification are based on thermal curing, despite the fact that its application presents many issues: long process cycles, energy consumption, non-uniform layer thickness.<sup>[131]</sup>

## 12.2 Polymer grafting

Grafting is a method that involves covalent attachment of a molecular moiety, such as a monomer or even a polymer, to a pre-formed polymeric backbone.<sup>[129]</sup> (**Figure 12.3**)



**Figure 12.3:** Schematic representation of grafting process.

Grafting may be achieved with many techniques, the most used is surely chemical graft, but others are known in literature and among these are worthy of mention:<sup>[136,137]</sup> radiation,<sup>[138,139]</sup> photochemical,<sup>[140]</sup> plasma,<sup>[141]</sup> and enzymatic grafting techniques.<sup>[136,137]</sup>

Many methods have been developed to carry out chemical grafting process, such as:<sup>[129,142]</sup>

- Grafting through living polymerization, it provides the possibility to graft directly to polymers surfaces thanks to immobilized radical reaction initiators and to control composition, ramification length and architecture of the final copolymer;<sup>[143-145]</sup>
- By use of ionic initiators, it is a process not widely used due to the stringent reaction conditions required. It finds some applications for grafting co-polymerization, wherein monomers are grafted and then polymerized by cationic or anionic processes;<sup>[146]</sup>
- By use of free radical initiators, it is the most used technique that presents many attractive characteristics such as wide applicability, possibility to functionalize the matrix with various

functional groups (COOH, NH<sub>2</sub>, OH, etc.), easy and inexpensive process, resistance to water and impurities compared to previously reported grafting techniques,<sup>[142,147,148]</sup>

- By use of amidation agents, these compounds have been recently discovered as efficient grafting agents for polymer matrices in amidation reactions to backbone chains.<sup>[124,149]</sup>

Grafting through living polymerization and by use of ionic initiators provide the possibility to synthesize only copolymers and these methods will be no longer considered in this work.

### 12.2.1 Free radical grafting and reactive extrusion (REX)

Until recently, academic studies about chemical grafting has been conducted mainly in solution<sup>[150,151]</sup> or in melting state.<sup>[151,152]</sup> by use of hydroperoxides and metal ions such as Fe<sup>2+</sup>, Cu<sup>+</sup>, Ag<sup>+</sup>, Co<sup>2+</sup>, Cr<sup>3+</sup> and Zn<sup>2+</sup>.<sup>[147,153]</sup> Reactive extrusion, another form of grafting was known, although it was almost completely confined to industrial field and therefore relatively few studies have been published.<sup>[154]</sup> Nowadays, it is common practice to use reactive extrusion in academic studies and many investigations about the topic have been reported for functionalization of many kinds of polymers, such as polyolefines, polylactic acid (PLA) or polyethylene terephthalate (PET).<sup>[148,155,156]</sup>

The term reactive extrusion (REX) refers to a method of chemical reactions for polymers melted with monomers, carried out in continuous process with short residence time, high temperature and in the presence of organic peroxides.<sup>[154]</sup> Such processes are carried out in equipment like torque rheometers, single or twin screw extruders, that allow to run the reaction in conditions at which the organic peroxides, thermally unstable, undergo homolytic cleavage of the oxygen-oxygen bonds to form free radicals. Thus, radicals produced afford hydrogen abstraction from polymer chains,<sup>[157]</sup> forming macroradicals that initiate the grafting process by the reaction with the monomers.<sup>[148]</sup>

One of the most important advantages of reactive extrusion process is to avoid the use of solvent, nevertheless, high temperatures may lead to secondary reactions like  $\beta$ -scissions,<sup>[148]</sup> cross-linking,<sup>[129]</sup> etc., which are known to alter the rheological characteristics of the matrix.<sup>[152]</sup> Moreover, in such conditions, yields are generally lower compared to processes carried out in solution.<sup>[148]</sup>

#### 12.2.1.1 Polypropylene reactive extrusion

Polypropylene (PP) belongs to the group of polyolefins, it is the second most produced polymer in the world after polyethylene (PE).<sup>[158]</sup> PP is a partially crystalline and non-polar thermoplastic polymer, that finds its application, mainly but not only, in packaging and laboratory or medicals

items.<sup>[159]</sup> Compared to polyethylene, the presence of the methyl group leads to higher mechanical and thermal resistances, but it decreases chemical resistance as well. Depending upon molecular weight, type and tacticity, many physical and chemical characteristics of polypropylene may be different. The steric position of CH<sub>3</sub> in the polymer backbone defines tacticity and thus its crystallinity, Glass Transition Temperature (T<sub>g</sub>) and Melting Point (T<sub>m</sub>). For example, in isotactic polypropylene (*i*-PP), methyl groups are all oriented on the same side of the chain, giving an high degree of crystallinity and the highest T<sub>m</sub> for PP.<sup>[160]</sup> (Figure 12.4)

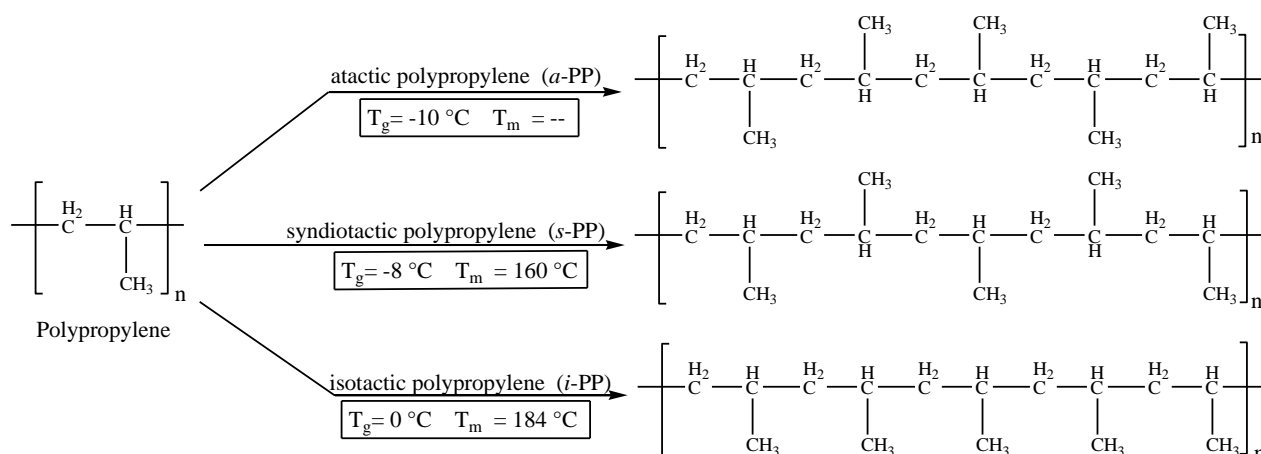


**Figure 12.4:** Changes in Glass Transition Temperature (T<sub>g</sub>) or Melting Point (T<sub>m</sub>) depending on tacticity of PP.

Besides tacticity, properties of PP may depend on possible amount of comonomer present in the chain, this leads to three possible type of polypropylene:<sup>[160]</sup>

- homopolymer, built only of propylene units, it shows higher stiffness and resistance to temperature, but lower impact strength below 0 °C;
- random copolymer (PP-r), it contains from 1.5% to 6% by weight of ethylene (or longer alkenes) with random distribution in the chain. The presence of ethylene leads to a lower degree in crystallinity and thus a lower melting point. PP-r is characterized by improved impact strength, resistance to creasing and improved clarity;
- block copolymer (PP-b), it contains a much higher quantity of PE, that is in a rubbery dispersed phase within the polypropylene matrix, leading to an higher impact strength at low temperatures but at the expense of transparency and softening point.

Demand of polypropylene, although increasing in recent years, is hampered by its non-polar nature, which makes it incompatible with metals, inorganic fillers, and polar polymers.<sup>[152]</sup> Nowadays, the reactive extrusion grafting represents one of the most known and investigated methods for



polypropylene functionalization and many studies have been reported about grafting of maleic anhydride (MA) on PP matrices.<sup>[148,151,152]</sup>

The grafting mechanisms still remain not clearly understood and different reaction pathways have been suggested. Nevertheless, it is generally accepted that grafting is induced by macroradicals, formed by  $\beta$ -scissions of PP chains, that react with MA to give the grafted polymer (PP-g-MA).<sup>[148]</sup> Grafting of maleic anhydride may confer to polypropylene the possibility to interact with substances otherwise incompatible or new reactive sites for further chemical functionalization. For example, recently Kaymakci *et al.* investigated the use of PP-g-MA as wood/polypropylene nanocomposites compatibilizer for the production of wood plastic composites (WPCs),<sup>[161]</sup> while Abbassian *et al.* reported the synthesis of polymer nanocomposites reinforced with carbon nanotubes starting from polypropylene grafting with MA.<sup>[162]</sup>

Grafting of PP is not limited to maleic anhydride, for instance, in a study about flame retardant plastics by Mai *et al.* it is reported the grafting of acrylic acid to polypropylene for the incorporation of aluminium hydroxide as inhibitor of polymer ignition and as smoke suppressant.<sup>[163]</sup>

Polypropylene grafting with acrylic acid has been also reported by Abudonia *et al.* for antimicrobial purposes by chitosan immobilization into the matrix, in the same study, methyl methacrylate is considered as another possible grafting unit for PP.<sup>[164]</sup> Another example of polypropylene functionalization with bioactive properties is reported by Yang *et al.* in a study about PP grafting with zwitterionic polymers for anti-biofouling.<sup>[165]</sup>

#### 12.2.1.2 Polylactic acid reactive extrusion

Polylactic acid, also known as polylactide (PLA), is a linear thermoplastic polyester, produced from renewable resources and reported to be biodegradable.<sup>[166]</sup> It finds applications in many sectors, from packaging materials to medical instruments and 3D printing.<sup>[155,167]</sup> Known since late nineteenth century, application of PLA has spread after the discovery of its synthesis in high molecular weight by lactide ring opening in a catalysed reaction.<sup>[168]</sup> Polylactic acid is an interesting polymer due to its modulable stereochemical structure, that may be easily modified by controlling the ratio of its L- or D- isomers during the polymerization. Indeed, generally PLA is a copolymer constituted by poly(L-lactic acid) (PLLA), which confers crystallinity to the structure, and poly(D,L-lactic acid) (PDLLA), which leads to amorphous polymers. Hence, tacticity, degree of crystallinity and many other important properties, such as Melting Point ( $T_m$ ), are largely controlled by the ratio between the enantiomers and, to lesser extent, by the catalytic system used. (**Figure 12.5**)

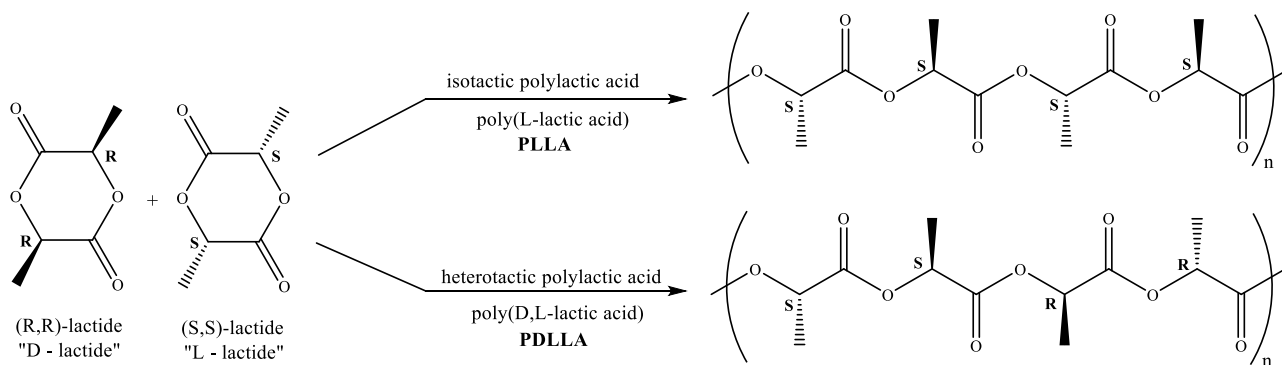


**Figure 12.5:** Tacticities of polylactic acid.

PLA presents many advantages:<sup>[169]</sup>

- Environmental friendly, it is derived from renewable resources, it is biodegradable, recyclable, and compostable. Moreover, the production of PLA consumes carbon dioxide;
- Biocompatibility, PLA does not produce toxic or carcinogenic effects in human tissues and possible chain degradation does not interfere with local tissues healing;
- Processability, it may be processed by many methods such as injection molding, film extrusion, blow molding with better performances compared to other commonly used polymers;
- Energy saving, production of PLA requires 25-55% less energy compared to petroleum-based polymers.

Maleic anhydride (MA) is by far the most commonly used monomer for grafting reactions and studies on PLA functionalization by reactive extrusion are reported. At high temperature, polylactic acid undergoes degradation, thus investigations about chain modification concern complex processes due the presence of simultaneous degradation and chain coupling reactions.<sup>[170]</sup> The first study on this topic is attributed to Carlson *et al.*, who achieved 0.5% wt. degree of grafting.<sup>[171]</sup>

Many applications are reported for grafted PLA, for example, it may be used as compatibilizer in blends with thermoplastic proteins or other biopolymers, resulting in products 100% bioderived.<sup>[155]</sup>

On this purpose, Zhang *et al.* investigated PLA-g-MA for compatibilization of polylactic acid with starch in order to produce eco-friendly composites.<sup>[172]</sup> As reported for polypropylene, grafting of many other monomers and polymers have been tested for PLA functionalization, such as, for example, itaconic anhydride or silk nanocrystals.<sup>[155,170]</sup>

### 12.2.2 Grafting by use of amidation agents

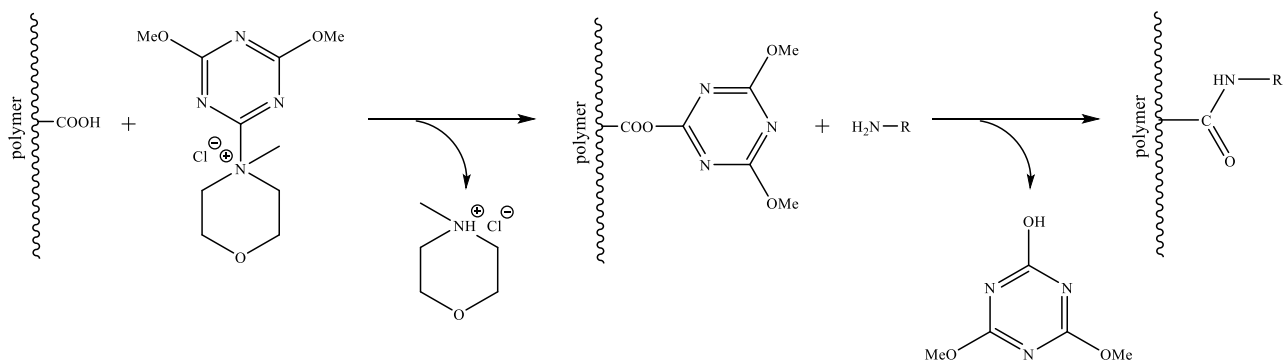
The application of amidation agents has been widely used in coupling reactions for the synthesis of polypeptides in many studies reported in literature.<sup>[5,31]</sup> Besides this kind of application, water soluble agents like *N*-(3-dimethylaminopropyl)-*N*'-ethylcarbodiimide (EDC) and 4-(4,6-dimethoxy-1,3,5-triazin-2-yl)-4-methylmorpholinium chloride (DMTMM), previously described in this work (**Chapter 1.6 and Chapter 1.7**), have been recently discovered as efficient grafting agents for polymer matrices in amidation reactions to the backbone chains.<sup>[124]</sup> D'este *et al.* reported a comparative study about the performance of EDC and DMTMM in hyaluronic acid functionalization with different water soluble moieties. DMTMM is individuated as the best amidation agent due to the higher yields obtained, minor quantity needed and the avoidance of pH control.<sup>[124]</sup>

DMTMM is capable to activate carboxylic groups towards amidation reaction, thus it is a good candidate both for natural and synthetic polymers presenting COOH groups. As example, Labre *et al.* investigated functionalization of alginates in order to improve their resistance to enzymatic activity for cosmetic purposes or as anti-infection agents.<sup>[173]</sup> Yamada *et al.* proposed a study where DMTMM has been used as grafting agent to synthesize starch-*g*-polyethylenimine copolymer for gene delivery vectors in order to reduce cytotoxicity and make the system enzymatically biodegradable.<sup>[174]</sup> Moreover, Thompson *et al.* reported the DMTMM-mediated synthesis of polyacrylamides by functionalization of poly(acrylic acid) with amines such as taurine, ethanolamine and butylamine, achieving yields up to 95%.<sup>[16]</sup>

Finally, 4-(4,6-dimethoxy-1,3,5-triazin-2-yl)-4-methyl morpholinium chloride has been used also on investigations for polymer surface treatments. Saraf *et al.* reported the functionalization of nylon 6,6 with DMTMM for superficial tension modulation. In this study, polymer terminal groups were amidated with different compounds to produce highly hydrophobic or oleophobic nonwoven fabrics.<sup>[175]</sup>

For radiopharmaceutical purposes, drug carriers polymers were instead investigated by Nie *et al.*, which reported a study about the treatment of polylactic acid membrane grafted with glycolic acid and further functionalized by DMTMM for radionuclides encapsulation.<sup>[176]</sup>

Studies like those by Saraf and Nie, in addition to Beghetto's investigation reported previously (**Chapter 7.2.3**),<sup>[125,126]</sup> demonstrated the capability of DMTMM to be active also towards heterogeneous surfaces both as cross-linking and grafting agent. (**Scheme 12.1**)



**Scheme 12.1:** Polymer grafting by DMTMM.

Hence, the idea to combine both grafting by reactive extrusion and DMTMM in a two steps process is interesting. In this way, it would be possible to use reactive extrusion for polymer grafting of carboxylic groups and further functionalization by DMTMM with amine moieties. This process is appealing because it would make possible to use compounds that may be chemically degradable or thermally unstable and thus not suitable for other kind of grafting processes, such as extrusion temperatures or presence of radical species.<sup>[177]</sup>

These compounds may have properties such as antimicrobial activity or ability to modulate polymer surface tension, with interesting application in sectors such as active packaging of food or plastic printing (coating, etc.).<sup>[178]</sup>

## **CHAPTER 13**

### **SCOPE OF THE WORK POLYMER GRAFTING**

This study has been carried out during the abroad research time at Aimplas, Instituto Tecnológico del Plástico located in Valencia, Spain. The scope of this part of PhD thesis is to verify the possibility to develop a protocol for the functionalization of polymers with amide moieties combining grafting by reactive extrusion (REX) and use of 4-(4,6-dimethoxy-1,3,5-triazin-2-yl)-4-methyl morpholinium chloride (DMTMM).

Reactive extrusion is a technique for the functionalization of polymer matrices with moieties such as carboxylic groups and is economically attractive. Nevertheless the individuation of the optimized process is a major challenge.

Grafting by amidation reaction using DMTMM is an appealing surface treatment because it would allow an high selective functionalization of polymers with stable chemical bonds, differently by other known grafting techniques (corona discharge, plasma treatment, migratory additives).<sup>[149]</sup>

The target of this part of the PhD thesis is to optimise the reactive extrusion of polypropylene (PP) and polylactic acid (PLA) for the further treatment with DMTMM for grafting of amide moieties.

In particular the objectives of this work are:

1. Individuation of the optimum conditions of polymer, monomer and peroxide ratio for grafting of PP and PLA;
2. Perform the reactive extrusion using optimum parameters to produce enough quantity of functionalized polymer to proceed with filmation;
3. Perform the surface functionalization with DMTMM and investigate the behaviour of modified polymers in comparison to the original matrices through the study of contact angle.

## **CHAPTER 14**

### **RESULTS AND DISCUSSION POLYMER GRAFTING**

In many processing applications, commercially available polymers do not always possess optimum characteristics in terms of mechanical or chemical properties. Thus, the polymer chain modification is a widely used process, where reactive extrusion (REX) stands out.<sup>[179]</sup>

Recently, another method has been developed for functionalization of polymers with carboxylic acid moieties in water media. 4-(4,6-dimethoxy-1,3,5-triazin-2-yl)-4-methylmorpholinium chloride (DMTMM) is a quaternary ammonium salt, previously illustrated (**Chapter 1.7** and **Chapter 12.2.2**), used as condensing agent in reactions between carboxylic acids and amines for the formation of the corresponding amides.<sup>[19]</sup> (**Figure 3.1**)

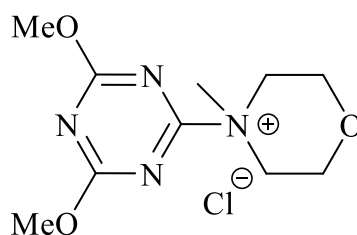
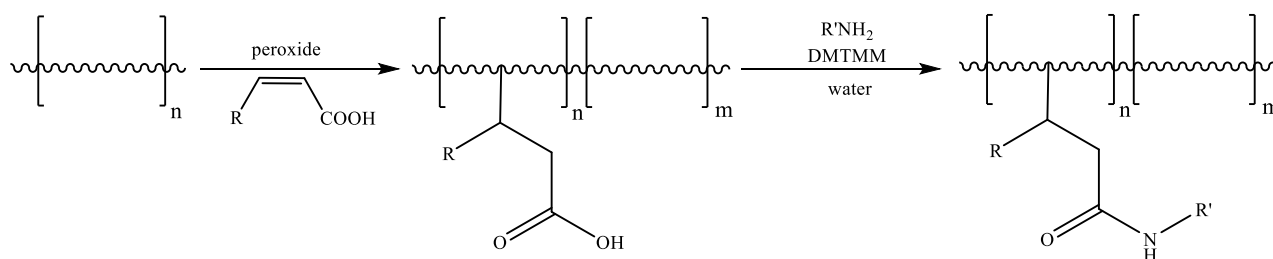


**Figure 14.1:** Chemical formula of 4-(4,6-dimethoxy-1,3,5-triazin-2-yl)-4-methylmorpholinium chloride (DMTMM).

Hence, below are reported the results for polypropylene (PP) and polylactic acid (PLA) functionalization, carried out by a two steps process: first REX extrusion followed by DMTMM as polymer surface grafting agent. (**Scheme 14.1**)



**Scheme 14.1:** Two steps process for polymer functionalization.

## 14.1 Grafting by reactive extrusion (REX)

In recent years, REX has been subject of many studies, first in industry and later by academic purposes. The main reason beyond this success is the characteristic of the extrusion process to carry out chemical reaction, in bulk phase, to produce speciality polymers with high added value.

Thanks to this process it is possible to carry out different reactions such as: bulk polymerisation, interchain copolymerization, grafting reaction, coupling reaction, cross-linking reaction, controlled degradation.<sup>[180]</sup>



The most common method to introduce the functionalities into a polymer substrate by reactive extrusion is the free radical grafting. This process involves the use of different compounds:

- The polymer matrix to be modified;
- A free radical initiator, typically a peroxide;
- The species to be grafted, which could be another polymer or a chemical compound. The latter need to present a double bond functionality in order to be attached to the polymer backbone.

Grafting of polyolefins, such as polypropylene (PP) or polyethylene (PE), has been the object of great interest in the industry due to their good processability and wide use in common life.<sup>[148]</sup> Recently, polylactic acid (PLA, also called polylactide) has been subject of grafting studies, being a biobased and biodegradable polymer.<sup>[155]</sup>

As described, reactive extrusion is carried out in the presence of free radical initiators, agents capable to generate radicals species, usually highly reactive peroxides, such as dicumyl peroxide (DCP). (**Figure 14.2**) DCP decomposes into free radicals at high temperature triggering hydrogen abstraction which initiates radicals on polymer backbone. It is widely used due to its capability to improve mechanical properties and melt strength of the matrix where it is used.<sup>[170]</sup>

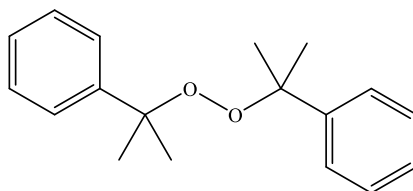
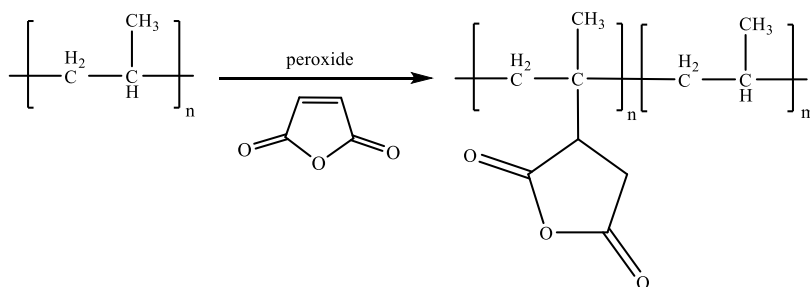


**Figure 14.2:** Chemical formula of dycumil peroxide (DCP).

Despite the great number of studies on the topic, mechanism of grafting is not yet fully understood because it involves many sub-reactions, such as  $\beta$ -scission, cross-linking, dismutation and recombination of the polymer chain as well as homopolymerization and termination reaction between free radicals.<sup>[154]</sup> To simplify, grafting reaction is reported with the mechanism showed below, using a functionalization of polypropylene with maleic anhydride (PP-*g*-MA) as example. (**Scheme 14.2**)



**Scheme 14.2:** Grafting mechanism for synthesis of PP-*g*-MA.

As reported by Jeziórska, optimization of grafting reactions in reactive extrusion depends by a large number of factors: different ratio between polymer, monomer and initiator or changes in residence time, reaction temperature and speed of extruder screws may lead to great differences in the final product, maximising grafting yields or minimizing side reactions for example.<sup>[154]</sup> In the case of maleic anhydride grafting, Berzin *et al.* reported a study about the importance of peroxide and monomer concentrations, indeed changing quantity of monomer or free radicals produced may lead to great difference in rheological characteristic, measured by Melt Flow Index (MFI), other than in chemical properties.<sup>[148]</sup>

Moreover, it is known that grafting may modify glass transition temperature ( $T_g$ ), melting temperature ( $T_m$ ), crystallinity and thermal stability, as the polymer matrix is modified.<sup>[155]</sup> Thanks to DSC analysis, changes in degree of crystallinity ( $\chi_c$ ), expressed as percentage, may be easily calculated by application of this formula:

$$\chi_c = \frac{\Delta H_m - \Delta H_{cc}}{\Delta H_{ref}}$$

Where  $\Delta H_m$  and  $\Delta H_{cc}$  are the heat of fusion corresponding to melting (m) and cold crystallization (cc), if present, of the DSC heating thermogram. While,  $\Delta H_{ref}$  is the theoretical enthalpy related to melting process of a polymer sample 100% crystalline, this value is reported as 209.2 J/g for isotactic polypropylene and 93.1 J/g for polylactic acid.<sup>[181,182]</sup>

Below, the results obtained by REX functionalization are reported. Polypropylene is grafted with fumaric acid (FMA) and linoleic acid (LNA), therefore, respectively polypropylene-*grafted*-fumaric acid (PP-*g*-FMA) and polypropylene-*grafted*-linoleic acid (PP-*g*-LNA) are produced. In the same way polylactic acid (PLA) is functionalized by grafting with the same chemicals in order to synthesize polylactide-*grafted*-fumaric acid (PLA-*g*-FMA) and polylactide-*grafted*-linoleic acid (PLA-*g*-LNA).

All functionalized polymers have been investigated using both an HAAKE and a Brabender Plasticorder (BBP) extruders. HAAKE instrument allows to extrude small amounts of polymer (7 g) presenting yet a reduced quantity of final product recovery (ca. 50% wt.) due to its structure. Instead, BBP extruder allows to run experiment with quantities between 30-100 grams of polymer depending on the matrix viscosity and allowing an increased recovery of the final product (ca. 75% wt.).

### 14.1.1 REX grafting of polypropylene

Polypropylene is a non-polar thermoplastic polymer with high processability, commonly used in REX grafting reactions for functionalization with many different chemicals, where maleic anhydride (MA) stands out.

In this work a random copolymer (PP-r) is used, where the polyethylene content is below 6% by weight.<sup>[160]</sup> Presence of ethylene decrease crystallinity and melting point of the polymers, moreover it offers good thermal and mechanical properties and chemical resistance along with transparency. Nevertheless, Heinen *et al.* reported that the ethylene units are disfavoured to grafting reaction compared to polypropylene units.<sup>[183]</sup> Heinen indeed reported that the tertiary carbon of polypropylene units is by far the most favoured site for grafting. Hence, as ethylene does not almost participate in the grafting reaction, from now on in this work, random copolymer (PP-r) is reported as pure polypropylene to simplify scheme reactions.

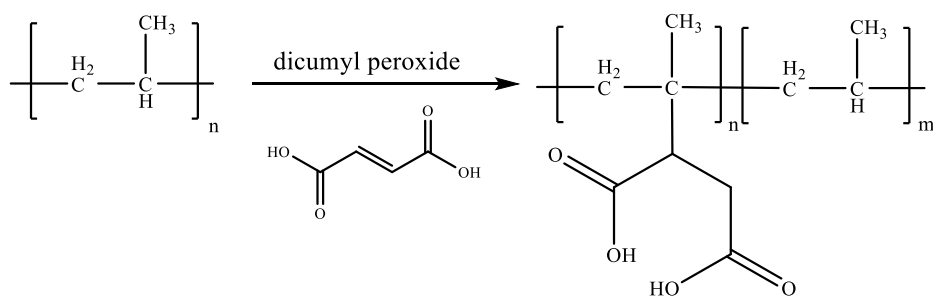
#### 14.1.1.1 Polypropylene-grafted-fumaric acid (PP-g-FMA)

Polyolefins modified by grafting functionalization with polar groups in their chain are commonly investigated for improvement of chemical-physical properties. As reported by De Vito *et al.*,<sup>[184]</sup> 1,2-disubstituted alkenes present low tendency to homopolymerization compared to other monomers, such as vinyl groups, thanks to steric hindrance associable to the double bond.

Fumaric acid (FMA), or *trans*-butenedioic acid, is an unsaturated dicarboxylic acid used as food additive,<sup>[185]</sup> which makes an excellent candidate for polyolefins functionalization with COOH groups.<sup>[186]</sup>

In a patent by the finnish company Neste Oyj, fumaric acid is used as grafted monomers with polyethylene and other olefins copolymers, achieving interesting results in terms of chemical-physical properties of the final product. Moreover, FMA is reported to show an higher graft efficiency and to be suitable for foodstuff compatibility.<sup>[187]</sup>

Below, the synthesis of polypropylene-grafted-fumaric acid (PP-g-FMA) is reported. The optimization of REX reaction has been investigated by polymer, monomer and initiator ratio modulation, keeping constant residence time (t), reaction temperature (T) and screws speed (v).  
(Scheme 14.3)



**Scheme 14.3:** Grafting reaction of PP-g-FMA.

The reaction was carried out at 220 °C, with a residence time of 30 minutes and a screws speed of 60 rpm in a HAAKE extruder. The average polymer recovery was ca. 50% in weight, samples were purified as reported in literature<sup>[188]</sup> and characterized by ATR FT-IR, DSC and TGA.

In **Table 14.1** are summarized all the experiments carried out at different conditions and the corresponding values of TGA and DSC analyses.

**Table 14.1:** Synthesis of PP-g-FMA at different PP/FMA/DCP ratios and related TGA, DSC and ATR FT-IR values.

Run	PP <sup>(a)</sup> (g)	FMA <sup>(a)</sup> (% wt.)	DCP <sup>(a)</sup> (% wt.)	TGA <sup>(b)</sup>			DSC <sup>(c)</sup>				
				T <sub>d</sub> (°C)	T <sub>5</sub> (°C)	T <sub>50</sub> (°C)	T <sub>m</sub> (°C)	ΔH <sub>m</sub> (J/g)	T <sub>c</sub> (°C)	ΔH <sub>c</sub> (J/g)	χ <sub>c</sub> <sup>(d)</sup> (%)
PP	7	-	-	336	432	465	147	42.8	90	- 59.2	20.4
1	7	1	0.25	206	422	469	146	44.6	99	- 60.0	21.3
2	7	5	0.25	204	421	470	146	42.8	102	- 58.4	20.5
3	7	10	0.25	203	418	467	147	41.9	103	- 56.9	20.0
4	7	10	1	203	419	465	147	40.4	101	- 53.4	19.3
5	7	20	1	204	422	466	145	39.7	101	- 52.0	19.0

Reaction conditions: temperature 220 °C, residence time 30 min., screws speed 60 rpm;

(a) reagents used are: polypropylene (PP), fumaric acid (FMA), dycumil peroxide (DCP).

(b) TGA analysis conditions: sample ca. 20 mg. Temperature programme: first heating cycle from 50 °C to 800 °C at 20 °C/min under N<sub>2</sub> atmosphere; isotherm at 900 °C for 15 minutes; cooling cycle at 30 °C/min until 450 °C under N<sub>2</sub> atmosphere, second heating cycle from 450 °C to 900 °C at 20 °C/min under air atmosphere.

(c) DSC analysis conditions: sample ca. 8 mg. Temperature programme: first heating cycle from 20 °C to 200 °C at 20 °C/min; isotherm at 200 °C for 5 minutes; cooling cycle at 20 °C/min until 20 °C; second heating cycle from 20 °C to 200 °C at 20 °C/min.

(d) degree of crystallinity (χ<sub>c</sub>) has been calculated with a ΔH<sub>ref</sub> of 209.2 J/g, corresponding to the theoretical melting enthalpy of a totally crystalline isotactic polypropylene sample.<sup>[181]</sup>

Thanks to DSC characterization (**Figure 14.3**), it was possible to confirm the grafting of FMA onto polypropylene chain, below it is reported a comparison between virgin PP and PP-g-FMA (Run 4).

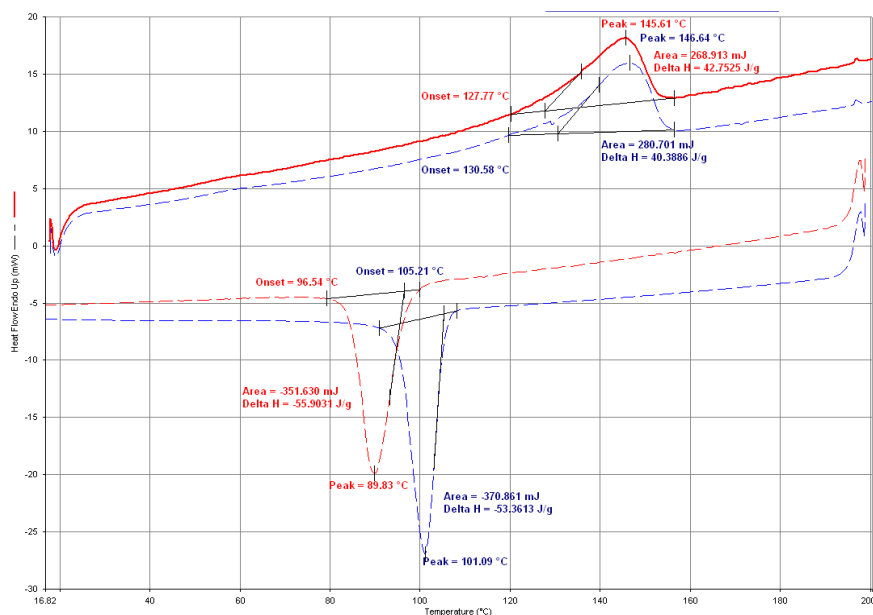


**Figure 14.3:** Comparison between DSC thermogram of virgin PP (red) and PP-g-FMA (blue).

In DSC thermogram (**Figure 14.3**), it is possible to observe that in the cooling cycles (bottom), crystallization ( $T_c = 101\text{ }^\circ\text{C}$ ) for PP-g-FMA occurs at higher temperatures compared to virgin PP ( $90\text{ }^\circ\text{C}$ ). Compared to the virgin polymer, differences in  $T_c$  are observable for all Runs of **Table 14.1**, while  $\Delta H$  and  $\chi_c$  are comparable. The changes in  $T_c$  are attributable to the presence of grafted fumaric acid. Crystallization processes involve kinetic and thermodynamic parameters: grafted species may interact both chemically and physically with polymeric lamellae. The influence on the progressive thickening of crystallized structures leads to differences in energy released (lower  $\Delta H$  modulus) or in temperatures.<sup>[189]</sup> A similar result is achieved by Sathe *et al.*, a higher crystallization temperature ( $T_c$ ) is reported for functionalized isotactic polypropylene and attributed to the action of grafted maleic anhydride as nucleating agent.<sup>[181]</sup>

DSC analyses of Runs 2, 3 and 5 of **Table 14.1** showed the presence of unreacted monomer, referred as blended fumaric acid, and needed further purification. Thus, values paragonable to the results obtained with lesser monomer content has been observed in the new DSC analyses. It is possible to assume that the optimal quantities for polypropylene REX extrusion require a monomer:initiator ratio lower than 20:1, in order to avoid the presence of blended monomer. Hence, for this reason, only Run 1 and Run 4 are further investigated.

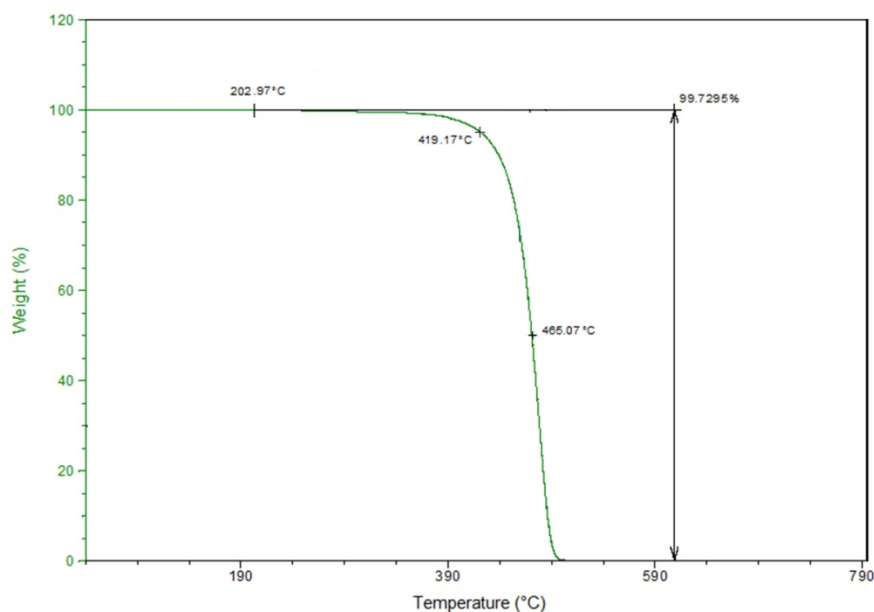


**Figure 14.4:** TGA thermogram of PP-g-FMA with PP/FMA/DCP ratio of 100/10/1.

In TGA thermogram (**Figure 14.4**), it is possible to observe the thermal decomposition of PP-g-FMA of Run 4 (**Table 14.1**), similar values have been obtained for Run 1 as well. In the curve are reported the temperature at which the polymer starts to degrade ( $T_d= 203$  °C), in addition to the temperatures of 5% ( $T_5= 419$  °C) and 50% ( $T_{50}= 465$  °C) of degradation. Compared to PP-g-FMA, virgin polypropylene presents a comparable  $T_{50}$ , while other values occur at higher temperatures ( $T_d= 336$  °C and  $T_5= 432$  °C)

Differences in these temperatures are attributable to the mechanism of chain-stripping, in which atoms or groups not part of the polymer chain are cleaved during the heating cycle. The bonds breaking process occurs at lower temperatures compared to backbone bonds cleaving mechanisms and is attributable to the presence of grafted species.<sup>[190]</sup>

Differently to what reported in literature, it has been surprising to observe that virgin PP and PP-g-FMA present very similar  $T_{50}$ . Sathe *et al.* reported that in the grafting of maleic anhydride to isotactic polypropylene,  $T_{50}$  increased with percentage of MA grafting.<sup>[181]</sup> This effect does not occur in the synthesis of PP-g-FMA, where  $T_{50}$  are practically unchanged in all collected analyses of **Table 14.1**. This may be attributed to reactive differences between maleic anhydride and fumaric acid combined to the occurrence of  $\beta$ -scissions in the backbone chain during REX reaction. However, additional investigations are necessary to clarify the significance of these tendencies as well as to confirm the proposed explanation.

Finally, ATR FT-IR characterization led to appreciable results only for Run 4 (**Figure 14.5**) and Run 5. It is possible that samples of Runs from 1 to 3 present a fumaric acid amount in quantity too reduced to be observable in ATR FT-IR spectroscopy due to the detection limits of the instrument.

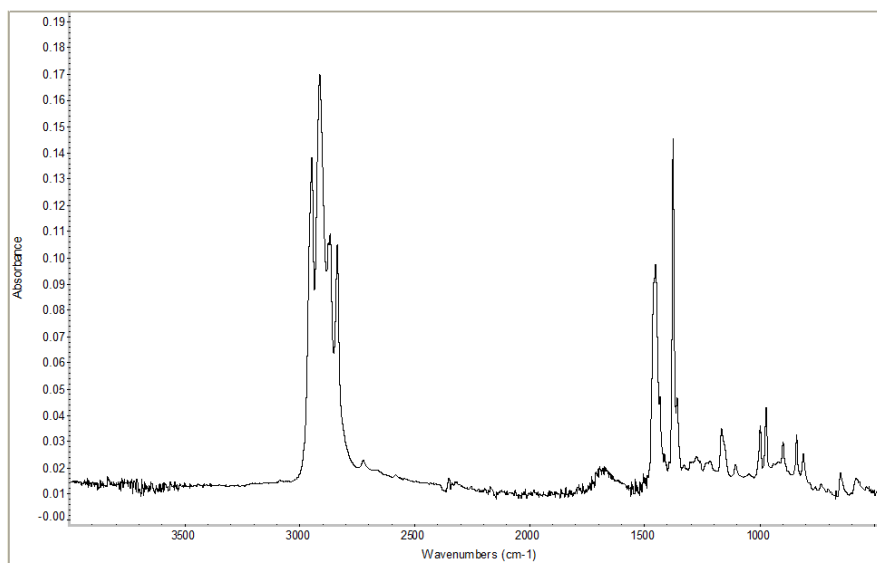


**Figure 14.5:** ATR FT-IR spectrum of PP-g-FMA with PP/FMA/DCP ratio of 100/10/1.

ATR FT-IR ( $\text{cm}^{-1}$ ): 2950, 2915, 2838, 1685, 1455, 1377, 1166, 997, 972, 840, 808.

In ATR FT-IR spectrum (**Figure 14.5**), it is possible to observe signals typical of polypropylene<sup>[191]</sup> and a large absorption peak at  $1685 \text{ cm}^{-1}$  of weak intensity, attributable to C=O stretching of fumaric acid. Reduced intensity for moieties signals is typical of grafted species due to the efficiency of the process for which is usually reported a functionalization of 0.1-1%.<sup>[162,181]</sup>

Even if grafting processes commonly reported in literature use a content in monomer and free radical initiator comparable to the quantities reported for Run 1,<sup>[192,181]</sup> characterization by ATR FT-IR has been considered of great importance and for this reason protocol reported for Run 4 has been favoured, considering that grafting by DMTMM is a surface treatment.

Thanks to good results achieved in REX reaction for synthesis of PP-g-FMA with HAAKE extruder, it has been decided to increase the quantities of polymer treated using a different extruder. Brabender plasticorder (BBP) is an extruder used for both industrial and academic studies.<sup>[188, 192]</sup>

The usual capacity of BBP is 30-100 grams, due to polypropylene viscosity, in this case ca. 40 g of reagents have been used. Thanks to BBP structure and better efficiency, PP-g-FMA extrusion led to a polymer recovery of 75% in weight. Moreover, it was possible to reduce the residence time to 15 minutes and it was possible to record the torque applied on the screws to keep constant their rotatory speed. This may give an idea of the rheological behaviour of the polymer during the

process and the effect of fumaric acid in grafting reaction. (**Figure 14.6**) Samples have been purified and characterized by ATR FT-IR, DSC and TGA, achieving results paragonable to products extruded by HAAKE in the same conditions. (**Chapter 16.2.1.1**)

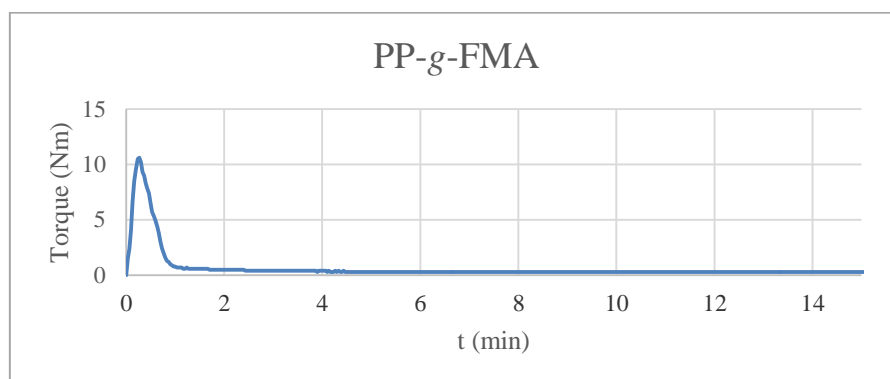


**Figure 14.6:** Comparison graph of torque vs residence time for PP-g-FMA in BBP extruder.

In the graph (**Figure 14.6**), it is possible to notice that the torque applied to keep 60 rpm speed for the screws drops close to zero, at the end of the process the torque value is 0.4 Nm. This effect may be attributed both to the occurrence of  $\beta$ -scissions reactions and to the presence of fumaric acid which make the polymer more fluid. Indeed in the same reaction conditions, grafting of maleic anhydride, carried out as comparison to synthesize PP-g-MA, led to a torque value of 4.6 Nm, while for virgin polypropylene extruded without monomers or DCP, torque value was 5.6 Nm. It may therefore be assumed that, even if  $\beta$ -scissions reactions occur during the process, the presence of fumaric acid strongly influences the viscosity of the polymer.

Finally, PP-g-FMA has been filmed with an hot platen press for the second reaction step with DMTMM and to perform surface analysis. (**Chapter 14.2**)

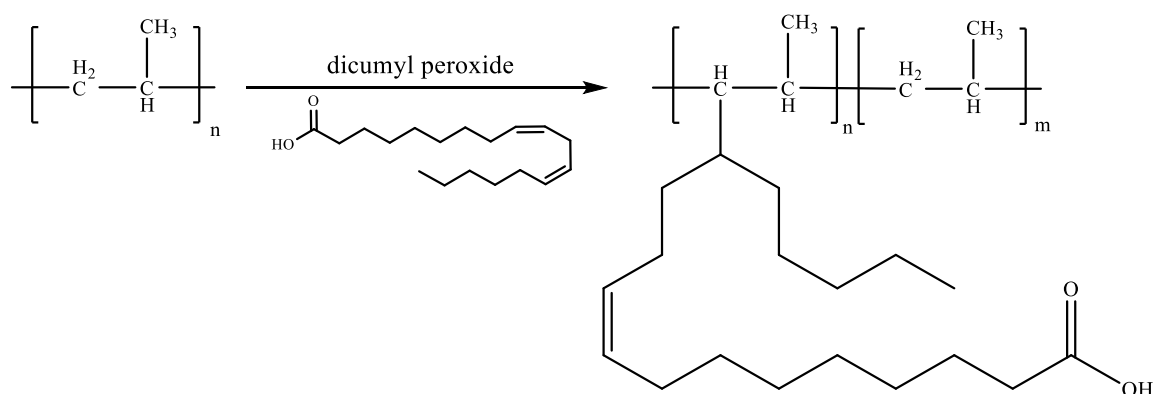
#### 14.1.1.2 Polypropylene-grafted-linoleic acid (PP-g-LNA)

Linoleic acid is an essential polyunsaturated omega-6 fatty acid, its properties as antimicrobial has been investigated in many studies,<sup>[193,194]</sup> also for food applications.<sup>[195]</sup> LNA can be found in many natural byproducts, such as almond shells,<sup>[196]</sup> used in many studies to produce green composites blends for enhancement of mechanical properties with recycling purposes. Few studies have been reported about grafting of linoleic acid on polymeric matrices. Recently, Çakmakli *et al.* for poly(methylmethacrylate) and Alli *et al.* for poly(*N*-isopropylacrylamide) studied the characteristic autooxidation of mixtures of LNA and similar fatty acids for preparation of polymeric oil peroxy initiators and their direct application. The process needs the fatty acids to be left in oxygenated environment and under sunlight for long time, before being directly grafted onto the polymer matrix without further use of radical initiator.<sup>[199,200]</sup>



To the best of our knowledge, only one study is reported about the reactive extrusion onto a polypropylene matrix for grafting of glycerol trilinoleate, a derivated triglyceride of linoleic acid. Xie *et al.* achieved interesting results for mechanical properties of the final product and observed a reduction in  $\beta$ -scissions reactions during the grafting process, possibly attributed to the high number of double bonds present in the tryglyceride.<sup>[201]</sup>

The synthesis of polypropylene-*grafted*-linoleic acid (PP-*g*-LNA) has been carried out reacting PP with 10% wt. of LNA and 1% of DCP in a HAAKE extruder, at 220 °C with a residence time of 30 minutes and a screws speed of 60 rpm. (**Scheme 14.4**)



**Scheme 14.4:** Grafting reaction of PP-*g*-LNA.

The recovery of polymer was 40% in weight, the sample has been purified as reported in literature<sup>[188]</sup> and characterized by ATR FT-IR, DSC and TGA analyses.

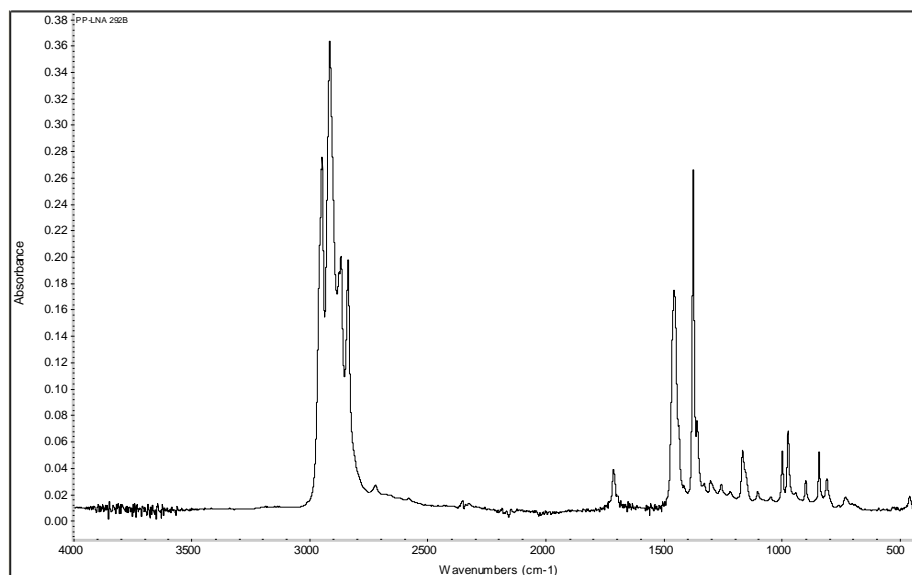


**Figure 14.7:** ATR FT-IR spectrum of PP-*g*-LNA.

ATR FT-IR ( $\text{cm}^{-1}$ ): 2950, 2915, 2838, 1712, 1455, 1377, 1166, 997, 972, 840, 808.

In ATR FT-IR spectrum (**Figure 14.7**), it is possible to observe signals typical of polypropylene and at  $1712\text{ cm}^{-1}$  a signal attributable to C=O stretching of linoleic acid groups.<sup>[191]</sup>

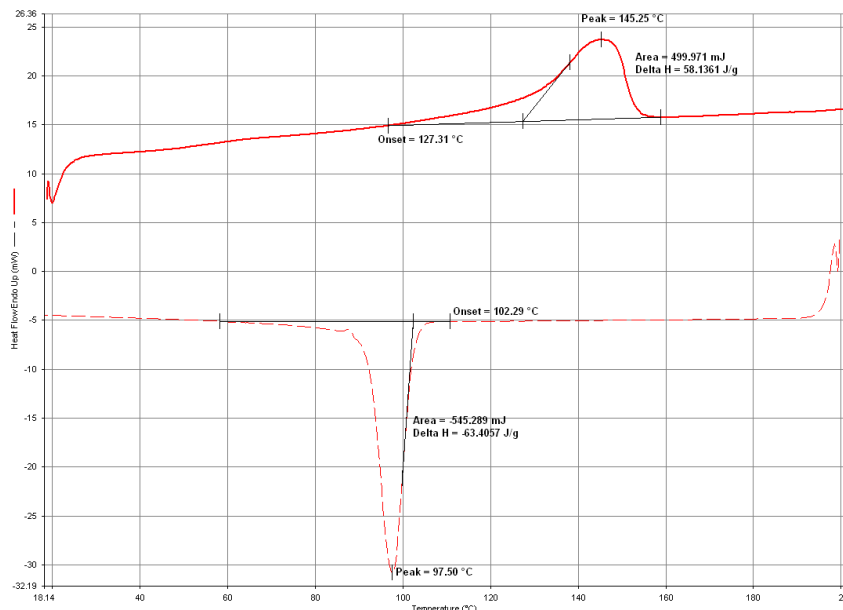


**Figure 14.8:** DSC thermogram of PP-g-LNA.

In DSC thermogram of PP-g-LNA (**Figure 14.8**), crystallization of the grafted polymer ( $T_c=98\text{ °C}$ ) occurs at higher temperature compared to virgin PP ( $T_c=90\text{ °C}$ ). Similarly to what reported for PP-g-FMA (**Chapter 14.1.1.1**), this may be attributed to grafted moieties interacting with the polymeric lamellae during the crystallization process.<sup>[181,189]</sup> Moreover, PP-g-LNA calculated degree of crystallization ( $\chi_c=27.8\%$ ) presents values slightly higher of virgin PP ( $\chi_c=20.4\%$ ), possibly attributable to the presence of linoleic acid in the extrusion process.

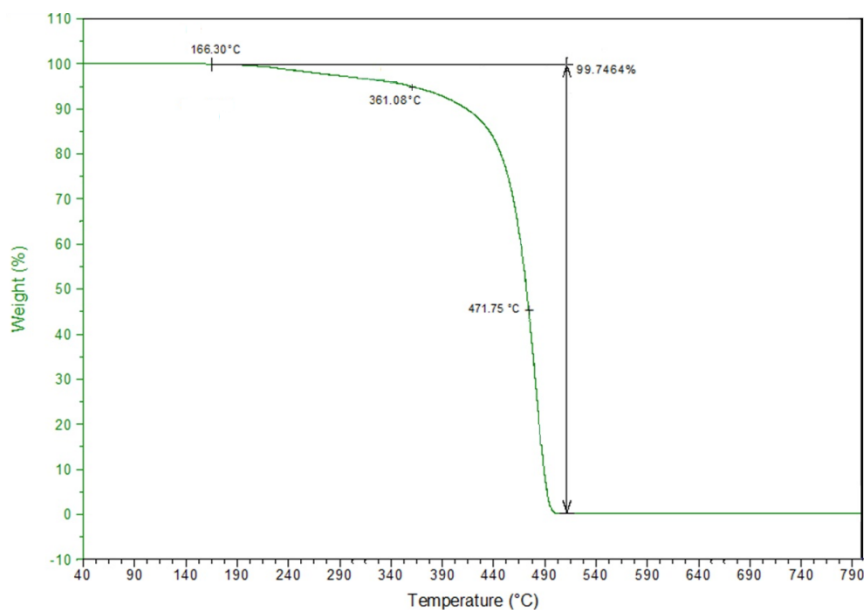


**Figure 14.9:** TGA thermogram of PP-g-LNA.

In TGA thermogram (**Figure 14.9**) the thermal decomposition of PP-g-LNA is reported, where it is possible to observe that the degradation temperatures of grafted polymer ( $T_d = 166\text{ }^\circ\text{C}$ ,  $T_5 = 361\text{ }^\circ\text{C}$ ,  $T_{50} = 472\text{ }^\circ\text{C}$ ) occur at lower values compared to virgin PP ( $T_d = 336\text{ }^\circ\text{C}$ ,  $T_5 = 432\text{ }^\circ\text{C}$ ,  $T_{50} = 465\text{ }^\circ\text{C}$ ). These results are attributable to the presence of grafted linoleic acid. Indeed, it is possible that due to chain-stripping mechanism polymer degradation starts at lower temperatures.<sup>[190]</sup>

In literature, linoleic acid and other compounds derived from linseed oil are known for their capability to naturally cross-link.<sup>[196,199]</sup> Moreover, as observed by Xie *et al.*, grafting of linoleic acid derivatives caused reduced  $\beta$ -scission reactions.<sup>[201]</sup> It is possible that for this reasons the polymer backbone shows extra stability and  $T_{50}$  occurs at slightly higher temperatures.

Similarly to what has been done for PP-g-FMA (**Chapter 12.1.1.1**), also synthesis of PP-g-LNA has been carried out in a Brabender plasticorder (BBP) extruder. Grafted polymer recovery was 93% in weight, also in this case residence time could be reduced to 15 minutes and the rheological behaviour of the polymer during the process has been recorded. (**Figure 14.10**) Samples have been purified and characterized by ATR FT-IR, DSC and TGA, achieving results paragonable to products extruded by HAAKE in the same conditions. (**Chapter 16.2.1.2**)

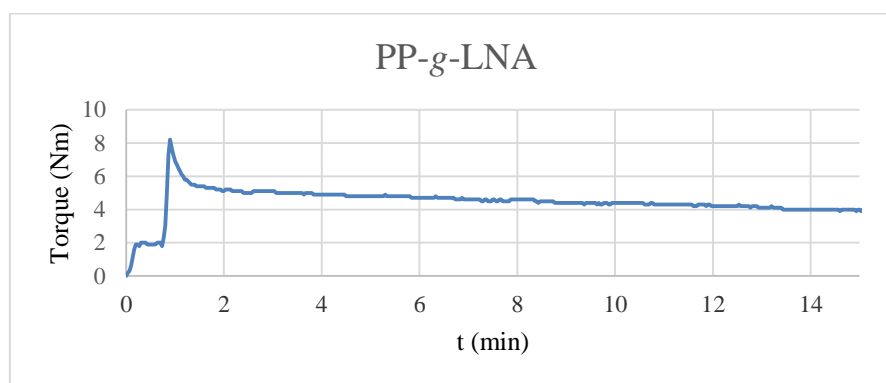


**Figure 14.10:** Comparison graph of torque vs residence time for PP-g-LNA in BBP extruder.

In the graph (**Figure 14.10**), it is possible to observe that after 15 minutes of reaction the torque applied on the screws by PP-g-LNA is 4.0 Nm. Differently to what has been recorded for PP-g-FMA, the value is closer to the initial viscosity of virgin PP (5.6 Nm). This behaviour may be attributed to reduced  $\beta$ -scissions reaction occurred in the grafting process, as reported by Xie *et al.*, and to the presence of linoleic acid which influences rheological properties of the matrix.<sup>[201]</sup> Additional studies will be necessary in order to clarify the significance of these tendencies as well as to confirm the proposed explanations.

Finally, PP-g-LNA has been filmed with an hot platen press for the second reaction step with DMTMM and to perform surface analysis. (**Chapter 14.2**)

### 14.1.2 REX Grafting of polylactic acid

Poly(lactic acid) presents many advantages, being a biobased, biodegradable, compostable and recyclable resource. Moreover, thanks to its good mechanical properties and transparency PLA is a good candidate as substitute of petrol based polymers. Nevertheless, due to its fragility and low heat deflection temperature, blending of PLA with other composites could be a good solution to these drawbacks. However, it is necessary to graft the polylactide to achieve an acceptable blend compatibility.<sup>[202]</sup>

It is important to highlight that PLA may undergo thermal degradation above 200 °C due to hydrolysis or chain breaking processes, lactide reformations or transesterification reactions. Thus, extrusion processing temperatures shall not exceed 185-190 °C.<sup>[182]</sup> Moreover, grafting efficiency on PLA is reduced compared to other polyesters, due to its limited reactivity.<sup>[155]</sup>

The mechanical properties and crystallization of polylactide are largely dependent on the isomers used to synthesize it. (**Chapter 12.2.1.2**)

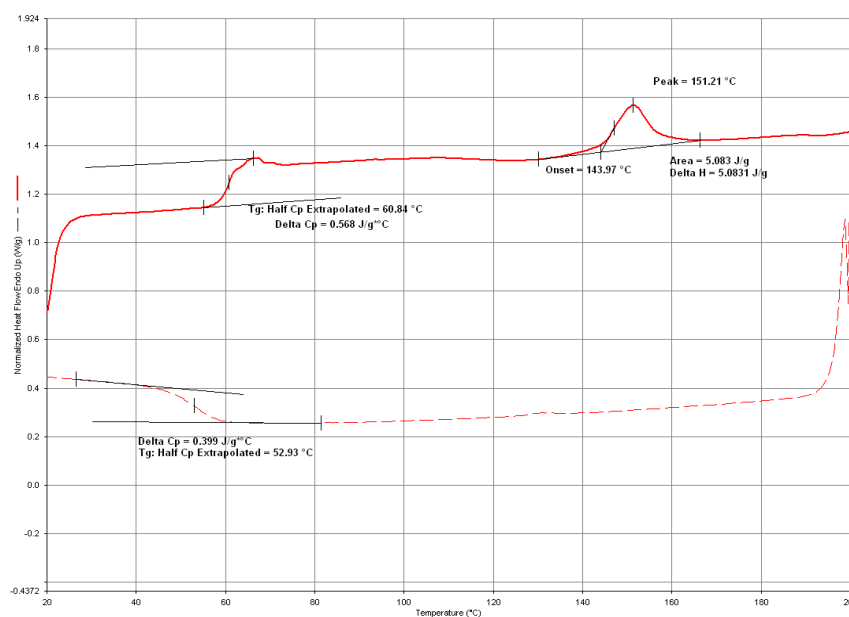


**Figure 14.11:** DSC thermogram of virgin PLA.

Above it is reported the DSC thermogram of the virgin PLA used in this work. (**Figure 14.11**) It presents a glass transition temperature ( $T_g$ ) at 61 °C and a melting temperature ( $T_m$ ) at 151 °C.

It is important to highlight that in DSC thermograms of functionalized polylactides after REX processes, the glass transition temperature undergoes an endothermic energy increase, this phenomenon is called relaxation enthalpy ( $\Delta H_{rlx}$ ). Polymers that have been cooled rapidly are prevented to find chain energetically favourable orientations and are, therefore, in a non-equilibrium

state when maintained below their glass transition temperature. Relaxation enthalpy leads thus to a significant interference on  $T_g$  measurements, due to modification in heat capacity of the transition.<sup>[203]</sup>

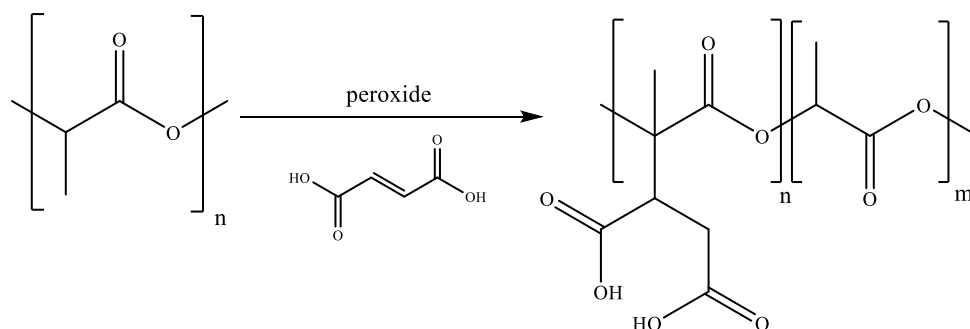
#### 14.1.2.1 Polylactic acid-grafted-fumaric acid (PLA-g-FMA)

Poly lactide grafting has been extensively investigated in the last years mainly with maleic anhydride (MA).<sup>[171,202,204]</sup> Zhang *et al.* reported that the production of a polylactide composites with starch has been possible only thanks to compatibility achieved by grafting of maleic anhydride.

To the best of our knowledge, few studies are reported about PLA grafting with monomers different from MA. Marsilla *et al.* investigated polylactic acid functionalization by grafting of itaconic anhydride, leading to a reduction in  $T_g$  and an increase in crystallinity.<sup>[155]</sup>

As reported by Detyothin *et al.*,<sup>[202]</sup> REX grafting on polylactic acid may be optimized by modulation of many different parameters. Similarly for what it has been reported for polypropylene (**Chapter 14.1.1.1**), fumaric acid (FMA) has been selected as monomer for grafting and the best ratio between reagents has been investigated.

Below, the synthesis of polylactic acid-grafted-fumaric acid (PLA-g-FMA) is reported. Different ratios between polymer, monomer and initiator have been tested, keeping constant residence time (t), reaction temperature (T) and screws speed (v). (**Scheme 14.5**)



**Scheme 14.5:** Grafting reaction of PLA-g-FMA.

The reaction was carried out at 180 °C, with a residence time of 30 minutes and a screws speed of 60 rpm in a HAAKE extruder. The average polymer recovery was ca. 50% in weight, purification of the samples was carried out by extraction with  $\text{CH}_2\text{Cl}_2$ , similarly to what reported in literature.<sup>[155]</sup> Finally, the purified samples have been characterized by ATR FT-IR, DSC and TGA.

In **Table 14.2** are reported all the tests carried out at different polymer, monomer and initiator ratios and in **Table 14.3** the corresponding values of TGA and DSC analyses.

**Table 14.2:** Synthesis of PLA-g-FMA at different PP/FMA/DCP ratios.

Run	PLA <sup>(a)</sup> (g)	FMA <sup>(a)</sup> (% wt.)	DCP <sup>(a)</sup> (% wt.)
PLA	7	-	-
1	7	1	0.25
2	7	5	0.25
3	7	10	0.25
4	7	5	0.5
5	7	10	0.5

Reaction conditions: temperature 180 °C, residence time 30 min., screws speed 60 rpm;

(a) reagents used are: polylactic acid (PLA), fumaric acid (FMA), dycumil peroxide (DCP).

**Table 14.3:** PLA-g-FMA values registered by TGA and DSC analyses.

Run	TGA <sup>(a)</sup>			DSC <sup>(b)</sup>						
	T <sub>d</sub> (°C)	T <sub>5</sub> (°C)	T <sub>50</sub> (°C)	T <sub>g</sub> (°C)	ΔH <sub>rlx</sub> (J/g)	T <sub>cc</sub> (°C)	ΔH <sub>cc</sub> (J/g)	T <sub>m</sub> (°C)	ΔH <sub>m</sub> (J/g)	χ <sub>c</sub> <sup>(c)</sup> (%)
PLA	282	340	389	61	-	-	-	151	5.1	5.5
1	124	342	390	66	8.6	-	-	148	2.9	3.1
2	121	344	393	66	8.6	-	-	150	12.0	12.9
3	119	339	392	66	8.6	-	-	151	17.5	18.8
4	112	341	376	62	7.0	113	-17.5	149	23.4	6.3
5	114	343	376	66	7.0	112	-14.8	150	25.8	11.8

(a) TGA analysis conditions: sample ca. 20 mg. Temperature programme: first heating cycle from 50 °C to 800 °C at 20 °C/min under N<sub>2</sub> atmosphere; isotherm at 900 °C for 15 minutes; cooling cycle at 30 °C/min until 450 °C under N<sub>2</sub> atmosphere, second heating cycle from 450 °C to 900 °C at 20 °C/min under air atmosphere;

(b) DSC analysis conditions: sample ca. 8 mg. Temperature programme: first heating cycle from 20 °C to 200 °C at 20 °C/min; isotherm at 200 °C for 5 minutes; cooling cycle at 20 °C/min until 20 °C; second heating cycle from 20 °C to 200 °C at 20 °C/min;

(c) Degree of crystallinity (χ<sub>c</sub>) has been calculated with a ΔH<sub>ref</sub> of 93.1 J/g, corresponding to the theoretical melting enthalpy of a totally crystalline PLA sample.<sup>[182]</sup>

In TGA data (**Table 14.3**), it may be observed that T<sub>5</sub> and T<sub>50</sub> values are comparable with virgin PLA (T<sub>5</sub>= 340 °C, T<sub>50</sub>= 389 °C) for Runs from 1 to 3. Instead, in thermogram of Run 4 (**Figure 14.12**) and Run 5, T<sub>50</sub> occurs at lower temperatures (376 °C).

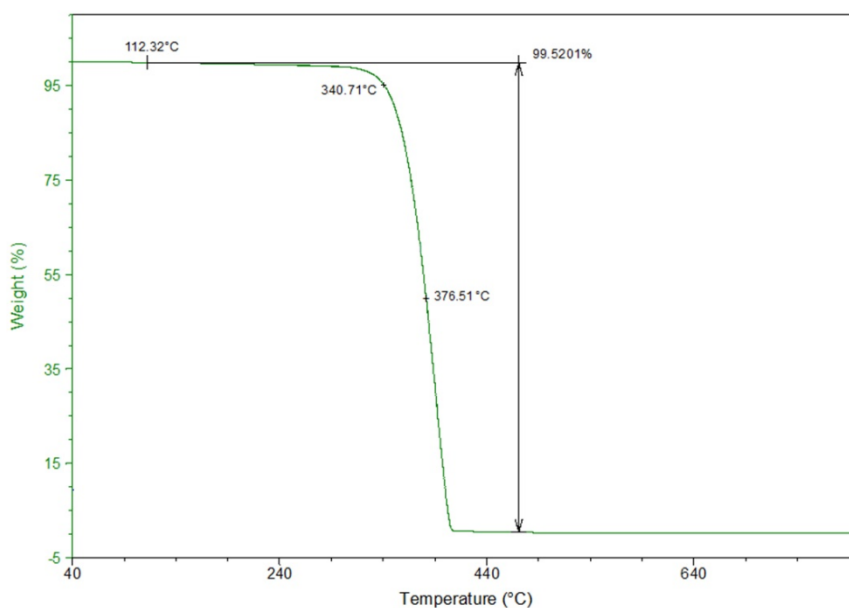


**Figure 14.12:** TGA thermogram of PLA-g-FMA with PLA/FMA/DCP ratio of 100/5/0.5.

As proposed by Carlson *et al.*,<sup>[171]</sup> during REX maleation (PLA with peroxide and MA), reactions possibly occurring are radical induced grafting,  $\beta$ -scission, cross-linking and thermo-hydrolysis, in addition to monomer homopolymerization.

In TGA thermogram of Run 4 (**Figure 14.12**) and Run 5, the decrease of  $T_{50}$  is possibly attributable to  $\beta$ -scission reactions which occur more frequently due to the higher quantity of peroxide used, as reported by Detyothin *et al.* for maleic anhydride grafting.<sup>[202]</sup>

All Runs present a decreased  $T_d$  compared to virgin PLA ( $T_d = 282$  °C), this value is further reduced for Run 4 ( $T_d = 112$  °C) and Run 5. This is possibly attributable to the limited reactivity of polylactide which leads to a poor grafting efficiency,<sup>[155]</sup> decreasing the  $T_d$  (due to chain stripping mechanism) without affecting  $T_5$  due to the reduced number of grafted species present.<sup>[190]</sup> However, titration tests will be necessary in order to confirm the proposed explanations.

In **Table 14.3**, it is possible to observe how changes in ratio of polymer, monomer and initiator ratios lead to variations of values measured by DSC analyses, such as degree of crystallinity ( $\chi_c$ ), and transitions attributable to relaxation enthalpy ( $\Delta H_{rlx}$ ) or cold crystallization ( $\Delta H_{cc}$ ).

Run 4 presents the most interesting changes in terms of energy transitions observed and differences from virgin PLA. For this reason its DSC thermogram is reported as example. (**Figure 14.13**)

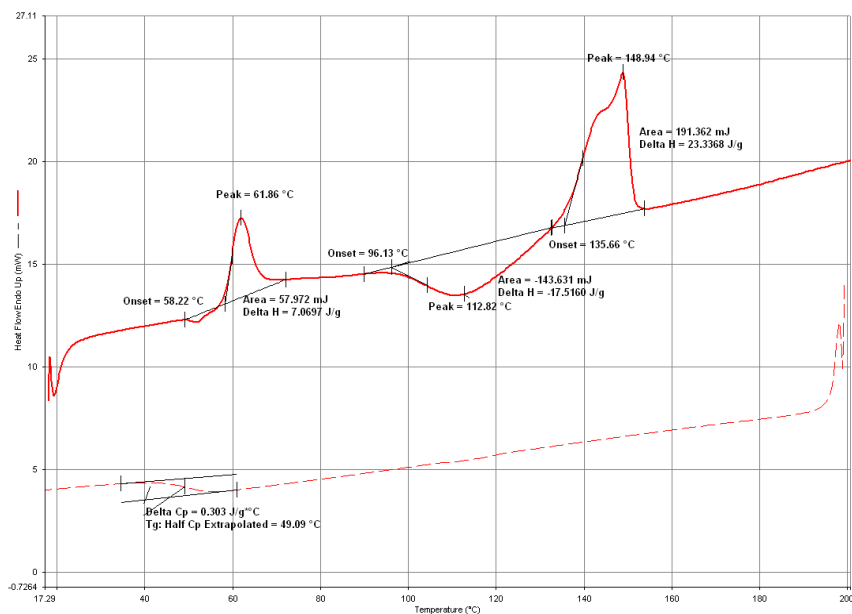


**Figure 14.13:** DSC thermogram of PLA-g-FMA with PLA/FMA/DCP ratio of 100/5/0.5.

In all DSC thermograms, relaxation enthalpy ( $\Delta H_{rlx}$ ) occurs with energy of ca. 7.7 J/g at similar temperatures of virgin PLA  $T_g$  (61 °C). In DSC thermogram of Run 4 (**Figure 14.13**), this transition has values slightly superior compared to virgin PLA (62 °C), while in the other Runs it occurs at ca. 66 °C. As reported before (**Chapter 14.1.2**), relaxation enthalpy is attributable to a rapid cooling below glass transition temperature that prevents energetically favourable orientations of the polymer chains.<sup>[203]</sup>

Degree of crystallinity ( $\chi_c$ ) is subject to great differences between the DSC analyses and it may be observed that:

- Runs 2, 3 and 5 show  $\chi_c$  values at least twice higher than virgin polymer, these tests present the highest ratio between monomer and initiator, with values from 20 to 40.
- Run 1 shows a slight decrease in the degree of crystallinity, leading to a more amorphous disposition of the chains.
- Run 4 and Run 5 present cold crystallization which occurs at ca. 112 °C with exothermic energies between 14.8 and 17.5 J/g.
- Run 4 presents the highest enthalpy energy in melting transition, but  $\chi_c$  value is comparable to virgin PLA, due to the presence of cold crystallization process.

Marsilla *et al.*, in a study about itaconic anhydride grafting observed an increase in  $T_g$  depending on the grafting percentage, moreover they witnessed an unexpected increase in crystallinity.<sup>[155]</sup> Marsilla *et al.* indeed noted that grafting process usually leads to lower degrees of crystallinity. They attributed this behaviour to the presence of monomer, impurities or chain fragments which



could act as nucleating agents leading to a higher values of  $\chi_c$ . These compounds are indeed well known in literature for their capability to influence polymers by increasing glass transition temperature and crystallinity.<sup>[205]</sup> Also Detyothin *et al.*, in a study about PLA grafting with maleic anhydride, discouraged use of high ratio between MA and radical initiator due to formation of impurities.<sup>[202]</sup> Furthermore, in the study by Hwang *et al.*, cold crystallization in DSC thermograms of functionalized PLA is reported as evidence for functionalization of polylactides.<sup>[204]</sup>

$T_d$  and  $\chi_c$  values obtained thanks to characterization analyses, in addition to the presence of cold crystallization transition in the DSC heating process, let to the decision to use the protocol reported in Run 4 for further reaction.

Finally, infrared spectroscopy has confirmed to be non-determinant for characterization of the samples, due to the presence of the strong peak attributable to carboxyl group of polylactic acid,<sup>[182]</sup> which made other possible distinctive signals of grafted COOH groups hardly observable.

REX for the synthesis of PLA-g-FMA has been carried out also in a Brabender plasticorder (BBP) extruder using 50 g of polylactide. Thanks to BBP greater efficiency, residence time has been reduced to 12 minutes and 82% wt. of polymer recovery has been achieved. Rheological behaviour of the polymer during the grafting process has been studied, recording the torque applied on the screws to keep constant their rotatory speed (60 rpm). (**Figure 14.14**) Samples have been purified and characterized by ATR FT-IR, DSC and TGA, achieving results paragonable to products extruded by HAAKE in the same conditions. (**Chapter 16.2.2.1**)

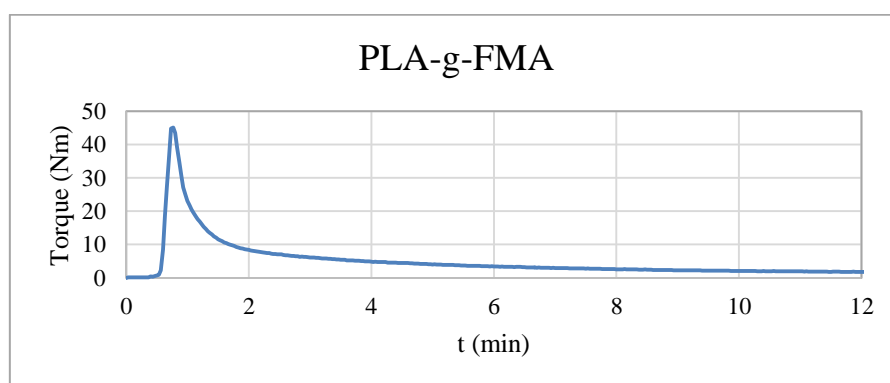


**Figure 14.14:** Comparison graph of torque vs residence time for PLA-g-FMA in BBP extruder.

In the graph (**Figure 14.14**), it is possible to notice that the torque applied to keep constant the rotation of the extruder screw after 12 minutes of reaction is 1.7 Nm. Considering that virgin PLA in extrusion process showed a torque of 14 Nm, this behaviour confirms what observed for PP-g-FMA (**Chapter 14.1.1.1**), with grafting of fumaric acid leading to a reduced viscosity of the polymer matrix.

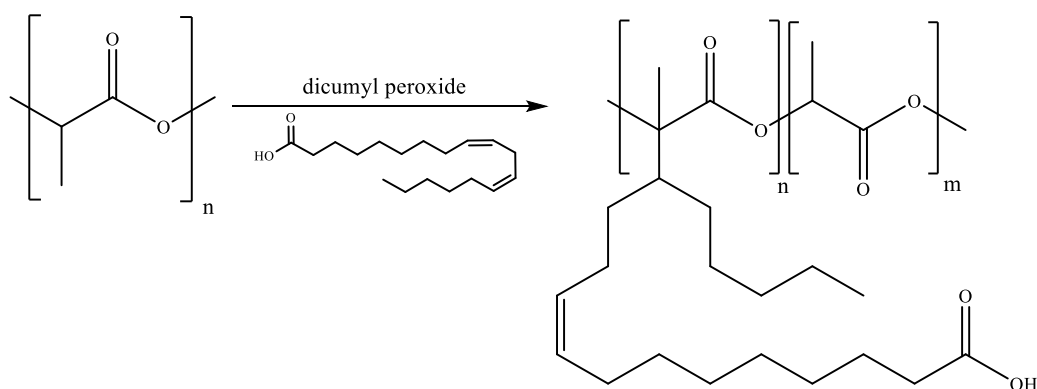
### 14.1.2.2 Poly(lactic acid)-grafted-linoleic acid (PLA-g-LNA)

Linoleic acid (LNA) is a fatty acid of 18-carbon chain with two double bonds which presents antimicrobial properties.<sup>[193,194]</sup> Due to food applicability of both linoleic acid and polylactide,<sup>[167,195]</sup> the study of this grafting process is very interesting.

Linoleic acid may be found in many natural products with other fatty acid compounds, such as in almond shell and linseed oil.<sup>[196,206]</sup> Investigations about linoleic acid or fatty acid mixture grafting onto different polymer matrices are reported in literature and have been discussed before. (**Chapter 14.1.1.2**) These studies reported grafting by autooxidation of the fatty acid for production of radical species,<sup>[199,200]</sup> or grafting of derivated triglycerides with radical initiators.<sup>[201]</sup>

To the best of our knowledge, no study is reported about the reactive extrusion of polylactide with linoleic acid in the presence of radical initiators. Nevertheless, it is worthy of mention the study of Quiles-Carrillo *et al.* about application of LNA with polylactic acid for biobased polymer blends. In this study, almond shells derivatives are reacted with PLA hydroxyl terminal groups, achieving biocomposites cost reduction, improved waste valorization and increased mechanical properties.<sup>[196,206]</sup>

Poly(lactic acid)-grafted-linoleic acid (PLA-g-LNA) synthesis has been carried out reacting PLA with 5% wt. of LNA and 0.5% of DCP in a HAAKE extruder, at 180 °C, with a residence time of 30 minutes and a screws speed of 60 rpm. (**Scheme 14.6**)



**Scheme 14.6:** Grafting reaction of PLA-g-LNA.

The yield of product was 51% in weight, samples were purified by extraction and the product has been characterized by ATR FT-IR, DSC and TGA analyses.

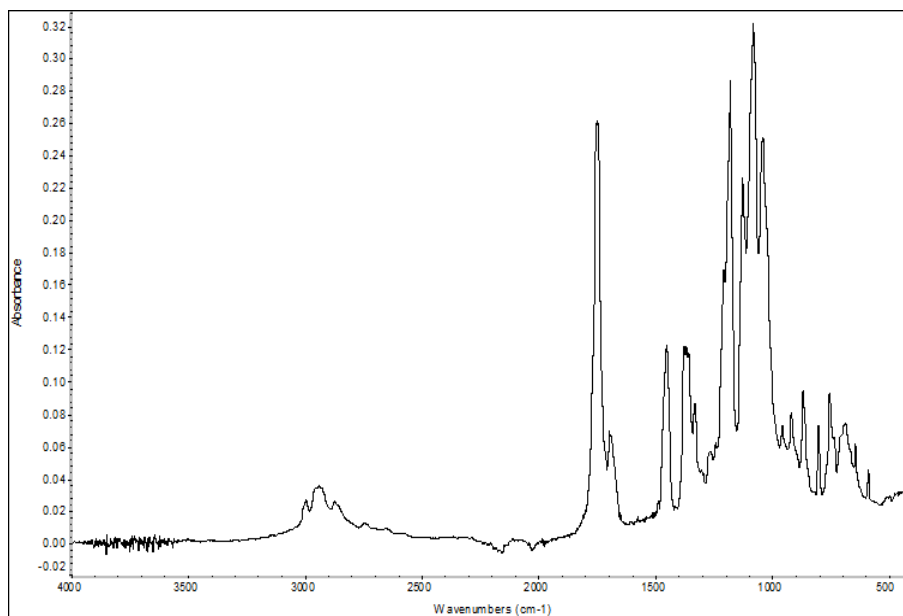


**Figure 14.15:** ATR FT-IR spectrum of PLA-g-LNA.

In ATR FT-IR spectrum of PP-g-LNA (**Figure 14.15**) it is possible to observe typical signals of the polylactide,<sup>[182]</sup> moreover, at  $1712\text{ cm}^{-1}$  a signal is present, attributable to C=O stretching of linoleic acid moieties, as reported for PP-g-LNA. (**Chapter 14.1.1.2**)

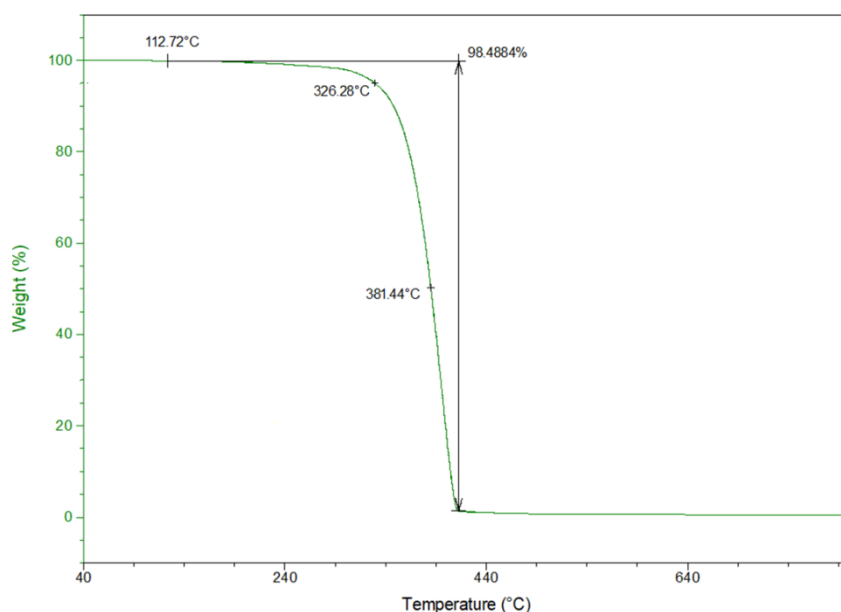


**Figure 14.16:** TGA thermogram of PLA-g-LNA.

In TGA thermogram (**Figure 14.16**), it may be observed that thermal decomposition curve of PLA-g-LNA ( $T_d=121\text{ }^\circ\text{C}$ ,  $T_5=326\text{ }^\circ\text{C}$ ,  $T_{50}=381\text{ }^\circ\text{C}$ ) presents lower values for decomposition temperatures compared to virgin PLA ( $T_d=282\text{ }^\circ\text{C}$ ,  $T_5=340\text{ }^\circ\text{C}$ ,  $T_{50}=389\text{ }^\circ\text{C}$ ). As reported for PP-g-LNA, the decrease of the values of  $T_d$  and  $T_5$  is attributable to chain-stripping mechanism of grafted species

occurred during the heating process.<sup>[190]</sup> Moreover,  $T_{50}$  registered for PLA-g-LNA occurs at higher temperature compared to PLA-g-FMA ( $T_{50}=376$  °C). Similar results have been observed also for the functionalization of polypropylene (**Chapter 14.1.1**), where the functionalization with linoleic acid led to higher  $T_{50}$  values compared to grafting of fumaric acid. LNA is known in literature for its capability to naturally cross-link and for its derivatives that are reported to grant reduced  $\beta$ -scission in grafting reactions.<sup>[196,199,201]</sup> Hence, it is possible that extra stability observed in the polymer may be caused by grafting of LNA.

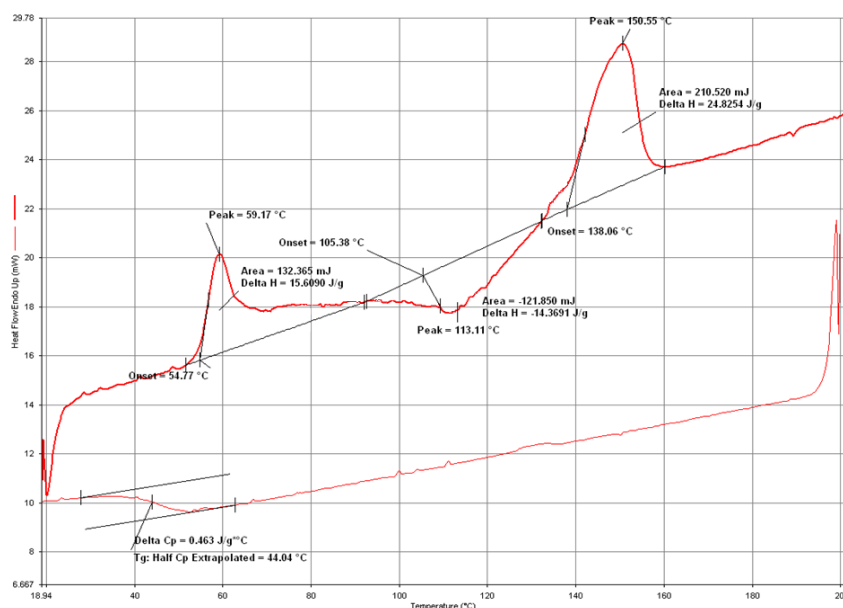


**Figure 14.17:** DSC thermogram of PLA-g-LNA.

In DSC thermogram (**Figure 14.17**), it is possible to observe that PLA-g-LNA heating cycle presents three transitions attributable to relaxation enthalpy (59 °C), cold crystallization (113 °C) and melting (151 °C). The calculated degree of crystallinity ( $\chi_c$ ) is 11%.

In this case, the presence of cold crystallization process is attributed to the interaction of grafted species with the polymer chain.<sup>[204]</sup> Nevertheless, considering virgin PLA values ( $T_g$  61 °C,  $\chi_c$  5.5%), it is surprising that in PLA-g-LNA glass transition temperature does not change, while an increase in the degree of crystallinity is present. Indeed, these two data may seem in disagreement to what reported about the presence of nucleating agents.<sup>[205]</sup> However, similar results were observed by Hwang and Marsilla, which implies that this phenomenon is shown in this kind of polymer.<sup>[155,204]</sup> Anyway, additional investigations will be necessary to clarify the significance of these data.

Finally, extrusion with in a Brabender plasticorder (BBP) instrument has been carried out for synthesis of PLA-g-LNA as well. Recovery of functionalized polymer was 90% in weight, moreover, also in this case residence time could be reduced to 12 minutes and the rheological behaviour of the polymer during the process could be recorded. (Figure 14.18) Samples have been purified and characterized by ATR FT-IR, DSC and TGA, achieving results paragonable to products extruded by HAAKE in the same conditions. (Chapter 16.2.2.2)

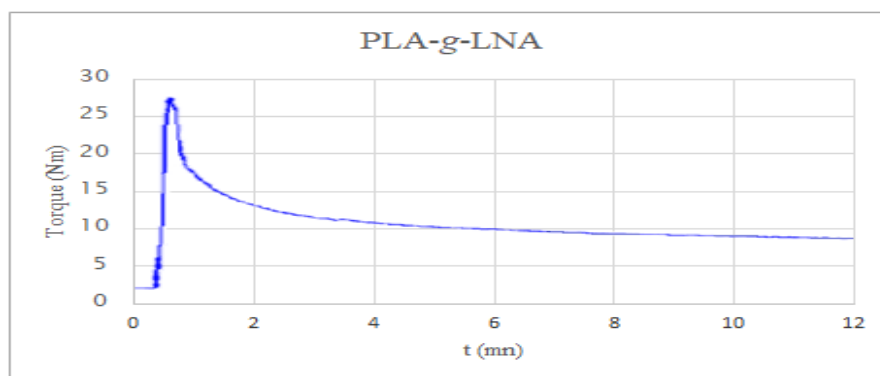


Figure 14.18: Comparison graph of torque vs residence time for PLA-g-LNA in BBP extruder.

In the graph (Figure 14.18), it is possible to observe that after 12 minutes of PP-g-LNA extrusion, the torque applied on the screws is 8.1 Nm. Torque value for virgin PLA at the same conditions is 14 Nm. Thus, similarly to what observed for PP-g-LNA (Chapter 14.1.1.2), it is possible to notice that grafting of linoleic acid cause a reduction in viscosity of the polymer matrix but with a lesser degree compared to what registered with fumaric acid.

## 14.2 Surface grafting by use of 4-(4,6-dimethoxy-1,3,5-triazin-2-yl)-4-methylmorpholinium chloride (DMTMM)

Polymer films may be processed by surface modification without affecting their bulk properties.<sup>[149]</sup> Specific compounds can be grafted to polymers for different applications, such as antimicrobial activity,<sup>[164,207]</sup> antifouling properties,<sup>[208]</sup> enhanced biocompatibility,<sup>[177]</sup> etc.

For this purpose, many techniques have been described in literature such as corona discharge,<sup>[164]</sup> plasma treatment,<sup>[207,208]</sup> UV irradiation,<sup>[164]</sup> in addition to the use of migratory additives.<sup>[209]</sup>

However, these techniques present some disadvantages such as lack of selectivity or short-lasting efficiency due to deactivation or removal by friction, heat or solvent treatment.<sup>[149]</sup> Covalent attachment is another technique developed recently which provides more durability and high selectivity to specific functional groups.<sup>[149]</sup>

In the last years many studies have been published about the application of amidation agents (AA) for reactions between carboxylic acids and primary amines.<sup>[5,19]</sup> Amidation agents commonly used to covalently bond moieties on polymer surfaces are dicyclohexylcarbodiimide (DCC), *N*-(3-dimethylaminopropyl)-*N'*-ethylcarbodiimide (EDC) and 4-(4,6-dimethoxy-1,3,5-triazin-2-yl)-4-methylmorpholinium chloride (DMTMM), previously described in this work (**Chapter 1**).

DCC has been used by Janorkar *et al.*, which activated carboxylic groups present in ethylene-acrylic acid copolymer for grafting of di- or tri-amine compounds. The purpose of this study is to further react the product with succinic anhydride in order to increase COOH groups on the polymer surface and consequently its hydrophilicity.<sup>[149]</sup>

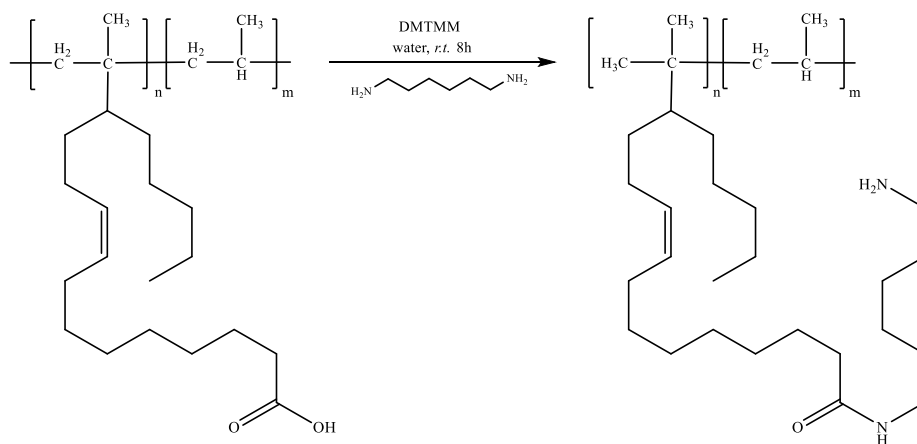
Homopolymers such as polyolefins or polylactic acid do not present carboxylic groups to be activated. In literature many studies overcome this problem by combination of other techniques with application of amidation agents.

Studies are reported about the use of plasma to functionalize polypropylene with COOH groups and later graft it by EDC with different purposes. Zannini *et al.* focused on the production of anti-fouling membranes: PP was treated with plasma in the presence of acrylic acid and then functionalized with mono-amino polyethylene glycole.<sup>[208]</sup> Similarly, Vartiainen *et al.* investigated antimicrobial activity by immobilization of an enzyme on a polypropylene film preventively activated with plasma.<sup>[207]</sup> Radical grafting has been used as well to functionalize polymers for treatment with amidation agents. In order to improve biocompatibility of the polymer, Zhang *et al.* reported a study about immobilization of collagen by EDC application on a polypropylene functionalized with acrylic acid.<sup>[177]</sup> Studies about use of DMTMM as amidation agent on polymer surfaces has been reported as well, Nie *et al.* studied encapsulation of radionuclides onto a poly(lactide-*co*-glycolide) membrane for radiopharmaceutical purposes.<sup>[176]</sup>

Surface functionalization grafting process with DMTMM has been carried out at *r.t.* and in water in order to avoid deactivation processes. Indeed, quaternary ammonium chloride salts may undergo dealkylation under heating or anhydrous conditions.<sup>[20,25,26]</sup>

Hence, below the results for surface treatments with amidation agent (*STAA*) on films of functionalized PP described above are reported. (**Chapter 14.1.1**) Polypropylene-*grafted*-fumaric acid (PP-*g*-FMA) and polypropylene-*grafted*-linoleic acid (PP-*g*-LNA) have been reacted in presence of DMTMM with 1,6-hexandiamine (HDA), butylamine (BU) and sodium 3-aminobenzenesulphonate (ABS). To simplify, an example of reaction and nomenclature used to describe polymers obtained by DMTMM treatment is reported below.

Polypropylene-*grafted*-linoleic acid (PP-*g*-LNA) is treated with DMTMM in presence of 1,6-hexandiamine (HDA) to produce polypropylene-*grafted*-*N*-(6-aminohexyl)-linoleamide (PP-*g*-LNA-HDA). (**Scheme 14.7**)



**Scheme 14.7:** Synthesis reaction of PP-*g*-LNA-HDA.

All processes have been carried out using the filmed polymer in a water solution of the desired amine (adjusted at pH 8) in the presence of DMTMM. After 8 hours at room temperature the films have been washed, dried and characterized by ATR FT-IR and by the study of surface tension.

Moreover, in order to investigate the role of grafted species on the polymer, the films have been treated with acid solution. The samples have been immersed in 40 mL of a 0.1 M HCl solution for 4 hours under stirring, then washed, dried and characterized again.

Infrared spectroscopy analyses confirmed the formation of amide bonds on the polymer surface. As example, the ATR-FT-IR spectrum of PP-*g*-LNA-HDA is reported. (**Figure 14.19**)

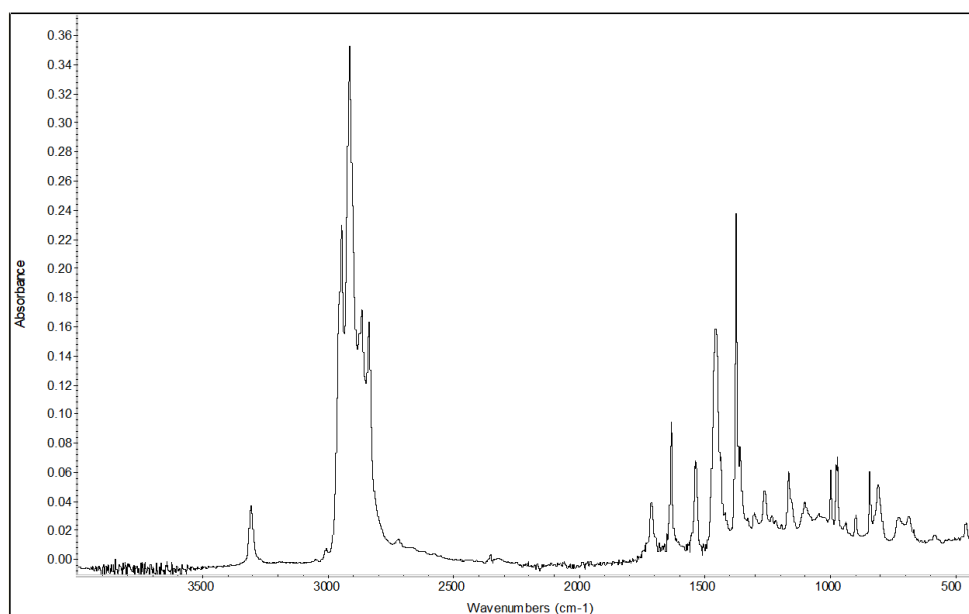


**Figure 14.19:** ATR FT-IR spectrum of PP-*g*-LNA-HDA.

In ATR FT-IR spectrum of PP-g-LNA-HDA (**Figure 14.19**), it is possible to observe signals typical of polypropylene<sup>[191]</sup> and a signal for C=O stretching at 1712 cm<sup>-1</sup> of linoleic acid. In addition, typical signals of amide-I and amide-II are observable at 1633 cm<sup>-1</sup> and at 1537 cm<sup>-1</sup>. Similar results have been reported by Janorkar *et al.* about amidation of acrylic acid.<sup>[154]</sup> Finally, a signal at 3308 cm<sup>-1</sup> is attributable to N-H stretching.

Analogous results have been obtained for others experiments as well, with the exception of PP-g-LNA-ABS. It is possible that the ionic charge present in sodium 3-amino benzenesulphonate prevented an optimal interaction with the polymer surface due to the hydrophobic nature of grafted linoleic acid. Moreover, no changes have been observed in the spectra after treatments in acid solution.

In order to further investigate the formation of amide bonds, the samples have been washed with water solutions at different pH and with organic solvents such as ethanol, CH<sub>2</sub>Cl<sub>2</sub> and acetone. The samples have been dried and characterized without observing any change in ATR FT-IR spectra. Hence, it is possible to assume that the amine moieties have been covalently bonded to the polymer surface.

Surface treating techniques have been found to increase the wetting tension of a polymer film. The more efficient the treatment, the more actively the surface reacts with different polar interfaces. Thus, it is possible to make a correlation between the contact angle of a polymer film surface and its interaction with inks, coatings and solvents, if these possess a polar functionality.<sup>[210]</sup>

Below are reported the contact angles registered for the films both after treatments with amidation agent (*STAA*) and with HCl solution. The tests have been carried out using a solution with a surface tension of 44 dynes. The data obtained are shown in **Table 14.4**.

**Table 14.4:** Contact angles values gathered for functionalized polypropylene.

Amine <sup>(a)</sup>	Contact angle (degree) <sup>(b)</sup>			
	(PP-g-FMA) <sup>(a)</sup>		(PP-g-LNA) <sup>(a)</sup>	
	STAA	HCl	STAA	HCl
blank <sup>(c)</sup>	72	71	94	94
(HDA)	72	46	79	71
(BU)	72	72	92	93
(ABS)	40	41	94	94

*STAA* process reaction conditions: 20x50x0.8 mm polymer film, 10% wt. amine, 10% wt. DMTMM, in 40 mL H<sub>2</sub>O at *r.t.* for 8 hours. Starting pH 8;



HCl treatment: immersion in 40 ml of 0.1 M HCl water solution, at *r.t.* for 4 hours;

(a) polymers treated are: polypropylene-*grafted*-fumaric acid (PP-*g*-FMA), polypropylene-*grafted*-linoleic acid (PP-*g*-LNA). Amines used are: 1,6-hexandiamine (HDA), butylamine (BU), sodium 3-aminobenzenesulphonate (ABS);

(b) contact angle measures have been carried out with the same method reported in the standard test method ASTM D5946 - 04 using a solution 22% ethylene glycole and 78% formamide (44 dynes);

(c) blank refers to a test carried out without the presence of amine.

Blank tests with virgin polypropylene have been carried out both for surface treatments with amidation agent (*STAA*) and with acid solution. In all the cases contact angle values for the film remained unchanged at 72° through all the processes. Thus, from data in **Table 14.4**, it is possible to observe:

- Contact angle of PP-*g*-AFM presents the same value of virgin polypropylene and does not change after treatment with HCl. This value is in agreement with what reported in literature, Janorakar *et al.* reported that a limited number of COOH groups is ineffective for changes of polymer hydrophilicity;<sup>[149]</sup>
- Measure of contact angle for PP-*g*-LNA increased to 94° compared to virgin PP, this is possibly attributable to the hydrophobic nature of linoleic acid. The value does not change after acid treatment;
- *STAA* process with HDA leads to a reduction in contact angle values for PP-*g*-LNA but not for PP-*g*-FMA, suggesting that influence of NH<sub>2</sub> groups is appreciable only in hydrophobic surfaces;
- Polymers treated with 1,6-hexandiamine undergo a reduction in contact angle values after treatments with HCl, probably due to the formation of ammonium species on the terminal group of the grafted chain;
- Treatment with butylamine leads to no changes in contact angles both with PP-*g*-AFM and PP-*g*-LNA, probably attributable to the presence of an alkyl moiety on the amide;
- PP-*g*-AFM-ABS shows a reduction in contact angle value after *STAA* process but does not change after acid treatment, possibly due to the presence of ionic group in ABS;
- After *STAA* process PP-*g*-LNA-ABS presents an unchanged value of contact angle. The latter result is in agreement with what previously reported in infrared spectroscopy about the interaction between PP-*g*-LNA and 3-amino benzenesulphonate.

By ATR FT-IR characterization and contact angle analyses it is possible to assume that DMTMM has successfully modified the polymeric surface even in heterogeneous phase, functionalizing

grafted polypropylene after the reactive extrusion process, in agreement with what reported in literature.<sup>[125,176]</sup>

Many studies reported the importance of polar groups on the polymers surface to achieve hydrophilicity.<sup>[149,176]</sup> Janorkar and Nie demonstrated that covalent attachment of polar groups may influence the surface energies of the treated polymers. By contact angle measures it is possible to observe that the presence of highly polar groups, such as ammonium chloride or sodium sulphonate species, lead to great changes in the hydrophilicity of the polymer surface. (**Figure 14.20**)

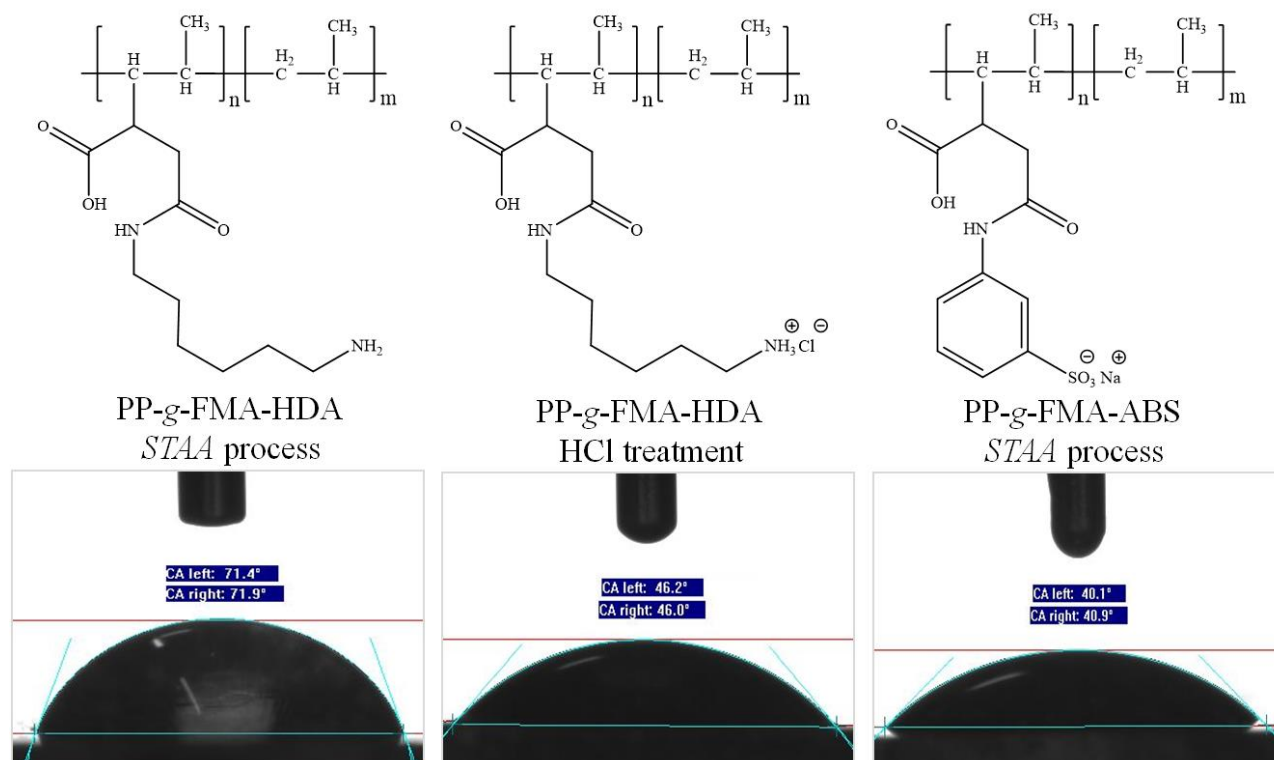


**Figure 14.20:** Changes in contact angle values for grafted polypropylene.

Hence, it may be assumed that covalent attachment of amine groups has been achieved, thanks to the use of DMTMM. Titration tests will be carried out in order to confirm these data and to evaluate the percentage of grafting both in the REX process and DMTMM treatment.

Moreover, PP-g-LNA and PP-g-LNA-HDA have been tested for explorative antimicrobial activity that seems to be promising for future studies. The analyses have been carried out by AATCC 147 test and are not further treated because it exceeds the purposes of this work.

Future developments will investigate the DMTMM functionalization of grafted polylactide films in similar way to what has been done for polypropylene. As well as the influence of the different ionic species of grafted terminal groups on polymers surface energies.

## **CHAPTER 15**

### **CONCLUSIONS POLYMER GRAFTING**

The research of this part of the PhD thesis has focused on the development of a protocol for the functionalization of polypropylene and polylactide by the combined use of reactive extrusion (REX) and an amidation agent such as 4-(4,6-dimethoxy-1,3,5-triazin-2-yl)-4-methylmorpholinium chloride (DMTMM). In addition, contact angle characterizations have been carried out to investigate the functionalized polymers surfaces.

The main results achieved are:

- Optimization of the reactive extrusion of polypropylene for the grafting of fumaric acid;
- Grafting of linoleic acid on polypropylene by reactive extrusion;
- Modification of hydrophobicity of polypropylene for the grafting of linoleic acid;
- Optimization of the reactive extrusion of polylactide for the grafting of fumaric acid;
- Grafting of linoleic acid on polylactide by reactive extrusion;
- Performed surface functionalization of amine moieties on grafted polymers;
- Modification of the final products characteristics measured by contact angle analysis, it has been possible to modulate the hydrophilicity of the extruded polymer by surface treatment with different amines. It may thus be assumed that the functionalization by DMTMM has been successfully achieved in heterogenous phases.

Future analyses by titration test will be carried out in order to investigate the percentage of grafting in both reactive extrusion and DMTMM application techniques.

These findings encourage further studies to investigate the effect of DMTMM surface treatment for grafting of different moieties for antimicrobial activity or antifouling characteristics, in addition to the study of surface treatments by triazine quaternary bis-ammonium salts developed in this PhD thesis.

## **CHAPTER 16**

### **EXPERIMENTAL SECTION POLYMER GRAFTING**

## 16.1 General methods

All chemicals were commercially available and procured from Sigma Aldrich, Merck, Alfa Aesar and Fluka with high grade of purity. Random polypropylene (ISPLEN PR 240 G1F) was purchased by Repsol and polylactic acid (Ingeo Biopolymer 2003D) by NatureWorks. Solvents were of analytical grade and used without further purification.

Extrusion processes have been carried out in Thermo Scientific Haake Minilab II by ThermoFisher Scientific and in a Brabender Plasti-Corder PL 2100 extruders.

Extruded polymers have been filmed in a Collin Hot Platen Press P 200 E. Filming process has been carried out at 160 °C with a 110 x 110 x 0.8 mm mold. Time (t) and pressure (P) programme: step<sub>1</sub> (t<sub>1</sub>:4 min, P<sub>1</sub>:2 bar), step<sub>2</sub> (t<sub>2</sub>:2 min, P<sub>2</sub>:30 bar), step<sub>3</sub> (t<sub>3</sub>:3 min, P<sub>3</sub>:60 bar), step<sub>4</sub> (t<sub>4</sub>:4 min, P<sub>4</sub>:150 bar), step<sub>5</sub> (t<sub>5</sub>:15 min, P<sub>5</sub>:90 bar).

Differential Scanning Calorimetry (DSC) analyses were recorded in a Perkin Elmer DIAMOND DSC, sealed Al pans were used for the analysis and deposited in a Pt pan. Analyses were run in a 20 mL/min N<sub>2</sub> flow and using an empty Al pan as standard. DSC temperature programme: first heating cycle from 20 °C to 200 °C at 20 °C/min, isotherm at 200 °C for 5 minutes, cooling cycle at 20 °C/min until 20 °C, second heating cycle from 20 °C to 200 °C at 20 °C/min. Temperature and enthalpies were determined in the first heating cycle. Values reported are glass transition temperature (T<sub>g</sub>), temperatures related to transitions of cold crystallization (T<sub>cc</sub>), melting (T<sub>m</sub>) and crystallization (T<sub>c</sub>) as well as the respective normalized enthalpies ( $\Delta H_{cc}$ ,  $\Delta H_m$ ,  $\Delta H_c$ ) and relaxation enthalpy ( $\Delta H_{rx}$ ). Degree of crystallinity was calculated by values of  $\Delta H_{ref}$  reported in literature for PP and PLA.<sup>[181,182]</sup>

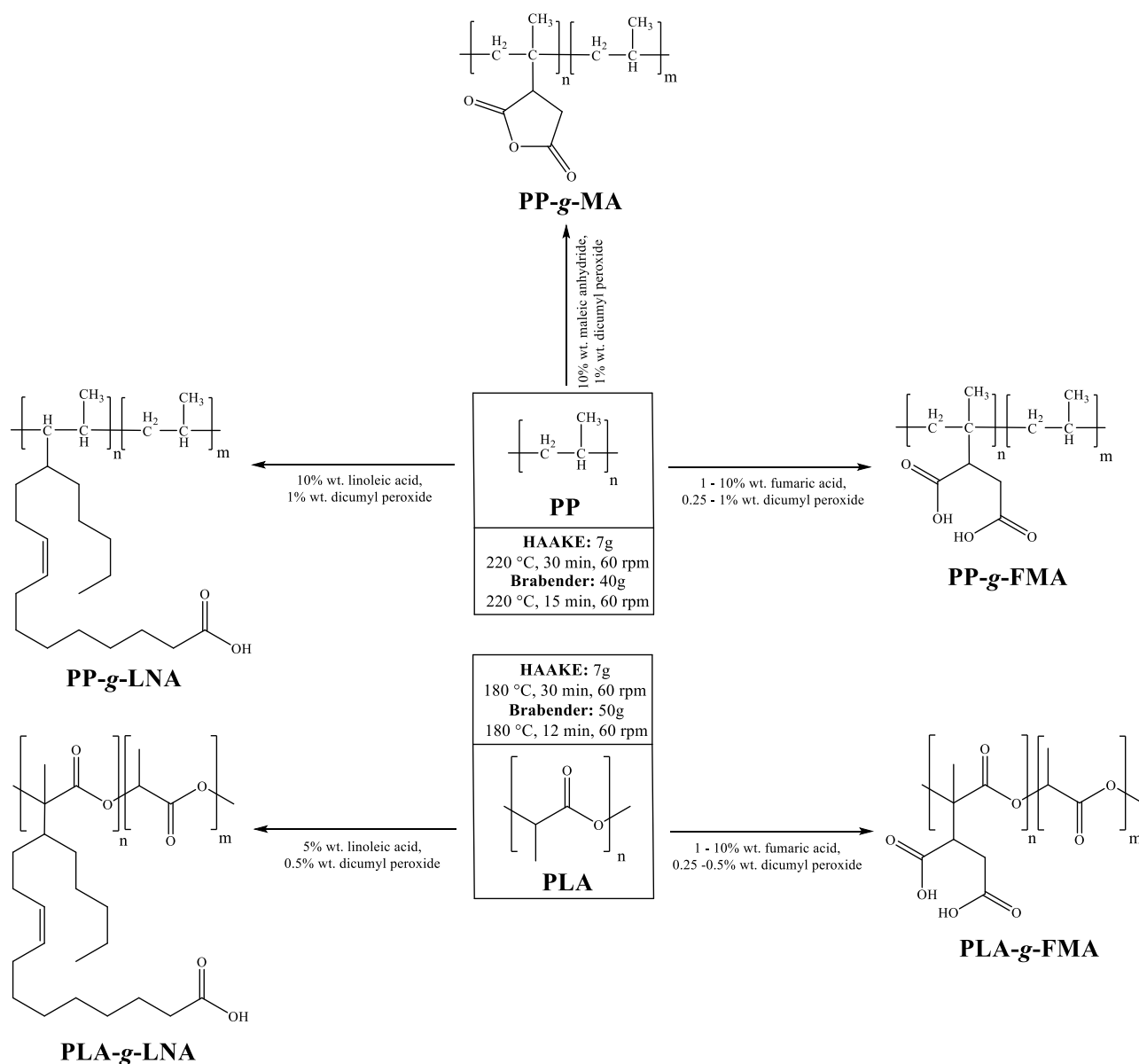
Spectra in the region of middle infrared (4000-400 cm<sup>-1</sup>) were recorded using a FT-IR Spectrophotometer Nicolet 6700 S/N AHR071021 by reflection in Smart Orbit with diamond glass.

Thermogravimetric analyses (TGA) were recorded on TA instruments TGA QIR5000 by method UNE-EN ISO 53375-3. TGA temperature programme: first heating cycle from 50 °C to 900 °C at 20 °C/min under N<sub>2</sub> flux, cooling cycle at 30 °C/min until 400 °C under N<sub>2</sub> flux, second heating cycle from 400 °C to 900 °C at 20 °C/min in air atmosphere. Values reported are the polymer decomposition beginning temperature (T<sub>d</sub>) and the temperatures for 5% (T<sub>5</sub>) and 50% (T<sub>50</sub>) of decomposition and were determined in the first heating scan.

Contact angle measures were performed on a Neurtek OCA15EC instrument static contact angle apparatus in according to ASTM D5946-04 Standard Test Method. A solution of 44 dynes (22% ethylene glycole and 78% formamide) was used and all the reported contact angle values were an average of 10 readings with 95% confidence intervals.

## 16.2 Reactive extrusion processes and characterizations

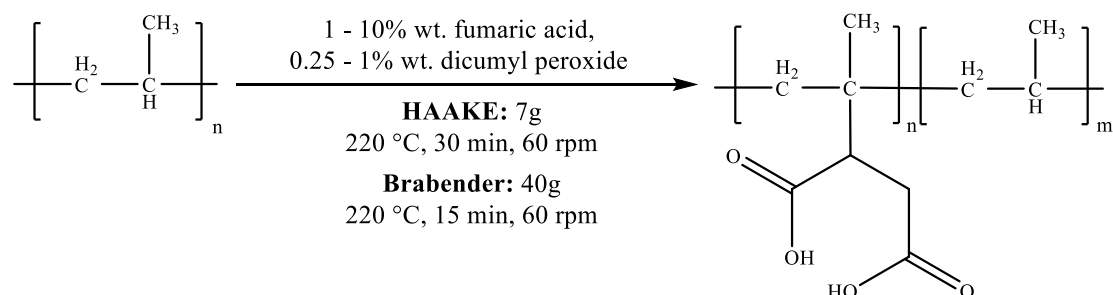
A general scheme is reported below for the reactive extrusions of polypropylene (PP) and polylactic acid (PLA) with fumaric acid (FMA), linoleic acid (LNA) and maleic anhydride (MA) in the presence of dicumyl peroxide (DCP) as free radical initiator. (**Scheme 16.1**)



**Scheme 16.1:** Reactive extrusions of polypropylene (PP) and polylactic acid (PLA).

## 16.2.1 Reactive extrusion of polypropylene (PP)

### 16.2.1.1 Synthesis of polypropylene-grafted-fumaric acid (PP-g-FMA)



**Scheme 16.2:** Grafting reaction of PP-g-FMA.

In a becker, polypropylene (PP) is mixed with different quantities of fumaric acid (FMA, 1-10% wt.) and dicumyl peroxide (DCP, 0.25-1% wt.). The reagents are fed into the extruder with the following protocol depending on the instrument:

- *Haake*: 7 g of polymer, at 220 °C and 60 rpm, with residence time of 30’;
- *Brabender Plasticorder*: 40 g of polymer, at 220 °C and 60 rpm, with residence time of 15’;

Then, the functionalized polypropylene is recovered, cooled and pelletized. As reported in literature,<sup>[188]</sup> the extrudate is dissolved into refluxing toluene (5 mL per gram of polymer) and precipitated into a large excess of acetone to remove unreacted fumaric acid and possible oligomers formed. The product is filtered and washed with 3 aliquotes of acetone (3 mL per gram of polymer). PP-g-FMA is dried under vacuum for 8 hours at 80 °C and characterized by ATR FT-IR, DSC and TGA, reported in **Table 16.1** as Runs from 1 to 5 for the process carried out by Haake extruder and as Run 6 for Brabender Plasticorder extrusion.

Finally, PP-g-FMA extruded with Brabender Plasticorder is filmed in an Hot Platen Press at 160 °C for surface characterization by contact angle studies reported below. (**Chapter 16.5**)

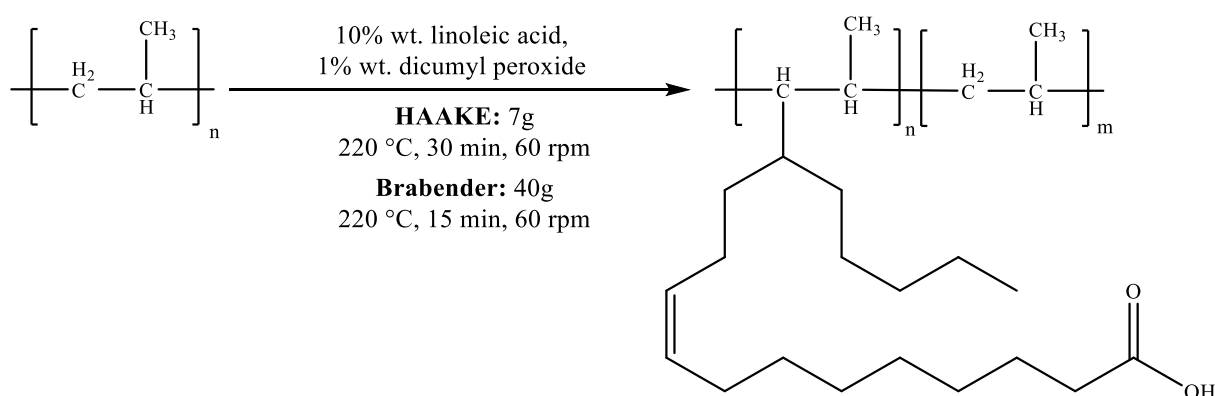
**Table 16.1:** Synthesis of PP-g-FMA at different PP/FMA/DCP ratios and related TGA, DSC and ATR FT-IR values.

Run	FMA (% wt.)	DCP (% wt.)	TGA <sup>(a)</sup>			DSC <sup>(b)</sup>					
			T <sub>d</sub> (°C)	T <sub>5</sub> (°C)	T <sub>50</sub> (°C)	T <sub>m</sub> (°C)	ΔH <sub>m</sub> (J/g)	T <sub>c</sub> (°C)	ΔH <sub>c</sub> (J/g)	χ <sub>c</sub> <sup>(c)</sup> (%)	
1	1	0.25	206	422	469	146	44.6	99	- 60.0	21.3	
2	5	0.25	204	421	470	146	42.8	102	- 58.4	20.5	
3	10	0.25	203	418	467	147	41.9	103	- 56.9	20.0	
4	10	1	203	419	465	147	40.4	101	- 53.4	19.3	
5	20	1	204	422	466	145	39.7	101	- 52.0	19.0	
6	10	1	204	420	464	146	41.1	101	-52.9	20.0	
ATR FT-IR (cm <sup>-1</sup> ):			2950, 2915, 2838, 1685 <sup>(d)</sup> , 1455, 1377, 1166, 997, 972, 840, 808								



- (a) TGA analysis conditions: sample ca. 20 mg. Temperature programme: first heating cycle from 50 °C to 800 °C at 20 °C/min under N<sub>2</sub> atmosphere; isotherm at 900 °C for 15 minutes; cooling cycle at 30 °C/min until 450 °C under N<sub>2</sub> atmosphere, second heating cycle from 450 °C to 900 °C at 20 °C/min under air atmosphere;
- (b) DSC analysis conditions: sample ca. 8 mg. Temperature programme: first heating cycle from 20 °C to 200 °C at 20 °C/min; isotherm at 200 °C for 5 minutes; cooling cycle at 20 °C/min until 20 °C; second heating cycle from 20 °C to 200 °C at 20 °C/min;
- (c) degree of crystallinity ( $\chi_c$ ) has been calculated with a  $\Delta H_{ref}$  of 209.2 J/g, corresponding to the theoretical melting enthalpy of a totally crystalline isotactic polypropylene sample;<sup>[181]</sup>
- (d) the value has been observed only for Runs 4, 5 and 6.

### 16.2.1.2 Synthesis of polypropylene-grafted-linoleic acid (PP-g-LNA)



**Scheme 16.3:** Grafting reaction of PP-g-LNA.

In a becker, polypropylene (PP) is mixed with 10% wt. of linoleic acid (LNA) and 1% wt. of dicumyl peroxide (DCP). The reagents are fed into the extruder with the following protocol depending on the instrument:

- *Haake*: 7 g of polymer, at 220 °C and 60 rpm, with residence time of 30’;
- *Brabender Plasticorder*: 40 g of polymer, at 220 °C and 60 rpm, with residence time of 15’;

Then, the functionalized polypropylene is recovered, cooled and pelletized. As reported in literature,<sup>[188]</sup> the extrudate is dissolved into refluxing toluene (5 mL per gram of polymer) and precipitated into a large excess of acetone to remove unreacted monomer and possible homopolymers formed. The product is filtered and washed with 3 aliquotes of acetone (3 mL per gram of polymer). PP-g-LNA is dried under vacuum for 8 hours at 80 °C and characterized by ATR FT-IR, DSC and TGA, reported in **Table 16.2** as Run 1 for the process carried out by Haake extruder and as Run 2 for Brabender Plasticorder extrusion.

Finally, PP-g-LNA extruded with Brabender Plasticorder is filmed in an Hot Platen Press at 160 °C for surface characterization by contact angle studies reported below. (**Chapter 16.5**)

**Table 16.2:** Synthesis of PP-g-LNA at different PP/LNA/DCP ratios and related TGA, DSC and ATR FT-IR values.

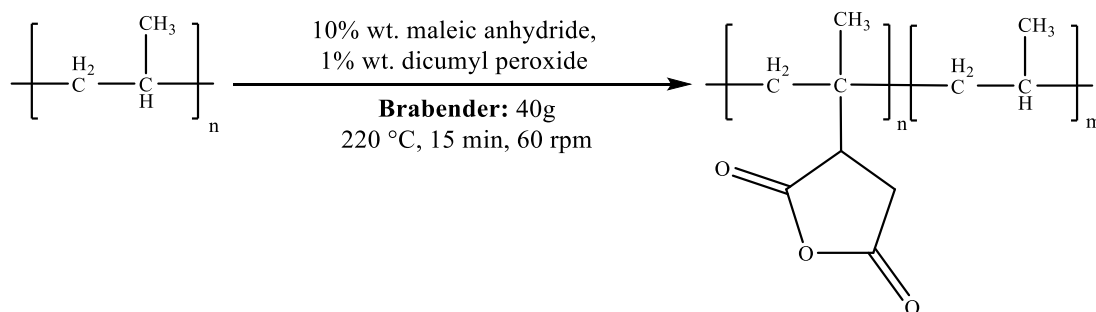
Run	LNA (% wt.)	DCP (% wt.)	TGA <sup>(a)</sup>			DSC <sup>(b)</sup>					
			T <sub>d</sub> (°C)	T <sub>5</sub> (°C)	T <sub>50</sub> (°C)	T <sub>m</sub> (°C)	ΔH <sub>m</sub> (J/g)	T <sub>c</sub> (°C)	ΔH <sub>c</sub> (J/g)	χ <sub>c</sub> <sup>(c)</sup> (%)	
1	10	1	166	361	472	145	58.1	98	- 63.4	27.8	
2	10	1	164	359	474	145	57.8	97	- 62.4	27.6	
ATR FT-IR (cm <sup>-1</sup> ):			2950, 2915, 2838, 1712, 1455, 1377, 1166, 997, 972, 840, 808								

(a) TGA analysis conditions: sample ca. 20 mg. Temperature programme: first heating cycle from 50 °C to 800 °C at 20 °C/min under N<sub>2</sub> atmosphere; isotherm at 900 °C for 15 minutes; cooling cycle at 30 °C/min until 450 °C under N<sub>2</sub> atmosphere, second heating cycle from 450 °C to 900 °C at 20 °C/min under air atmosphere;

(b) DSC analysis conditions: sample ca. 8 mg. Temperature programme: first heating cycle from 20 °C to 200 °C at 20 °C/min; isotherm at 200 °C for 5 minutes; cooling cycle at 20 °C/min until 20 °C; second heating cycle from 20 °C to 200 °C at 20 °C/min;

(c) degree of crystallinity (χ<sub>c</sub>) has been calculated with a ΔH<sub>ref</sub> of 209.2 J/g, corresponding to the theoretical melting enthalpy of a totally crystalline isotactic polypropylene sample.<sup>[181]</sup>

### 16.2.1.3 Synthesis of polypropylene-grafted-maleic anhydride (PP-g-MA)

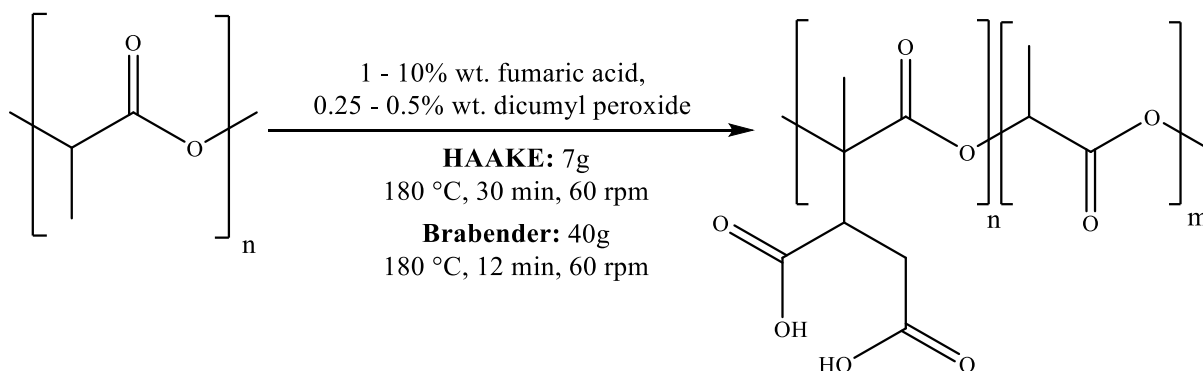
**Scheme 16.4:** Grafting mechanism for synthesis of PP-g-MA.

In a 100 mL becker, 40 g of polypropylene (PP) are mixed with 4 g of maleic anhydride (MA, 10% wt.) and 0.4 g of dicumyl peroxide (DCP, 1% wt.). The reagents are fed into a Brabender Plasticorder extruder set at 220 °C and 60 rpm, with residence time of 15 minutes. Then, the functionalized polypropylene is recovered, cooled and pelletized. As reported in literature,<sup>[188]</sup> the extrudate is dissolved into 200 mL of refluxing toluene and precipitated into a large excess of acetone to remove unreacted monomer and possible oligomers formed. The product is washed with 3 x 20 mL aliquotes of acetone. Finally, PP-g-MA is dried under vacuum for 8 hours at 80 °C and characterized by ATR FT-IR.

ATR FT-IR (cm<sup>-1</sup>): 2950, 2915, 2838, 1782, 1455, 1377, 1166, 997, 972, 840, 808.

## 16.2.2 Reactive extrusion of polylactic acid (PLA)

### 16.2.2.1 Synthesis of polylactic acid-grafted-fumaric acid (PLA-g-FMA)



**Scheme 16.5:** Grafting reaction of PLA-g-FMA.

In a becker, polylactic acid (PLA) is mixed with different quantities of fumaric acid (FMA, 1-10% wt.) and dicumyl peroxide (DCP, 0.25-0.5% wt.). The reagents are fed into the extruder with the following protocol depending on the instrument:

- *Haake*: 7 g of polymer, at 180 °C and 60 rpm, with residence time of 30’;
- *Brabender Plasticorder*: 50 g of polymer, at 180 °C and 60 rpm, with residence time of 12’;

Then, the functionalized polylactide is recovered, cooled and pelletized. The polymer is dissolved in CH<sub>2</sub>Cl<sub>2</sub> (5 mL per gram of polymer) and purified by extraction with water. PLA-g-FMA is dried under vacuum for 8 hours at 80 °C and characterized by ATR FT-IR, DSC and TGA, reported in **Table 16.3** as Runs from 1 to 5 for the process carried out by Haake extruder and as Run 6 for Brabender Plasticorder extrusion.

**Table 16.3:** Synthesis of PLA-g-FMA at different PLA/FMA/DCP ratios and related TGA, DSC and ATR FT-IR values.

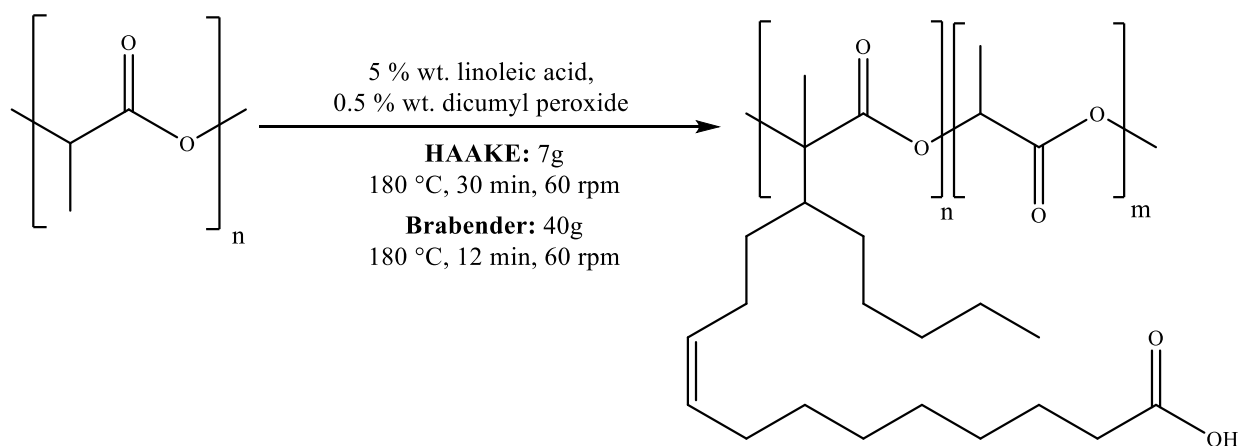
Run	FMA (% wt.)	DCP (% wt.)	TGA <sup>(a)</sup>			DSC <sup>(b)</sup>						
			T <sub>d</sub> (°C)	T <sub>5</sub> (°C)	T <sub>50</sub> (°C)	T <sub>g</sub> (°C)	ΔH <sub>rlx</sub> (J/g)	T <sub>cc</sub> (°C)	ΔH <sub>cc</sub> (J/g)	T <sub>m</sub> (°C)	ΔH <sub>m</sub> (J/g)	χ <sub>c</sub> <sup>(c)</sup> (%)
1	1	0.25	124	342	390	66	8.6	-	-	148	2.9	3.1
2	5	0.25	121	344	393	66	8.6	-	-	150	12.0	12.9
3	10	0.25	119	339	392	66	8.6	-	-	151	17.5	18.8
4	5	0.5	112	341	376	62	7.0	113	-17.5	149	23.4	6.3
5	10	0.5	114	343	376	66	7.0	112	-14.8	150	25.8	11.8
6	5	0.5	111	339	378	61	6.8	112	-16.7	150	22.8	6.6
<b>ATR FT-IR (cm<sup>-1</sup>):</b>			2995, 2944, 1759, 1453, 1382, 1194, 1130, 1093, 1047, 868									

(a) TGA analysis conditions: sample ca. 20 mg. Temperature programme: first heating cycle from 50 °C to 800 °C at 20 °C/min under N<sub>2</sub> atmosphere; isotherm at 900 °C for 15 minutes; cooling cycle at 30 °C/min until 450 °C under N<sub>2</sub> atmosphere, second heating cycle from 450 °C to 900 °C at 20 °C/min under air atmosphere;

(b) DSC analysis conditions: sample ca. 8 mg. Temperature programme: first heating cycle from 20 °C to 200 °C at 20 °C/min; isotherm at 200 °C for 5 minutes; cooling cycle at 20 °C/min until 20 °C; second heating cycle from 20 °C to 200 °C at 20 °C/min;

(c) Degree of crystallinity ( $\chi_c$ ) has been calculated with a  $\Delta H_{ref}$  of 93.1 J/g, corresponding to the theoretical melting enthalpy of a totally crystalline PLA sample.<sup>[182]</sup>

### 16.2.2.2 Synthesis of poly(lactic acid-*g*-linoleic acid) (PLA-*g*-LNA)



**Scheme 3.2:** Grafting reaction of PLA-*g*-LNA.

In a becker, polylactic acid (PLA) is mixed with 5% wt. of linoleic acid (LNA) and 0.5% wt. of dicumyl peroxide (DCP). Thus, the reagents are fed into the extruder with the following protocol depending on the extruder:

- *Haake*: 7 g of polymer, at 180 °C and 60 rpm, with residence time of 30’;
- *Brabender Plasticorder*: 50 g of polymer, at 180 °C and 60 rpm, with residence time of 12’;

Then, functionalized polylactide is recovered, cooled and pelletized. The polymer is dissolved in  $\text{CH}_2\text{Cl}_2$  (5 mL per gram of polymer) and purified by extraction with water. Finally, PLA-*g*-LNA is dried under vacuum for 8 hours at 80 °C and characterized by ATR FT-IR, DSC and TGA, reported in **Table 16.4** as Run 1 for the process carried out by Haake extruder and as Run 2 for Brabender Plasticorder extrusion.

**Table 16.4:** Synthesis of PLA-*g*-LNA at different PLA/LNA/DCP ratios and related TGA, DSC and ATR FT-IR values.

Run	LNA (% wt.)	DCP (% wt.)	TGA <sup>(a)</sup>			DSC <sup>(b)</sup>						
			T <sub>d</sub> (°C)	T <sub>5</sub> (°C)	T <sub>50</sub> (°C)	T <sub>g</sub> (°C)	$\Delta H_{rlx}$ (J/g)	T <sub>cc</sub> (°C)	$\Delta H_{cc}$ (J/g)	T <sub>m</sub> (°C)	$\Delta H_m$ (J/g)	$\chi_c$ <sup>(c)</sup> (%)
1	5	0.5	113	326	381	59	15.6	113	-14.4	151	24.8	11.2
2	5	0.5	111	325	383	59	14.9	112	-13.5	151	23.6	10.8
<b>ATR FT-IR (cm<sup>-1</sup>):</b>			2995, 2944, 1759, 1712, 1453, 1382, 1194, 1130, 1093, 1047, 868									

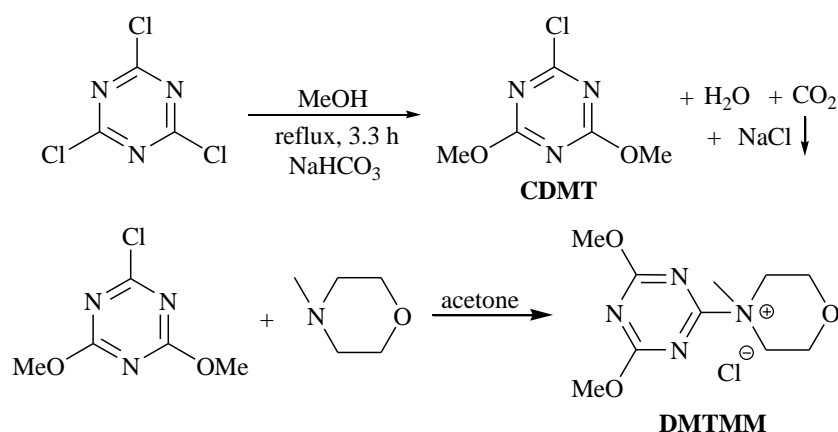
(a) TGA analysis conditions: sample ca. 20 mg. Temperature programme: first heating cycle from 50 °C to 800 °C at 20 °C/min under N<sub>2</sub> atmosphere; isotherm at 900 °C for 15 minutes; cooling cycle at 30 °C/min until 450 °C under N<sub>2</sub> atmosphere, second heating cycle from 450 °C to 900 °C at 20 °C/min under air atmosphere;

(b) DSC analysis conditions: sample ca. 8 mg. Temperature programme: first heating cycle from 20 °C to 200 °C at 20 °C/min; isotherm at 200 °C for 5 minutes; cooling cycle at 20 °C/min until 20 °C; second heating cycle from 20 °C to 200 °C at 20 °C/min;

(c) Degree of crystallinity ( $\chi_c$ ) has been calculated with a  $\Delta H_{ref}$  of 93.1 J/g, corresponding to the theoretical melting enthalpy of a totally crystalline PLA sample.<sup>[182]</sup>

### 16.3 Synthesis of 2-chloro-4,6-dimethoxy-1,3,5-triazine (CDMT) and 4-(4,6-dimethoxy-1,3,5-triazin-2-yl)-4-methylmorpholinium chloride (DMTMM)

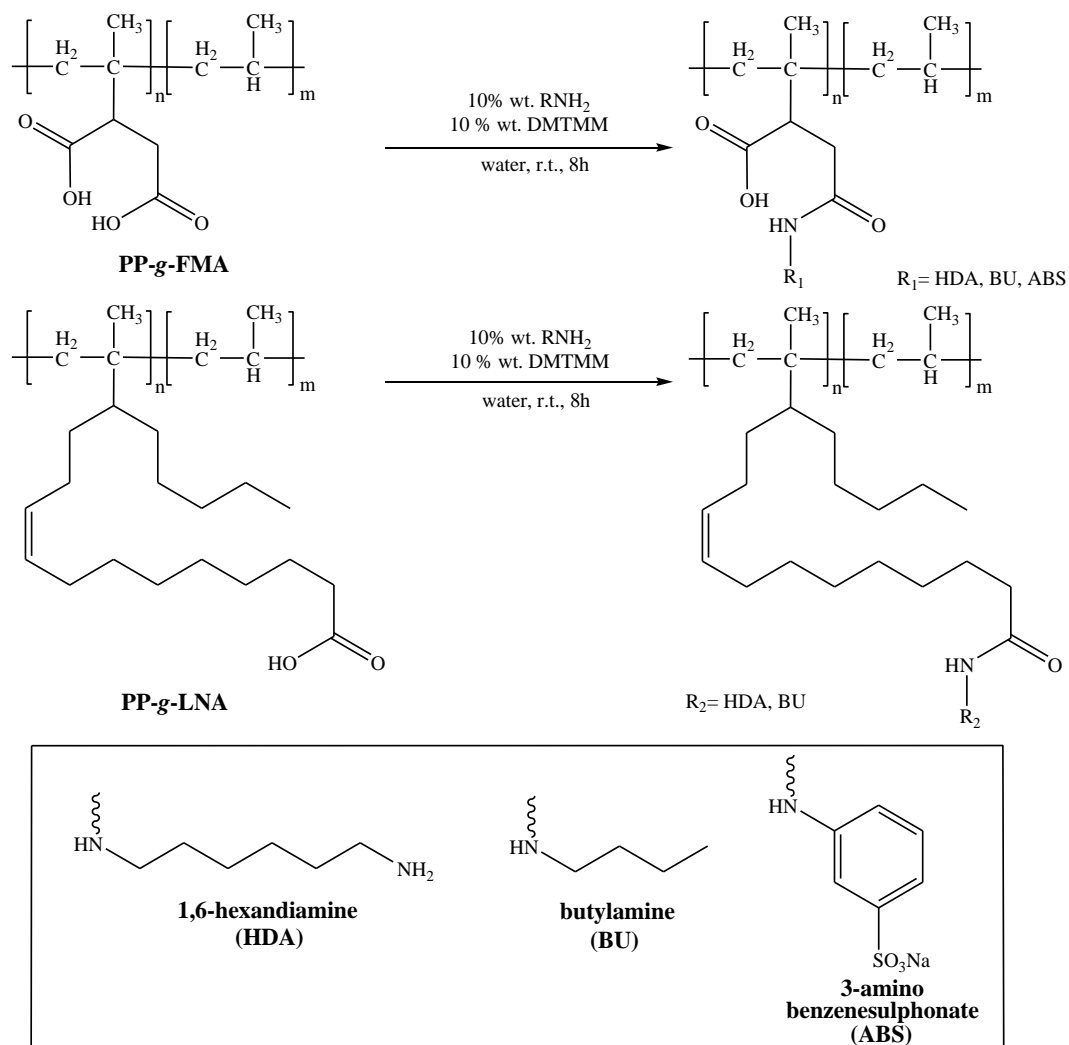
The syntheses of 2-chloro-4,6-dimethoxy-1,3,5-triazine (CDMT) and 4-(4,6-dimethoxy-1,3,5-triazin-2-yl)-4-methylmorpholinium chloride (DMTMM) have been carried out following the method proposed by Kaminski.<sup>[29,32]</sup> (**Scheme 16.6**)



**Scheme 16.6:** Synthesis of 2-chloro-4,6-dimethoxy-1,3,5-triazine (CDMT) and 4-(4,6-dimethoxy-1,3,5-triazin-2-yl)-4-methylmorpholinium chloride (DMTMM).

The syntheses and the characterizations of the products have been previously reported in this work. (**Chapter 11.2.1**)

## 16.4 Surface grafting treatment with DMTMM



**Scheme 16.7:** Surface grafting treatment of functionalized polypropylene (PP) with DMTMM.

In a 50 mL flask equipped with magnetic stirrer, a 25 x 50 x 0.8 mm filmed functionalized polymer is added to a 40 mL water solution with 10% wt. of the desired amine. pH is adjusted to 8 and DMTMM (10% wt.) is solubilized into the solution. The reaction is left under stirring for 8 h at *r.t.*, then the polymer is recovered and washed with water. Finally, the film is dried under vacuum for 8 hours at 80 °C and characterized by ATR FT-IR.

Characterization:

- polypropylene-grafted-fumaric acid mono *N*-(6-aminohexyl)amide  
(PP-*g*-FMA-HDA)  
**ATR FT-IR** (cm<sup>-1</sup>): 3310, 2951, 2915, 2838, 1685, 1627, 1541, 1454, 1377, 1165, 997, 971, 840, 807.
- polypropylene-grafted-fumaric acid mono *N*-(butyl)amide  
(PP-*g*-FMA-BU)  
**ATR FT-IR** (cm<sup>-1</sup>): 3299, 2950, 2915, 2837, 1686, 1655, 1559, 1455, 1374, 1166, 998, 972, 841, 809.
- polypropylene-grafted-fumaric acid mono *N*-(3-benzen sodium sulphonate)amide  
(PP-*g*-FMA-ABS)  
**ATR FT-IR** (cm<sup>-1</sup>): 3284, 2950, 2914, 2837, 1688, 1659, 1555, 1455, 1377, 1171, 999, 973, 841, 807.
- polypropylene-grafted-*N*-(6-aminohexyl)linoleamide  
(PP-*g*-LNA-HDA)  
**ATR FT-IR** (cm<sup>-1</sup>): 3308, 2949, 2915, 2838, 1712, 1633, 1537, 1455, 1377, 1165, 997, 972, 839, 808.
- polypropylene-grafted-*N*-( butyl)linoleamide  
(PP-*g*-LNA-BU)  
**ATR FT-IR** (cm<sup>-1</sup>): 3291, 2949, 2916, 2840, 1712, 1654, 1558, 1455, 1378, 1166, 999, 972, 840, 808.

## 16.5 Contact angle characterization

The surface treatment techniques have been found to increase the wetting tension of a polymer film.<sup>[210]</sup> The analyses have been carried out following the standard test method ASTM D5946 - 04, knowing that it has been designed for polymers activated by corona-treatment and with the difference of using a solution of 44 dyne (22% ethylene glycole and 78% formamide) instead of water.<sup>[210]</sup>

Samples have been dried under vacuum for 8 hours at 80 °C and positioned on instrument holder. Then, a 5-8 µL droplet has been suspended on the syringe needle and the polymer surface is brought in contact with the droplet for deposition. The contact angle is measured and the process is repeated 10 times. Contact angle is considered by the average of the values.

## **CHAPTER 17**

## **REFERENCES**



- [1] Z.J. Kamiński, B. Kolesińska, J. Kolesińska, G. Sabatino, M. Chelli, P. Rovero, M. Błaszczuk, M.L. Główka and A.M. Papini, *J. Am. Chem. Soc.*, **2005**, 127, 16912-16920.
- [2] C.A.G.N. Montalbetti and V. Falque, *Tetrahedron*, **2005**, 61, 10827-10852.
- [3] J.A. Mitchell and E.E.J.A. Reid, *J. Am. Chem. Soc.*, **1931**, 53, 1897-1883.
- [4] B.S. Jursic and Z. Zdravkovski, *Synth. Commun.*, **1993**, 23, 2761-2770.
- [5] A. El-Faham and F. Albericio, *Chem. Rev.*, **2011**, 111, 6557-6602.
- [6] E. Valeur and M. Edric, *Chem. Soc. Rev.*, **2009**, 38, 606-631.
- [7] T. Curtius, *Ber. Deutsch. Chem. Ges.*, **1902**, 35 (3), 3226-3228.
- [8] J. Meienhofer, The azide method in peptide synthesis. In: *The Peptides: Analysis, Synthesis, Biology*; E. Gross, J. Meienhofer, Academic Press Inc., **1979**.
- [9] A. El-Faham, R. Subirós Funosas, R. Prohens and F. Albericio, *Chem. Eur. J.*, **2009**, 15 (37), 9404 - 9416.
- [10] L.M. Durán-Riveroll and A.D. Cambell, *Mar. Drugs*, **2017**, 15 (10), 303-331.
- [11] K.D. Wehrstedt, P.A. Wandrey and D. Heitkamp, *J. Hazard. Mater.*, **2005**, 126 (1-3), 1-7.
- [12] A. El-Faham and F. Albericio, *J. Pept. Sci.*, **2010**, 16 (1), 6-9.
- [13] J.C. Sheehan and G.P. Hess, *J. Am. Chem. Soc.*, **1955**, 77 (4), 1067-1068.
- [14] F.A. Tobiesen and S. Michielsen, *J. of Polym. Sci., Part A: Polym. Chem.*, **2002**, 40 (5), 719-728.
- [15] J. Sheehan, P. Cruickshank and G. Boshart, *J. Org. Chem.*, **1961**, 26 (7), 2525-2528.
- [16] K. Thompson and S. Michielsen, *J. of Polym. Sci., Part A: Polym. Chem.*, **2006**, 44 (1), 126-136.
- [17] C. Wang, Q. Yan, H. Liu, X. Zhou and S. Xiao, *Langmuir*, **2011**, 27 (19), 12058-12068.
- [18] Z.J. Kamiński, *Tetrahedron Letters*, **1985**, 26 (24), 2901-2904.
- [19] M. Kunishima, C. Kawachi, K. Hioki, K. Terao and S. Tani, *Tetrahedron*, **2001**, 57 (8), 1551-1558.
- [20] M. Kunishima, C. Kawachi, J. Morita, K. Terao, S. Tani, F. Iwasaki and S. Tani, *Tetrahedron*, **1999**, 55 (46), 13159-13170.
- [21] M. Kunishima, T. Ujigawa, Y. Nagaoka, C. Kawachi, K. Hioki and M. Shiro, *Chem. Eur. J.*, **2012**, 18 (49), 15856-15867.
- [22] J. Fraczyk, Z. Kamiński, J. Katarzynska and B. Kolesinska, *Helv. Chim. Acta*, **2018**, 101, 1-21.
- [23] M. Kunishima, K. Hioki, A. Wada, H. Kobayashi and S. Tani, *Tetrahedron Letters*, **2002**, 43 (18), 3323-3326.

- [24] K. Jastrzabek, P. Bednarek, B. Kolesinska and Z.J. Kamiński, *Chemistry & Biodiversity*, **2013**, 10 (5), 952-961.
- [25] B. Kolesinska and Z. J. Kamiński, *Pol. J. Chem.*, **2008**, 82, 2115-2123.
- [26] P. Rushton and M.F.G. Stevens, *J. Chem. Soc. Perkin Trans. 1*, **1985**, 0, 1533-1539.
- [27] J. Yu, F. Teng and J. Cheng, *Adv. Synth. Catal.*, **2017**, 359 (1), 26-38.
- [28] S. Rydergren, *Chemical Modifications of Hyaluronan using DMTMM-Activated Amidation*, PhD thesis, Uppsala Universitet, **2018**.
- [29] Z. J. Kamiński, *Biopolymers (Peptide Science)*, **2000**, 55 (2), 140-164.
- [30] J. Fraczyk, M. Walczak, L. Szymanski, Z. Kolacinski, H. Wrzosek, I. Majsterek, K. Przybylowska-Sygut and Z.J. Kamiński, *Nanomedicine (Lond.)*, **2017**, 12 (18), 2161-2182.
- [31] B. Kolesinska, K.K. Rozniakowski, J. Fraczyk, I. Relich, A.M. Papini and Z.J. Kamiński, *Eur. J. Org. Chem.* **2015**, 2, 401-408.
- [32] Z.J. Kamiński, P. Paneth and J. Rudzinski, *J. Org. Chem.*, **1998**, 63 (13), 4248-4255.
- [33] M. Kunishima, D. Kato, N. Kimura, M. Kitamura, K. Yamada and K. Hioki, *Beilstein J. Org. Chem.* **2016**, 12, 1897-1903.
- [34] M. Kitamura, S. Sasaki, R. Nishikawa, K. Yamada and M. Kunishima, *RSC Adv.*, **2018**, 8, 22482-22489.
- [35] D. Azarifar and A. Forghaniha, *Heterocycles*, **2006**, 68 (4), 807-810.
- [36] A.R. Katritzky, D.C. Oniciu, I. Ghiviriga and R.A. Barcock, *J. Chem. Soc. Perkin Trans. 2*, **1995**, 785-792.
- [37] H.K. Hall Jr., *J. Am. Chem. Soc.*, **1957**, 79, 5441-5444.
- [38] C.W. Bird, *Tetrahedron*, **1985**, 41 (7), 1409-1414.
- [39] D. Bartholomew, Zeneca Agrochemicals, Bracknell, UK, In: *Comprehensive Heterocyclic Chemistry II*, Elsevier **1996**, 575-636.
- [40] R.M. Silverstein, G.C. Bassler and T.C. Morrill, *Spectrometric Identification of Organic Compounds*, 5th ed., Wiley, New York, **1991**.
- [41] A.R. Katritzky, I. Ghiviriga, P.J. Steel and D.C. Oniciu, *J. Chem. Soc. Perkin Trans. 2*, **1995**, 443-447.
- [42] A. M. Rana, P. Trivedi, K. R. Desai and S. Jauhari, *Med Chem Res*, **2014**, 23, 4320-4336.
- [43] P. Gahtori and S. K. Ghosh, *Journal of Enzyme Inhibition and Medicinal Chemistry*, **2012**, 27 (2), 281-293.
- [44] X. Wang, Y. Xu, L. Yang, X. Lu, H. Zou, W. Yang, Y. Zhang, Z. Li, M. Ma, *Journal of Fluorescence* **2018**, 28 (2), 707-723.

- [45] T.C. Johnson, A.V. Brown, K.K. Bryan, K.K. Guentenspberger, R. Hunter, T.P. Martin, N. Niyaz, G.F. Tisdell and T.Trullinger, *Pest Management Sci.*, **2017**,73 (10) , 2138 – 2148.
- [46] N.S. Mewada, D.R. Shah, H.P. Lakum and K.H. Chikhalia, *Journal of the Association of Arab Universities for Basic and Applied Sciences*, **2016**, 20 (1), 8-18.
- [47] S.Kusano, S. Konishi, R. Ishikawa, N. Sato, S. Kawata, F. Nagatsugi and O. Hayashida, *Eur. J. Org. Chem.* **2017**, 12, 1618-1623.
- [48] J. Yuan, Y. Zhu, M. Lian, Q. Gao, M. Liu, F. Jia and A. Wu, *Tetrahedron Letters* , **2012**, 53, 1222-1226.
- [49] E.A. Braude and F.C. Nachod, in: *Determination of Organic Structures by Physical Methods*, Academic Press, New York, **1955**.
- [50] M. Bazargani and M. Tafazzoli, *APCBEE Procedia*, **2013**, 7, 145-150.
- [51] T.I. Atta-Ur-Rahman, *Nuclear Magnetic Resonance: Basic Principles*, Springer-Verlag, **1989**.
- [52] P. Zassowski, P.Ledwon, A. Kurowska, A.P. Herman, M. Lapkowski, V. Cherpak, Z. Hotra, P. Turyk, K. Ivaniuk, P. Stakhira, G. Sych, D. Volyniuk and J.V. Grazulevicius, *Dyes and Pigments*, **2018**, 149, 804-811.
- [53] A. Ullah, F. Iftikhar, M. Arfan, S.T. Batool Kazmi, M.N. Anjum, I.U. Haq, M. Ayaz, S. Farooq and U. Rashid, *Eur. J. of Med. Chem.*, **2018**, 145, 140-153.
- [54] L. Xiaolian and C. Xuehui, *Dalian University of Technology*, CN107739367, **2018**, A.
- [55] A. Locher, F. Reisser and K. Hofer, *Sandoz Ltd.*, BE636144, **1963**, A.
- [56] S. Vijayaraghavan and S. Mahajan, *Bio. & Med. Chem. Lett.*, **2017**, 27 (8), 1693-1697.
- [57] S. Jana and A. Das, *As. J. of Chem.*, **2013**, 25 (1),186-190.
- [58] J. Vaughan, D.J. Carter, A.L. Rohl, M.I. Ogden, B.W. Skelton, P.V. Simpson and D.H. Brown, *Dalton Trans.*, **2016**, 45 (4), 1484-1495.
- [59] Y. Shibasaki, T. Kotaki, T. Bito, R. Sasahara, N. Idutsu, A. Fujimori, S. Miura, Y. Shidara, N. Nishimura and Y. Oishi, *Polymer*, **2018**, 146, 12-20.
- [60] D. W. Wang and M..M. Fisher, *J. of Pol. Sc.: Pol. Chem. Ed.*, **1983**, 21, 671-677.
- [61] W.C. Austin, L.H. Lunts, M.D. Potter and E.P. Taylor, *J. of Pharmacy and Pharmacology*, **1959**, 11, 80-93.
- [62] J. Bjerrum, *Stability Constants*, Chemical Society, London, **1958**.
- [63] U.S. EPA. *Carcinogenic Effects of Benzene: An Update (Draft Report)*. U.S. Environmental Protection Agency, Office of Research and Development, National Center for Environ. Assessment, Washington Office, Washington, DC, EPA/600/P-97/001F, **1998**.

- [64] R.K. Singh and F.W. Bansode, *J. Environ. Biol.*, **2011**, 32 (6), 687-694.
- [65] A.A. Chesniuk, S.N. Mikhailichenko, V.S. Zavodnov and V.N. Zaplishny, *Chem. of Heteroc. Comp.*, **2002**, 38 (2), 177-182.
- [66] T. Borke, F.M. Winnik, H. Tenhu and S. Hietala, *Carb. Polym.*, **2015**, 116, 42-50.
- [67] B. Fuchs, *Conformations of Five-Membered Rings*, in: *Topics in Stereochemistry*, Vol.10, John Wiley & Sons, Inc., **1978**.
- [68] A.R. Katritzky, C.A. Ramsden, E.E.V. Scriven and R.J.K. Taylor, *Comprehensive Heterocyclic Chemistry*, 4. Elsevier Science **2008**, Vol. 4.
- [69] S. N. Riduan and Y. Zhang, *Chem. Soc. Rev.*, **2013**, 42, 9055-9070.
- [70] K. Hoffman, *Imidazole and Its Derivatives. Part I. The Chemistry of heterocyclic compounds*, Interscience Publishers, **1953**.
- [71] T.L. Amyes, S.T. Diver, J.P. Richard, F.M. Rivas and K. Toth, *J. Am. Chem. Soc.*, **2004**, 126 (13), 4366-4374.
- [72] V. Mullangi, X. Zhou, D.W. Ball, D.J. Anderson and M. Miyagi, *Biochem.*, **2012**, 51, 7202-7208.
- [73] M. Cebo, M. Kielmas, J. Adamczyk, M. Cebrat, Z. Szewczuk and P. Stefanowicz, *Anal. Bioanal. Chem.*, **2014**, 406 (30), 8013-8020.
- [74] J. Myllyharju and K.I. Kivirikko, *Trends in Genetics*, **2004**, 20 (1), 33-43.
- [75] W. Friess, *Eur. J. of Pharm. and Biopharm.*, **1998**, 45, 113-136.
- [76] C.H. Lee, A. Singla and Y. Lee, *Int. J. of Pharm.*, **2001**, 221, 1-22.
- [77] A. Birbrair, T. Zhang, D.C. Files, S. Mannava, T. Smith, Z.M. Wang, M.L. Messi, A. Mintz and O. Delbono, *Stem Cell Res. & Ther.*, **2014**, 5, 122-140.
- [78] R. Parenteau-Bareil, R. Gauvin and F. Berthod, *Materials*, **2010**, 3, 1863-1887.
- [79] X. Duan and H. Sheardown, *Biomaterials*, **2006**, 27, 4608-4617.
- [80] A. Barbetta, M. Massimi, B. Di Rosario, S. Nardecchia, M. De Colli, L.C. Devirgiliis, M. Dentini, *Biomacromolecules*, **2008**, 9, 2844-2856.
- [81] K.S. Weadock, E.J. Miller, E.I. Keuffel and M.G. Dunn, *J. Biomed. Mater. Res.*, **1996**, 32, 221-226.
- [82] S.T. Boyce, D.J. Christianson and J.F. Hansborough, *J. Biomed. Mater. Res.*, **1988**, 22, 939-957.
- [83] M.G. Haugh, M.J. Jaasma and F.J. O'Brien, *J. of Biomed. Mater. Res. Part A*, **2009**, 89A, 363-369.

- [84] L. Ma, C.Gao, Z. Mao, J. Shen, X. Hu and C. Han, *J. of Biomat. Sci., Polym. Ed.*, **2003**, 14, 861-874.
- [85] E. Jorge-Herrero, P. Fernández, J. Turnay, N. Olmo, P. Calero, R. García, I. Freile and J.L. Castillo-Olivares, *Biomaterials*, **1999**, 20 (6), 539-545.
- [86] K. E. Kadler, C. Baldock, J. Bella and R.P. Boot-Handford, *J. Cell Science*, **2007**, 120 (12), 1955-1958.
- [87] P. Li and G. Wu, *Amino Acids*, **2018**, 50 (1), 29-38.
- [88] M.L. Chu, K. Mann, R. Deutzmann, D. Pribula-Conway, C.C. Hsu-Chen, M.P. Bernard and R. Timpl, *Eur. J. Biochem.*, **1987**, 168, 309-317.
- [89] J.E. Eastoe, *Biochem. J.*, **1955**, 61 (4), 589-600.
- [90] J. Bella, *Biochem. J.*, **2016**, 473 (8), 1001-1025.
- [91] A. Covington, *Tanning Chemistry: The Science of Leather*, RSC Publishing, Cambridge, UK, **2009**.
- [92] P.L. Privalov, *Advances in Protein Chemistry*, Vol. 35, Academic Press Inc., **1982**.
- [93] G.N. Ramachandran and G. Kartha, *Nature*, **1955**, 176, 593-595.
- [94] J. Kopp, M. Bonnet and J.P. Renou, *Matrix*, **1989**, 9, 443-450.
- [95] P.J. Flory and R.R. Garrett, *J. Am. Chem. Soc.*, **1958**, 80 (18), 4836-4845.
- [96] L.Bozec and M. Odlyha, *Biophys. J.* **2011**, 101 (1), 228-236.
- [97] A. Rochdi, L. Foucat and J. P. Renou, *Biopolymers*, **1999**, 50 (7), 690-696.
- [98] E. Onem, A. Yorgancioglu, H.A. Karavana and O. Yilmaz, *Journal of Thermal Analysis and Calorimetry*, **2017**, 129 (1), 615-622.
- [99] C.A. Miles, *Int. J. Biol. Macromol.*, **1993**, 15, 265-271.
- [100] H. Hoermann and H. Schlebusch, *Biochemistry*, **1971**, 10 (6), 932-937.
- [101] A. Covington, *Chem. Soc. Rev.*, **1997**, 26, 111-126.
- [102] C.A. Miles, N.C. Avery, V.V. Rodin and A.J. Bailey, *J. Mol. Biol.*, **2005**, 346, 551-556.
- [103] M. Schroepfer and M. Meyer, *Int. J. of Bio. Macromol.*, **2017**, 103, 120-128.
- [104] L.H.H. Olde Damink, P.J. Dijkstra, M.J.A. van Luyn, P.B. van Wachem, P. Nieuwenhuis and J. Feijen, *Biomaterials*, **1996**, 17 (8), 765-773.
- [105] X. Duan and H. Sheardown, *J. Biomed. Mater. Res.*, **2005**, 75A (3), 510-518.
- [106] N.Z. Bjerrum, *Phys. Chem.*, **1910**, 73, 724-759.
- [107] Y.Q. Ding, C.L. Chen, T.D. Li, J.Y. Cheng and H.Y. Zhang, *Soft Mat.*, **2015**, 13, 24-31.
- [108] *World Statistical Compendium for Raw Hides and Skins, Leather and Leather Footwear 1990-2009*. Food and Agricultural Organisation Database, FAO, **2010**.

- [109] J.M. Morera, E. Bartolí, R. Chico, C. Solé and L.F. Cabeza, *J. of Cleaner Prod.*, **2011**, 19 (17-18), 2128-2132.
- [110] M. Costa, *Crit. Rev. Toxicol.*, **1997**, 27 (5), 431-442.
- [111] Z. Kirpnick-Sobol, R. Reliene and R.H. Schiestl, *Cancer. Res.*, **2006**, 66 (7), 3480-3484.
- [112] R. Usha and T. Ramasami, *Thermochimica Acta*, **2000**, 356 (1-2), 59-66.
- [113] J.M. Ruijgrok, J.R. de Wijn and M.E. Boon, *Clinic. Mater.*, **1994**, 17 (1), 23-27.
- [114] A. Marsal, S. Cuadros, A.M. Manich, F. Izquierdo and J. Font, *J. of Cleaner Prod.*, **2017**, 148, 518-526.
- [115] B. Madhan, C. Muralidharan and R. Jayakumar, *Biomaterials*, **2002**, 23 (14), 2841-2847.
- [116] L.H.H. Olde Damink, P.J. Dijkstra, M.J.A. van Luyn, P.B. van Wachem, P. Nieuwenhuis and J. Feijen, *J. of Mater. Sci.: Mater. in Med.*, **1995**, 6 (8), 460-472.
- [117] S. Dixit, A. Yadav, P.D. Dwivedi and M. Das, *J. of Cleaner Prod.*, **2015**, 87, 39-49.
- [118] H. Shadnia and J.S. Wright, *Chem. Res. Toxicol.*, **2008**, 21 (6), 1197-1204.
- [119] J.E. Gough, C.A. Scotchford and S. Downes, *J. of Biomed. Mater. Res.*, **2002**, 61 (1), 121-130.
- [120] H. Petite, I. Rault, A. Huc, P. Menasche and D. Herbage, *J. Biomed. Mater. Res.*, **1990**, 24 (2), 179-187.
- [121] N. Davidenko, C.F. Schuster, D.V. Bax, N. Raynal, R.W. Farndale, S.M. Best and R.E. Cameron, *Acta Biomaterialia*, **2015**, 25, 131-142.
- [122] A. Falchi, G. Giacomelli, A. Porcheddu and M. Taddei, *Synlett.*, **2000**, 2, 275-277.
- [123] P. Farkas and S. Bystricky, *Carbohydr. Polym.*, **2007**, 68, 187-190.
- [124] M. D'Este, D. Eglin and M. Alini, *Carbohydr. Polym.*, **2014**, 108, 239-246.
- [125] V. Beghetto, A. Zancanaro and G. Pozza, WO2015/044971 A2, **2014**.
- [126] V. Beghetto, WO2016/103185A3, **2016**.
- [127] Leather, Physical and mechanical tests. Determination of the shrinkage temperature of leather up to 100 °C, IULTCS/IUP 16, EN ISO 3380, **2015**.
- [128] H. Namazi, *BioImpacts*, **2017**, 7 (2), 73-74.
- [129] A. Bhattacharya and B.N. Misra, *Prog. Polym. Sci.*, **2004**, 29, 767-814.
- [130] G.R. Strobl, *The Physics of Polymers: Concepts for Understanding Their Structures and Behavior*, 3rd ed., Springer, **2007**.
- [131] D. Abliz, Y. Duan, L. Steuernagel, L. Xie, D. Li and G. Ziegmann, *Polymers & Polymer Composites*, **2013**, 21(6), 341-348.
- [132] M.M. Reboredo and A. Vazquez, *Polym. Eng. & Sci.*, **1995**, 35 (19), 1521-1526.

- [133] R. Kay, A.R. Westwood *Eur. Polym. J.*, **1975**, 11 (1), 25-30.
- [134] X. Liu, W. Xin and J. Zhang, *Green. Chem.*, **2009**, 11, 1018-1025.
- [135] L.J. Lee and C.W. Macosko, *Int. J. of Heat and Mass Tran.*, **1980**, 23 (11), 1479-1492.
- [136] T. Chen, G. Kumar, M.T. Harris, P.J. Smith, G.F. Payne, *Biotech. and Bioeng.*, **2000**, 70 (5), 564-573.
- [137] S. Cosnier, D. Fologea, S. Szunerits and R.S. Marks, *Electrochem. Comm.*, **2000**, 2 (12), 827-831.
- [138] V.T. Stannett, *Int. J. of Rad. App. and Instr. Part C. Rad. Physics and Chem.*, **1990**, 35 (1-3), 82-87.
- [139] N. Friis and A.E. Hamielec, *ACS Symposium Series*, **1975**, 16 (1), 192-197.
- [140] H. Kubota, I.G. Suka, S. Kuroda and T. Kondo, *Eur. Polym. J.*, **2001**, 37 (7), 1367-1372.
- [141] T. Yamaguchi, S. Yamahara, S. Nakao and S. Kimura, *J. of Membrane Sci.*, **1994**, 95 (1), 39-49.
- [142] D. Roy, M. Semsarilar, J.T. Guthrie and S. Perrier *Chem. Soc. Rev.*, **2009**, 38, 2046-2064.
- [143] M. Szwarc, *Nature*, **1956**, 178, 1168-1169.
- [144] K. Matyjaszewski, *Controlled/Living Radical Polymerization. Progress in ATRP, NMP, and RAFT*, American Chemical Society, **2000**.
- [145] G. Odian, *Principles of Polymerization*, Wiley-Interscience, 4th ed., **2004**.
- [146] H.C. Haas, P.M. Kamath and N.W. Schuler, *J. of Polym. Sci.*, **1957**, 24 (105), 85-92.
- [147] B.N. Misra, R. Dogra and I.K. Mehta, *J. of Polym. Sci.: Polym. Chem. Ed.*, **1980**, 18, 749-752.
- [148] F. Berzin, J. Flat and B. Vergnes, *J. Polym. Eng.*, **2013**, 33(8), 673-682.
- [149] A.V. Janorkar, N. Luo and D.E. Hirt, *Langmuir*, **2004**, 20 (17), 7151-7158.
- [150] I. Kaur and R. Barsola, *J. of App. Polym. Sci.*, **1990**, 41 (9-10), 2067-2076.
- [151] J.M. García-Martínez, O. Laguna and E.P. Collar, *J. of App. Polym. Sci.*, **1998**, 68 (3), 483-495.
- [152] S.H.P. Bettini and J.A.M. Agnelli, *J. of App. Polym. Sci.*, **1999**, 74 (2), 247-255.
- [153] Y. Ogiwara and H. Kubota, *J. of App. Polym. Sci.*, **1969**, 13 (8), 1613-1620.
- [154] R.M. Jeziórska, *Reactive extrusion of polymers*, in: *Advances in Polymer Processing, From Macro- to Nano-Scales*, S. Thomas and W. Yang, Woodhead Publishing, 1st ed., **2009**.
- [155] K.I. Ku Marsilla, C.J.R. Verbeek, *Eur. Polym. J.*, **2015**, 67, 213-223.
- [156] M.A. Mohsin, T. Abdulrehman and Y. Haik, *Int. J. of Chem. Eng.*, **2017**.
- [157] W. Lai, C. Li, H. Chen and S. Shaik, *Angew. Chem. Int. Ed.*, **2012**, 51 (23), 5556-5578.

- [158] Market Study: Polypropylene, Ceresana, 4th edition, **2017**.
- [159] Ullmann's Encyclopedia of Industrial Chemistry, Wiley-VCH; 7th ed., **2005**.
- [160] D. Tripathi, Practical Guide to Polypropylene, Smithers Rapra Press, **2002**.
- [161] A. Kaymakci, E. Birinci and N. Ayrimis, Comp. Part B: Eng., **2018**, 157, 43-46.
- [162] M. Abbasian, H. Ghaemina and M. Jaymand, M. Appl. Phys. A, **2018**, 124-522.
- [163] K. Mai, Z. Li, Y. Qiu and H. Zeng, J. of Appl. Polym. Sci., **2001**, 81 (11), 2679-2686.
- [164] K.S. Abudonia, G.R. Saad, H.F. Naguib, M. Eweis, D. Zahran and M. Z. Elsabee, J. of Polym. Res., **2018**, 25-125.
- [165] Y.F. Yang, Y. Li, Q.L. Li, L.S. Wan and Z.K. Xu, J. of Membrane Sci., **2010**, 362 (1-2), 255-264.
- [166] O. Martiin and L. Avérous, Polymer, **2001**, 42 (14), 6209-6219.
- [167] M. Jamshidian, E.A. Tehrany, M. Imran, M. Jacquot, and S. Desobry, Compreh. Rev. in Food Sci. and Food Safety, **2010**, 9(5), 552-571.
- [168] R.A. Auras, L.T Lim, S.E.M. Selke and H. Tsuji, Poly(lactic acid): Synthesis, Structures, Properties, Processing, and Applications, Wiley, 1st ed., **2011**.
- [169] T.Maharana, S. Pattanaik, A. Routaray, N. Nath and A.K.Sutar, Reactive and Functional Polymers, **2015**, 93, 47-67.
- [170] M. Tesfaye, R. Patwa, P. Dhar, and V. Katiyar, *ACS Omega*, **2017**, 2 (10), 7071-7084.
- [171] D. Carlson, L. Nie, R. Narayan and P. Dubois, J. of Appl. Polym. Sci., **1999**, 72 (4), 477-485.
- [172] J.F. Zhang and X. Sun, Biomacromolecules, **2004**, 5 (4), 1446-1451.
- [173] F. Labre, S. Mathieu, P. Chaud, P.Y. Morvan, R. Vallée, W. Helbert and S. Fort, Carbohydr. Polym., **2018**, 184, 427-434.
- [174] H. Yamada, B. Loretz and C.M. Lehr, Biomacromolecules, **2014**, 15 (5), 1753-1761.
- [175] R. Saraf, H.J. Lee, S. Michielsen, J. Owens, C. Willis, C. Stone and E. Wilusz, J. of Mat. Scie., **2011**, 46 (17), 5751-5760.
- [176] H. Nie, A. He, B. Jia, F. Wang, Q. Jiang and C.C. Han, Polymer, **2010**, 51 (15), 3344-3348.
- [177] Y. Zhang, W. Wang, Q. Feng, F. Cui and Y. Xu, Mat. Sci. and Eng. C, **2006**, 26 (4), 657-663.
- [178] P. Suppakul, J. Miltz, K. Sonneveld and S.W. Bigger, J. of Food Sci., **2003**, 68 (2), 408-420.
- [179] G. Moad, Progress in Polym. Sci., **1999**, 24 (1), 81-142.
- [180] I. Sheelakumari, *Modification of Polyethylenes by Reactive Extrusion*, PhD thesis, Cochin University Of Science And Technology, **2001**.



- [181] S.N. Sathe, G.S.S. Rao and S. Devi, *J. of Applied Polym. Sci.*, **1994**, 53 (2), 239-245.
- [182] D. Garlotta, *J. of Polym. and the Envir.*, **2001**, 9 (2), 63-84.
- [183] W. Heinen, C.H. Rosenmüller, C.B. Wenzel, H.J.M. de Groot and J. Lugtenburg, *Macromolecules*, **1996**, 29 (4), 1151-1157.
- [184] G. De Vito, N. Lanzetta, G. Maglio, M. Malinconico, P. Musto, and R. Palumbo, *J. of Polym. Sci.: Polym. Chem. Ed.*, **1984**, 22 (6), 1335-1347.
- [185] Food Standard Agency, *Food Additives Legislation Guidance to Compliance*, **2015**.
- [186] Y.M. Krivoguz, A.M. Guliyev and S.S. Pesetskii, *eXPRESS Polym. Lett.*, **2010**, 4 (3), 161-170.
- [187] C. Bergstrom and T.H. Palmgren, *US4877685A*, **1986**.
- [188] G.R.P. Henry, X. Drooghaag, D.D. J. Rousseaux, M. Sclavons, J. Devaux, J. Marchand-Brynaert and V. Carlier, *J. of Polym. Sci.: Part A: Polym. Chem.*, **2008**, 46 (9), 2936-2947.
- [189] Y. Kong and J.N. Hay, *Eur. Polym. J.*, **2003**, 39 (8), 1721-1727.
- [190] C.L. Beyler and M.M. Hirschler, *Thermal Decomposition of Polymers*, in *SFPE Handbook of Fire Protection Engineering*, M.J. Hurley, Springer Verlag; 5th ed., **2015**.
- [191] M.R. Jung, F.D. Horgen, S.V. Orski, V. Rodriguez, K.L. Beers, G.H. Balazs, T.T. Jones, T.M. Work, K.C. Brignac, S.J. Royer, K.D. Hyrenbach, B.A. Jensen and J.M. Lynch, *Marine Pollution Bulletin*, **2018**, 127, 704-716.
- [192] G. Moad, E. Rizzardo and S.E. Thang, *Aust. J. Chem.*, **2009**, 62 (11), 1402-1472.
- [193] F. Dilika, P.D. Bremner and J.J.M. Meyer, *Fitoterapia*, **2000**, 71 (4), 450-452.
- [194] J.B. Parsons, J. Yao, M.W. Frank, P. Jackson and C.O. Rock, *J. of Bacteriology*, **2012**, 194 (19), 5294-304.
- [195] E. Freese, C.W. Sheu and E. Galliers, *Nature*, **1973**, 241, 321-325.
- [196] L. Quiles-Carrillo, N. Montanes, C. Sammon, R. Balart and S. Torres-Giner, *Industrial Crops and Products*, **2018**, 111, 878-888.
- [197] A. Lashgari, A. Eshghi and M. Farsi, *Asian J. of Chem.*, **2013**, 25 (2), 1043-1049.
- [198] H. Essabir, S. Nekhlaoui, M. Malha, M.O. Bensalah, F.Z. Arrakhiz, A. Qaiss and R. Bouhfid, *Materials and Design*, **2013**, 51, 225-230.
- [199] B. Çakmakli, B. Hazer, S. Açıkgöz, M. Can and F.B. Cömert, *J. of Applied Polym. Sci.*, **2007**, 105 (6), 3448-3457.
- [200] A. Alli and B. Hazer, *J. of the Am. Oil Chem. Soc.*, **2011**, 88 (2), 255-263.
- [201] X. Xie and X. Zheng, *Materials and Design*, **2001**, 22 (1), 11-14.

- [202] S. Detyothin, S.E.M. Selke, R. Narayan, M. Rubino and R. Auras, *Polym. Degrad. and Stab.*, **2013**, 98 (12), 2697-2708.
- [203] M.J. Parker, *Test Methods, Nondestructive Evaluation and Smart Materials*, in *Comprehensive composite materials*, A. Kelly and C. Zweben, Elsevier, **2000**.
- [204] S.W. Hwang, S.B. Lee, C.K. Lee, J.Y. Lee, J.K. Shim, S.E.M. Selke, H. Soto-Valdez, L. Matuana, M. Rubino and R. Auras, *Polymer Testing* **2012**, 31 (2), 333-344.
- [205] G. Wypych, *Handbook of Nucleating Agents*, ChemTec Publishing, **2016**.
- [206] L. Quiles-Carrillo, M.M. Blanes-Martínez, N. Montanes, O. Fenollar, S. Torres-Giner and R. Balart, *Eur. Polym. J.*, **2018**, 98, 402-410.
- [207] J. Vartiainen, M. Rättö and S. Paulussen, *Packag. Technol. Sci.*, **2005**, 18 (5), 243-251.
- [208] S. Zanini, M. Müller, C. Riccardi and M. Orlandi, *Plasma Chem. & Plasma Process*, **2007**, 27, 446-457.
- [209] R.M. Rasal, A.V. Janorkar and D.E. Hirt, *Progress in Polym. Sci.*, **2010**, 35 (3), 338-356.
- [210] ASTM D5946-04, *Standard test method for corona-treated polymer films using water contact angle measurements*, ASTM International, West Conshohocken, PA, **2004**.